

# THESIS AIM

Glutamate is the main excitatory neurotransmitter of the mammalian nervous system and is involved in neuronal plasticity, memory and learning.

Emerging evidences suggest that glutamate is also present in peripheral tissues, where it plays a role in both cellular homeostasis and in autocrine/paracrine communication as extracellular signalling molecule.

Particular interesting is the role played by this amino acid in islets of Langerhans, the endocrine part of the pancreas which controls whole body glucose homeostasis, by releasing hormones.

Islet cells use a sophisticate system of endocrine, paracrine and autocrine signals to synchronize their activities, among these is glutamate. By activating specific glutamate receptors, the amino acid controls hormone release and  $\beta$ -cell viability. However, the glutamate signalling machinery and the precise mechanisms by which it modulates islet functions are poorly understood.

The extracellular glutamate concentration is tightly controlled by high affinity glutamate transporters. The main isoform expressed in the islet is the  $\text{Na}^+$ -dependent high affinity glutamate transporter GLT1/EAAT2 (glutamate transporter 1/ excitatory amino acid transporter 2) which is prevalently expressed on the plasma membrane of insulin-secreting cell ( $\beta$ -pancreatic cells). We have previously shown that GLT1, by transporting glutamate within the cell, exerts a key role in the control of extracellular glutamate concentration and in the modulation of hormone release and  $\beta$ -cell viability.

In this study, we focus on GLT1 and we examine the molecular mechanisms which control its expression and function, using murine clonal  $\beta$ -cell lines and isolated human islets of Langerhans as experimental models.

In chapter I, we focus on the effects of rapid physiological modifications of glucose concentrations on GLT1 activity and localization and we investigate the molecular mechanisms responsible for this acute regulation.

In chapter II, we analyse the effects of chronic hyperglycaemia (a condition typical of diabetes mellitus) on modulation of GLT1 expression and activity and we investigate the consequences of such as modulation on  $\beta$ -cell function. The localization of GLT1 was also assessed on pancreas sections from control and diabetic subjects.

In chapter III we highlight the possible pathological role of GLUT1 in type 1 of diabetes mellitus (T1DM). We investigate the potential involvement of this transporter in the development of T1DM autoimmunity, as a new membrane antigen of diabetes mellitus.

Chapter IV reports two side projects of these three-years of doctoral activity. The first project is related to the characterization of islet remodelling during diabetes, in baboons. This is collaboration with Prof. Folli Franco of Texas University and my role in the project was to characterize the apoptotic cells in islets of Langerhans.

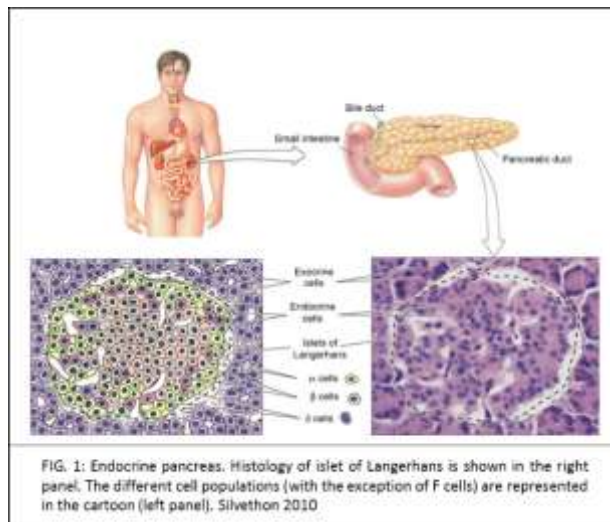
The second project is a technical project; the lab is interested in developing imaging techniques and protocols for studying vesicle dynamics. Using the genetically encoded synapto-pHluorin and Total Internal Reflection Fluorescence Microscopy we developed a new macro for the analysis of endocytic and exocytic events at the plasma membrane. This macro could be very useful for future studies related to the effect of glutamate on hormone secretion.

# GENERAL INTRODUCTION:

## 1) The islets of Langerhans

### *Pancreas*

The pancreas is composed of two functionally different portions: the exocrine pancreas, the main digestive gland of the body, and the endocrine pancreas (islets of Langerhans) responsible for the release of several important hormones (insulin, glucagon, somatostatin and pancreatic polypeptide). While the main products of the exocrine pancreas (digestive enzymes) have the function to process the ingested food to make them available for cells, the hormones produced by the endocrine pancreas regulate several aspects of cell nutrition such as the speed of food absorption, the nutrients metabolism and intracellular storage (Silverthorn 2010). Functional alteration of the endocrine pancreas, or an abnormal response to pancreatic hormones by the target tissues, causes significant alterations in the homeostasis of nutrients, including the syndromes of diabetes mellitus. (FIG. 1, Silverthorn 2010).



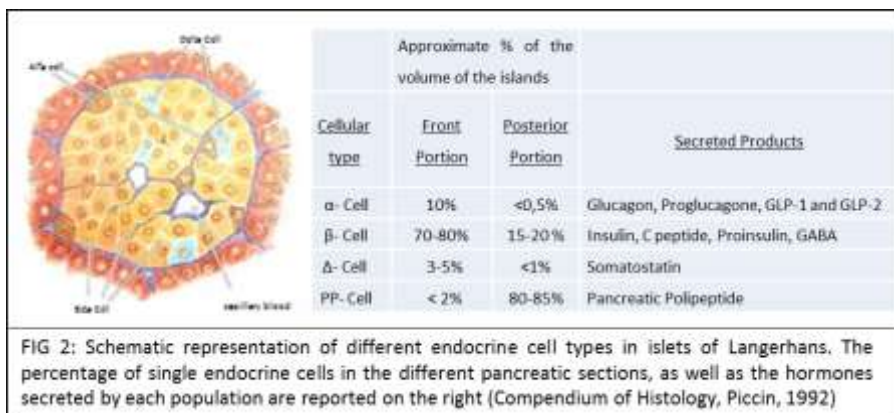
### *The islets of Langerhans*

Islets of Langerhans control whole body glucose homeostasis, as they respond, releasing hormones, to changes in nutrient concentrations in the blood stream. The regulation of hormone secretion has been the focus of attention for a long time because it is related to many metabolic disorders, including diabetes mellitus.

Pancreatic islets are islands of endocrine tissue dispersed in the exocrine pancreas. They are composed not only of hormone secreting endocrine cells but also of vascular cells, resident immune cells and, in many species, neurons and glial cells of the neuroinsular complex (Caicedo et al., 2012).

**The architecture of islets of Langerhans**

A human pancreas contains approximately 1 million pancreatic islets of Langerhans (Hellman 1959). The pancreatic islets consist of several types of endocrine cells: the insulin-secreting  $\beta$  cells (50% of the cells in human islets), the glucagon-releasing  $\alpha$  cells (35–40%), the somatostatin-releasing  $\delta$  cells (10–15%), the ghrelin-releasing  $\epsilon$ -cells and F-cells for the pancreatic polypeptide production (FIG. 2 and FIG. 3; Compendium of Histology, Piccin, 1992; Cabrera et al., 2006). The percentage of the different endocrine cell populations changes from islet to islet, from individual to individual, from species to species (Gloyn et al., 2005; Schuit et



al., 1997). Human islets have a larger proportion of alpha cells than mouse islets (38% versus 18%) (McCulloch et al., 2011). Not only is important the relative proportion of endocrine cell types but also their distribution within the islets.

Human islets are surrounded by a complex double basement membrane (Fraysn 2010; Cbrera et al., 2005). Each islet is a functional unit given that it has all the cells necessary to produce adequate responses to changes in glucose concentrations. Indeed, *in vitro*, hormone release from isolated islets in response to glucose faithfully reflects the secretory activity of the endocrine pancreas in the organism (Doliba et al., 2012). When transplanted into diabetic individuals, islets take over glucose homeostasis and restore normoglycemia (Kahn SE 2003). In human islets, alpha and delta cells are not segregated to the periphery as they are in the mouse islet (Rodriguez-Diaz et al., 2011b). Instead, they are intermixed and this distribution has multiple effects on endocrine cell function (Rebelato et al., 2011). For example, beta cells that are associated with alpha cells secrete more insulin when stimulated with glucose (MacDonald et al., 2011). Morphological studies reveal the

presence of tight and gap junctions between islet cells. Those junctions create narrow intercellular spaces of only 15-20 nm where the chemical signals can be released and reach relevant concentrations (Orci et al., 1975).

### ***Vascularization of Islets of Langerhans***

The islets receive a rich systemic vascular supply via the splenic and superior mesenteric arteries, and the effluent empties into the portal vein. Although islets represent only 1–2% of the pancreas, they receive ~10% of the blood supply (Jansson and Hellerstrom 1986).

Because of a rich network of capillaries, endocrine cells in islets detect glucose and other nutrients and release their hormones in the bloodstream. Despite the importance for islets function, there are no detailed studies of the human islet vasculature. Blood vessels in mouse islets are mainly capillary endothelial tubes connected to one or two feeding arterioles that penetrate the islet. As in other organs, blood flow can be locally regulated by vascular smooth muscle cells acting as sphincters. The presence of such sphincters, deep within the islet, suggests that these cells can be regulated by paracrine signals released from endocrine cells. The possibility that endocrine cells regulate their own blood supply by influencing adjacent vascular smooth muscle cells needs to be tested experimentally.

Recent findings indicate that blood vessels in human islets may contain more smooth muscles than those in mouse islets (Bosco et al., 2010). These contractile cells seem to be present throughout the islet vasculature and are the preferred target of sympathetic axons in the human islets (Caicedo et al., 2012). In mice, where  $\beta$ -cells are segregated in the islets core and non  $\beta$ -cells in the periphery, blood flows sequentially through distinct regions containing either  $\beta$ -cells or non- $\beta$  cells. In human islets, endocrine cells are intermixed and are all distributed along blood vessels (McCulloch et al., 2011). As a result, any given region of the human islet contains a heterogeneous cell population through which blood flows and any given cell type can influence other cell types (Cabrera et al., 2006). Therefore, from an anatomical point of view human islets seem to be predisposed for paracrine signaling.

### ***Innervation of Islets of Langerhans***

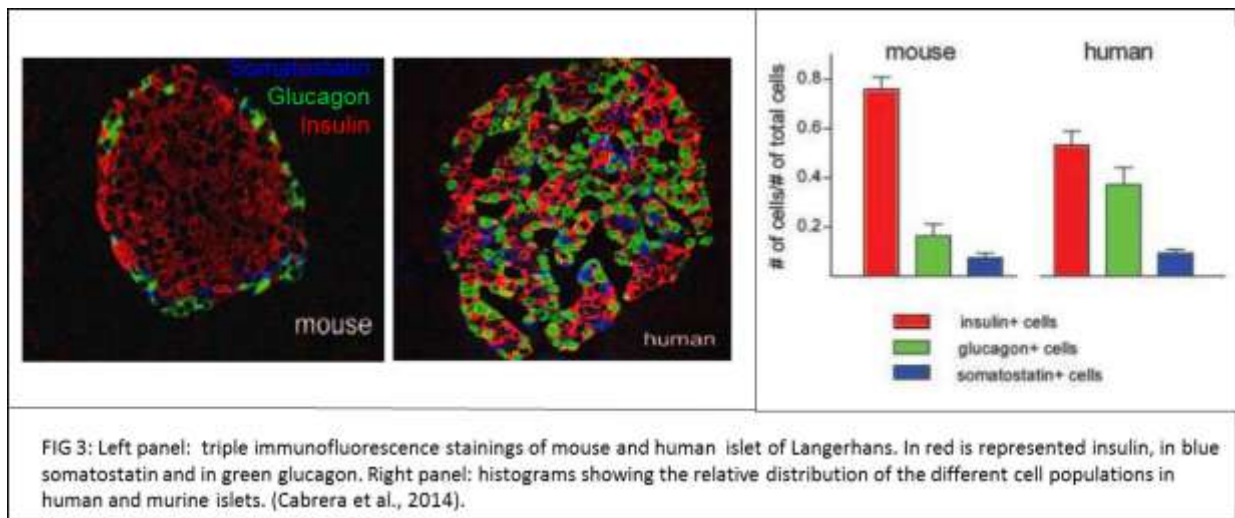
The autonomic nervous system influences insulin and glucagon secretion but mouse and human islets differ in their innervation patterns. In mouse islets, the sympathetic fibers preferentially innervate alpha cells and parasympathetic fibers innervate alpha cells and beta cells equally. In striking contrast, in human islets, sympathetic fibers preferentially innervate central islet blood vessels and parasympathetic fibers are few and far (Karlsson et al., 1994). Although the animal studies demonstrate that nerves can influence islet hormone secretion, they did not establish when they actually do so. Studies measuring norepinephrine spillover

demonstrated that pancreatic sympathetic nerves are activated by hypoglycemic stress, but not by either hypoxic or hypotensive stress (Havel et al., 1988). Analogous measurements of acetylcholine spillover from parasympathetic nerves are rarely, possible because of avid and ubiquitous acetylcholinesterases. Fortunately, pancreatic polypeptide, secreted from the islet F cell, is under strong parasympathetic control (Schwartz et al., 1978). Using the latter as a marker of parasympathetic activation, it has been found that pancreatic parasympathetic nerves are activated during both hypoglycemia and feeding. Studies using autonomic blockade or ablation, implicate autonomic innervation in the control of the glucagon response to severe hypoglycemia (Taborsky et al., 1998). This increased glucagon secretion helps to restore normo-glycemia by stimulating hepatic glucose production. Studies using vagotomy or cholinergic antagonists, suggest that parasympathetic nerves help mediating the very early insulin response to feeding (Ahrén, 2000), which primes the liver to store the incoming glucose load.

The discovery and elucidation of neural control of the human islet will yield new insight into modulation of alpha and beta cell function with the potential to influence future diabetic therapeutics.

**Human and rodent islets show several differences in their architecture.**

As mentioned previously, human and mouse islets have anatomical and functional differences that profoundly affect their physiology:



- The innervation: whereas the pancreatic islets of rodents are extensively innervated, human islet cells are more sparsely innervated (Rodriguez-Diaz et al., 2011a; Rorsman and Braun 2013).

- Cell proportion: the number of  $\alpha$ -cells is unusually high in human islets if compared to rodent (40% in human vs 20% in rodent) with a ratio of  $\alpha$  to  $\beta$  cells of 1:1.25 (Cabrera et al, 2006); therefore, the possibility of  $\alpha$ - $\beta$  cell interactions is increased (Figure 3).

- Cell arrangement in the islet: rodent islets consist of a clearly demarcated core of  $\beta$  cells surrounded by a mantle of non- $\beta$  cells, principally  $\alpha$  cells. On the contrary, in human islets, the different cell populations are intermixed, supporting the possibility of a crosstalk among the different cell types (Cabrera et al., 2006; Bosco et al., 2010).

- Islet blood vessels: in rodents, the intra-islet vascular perfusion enables blood flow from  $\beta$ -cell to  $\alpha/\delta$ , therefore  $\beta$ -cells can directly control secretion from  $\alpha$  and  $\delta$  cells via the vascular route, whereas the opposite looks unlikely (Stagner and Samols 1992). In humans, all endocrine cell types are closely associated with the islet vessels; therefore, blood flows without any defined order and any given cell type can influence other cell types (Cabrera et al., 2006). Furthermore, blood vessels in human islets may contain more smooth muscle than those in mouse islets. These contractile cells, controlled by the autonomic system, act as sphincters and regulate local blood flow increasing the possibility of paracrine interactions (Rodriguez-Diaz et al., 2011).

These morphological, anatomical and functional differences between rodent and human islets suggest that the mechanisms and the molecules involved in cells interactions may be very different between the two species and the cell arrangement of human islets predisposes this islet to paracrine and autocrine interactions.

### ***Physiology of Islets of Langerhans***

The islets of Langerhans are mainly responsible for the production and secretion of insulin, glucagon, somatostatin and pancreatic polypeptide principally. The primary focus of islet research is therefore to understand the physiology of human islets and to unravel the molecular mechanisms that lead to hormone synthesis and secretion. Indeed, the complex mechanisms underlying such a regulation are strictly related to many metabolic disorders, including diabetes mellitus, which results from beta cells specific dysfunction and death (Caicedo et al., 2012).

Although the endocrine cells of pancreas are able to detect other nutrients such as amino acids, the islets are considered a glucose sensor. Unlike other chemoreceptors in the body that use G protein coupled receptors for detecting sugars, islet endocrine cells transduce glucose stimulation by a series of metabolic processes that lead to changes in the cell's membrane potential (Henquin 2009). These processes include glucose transport into the cells via the low-affinity glucose transporter type 1, glucose phosphorylation by the enzyme glucokinase and the subsequent metabolism of glucose that increases the intracellular ATP-to-ADP ratio.

Elevated ATP closes ATP-gated  $K^+$  channels, depolarizes the membrane, and opens voltage-gated  $Ca^{2+}$  channels, triggering hormone secretion. This complex chain of events not only ensures that glucose metabolism is coupled to membrane electrical activity but also provides multiple points where extracellular and intracellular signals can modulate hormone secretion.

Increases in glucose concentration stimulate insulin secretion but inhibit glucagon release. Instead of relying on different mechanisms to transduce increases in glucose concentration into decreased cellular activity, alpha cells have additional mechanisms beyond those they share with beta cells. Thus, like beta and delta cells, alpha cells are depolarized by glucose. However, in alpha cells voltage-gated  $Na^+$  channels become inactivated and/or they become inhibited by paracrine signals released from beta cells (Ramracheya et al., 2010; Gromada et al., 2007). Both proposed mechanisms invert the effects of glucose by inhibiting electrical activity in alpha cells.

Because electrical activity is closely associated with exocytosis, islet hormone secretion can be modulated by activating ligand-gated membrane channels (i.e. ionotropic neurotransmitter receptors) or via signaling pathways affecting ion channel conductance. Many signals impinging on islet endocrine cells affect membrane electrical activity. Islet endocrine cells express voltage-gated ion channels that make them excitable; they display complex electrical activity with bursts of action potentials.

Function of islet endocrine cells can also be regulated at the level of the secretory pathway. Islet endocrine cells possess dense core granules containing hormones and neurotransmitters. In response to a rise in cytoplasmic  $Ca^{2+}$ , these granules fuse with the plasma membrane in a process requiring soluble N-ethylmaleimide-sensitive factor attachment protein receptor (SNARE) (Braun et al., 2008). This mechanism is similar to vesicular transmitter release in neurons. Stimuli that increase intracellular  $Ca^{2+}$ , either via  $Ca^{2+}$  influx or via  $Ca^{2+}$  release from intracellular stores, trigger granule fusion. Granule fusion is crucial for insulin secretion and glucose homeostasis. Single nucleotide polymorphisms (SNPs) and alterations in the abundance of SNARE proteins have been linked to type 2 diabetes (T2D) (Wang et al., 2009). In addition to fusion, secretion also involves the mobilization of granules to the plasma membrane. Trafficking of granules to the plasma membrane requires cytoskeletal reorganization, which is accomplished with the help of the small Rho-family GTPases Cdc42 and Rac1 (Braun et al., 2008).

Neuronal, paracrine, or autocrine signals can therefore use different intracellular signaling cascades to regulate islet hormone exocytosis.

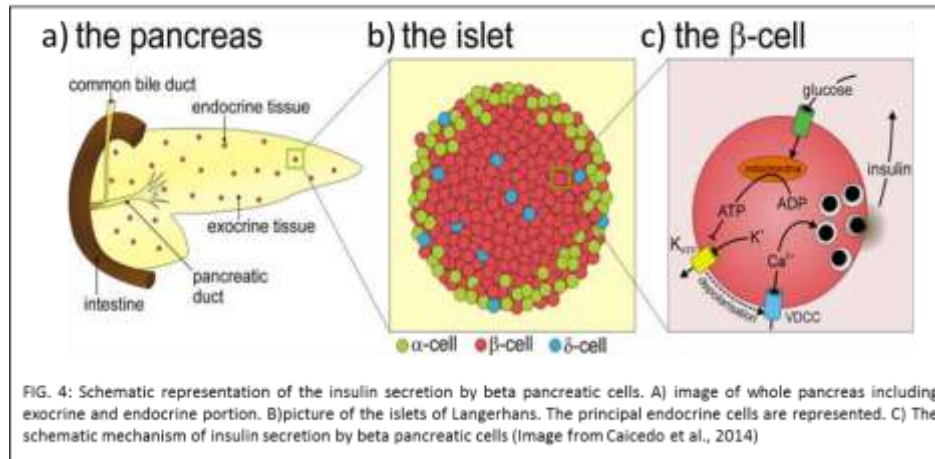
### ***Physiology of Islets of Langerhans: a focus on INSULIN SECRETION by $\beta$ -pancreatic cells.***

As for neurotransmitter release in neurons and muscle contraction, the secretion of insulin is dependent on electrical activity and calcium ( $Ca^{2+}$ ) entry.  $\beta$ -cells have channels in their membranes that mediate ions flow

(mainly  $\text{Ca}^{2+}$  and  $\text{K}^+$ ) into and out of the cell. Because ions are electrically charged, their flux across the membrane may give rise to sharp changes in voltage which resemble “action potentials” (MacDonald and Rorsman, 2006). Glucose stimulation elicits depolarization of the cell membrane and electrical activity in  $\beta$  cells (Dean et al., 1968; Henquin et al., 1984; Ashcroft et al., 1989). This serves to open voltage-dependent  $\text{Ca}^{2+}$  channels in the membrane (VDCCs) and allow  $\text{Ca}^{2+}$  entry and action potential firing.  $\text{Ca}^{2+}$  acts on the exocytotic machinery to stimulate fusion of insulin-containing vesicles with the plasma membrane for secretion into the bloodstream (Rorsman and Renstrom 2003). Removal of extracellular  $\text{Ca}^{2+}$  prevents action potential firing (Matthews and Sakamoto 1975) and insulin secretion (Curry et al., 1968; Hales and Milner 1968). Numerous subsequent studies have confirmed the essential roles of glucose-stimulated membrane depolarisation, action potential firing and influx of  $\text{Ca}^{2+}$  in the regulation of insulin secretion (Figure 4).

Metabolism of glucose is essential for insulin secretion and inhibition of mitochondrial metabolism blocks insulin secretion (Ashcroft et al., 1980). The breakdown of glucose results in the generation of ATP, one of the key molecules fueling cellular reactions. An increased ATP:ADP ratio represents the critical link between mitochondrial metabolism and insulin secretion through its ability to close ATP-dependent  $\text{K}^+$  ( $\text{K}_{\text{ATP}}$ ) channels and depolarise the cell (Rorsman and Trube 1985).  $\text{K}_{\text{ATP}}$  channels are composed of four pore-forming subunits ( $\text{K}_{\text{ir}}6.2$  in  $\beta$  cells) and four accessory sulfonylurea receptor subunits (SUR1 in  $\beta$  cells). The latter are the target of the anti-diabetic sulphonylurea drugs, which stimulate insulin secretion by mimicking the effect of glucose to close  $\text{K}_{\text{ATP}}$  channels. Polymorphism in  $\text{K}_{\text{ATP}}$  subunits contribute to diabetes susceptibility by altering the biophysical properties of the channels (Ashcroft and Rorsman 2004).

Under low glucose conditions,  $\text{K}_{\text{ATP}}$  channels are open, allowing the outward flux of  $\text{K}^+$  and holding the cell membrane potential at about  $-70$  mV. Closure of  $\text{K}_{\text{ATP}}$  channels, by glucose-induced increases in ATP, drives the membrane voltage to more positive potentials, and eventually triggers the firing of action potentials resulting from activation of VDCCs. The major VDCC subtype expressed in  $\beta$  cells regulating insulin secretion is the L-type  $\text{Ca}^{2+}$  channel ( $\text{Ca}_v1.2$ ). The essential role of this channel has been demonstrated both by pharmacological (Malaisse and Boschero 1977) and genetic (Schulla et al., 2003) inhibition of the channel. Both of these approaches result in a severe reduction in glucose stimulated insulin secretion. Although the L-type  $\text{Ca}^{2+}$  channel certainly plays a primary role in the regulation of insulin secretion, it is not the only VDCC expressed in  $\beta$  cells and recent work suggests an important role for the R-type  $\text{Ca}^{2+}$  in insulin secretion during prolonged stimulation (Figure 4; Caicedo et al., 2014; Jing et al., 2005).



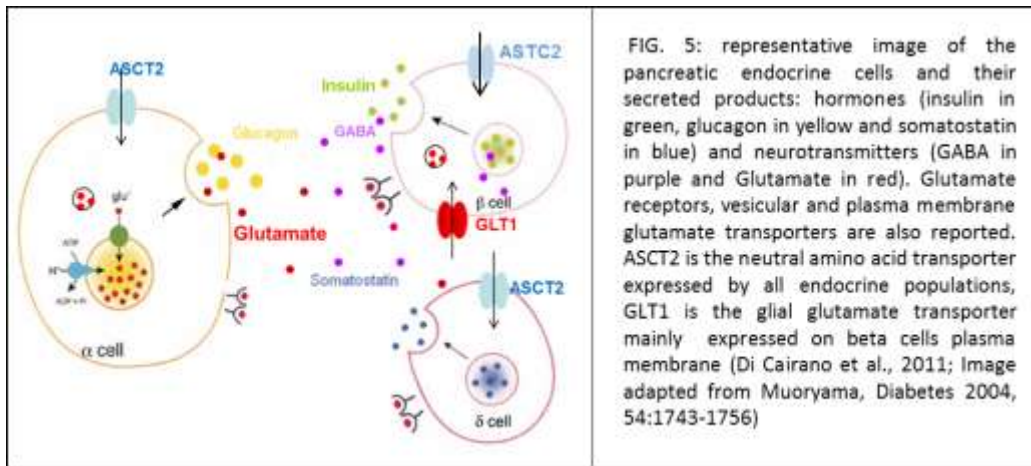
Because the membrane voltage is sensitive to changes in ATP levels within the cell, perturbations of the metabolic pathways that generate ATP can have a strong effect on insulin secretion. ATP is generated in mitochondria through the electron transport chain and is dependent upon the presence of a proton gradient ( $H^+$ ) across the mitochondrial membrane. In  $\beta$  cells, expression of uncoupling protein-2 (UCP2) can disrupt the generation of ATP in mitochondria by leading protons to leak across the mitochondrial membrane. When UCP2 is overexpressed, the generation of ATP is bypassed (Chan et al., 2001), while loss of UCP2 expression results in increased ATP levels and also enhanced insulin release by islets (Zhang et al., 2001; Figure 4).

This initial phase is called first phase of insulin secretion, is characterized by the release of the hormone contained in a pool of granules immediately ready to release because they are located in proximity to the plasma membrane. The first phase of insulin release, also identified as  $K_{ATP}$  channel dependent pathway, is driven by glucose metabolism and has been defined Glucose stimulated insulin secretion (GSIS).

There is also a second phase of insulin release, which is also called “amplification phase”. This phase in fact enhances the effect of the first phase, induced by calcium ions, and acts on storage granules. This pool of insulin granules is close to the plasma membrane but not enough to be able to fuse with the cell surface during the first phase of insulin secretion. The second phase is also associated with activation of enzymes responsible for the synthesis and maturation of new insulin molecules. Several metabolic factors downstream glucose entry in the beta cell have been proposed to support the second phase of insulin release, among these citrate, glutamate itself and GDP (Straub and Sharp, 2002).

## 2) The Paracrine / Autocrine signals in islets of Langerhans

Paracrine and autocrine signals represent a potent and rapid mechanism to control hormone release and provide positive and negative feedbacks that in turn secure glucose homeostasis. Hormones are the major auto/paracrine signaling molecules within the islet but also neuropeptides and neurotransmitters play a crucial role in this kind of interactions.



### Paracrine regulation by HORMONES in islets of Langerhans

Several hormones are stored in secretory granules of  $\alpha$ ,  $\beta$ ,  $\delta$ ,  $\epsilon$  cells and their receptors are expressed by pancreatic endocrine cells, suggesting an involvement of these hormones in the paracrine signals (Figure 5).

**INSULIN:** type A and B insulin receptors (INSR) have been identified in both murine and human  $\alpha$  and  $\beta$  cells and their activation induces a cascade of signal transduction (Muller et al. 2006; Uhles et al. 2003). At high concentrations, insulin also activates the Insulin growth factor-1 receptor (IGF1-R) express in  $\beta$ -cells (Yarden and Ullrich, 1988). This suggests the existence of an autocrine mechanism whereby insulin secreted by  $\beta$ -cells affects  $\beta$ -cell activity via InsRs and IGF1 receptors (Katz et al. 1997; Van Schravendijk et al. 1987). Short and long-term mechanisms of insulin actions have been proposed:

- a) *long-term insulin action* requires the activation of the IGF1 receptor maintains  $\beta$ -cell mass, by increasing proliferation and reducing apoptosis (Leibiger et al. 2008). IGF1-R signaling pathway mediates the activation of the insulin receptor substrates 1 and 2 (IRS1, IRS2) and the phosphatidylinositol 3-kinase (PI3K). The latter, in turn, targets the transcription factor PDX-1 (pancreatic and duodenal homeobox factor 1) to modulate  $\beta$ -cell proliferation and differentiation (Leibiger et al. 2001; Muller et al., 2006; Wu et al. 1999). The long-term effect on insulin secretion, however, is still unclear and controversial hypotheses have been proposed so far.
- b) *short term insulin action* is mediated by activation of the InsR and IRS1 on  $\beta$  cells. The resulting cascade of signal transduction leads to increased  $Ca^{2+}$  flow which promotes insulin granules exocytosis (Aspinwall et

al. 2000). Alternatively, activation of the insulin signaling can directly promote exocytosis via AKT (Bernal-Mizrachi et al. 2004). Paradoxically, activation of InsR may also inhibit insulin secretion, a reaction mediated by activation of the PI3-kinase, increased PI(3,4,5)P3 levels and activation of ATP-gated K<sup>+</sup>-channels.(Spanswick et al. 2000). Consequently, also short-term effects of insulin on its own secretion are complex and appear to be modified, depending on the intracellular metabolic state (Swanson et al., 1997)

The InsR receptors are abundantly expressed even in pancreatic  $\alpha$ -cells, at levels similar to those found in the liver, the main target of insulin action. Activation of InsR in  $\alpha$ -cells inhibits glucagon release, a mechanism mediated by activation of PI3-kinase, opening of ATP-gated K<sup>+</sup>-channels and membrane hyper-polarization (Franklin et al., 2005; Leung et al. 2006). Part of the inhibitory effect is mediated also by activation of GABA-A receptor expressed on  $\alpha$ -cell plasma membrane. Indeed, GABA is co-released together with insulin and, by acting on GABA-A receptor, mediates the influx of chloride ions and reduces cell excitability (Xu et al. 2006). Finally, also Zn<sup>++</sup>, which is co-released together with insulin and GABA, can affect glucagon secretion, although the direction of this modulation (inhibition vs stimulation) is specie-specific (inhibition in rodent model, activation in human islets) (Cooperberg and Cryer 2010).

**GLUCAGON:** also glucagon receptors (GlucR) have been identified on  $\alpha$  and  $\beta$  cell membranes (Ahren 2009; Gromada et al. 2007), thus indicating that the endocrine hormone exerts also autocrine and paracrine effects. In rodents and humans, GlucR is coupled to an eteromeric G<sub>s</sub> protein that stimulates adenylate cyclase and increases the cAMP production (Ahren 2009). This in turn leads to protein kinase A (PKA) activation and Ca<sup>2+</sup> dependent exocytosis of glucagon reserve granules (Gromada et al. 2007). Transgenic mice lacking the GlucR showed  $\alpha$ -cells hyperplasia, indicative of a role of this hormone in the autocrine regulation of  $\alpha$ -cell proliferation.

**SOMATOSTATIN:** is produced by  $\delta$  cells and is able to inhibit the secretion of both insulin and glucagon (Ahren 2009) via three mechanisms: 1) the activation of K<sup>+</sup> channels in  $\alpha$  cell that leads to hyper-polarization of the plasma membrane and inhibition of glucagon secretion; 2) the activation of a G<sub>i</sub> protein and calcineurin which inhibits the fusion of secretory granules with the plasma membrane and 3) the inhibition of adenylate cyclase in  $\alpha$  cells. The resulting decreased cytosolic cAMP concentrations reduce hormones secretion.

Five different somatostatin receptors (SSTR1-5) have been identified (Gromada et al. 2007; Quesada et al. 2008);  $\alpha$ -cells mainly express the SSTR2 isoform, while  $\beta$ -cells express substantially SSTR1 and SSTR5 (Gromada et al. 2007; Quesada et al. 2008). In line with these findings, SSTR2 specific agonists significantly reduce glucagon secretion in both mouse and rat islets, without effects on insulin secretion (Rossowski and Coy 1994;

Strowski et al. 2006). Consequently, selective agonists of different SSTR receptors may be used in the treatment of hyperglycaemia and hyperglucagonemia in fasting state.

**GHRELIN:** initially described as a growth hormone related peptide, it is now clear that ghrelin is abundantly released by the stomach during the meal (Kojima et al. 1999). More recently, its expression has been detected also in the endocrine pancreas, in a new class of cells called islets ghrelin-secreting cells or  $\epsilon$ -cells (Ahren 2009). Ghrelin receptors (GHSR) were found in  $\alpha$  and  $\beta$  cells. The release of ghrelin in the islets microenvironment leads the inhibition of insulin secretion, an effect probably mediated by the GHSR receptor associated  $G_i$  protein. The signal cascade triggered by  $G_i$  protein activation induces the opening of voltage-gated  $K^+$ -channels and inhibition of calcium influx in the cytosol (Ahren 2009). Conflicting results have been obtained regarding the acute effects of ghrelin on glucagon secretion (Gromada et al.2007), consequently, the ghrelin effects on glucagon secretion from  $\alpha$  cells remain still unexplored.

The long-term stimulation with ghrelin induces in the islets the up-regulation of the UCP2 protein (uncoupling protein 2) while the ablation of the ghrelin gene in the ob / ob mice leads to a reduction of UCP2 expression. Because the UCP2 protein is responsible for the uncoupling of the mitochondrial oxidation with ATP synthesis, the long-term metabolic effects of ghrelin are probably mediated by changes in the UCP2 expression (Sun et al., 2006).

**INCRETINS:** are released by the intestine following food ingestion and stimulate glucose-induced insulin secretion (GSIS). The most important are the glucagon-like peptide-1 (GLP-1) and glucose-dependent-insulinotropic-polypeptide (GIP) (Meier and Nauck 2006). The GLP1 and GIP receptors expression was confirmed in the pancreatic  $\beta$  cells (Ahren 2009). They are coupled to a stimulatory  $G_s$  protein whose activation results in the increase of cAMP, a potent activator of insulin secretion. Interestingly, long term effects of incretins hormones cause a reduction of  $\beta$  cells apoptosis and an increase in their proliferation, probably through activation of PKB and the PDX-1 transcription factor (Ahren 2009). In animal models of obesity and diabetes, the GLP1 and GIP signalling are altered especially in T2D. Therefore they represent a potential therapeutic target (Meier and Nauck 2006). In  $\alpha$ -cells the effects of the two hormones are different: the GIP stimulates the secretion of glucagon while GLP1 seems to suppress it, although the molecular mechanisms at the basis of this inhibition are still unknown (Meier and Nauck 2006). The expression of the GLP1-R mRNA was observed in subpopulations of  $\alpha$  cells derived from rats (Heller et al. 1997) but, in contrast it was not detected the mature protein or its transcript (Moens et al. 1996). This suggests that inhibition of  $\alpha$  cell from the GLP1 probably occurs through an indirect mechanism.

### **Paracrine regulation by NEUROPEPTIDE in islets of Langerhans**

Nerve endings of the sympathetic, parasympathetic and sensory types innervate islet cells.

- The parasympathetic neuropeptides released in the islets of Langerhans are the pituitary adenylate cyclase activating polypeptide (PACAP), vasoactive intestinal polypeptide (VIP) and gastrin releasing peptide (GRP) (Ahren 2000). They are released after vagal stimulation and induce insulin and glucagon release.

- The most important sympathetic neuropeptides is the neuropeptide Y (NPY) which inhibits insulin secretion in vivo and in vitro (Ahren 2000) through activation of its receptor, expressed on  $\beta$ -cells. NPY-R activation leads to inhibition of the adenylate cyclase and cAMP reduction. Conversely, NPY stimulates  $\alpha$ -cells to release glucagon by a yet unknown mechanism (Ahren 2000).

-The islets are also characterized by sensory innervations. These terminals release peptides in the islets microenvironment such as CGRP (calcitonin-gene-related peptide) and substance P (Ahren 2000). The CGRP inhibits the insulin secretion, while substance P shows both stimulatory and inhibitory effects (Ahren 2000).

### **Paracrine regulation by NEUROTRANSMITTERS: in islets of Langerhans**

Neurotransmitters are another class of paracrine and autocrine signals within the islet. All neurotransmitters present in the CNS have been identified in human islets of Langerhans. They are selectively synthesized, packaged in synaptic-like micro vesicles (SLMV) present in the endocrine cells themselves and released under stimulated conditions. As in the nervous system, neurotransmitters are specifically segregated in different endocrine cell types within the islet: glutamate and acetylcholine are released by  $\alpha$ -cells; conversely,  $\beta$ -cells release GABA, ATP, serotonin and dopamine (Hille 2001; Gonzales 2004; Di Cairano 2014).

They are molecules with low molecular weight and can rapidly diffuse in the intracellular spaces, where they can directly modulate the membrane potential (onset time  $<1$  sec; Hille 2001).

**ACETYLCHOLINE**: acetylcholine (ACh) is known as a parasympathetic neurotransmitter within the islets, but it is also a signaling molecule produced by human  $\alpha$ -cells. Studies performed in the last years have shown that  $\alpha$ -cells express the enzyme Choline acetyltransferase (ChAT) for its synthesis and the selective vesicular transporter VACHT for its storage in vesicular compartments, proving that Acetylcholine is actually synthesized and stored in human  $\alpha$ -cells and does not simply derive from nerve terminals (Rodriguez-Diaz et al., 2011b).

ACh is stored in vesicles that do not contain glucagon. ACh immunoreactivity has been found also in a cohort of  $\delta$ -cells, although the significance of its expression deserves further investigations (Rodriguez-Diaz et al., 2011b).

$\alpha$ -cells release ACh during low glucose conditions or upon stimulation of glutamate receptors with Kainate (Rodriguez-Diaz et al., 2011b). The released ACh reaches concentration of 100-300 nM that is able to activate

nicotinic and muscarinic receptors expressed on the plasma membrane of all endocrine cell populations of the islet (Iismaa et al., 2000; Yoshikawa et al., 2005). In humans, metabotropic muscarinic receptors are generally implicated in the increase of hormone release, since ACh is able to stimulate insulin-secreting  $\beta$ -cells via the M3 and M5 receptors, somatostatin-secreting  $\delta$ -cells via the M1 receptor and glucagon-secreting  $\alpha$ -cells via the M3 receptor (Rodriguez-Diaz et al., 2011b; Molina et al., 2014). Interestingly, M3 receptor expression is down regulated by high glucose treatment in mouse and human islets, thus suggesting that impaired glucose sensing and insulin secretion observed in diabetes may also be due to alteration of paracrine signaling systems (Hauge-Evans et al., 2014).

So far, no studies have directly addressed the role of ACh in the control of cell proliferation and survival; however, as in other systems, ACh may act as a trophic factor to promote  $\beta$ -cell survival (Wessler and Kirkpatrick, 2012).

**SEROTONIN:** serotonin (5-HT) is a biogenic amine synthesized by the central, peripheral and enteric nervous system. In the pancreas it is released by neuronal projections and modulates exocrine secretion (Zhang et al., 2013). More recently, a role of this neurotransmitter as paracrine signal in the endocrine pancreas has been proposed. In particular, serotonin is synthesized, stored in insulin granules and secreted by  $\beta$ -cells (Ekholm et al., 1971).

5-HT is synthesized from tryptophan in two steps promoted by tryptophan hydroxylase (TPH), which represents the rate limiting step, followed by aromatic L-aminoacid decarboxylase.  $\beta$ -cells express TPH (Ohta et al., 2011) and, interestingly, TPH deficiency in mice has been assimilated to Maturity Onset Diabetes of the Young (MODY) (Paulmann et al., 2009); further studies are needed to clarify this relationship. Once synthesized, 5-HT is stored in LDCVs (large dense core vesicles) by VMAT2 together with insulin, ATP and GABA.

The 5-HT receptor 2C (5-HT<sub>2C</sub>R) is expressed in mice islets and its activation inhibits insulin release. Interestingly, this receptor is over-expressed in diabetic mouse models (Zhang et al., 2013).

Intra-islet serotonin has been recently implicated in the expansion of  $\beta$ -cell mass during conditions of higher insulin demand such as pregnancy. Indeed, under the action of lactogenic hormones, the production of serotonin increases in the islet and drives, in a paracrine-autocrine fashion,  $\beta$ -cell cell replication; an effect mediated by the 5-HT receptor 2B (Oh et al., 2015). The study has been carried out in mice and it is not known whether similar mechanisms operate in humans. If that turns out to be the case, serotonin agonists may provide a therapeutic approach to improve the outcome of gestational diabetes, and more in general, to control  $\beta$ -cell expansion *in vitro*.

**DOPAMINE:** the presence of dopamine (DA) has been documented also within the pancreas: beside nerve terminals and the exocrine tissue of the pancreas, endocrine cells within the islets are dopamine sources (Mezey et al., 1996; Ustione and Piston, 2012).

Rodent and human islet tissues express a variety of molecules associated with the biosynthesis, storage, degradation and response to DA, thus suggesting a role of the neurotransmitter in islet paracrinology. The acid decarboxylase necessary for *the novo* synthesis of DA and monoamine oxidase activities have been identified in mouse islet homogenates (Lindström P. 1986; Lundquist et al., 1991) and the vesicular monoamine transporter type 2 (VMAT2), important for the neurotransmitter accumulation in vesicular compartments, is expressed in rodent islets and in human  $\beta$ -cells (Raffo et al., 2008). Once stored, DA is co-released into the extracellular space with insulin, upon glucose stimulation and can reach a concentration of approximately 7  $\mu$ M per islet (Ustione and Piston, 2012). Morphological and functional studies in human reveal the expression of the D1 receptors in  $\beta$ -cells, D2 in  $\alpha$ -,  $\beta$ -  $\delta$ - and PP cells, D4 in  $\beta$ - and PP cells and D5 in  $\delta$ -cells (Simpson et al., 2012; Zhang et al., 2015).

The dopaminergic signal is switched off by the plasma membrane dopamine transporter (DAT) which is expressed in mouse islets (Ustione and Piston 2012).

Within the islet, dopamine controls a negative feedback circuit that regulates insulin secretion in the islet (Shankar et al., 2006, Simpson et al., 2012). Indeed, the neurotransmitter inhibits glucose-stimulated insulin secretion in both  $\beta$ -cell lines and isolated islets from rodents and humans. This inhibition correlates with a reduction in the frequency of intracellular  $Ca^{2+}$  oscillations and it is mainly mediated by the D2 receptor (Rubí et al. 2005; Shankar et al., 2006; Simpson et al., 2012).

Interestingly, in humans, the rs1800497 variant in the coding region of the D2 is associated with increased susceptibility to T2D in women (Guigas et al., 2014), thus indicating that the D2 receptor may represent an interesting pharmacological target for diabetes treatment.

The dopaminergic signaling has been recently involved in the control of  $\beta$ -cell viability; following DA treatment,  $\beta$ -cell proliferation rate is decreased and apoptosis increased in rat islets, suggesting another opportunity for pharmacological intervention (Garcia Barrado et al., 2015).

Although the role of DA receptors and transporters in islet physiology has not yet completely clarified, drugs affecting the dopaminergic signaling are already used in the T2D treatment. In particular, the D2 agonist bromocriptine has been approved by the U.S. Food and Drug Administration (FDA) for the treatment of T2D (DeFronzo 2011). Bromocriptine administration improves glycemic control and glucose tolerance in obese

patients with T2D. However, part of the observed effects are central and peripheral nervous system-driven (Guigas et al., 2014).

**ATP:** besides the brain, purinergic signaling is also important in islets of Langerhans where it exerts both intracellular and extracellular functions in pancreatic  $\beta$ -cells. Adenosine triphosphate (ATP), deriving from glucose metabolism in the cytosol, regulates the ATP/ADP ratio which controls  $\beta$ -cell excitability. ATP is stored in insulin containing secretory granules of  $\beta$ -cells, at a concentration of about 5 mM (MacDonald et al., 2006). Low glucose concentrations favor the so-called “kiss-and-run” exocytosis (transient formation of a fusion pore between the secretory granule and the plasma membrane) which causes release of the small molecular weight ATP, but not insulin secretion. High glucose concentrations induce the complete vesicle fusion with the plasma membrane and the release of both molecules (MacDonald et al., 2006).

When released, ATP can act on selective ionotropic (P2X) and metabotropic (P2Y) purinergic receptors. Human  $\beta$ -cells express the ionotropic P2X3, P2X5, P2X7 and the metabotropic P2Y11 and P2Y12, while  $\alpha$ -cells express P2X4, P2Y1 and P2Y6 (for a review see Burnstock and Novak, 2012).

Due to the heterogeneity of purinergic receptors expressed in the islets, the observed effects of ATP on hormone release are various and species-specific.

In humans, ATP mediates the increase in basal and stimulated insulin release via P2X receptors activation (Fernandez-Alvarez et al., 2001; Jacques-Silva et al., 2010). In mice ATP decreases insulin release via activation of P2Y receptors, while in rat, both inhibition and stimulation have been detected upon receptor activation (Petit et al., 2009).

As regards glucagon release, both stimulation (via P2Y6) and inhibition (via P2Y1) of secretion have been observed (Burnstock and Novak, 2012).

As described for the other neurotransmitters, purinergic signal not only modulates hormone release but also controls  $\beta$ -cell mass in endocrine pancreas. In particular, P2Y6 has been shown to prevent  $\beta$ -cell death induced by tumor necrosis factor (TNF) (Balasubramanian et al., 2010); P2X7 is able to regulate  $\beta$ -cell mass and its expression is upregulated in obesity and decreased in diabetes (Glas et al., 2009).

The purinergic system is active also on non-endocrine, islet-resident cells. ATP, by acting on vascular smooth muscle cells, particularly abundant in human islets, can induce vasoconstriction, thus modifying the islet blood flow locally, depending on metabolic demand. ATP can be released by endothelial cells in response to changes in blood flow and hypoxia and in turn may act as autocrine signal to control endothelial cell permeability, proliferation and remodeling (Burnstock, 2008). Finally, the purinergic signaling controls immune cell activation

(Junger, 2011) and allows immune cells to adjust their functional responses locally, based on the extracellular cues provided by the islet environment.

Therefore, we cannot exclude at the moment that part of the effects observed on endocrine cells function and survival may be indirect and mediated by modification of their relationships with the other islet-resident cells.

**GABA:** the  $\gamma$ -aminobutyric acid, is the major inhibitory neurotransmitter in the central nervous system and it is also an autocrine and paracrine signal in islets of Langerhans.

In rodents, it is produced mainly in  $\beta$ -cells which express huge amount of Glutamic Acid Decarboxylase (GAD) and GABA transaminase, the enzymes responsible for conversion of glutamate into GABA and its catabolism (Reetz et al., 1991). In  $\beta$ -cells, GABA is stored in small synaptic-like microvesicles (SLMV) and in a subpopulation of insulin secretory granules (Reetz et al., 1991; Braun et al., 2004 and 2007). The vesicular transporter VGAT, identified in rat but not human islets, is responsible for GABA accumulation in vesicles (Thomas-Reetz et al., 1993). VGAT has also been detected in glucagon-containing secretory granules in  $\alpha$ -cells (Hayashi et al., 2003b). Conversely, in humans, GABA is present in  $\alpha$ -,  $\beta$ - and  $\delta$ -cells that express high levels of GAD65 (Braun et al., 2010).

GABA concentration in human islets has been proved to be 1.5 nmol/ $\mu$ g DNA (Wang et al., 2005).

The GABA effects within the islet are mediated by ionotropic (GABA-A) and metabotropic (GABA-B) receptors, expressed on the plasma membrane of all islet cell populations. GABA-A activation increases the  $\text{Cl}^-$  conductance, but the direction of  $\text{Cl}^-$  currents (inwards vs outwards) and the effect on hormone secretion depend on the  $\text{Cl}^-$  equilibrium potential (which is cell-specific) and membrane potential which is influenced by glucose concentrations. Therefore, GABA-A activation stimulates somatostatin release from human  $\delta$ -cells, but inhibits glucagon release from  $\alpha$ -cells (Rorsman et al., 1989). In human  $\beta$ -cells, GABA has opposite effects depending on glucose concentrations: at low glucose concentrations, GABA facilitates insulin release, while at high glucose GABA inhibits insulin release (Braun et al., 2010).

In rodent  $\beta$ -cells, GABA-B receptors activation reduces insulin secretion; however, at present it is not known how it affects  $\alpha$ -cells (Bonaventura et al., 2008; Ligon et al., 2007).

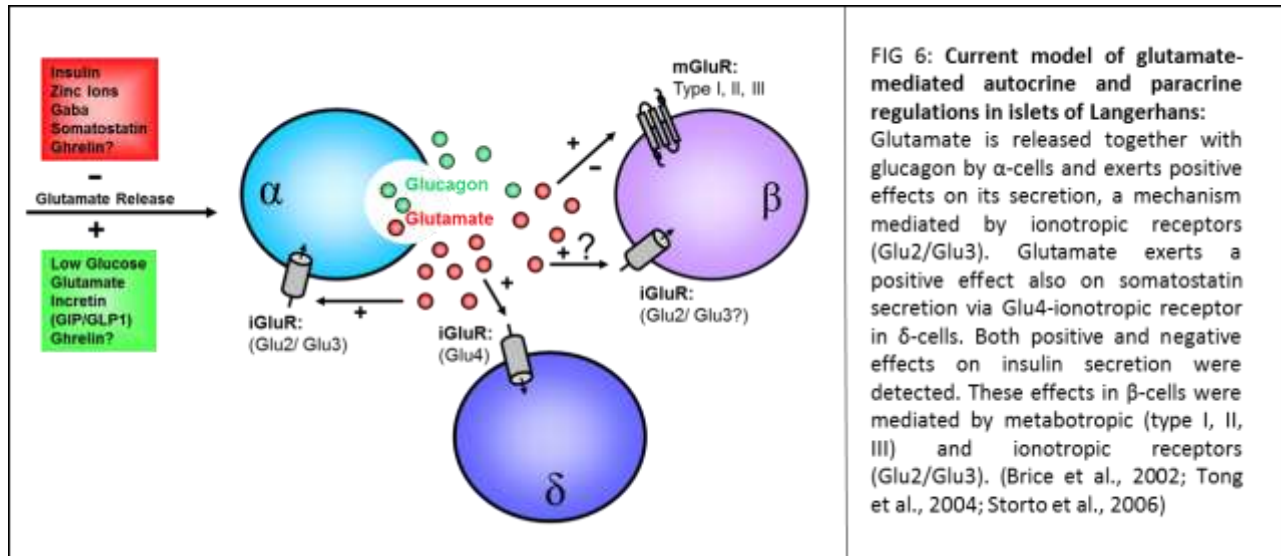
A role of GABA in the control of  $\beta$ -cell viability has emerged in the last years. Activation of GABA-B receptors decreases apoptosis and increases  $\beta$ -cells viability, leading to an overall increased  $\beta$ -cell mass (Ligon et al., 2007). GABA-A activation enhances  $\beta$ -cell replication in mice and human islets implanted into non-obese diabetic/scid mice. (Tian et al., 2013).

In T1D mouse models, GABA prevents and reverses the disease by exerting protective and regenerative effects on islet  $\beta$ -cells (Soltani et al., 2011). GABA also showed anti-inflammatory effects in high-fat-diet induced obesity in mice (Tian et al., 2013). If these effects will be confirmed in humans, GABA administration would represent a promising strategy to treat diabetes.

In the next section will detail the role of glutamate as a paracrine/autocrine messenger in the islets of Langerhans.

### 3) The Glutamate signal in islets of Langerhans

In the endocrine pancreas, the presence of glutamate as a signalling molecule is well established (Hayashi et al., 2003) and glutamate-mediated paracrine-like signalling has been proposed as a novel regulatory mechanism of islet hormone secretion (Figure 6; Moriyama and Hayashi, 2003; Bertrand et al., 1995).



Islets have all required components for glutamate transmission:

- i) Enzymes and vesicular glutamate transporters for glutamate synthesis and storage in vesicles (Storage System),
- ii) Expression of ionotropic and metabotropic receptors (Receptors System),
- iii) Expression of glutamate transporters responsible for the glutamate clearance (Clearance system)

#### I) GLUTAMATE STORAGE SYSTEM in the islets

The principal source of glutamate in the islet is  $\alpha$ -cells, where the neurotransmitter is stored in large dense-core vesicles containing glucagon. L-glutamate is co-stored and co-secreted with glucagon in alpha cells and the stoichiometric amounts of glutamate and glucagon are 2000:1 (molar ratio)(Bai *et al.*, 2003). This implies that L-glutamate is co-secreted with glucagon when blood glucose levels decrease or following stimulation of  $\beta$ -adrenergic receptors. Glutamate in alpha cells might originate not only from intracellular synthesis by means of glutaminase, but it has been proposed that it can also derive by uptake of plasma L-glutamate through a sodium dependent glutamate transporter not yet identified (Weaver *et al.*, 1998).

The vesicular glutamate transporters VGLUT1 and VGLUT2 (Hayashi et al., 2003a; Cabrera et al., 2008), identical to those expressed in neurons, are responsible for the neurotransmitter accumulation in the granules.

In low glucose the reported glutamate secretion per islet per second is 15 fmol. This means that in the narrow extracellular space, glutamate concentration would rise to 3 mM in 1 sec, a concentration relevant for receptor activation.

The accumulation of glutamate in insulin granules is controversial. VGLUT1-3 transporters have been identified in insulin granules of pancreatic  $\beta$ TC6, RINm5F and INS-1E  $\beta$  cell lines, thus suggesting that glutamate may accumulate within these granules (Bai et al., 2003; Gammelsaeter et al., 2004). Beside to a vesicle-mediated glutamate release, there is evidence supporting the possibility that glutamate may be released in the extracellular space, also via plasma membrane glutamate transporters or exchangers, by uptake reversal (Vetterli et al., 2012).

Some early reports highlight the expression of vesicular glutamate transporters also in F cells and are associated with pancreatic polypeptide-containing secretory granules, suggesting that F cells are also glutamatergic and that pancreatic polypeptides and L-glutamate are co-secreted (Hayashi *et al.*, 2003b). By contrast, neither VGLUT1, 2 nor 3 are expressed in  $\delta$  cells (Moriyama and Hayashi, 2003; Moriyama and Omote 2008).

## **II) GLUTAMATE RECEPTORS SYSTEM in the islets**

Once released, glutamate act on glutamate receptors (Bai et al., 2003, Cabrera et al., 2008) which are expressed on the plasma membrane of all endocrine cells of the islet. Several independent lines of evidence indicate expression of both ionotropic and metabotropic glutamate receptors (iGluRs and mGluRs) in pancreatic islets, but as reported in the summary table (Figure 7) several controversies emerged from literature studies and species-specific differences in subtype expression and localization have been detected.

Receptors	Cells / Species	Method	Effects	Refs
GluR2, GluR3, KA2, NR1, NR2D (no other subunits were identified)	MIN6	RT-PCR	AMPA-, kainate- and NMDA-evoked currents and increase in the intracellular concentration of Ca <sup>2+</sup>	Gonoi et al., 1994
GluR2, KA1, KA2, NR1, NR2D	RIN	RT-PCR	AMPA-, kainate- and NMDA-evoked currents and increase in the intracellular concentration of Ca <sup>2+</sup>	Inagaki et al., 1995
GluR2, GluR3, GluR6, GluR7, KA2, NR1, NR2D	Rat islets	RT-PCR	AMPA-, kainate- and NMDA-evoked currents and increase in the intracellular concentration of Ca <sup>2+</sup>	Inagaki et al., 1995
NR1 and KA2 (no GluR1)	Rat islets, MIN6, RIN, HIT	IB	Specific AMPA and kainate binding in MIN6 and RIN membranes	Molnar et al., 1995
GluR2 and GluR3 (no GluR1,4 or NR1)	α-, β- and F-cells (not in δ-cells)	IHC	L-Glutamate-, AMPA- and kainate-evoked currents	Weaver, et al. 1996
GluR6 and GluR7 (no GluR1,4 or NR1)	α-cells, but not in β-, δ- or F-cells,	IHC	L-Glutamate-, AMPA- and kainate-evoked currents	Weaver, et al. 1996
KA2 (no GluR1,4 or NR1)	δ-cells	IHC	L-Glutamate-, AMPA- and kainate-evoked currents	Weaver, et al. 1996
GluR2 and GluR3	Rat islets	IB	L-Glutamate-, AMPA- and kainate-evoked currents	Weaver, et al. 1996
GluR6, GluR7 and KA2	αTC6	IB	L-Glutamate-, AMPA- and kainate-evoked currents	Weaver, et al. 1996
NR1, low level of NR2A, NR2B, GluR2, very low level of both GluR3 and GluR4	MIN6	RT-PCR	AMPA- and kainate-evoked increase in the intracellular concentration of Ca <sup>2+</sup> ; no response to NMDA; stimulation by cyclothiazide (CTZ) <sup>b</sup>	Morley, et al. 2000
GluR2 and GluR3 (no GluR1 and GluR4)	GK-P3	IB	L-Glutamate-, AMPA- and kainate-evoked currents and an increase in the intracellular concentration of Ca <sup>2+</sup> ; stimulation by CTZ	Weaver, et al. 1998
No mGlu receptors were identified	MIN6	IB, RT-PCR	-	Wang, et al., 1997
mGlu <sub>8</sub> receptor (only class III mGlu receptors were examined)	α-cells	RT-PCR, IB, IHC	-	Tong et al., 2002
mGlu <sub>2</sub> receptor	MIN6	RT-PCR	-	Brice, et al. 2002
mGlu <sub>3</sub> and mGlu <sub>5</sub> receptors	Human and rat islets, αTC6, RIN, MIN6	RT-PCR	-	Brice, et al. 2002
mGlu <sub>4</sub> receptor	Rat islets	RT-PCR	-	Brice, et al. 2002
mGlu <sub>8</sub> receptor	Rat islets, RIN, MIN6	RT-PCR	-	Brice, et al. 2002
mGlu <sub>2</sub> , mGlu <sub>3</sub> and mGlu <sub>5</sub> receptors	Human and rat islets	IB	-	Brice, et al. 2002

FIG. 7 Summary table of glutamate receptors identified in the endocrine pancreas. Abbreviations: CNQX, 6-cyano-7-nitroquinoxaline-2,3-dione; EAAT2, excitatory amino acid transporter 2; GluR1-4, AMPA receptor subunits; GluR5-7, kainate receptor subunits; IB, immunoblotting; IHC, immunohistochemistry; KA1,2, kainate receptor subunits; mGlu receptor, metabotropic glutamate receptor; NR1,2A,2B,2D, NMDA receptor subunits; RT-PCR, reverse transcriptase-polymerase chain reaction; VGLUT, vesicular glutamate transporter.

<sup>b</sup> CTZ potentiates neuronal AMPA receptors by blocking rapid desensitization

Among iGluRs, AMPA are expressed and functional in alpha and beta cells (Gonoi *et al.*, 1999; Inagaki *et al.*, 1995; Molnar *et al.*, 1995; Weaver *et al.*, 1996; Morley *et al.*, 2000; Weaver *et al.*, 1998; Bertrand *et al.*, 1992). On the other hand, the expression of functional kainate receptors is negligible, even though kainate currents similar to those reported in neuronal cells have been measured in β-cells (Weaver *et al.*, 1996). mRNA

transcripts for NMDA receptors have been detected in rat islets and MIN6 cells in islets, although neither NMDA receptor subunits expression, nor NMDA-evoked ion currents have been observed, thus raising the question whether functional NMDA receptors are effectively active in these models.

The modulation of hormone release is the main effect of glutamate on cells of the islet. Due to the heterogeneity of glutamate receptors, the reported effects of glutamate on hormone secretion are diverse and species-specific. In general, it is thought that activation of ionotropic receptors increases hormone release via membrane depolarization, activation of voltage-gated  $\text{Ca}^{2+}$  channels and  $\text{Ca}^{2+}$ -triggered secretory granule exocytosis.

In human  $\alpha$ -cells, glutamate stimulates glucagon release via ionotropic AMPA/kainate receptors (Bertrand et al., 1993; Cabrera et al., 2008; Moriyama and Hayashi, 2003). As glutamate is released together with glucagon, this represents an autocrine positive feedback, which further sustains glucagon release in low glucose concentrations (Cabrera et al., 2008).

In rodent  $\beta$ -cells and islets, activation of ionotropic (AMPA/kainate subtype) and metabotropic receptors mediates insulin release (Bertrand et al., 1995; Storto et al., 2006). This pathway is unlikely in human cells in which ionotropic receptors localize in intracellular compartments; hence as a result, glutamate does not influence insulin release (Cabrera et al., 2008; Cho et al., 2010; Di Cairano et al., 2011).

$\delta$ -cells express a novel variant of ionotropic glutamate receptor (GluR4c-flip), its activation promotes somatostatin release (Muroyama et al., 2004).

Also mGlu receptors have been reported to be expressed in islet of Langerhans and in endocrine cell lines. Similarly to iGluRs, they modulate hormone secretions although both, stimulation and inhibition of hormone release have been detected, depending on the metabotropic receptor subtype expressed. Group I and II agonists increase the release of insulin in the presence of glucose at low concentration, whereas group III agonists inhibit insulin release at high glucose concentrations (Brice *et al.*, 2002). In rodent  $\alpha$ -cell lines and islets, activation of class III metabotropic receptors inhibits glucagon release (Uehara et al., 2004; Di Cairano et al., 2011; Tong *et al.*, 2002).

### III) GLUTAMATE CLEARANCE SYSTEM in the islets

The glutamate signal in the CNS is spatially and temporally controlled by plasma membrane glutamate transporters that regulate the extracellular glutamate concentrations by transporting glutamate inside the cells.

Similarly, in the islet, the cellular response to glutamate may be controlled by regulating the amino acid transport across the plasma membrane. In particular, glutamate flux through transporters may act as a modulator of hormone secretion by increasing the intracellular amino acid content or by controlling the extracellular amino acid concentration and therefore glutamate receptors activation. In the islet, the extracellular L-glutamate is controlled by high-affinity glutamate/aspartate (excitatory amino acid transporter or EAATs) of the solute carrier family 1 (SLC1A) similar to those described in the CNS (Di Cairano et al., 2011). The SLC1 family, includes five different transporter subtypes: glutamate aspartate transporter (GLAST/EAAT1), glutamate transporter 1 (GLT1/EAAT2), excitatory amino acid carrier (EAAC1/EAAT3), EAAT4 and EAAT5 (Arriza et al., 1997; Arriza et al., 1994; Kanai et al., 2003; Robinson and Dowd 1997) and two neutral amino acid transporter (ASCT1 and ASCT2). They share 40% to 65% of sequence identity and are characterized by a common structure: 8 transmembrane domains and two re-entrant hairpin loops (HP1 and HP2), that partially span the phospholipidic bilayer. The structure has been confirmed by the crystallised prokaryotic analogous (Yernool *et al.*, 2004). The 8<sup>th</sup> transmembrane domain and the two re-entrant loops are the sodium and substrate binding sites, respectively (Figure 8; Torres and Amara, 2007).

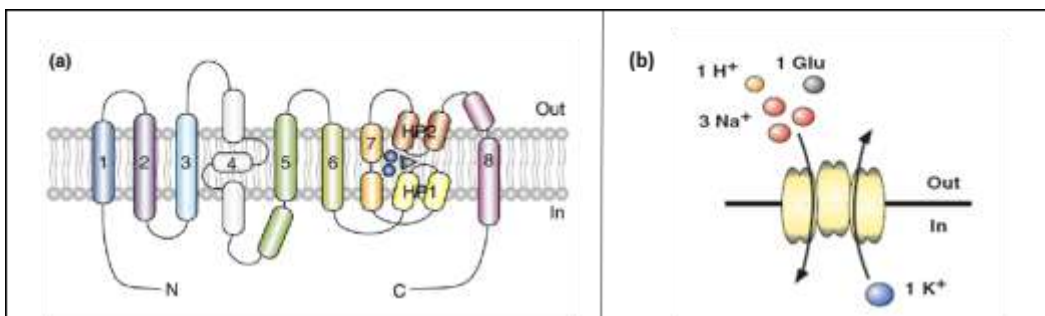


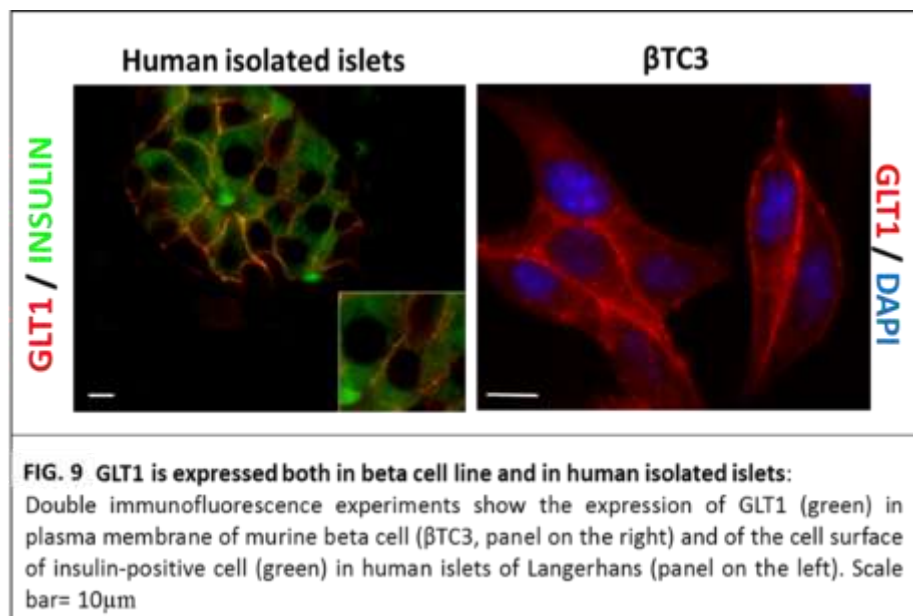
**FIG 8 : Membrane structure and surface transport activity of GLT1.**

(a) draft representation of the complex membrane structure of the GLT1/EAAT2 transporter. There are 8 transmembrane domains and two hairpin loop responsible for the interaction with substrates. The C and the N terminals are both cytosolic (Torres and Amara, 2007).

(b) GLT1 is a Na<sup>+</sup>/K<sup>+</sup>-dependent glutamate transporter. It is an electrogenic transporter, as it couples the transport of the amino acids with the translocation of a net positive charge across the membrane. This transporter utilizes the free energy stored by the antiport of three Na<sup>+</sup> ions (internalized into the cell) and an ion K<sup>+</sup> (which passes into the extracellular environment), for driving a molecule of glutamate (Glu) together with a proton inside the cell (Gonzales and Robinson, 2004).

Endocrine cells of the pancreas express ASTC2 (unpublished data), a neutral amino acid transporter that exhibits the properties of the classical Na<sup>+</sup>-dependent amino acid transport and it is able to transport

glutamate, even though with low affinity, in conditions of low pH (Kanai et al., 2003; Pochini et al., 2014). The key regulator of the extracellular glutamate clearance in the islet of Langerhans is the glutamate transporter 1 or excitatory amino acid transporter 2 (GLT1/EAAT2; Figure 8). GLT1 uses the free energy, stored by the antiporter of three sodium ions ( $3\text{Na}^+$ ) (internalized into the cell) and a potassium ion ( $1\text{K}^+$ , that is released into the extracellular environment), for transporting one molecule of glutamate (Glu), together with a proton ( $1\text{H}^+$ ) inside the cell (Figure 8). It is therefore a  $\text{Na}^+$ -dependent transporter and an electrogenic transporter because it couples the amino acid transport with the influx of electric current. The affinity of this transporter for glutamate is in the range of the blood glutamate concentrations (50-100  $\mu\text{M}$ ), thus its activity and density can finely tune glutamate concentrations within the narrow intercellular spaces of the islet.



GLT1 is the only high affinity glutamate transporter expressed in the islets and localizes specifically to the  $\beta$ -cell plasma membrane (Figure 9). Pharmacological blockade or RNA interference experiments show that GLT1 is the main regulator of the glutamate clearance in isolated islets. In fact, selective GLT1 inhibition with DHK almost completely blocks the uptake of glutamate in isolated human islets and increases the extracellular glutamate concentration.

Although data are somewhat controversial, a recognized effect of glutamate is to modulate the release of insulin, glucagon and somatostatin induced by changes in glucose concentration (Cabrera et al., 2008; Caicedo et al., 2014; Di Cairano et al., 2011; Broun et al., 2010). Similarly, GLT1 by regulating the extracellular glutamate concentration may modulate hormone secretion. In previous experiments, we found that glutamate decreased the physiological release of glucagon in response to an acute fall in glucose concentrations, whereas glutamate

did not potentiate insulin secretion in response to an acute glucose change as previously reported by others (Di Cairano et al., 2010; Brice et al., 2002; ; Tong et al., 2004; Storto et al., 2006). Similar results were obtained in the presence of DHK, suggesting that GLT1 may be involved in the regulation of hormone secretion.

## **The goal of the PhD project**

Given the key role of this glutamate transporter in modulating hormone release the project purpose was to evaluate the modification of GLT1 expression and activity in physiological conditions (Chapter1) and to evaluate the possible pathological implications of GLT1 dysfunction (Chapter2 and 3).

Since the beta cells are physiologically exposed to rapid changes in extracellular glucose level, which affects the hormones secretion, we evaluated in mouse beta cell line ( $\beta$ TC3) the effect of acute exposure (30 minutes) to low and high glucose concentrations on GLT1 activity and localization (Chapter1). In addition, we focused on intracellular kinases, which are regulated by modification of glucose metabolism and are involved in the regulation of membrane proteins trafficking. In particular, we evaluated the role of PKC and PI3K, which are normally active in conditions of hyperglycaemia and are induced following the activation of the insulin receptor and the role of AMPK, which is activated by hypoglycaemic conditions.

Given the key role of GLT1 in preserving  $\beta$ -cell viability, in chapter 2 we monitored the effects of long-term treatment (3 days) with high extracellular glucose concentrations (chronic hyperglycaemia) or inflammatory cytokines on GLT1 activity and localization.

Finally, in Chapter 3 we tested the possibility that GLT1 may be the target antigens of cytotoxic islet cell surface autoantibodies described in sera of Type 1 Diabetes Mellitus patients (T1DM).

# CHAPTER I

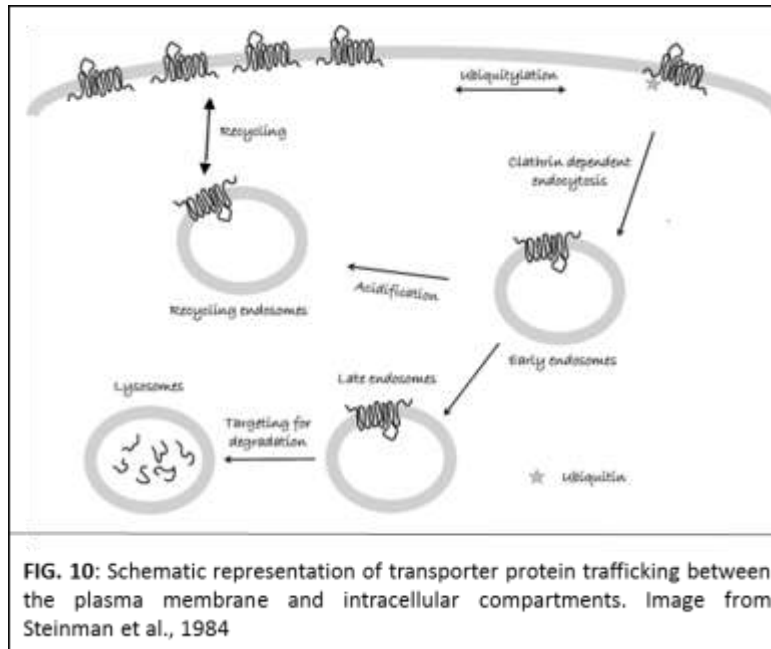
## **Short-term regulation of GLT1 membrane activity and localization**

Early studies suggested that the activity of glutamate transporters can be fine tuned by a number of different signaling pathways. In the past five years, several groups have provided compelling evidence that changing the cell surface availability of these transporters contributes to this fine tuning. This regulated trafficking can result in rapid (within minutes) increases or decreases in the plasma membrane expression of these transporters and is independent of transcriptional or translational control mechanisms. Many signaling molecules, including protein kinase C (PKC), tyrosine kinase, phosphatidylinositol 3-kinase (PI3-K), and protein phosphatase, regulate the transporters of different neurotransmitters (for reviews, see Danbolt, 2001, [González and Robinson, 2003](#) and [Beart and O'Shea, 2007](#)). Interestingly, these same signalling pathways are activated by modification of plasma glucose concentrations.

In this chapter we explore the possibility that physiological modifications in the extracellular glucose concentration may modify GLT1 activity/expression, and we investigate the molecular mechanism of these modifications.

### ***Dynamic Regulation of glutamate transporter trafficking***

The organization of the plasma membrane is both highly complex and highly dynamic. The modes by which proteins move in the plane of the membrane provide insights into the molecular interactions between these proteins and neighboring membrane proteins, membrane lipids, the underlying cytoskeleton and receptors on cells or other structures in the extracellular environment (Figure 10; Alenghat and Golan, 2013).



The balance between endocytic uptake and recycling on the cell surface controls the composition of the plasma membrane and contributes to different cellular processes, including nutrient uptake and signal transduction (Figure 10; Steinman et al., 1984).

The basic mechanism to transfer proteins between organelles and plasma membrane is mediated by carrier vesicles that continually bud from one membrane and fuse with other and is driven by protein-protein interactions (Bonifacino and Glick, 2004). A fundamental element of membrane traffic is vesicle formation, or budding, that is initiated by the selection and concentration of cargo proteins within membrane subdomains. This occurs through interactions between sorting determinants on cargo proteins and cytosolic coat components that direct cargo to the forming vesicles (Aridor *et al.*, 1996). Protein coats are dynamic structures that are recruited from the cytosol onto donor membrane by small GTPases and they deform flat membranes into round buds, which lead to the release of the coated vesicle.

Vesicular transport within the early secretory pathways is mediated by two types of non-clathrin coated vesicles: COP-I and COP-II (Allan and Balch 1999). COP-I primary acts from the Golgi to the endoplasmic reticulum (ER) and between Golgi cisterna,. COP-II mediates trafficking from the ER to Golgi (Barlowe *et al.*, 1994; Letourneur *et al.*, 1994; Waters *et al.*, 1991).

Clathrin coated vesicles, the first identified (Pearse, 1975), mainly derives from the plasma membrane or the Trans-Golgi network (TGN) and are transported to endosomes (Owen *et al.*, 2004). The main adaptors are proteins of AP2 complex.

Coat recruitment is coupled with the acquisition of SNAREs (SNAP: Soluble N-ethylmaleimide sensitive-factor Attachment Protein Receptors) proteins that direct the vesicles to their target membranes (Söllner *et al.*, 1993). After budding, cargo vesicles are transported to their final destination by diffusion or by motor-mediated transport along a cytoskeletal track. In particular, vesicles interact with microtubules, by means of the so-called “microtubule motors”, dynein and kinesin families (Schroer and Sheetz, 1991; Brown and Stow, 1996). Also the actin cytoskeleton may serve as mechanical element that drives and guides vesicles movement within the cells (Rogers and Gelfand, 1998). In addition, the actin cytoskeleton may directly concur to cell polarity by anchoring proteins in specific plasma membrane domain (Hammerton *et al.*, 1991).

The last step in vesicle-mediated transport is the recognition and fusion of the vesicle with its target membrane, a process that involves the so-called tethering factors and SNAREs. Acting upstream to SNAREs, tethering factors, interacting and working together with coat proteins, mediate the first point of contact of vesicle with the target membrane and the specificity of vesicle targeting.

Tethering factors may couple the recognition of a vesicle to the process of vesicle uncoating and then bring the vesicles in closer contact with its target compartment (Malsam *et al.*, 2005). To date, eight conserved complexes have been identified as crucial for exocytic and endocytic trafficking events (Cai *et al.*, 2007). Tethers can be also Rab effectors and Rab exchange factors. Rabs are small GTPases of the Ras superfamily that continuously cycle between the cytosol and membranes. Rabs act at multiple stages of the exocytic and endocytic pathway and in their GTP-bound form they appear to facilitate the recruitment of tethers to specific locations.

Tethering factors may actively promote SNARE-mediated membrane fusion by stimulating the formation of trans SNARE complexes (Shorter *et al.*, 2002). SNAREs is a family of membrane proteins that are related to three different neuronal proteins: synaptobrevin, syntaxin and SNAP-25. Specific membrane associated SNAREs form a sort of lock and key that is activated by selective recognition among these proteins. A SNARE on a transport vesicle (v-SNARE) pairs with its cognate SNARE-binding partner (t-SNARE) on the appropriate target membrane (Rothman, 1994; Söllner *et al.*, 1993).

Activation of signalling pathway may modify protein trafficking within the cells, by phosphorylating cargo, adaptors, tethering factors and SNARE proteins.

## **PROTEINS INVOLVED IN MEMBRANE TRAFFICKING AND GLUCOSE METABOLISM**

Among the different protein kinases, which are involved in protein trafficking and are regulated by modification of glucose metabolism, we focused on PKC and PI3K, which are normally active in hyperglycaemic conditions and AMPK which is activated by hypoglycaemic conditions.

### **PKC: protein kinase C**

The PKC family plays important roles in many intracellular signaling events, cell growth and differentiation (Buchner 1995; Nishizuka 1984; Nishizuka 1989; Nishizuka 1986; Nishizuka 1988). It is composed of a number of individual isoforms which belong to three distinct categories-conventional, novel and atypical- based upon their structurally distinct N-terminal regulatory domains. The basic PKC structure of the conventional and novel categories is composed of the N-terminal regulatory domains (that contain an autoinhibitory pseudosubstrate domain and two membrane-targeting modules termed C1 and C2) and a highly conserved C-terminal catalytic domain (that contains the C3 and C4 motifs required for ATP/substrate binding and catalytic activity). The "**conventional isoforms**" (cPKCs— $\alpha$ ,  $\beta$ I,  $\beta$ II,  $\gamma$ ) contain two membrane-targeting regions, designated C1 and C2. The C1 domain can bind PMA (or endogenously generated DAG). The interfacing of the C1 region with PMA or DAG promotes PKC binding to membranes (Cho 2001; Hurley and Misra 2000). The C2 domain contains a motif found in many proteins that participate in membrane trafficking and signal transduction. C2 domains of cPKC isoforms bind anionic phospholipids in a calcium-dependent manner due to the presence of several calcium-binding residues. The "**novel isoforms**" (nPKCs— $\delta$ ,  $\epsilon$ ,  $\eta$  and  $\theta$ ) also have similar N-terminal regulatory regions but differ in that the C2 domain lacks the calcium-binding side chains. Therefore, nPKCs are maximally activated by DAG/PMA independent of calcium. The "**atypical isoforms**" (aPKCs— $\zeta$  and  $\iota/\lambda$ ) are the third PKC isoform subfamily. aPKCs lack a calcium-sensitive C2 domain and also do not bind DAG or PMA. Consequently, aPKCs are activated by a distinct set of phospholipid cofactors as well as by stimulus-induced phosphorylation events (Sampson and Cooper, 2009).

### **Mechanisms of PKC activation**

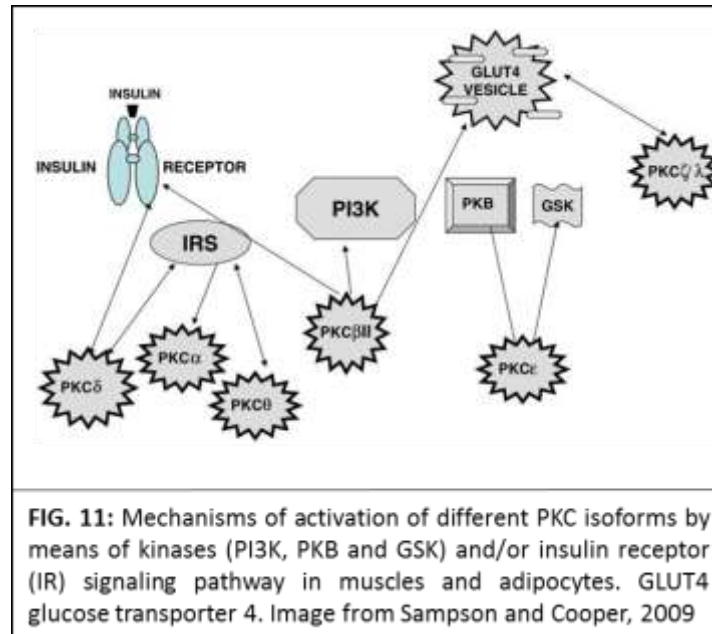
The conventional and novel PKC isoforms ( $\alpha$ ,  $\beta$ II,  $\delta$ ,  $\epsilon$  and  $\theta$ ) are expressed in each of the insulin-responsive tissues and the presence of binding sites for  $\text{Ca}^{2+}$  (conventional), DAG and phosphatidyl serine and fatty acids makes their activation a virtual certainty also in  $\beta$ -cells.

Several isoforms of PKC have been identified in pancreatic  $\beta$ -cells and many have been reported to undergo translocation after stimulation by glucose, acetylcholine, glucagon-like peptide 1 or fatty acids (Baluch and Capco 2002; Mochly-Rosen and Gordon 1998; Feliciello et al., 2001; Pouyssegur et al., 2002). When activated, these PKC translocate to their effector site and bind an anchoring protein, which keeps them in close proximity with downstream effectors (Baluch and Capco 2002; Mochly-Rosen and Gordon 1998; Feliciello et al., 2001;

Pouyssegur et al., 2002). Signal termination usually results in dissociation of the kinase from its scaffold protein (Baluch and Capco 2002; Mochly-Rosen and Gordon 1998; Feliciello et al., 2001; Pouyssegur et al., 2002).

In pancreatic  $\beta$ -cells decreased levels and/or activation of PKC $\alpha$ , PKC $\epsilon$ , PKC $\theta$ , and PKC $\zeta$  are associated with defective signals downstream to glucose metabolism responsible for the deranged insulin secretion in  $\beta$  cells of diabetic rats. PKC $\alpha$  has a role in glucose-induced insulin granule recruitment for exocytosis; while PKC $\epsilon$  is involved in the glucose-generated time-dependent potentiation signal for insulin release. For PKC $\zeta$  a dual function has been proposed: as promoter of insulin release and as regulator of the transcriptional machinery (Pouyssegur et al., 2002; Yedovitzky et al., 1997; Tang and Sharp 1998; Gao et al., 1994; Buteau et al., 2001; Yaney et al., 2002; Deeney et al., 1996; Nesher and Cerasi 1987). Of particular importance for the pancreatic  $\beta$  cell are the PKC $\alpha$  and PKC $\epsilon$  isoforms. These PKC are involved in the second phase of insulin release and the selective inhibition of PKC $\alpha$  or PKC $\epsilon$  translocation to the plasma membrane, results in a partial inhibition of glucose-induced insulin release (Yedovitzky et al., 1997).

Furthermore, PKC may also be a downstream target of insulin receptor activation. The binding of insulin to its receptor initiates a cascade of events leading to its many biological effects. The first step in this cascade is activation of the insulin receptor intrinsic tyrosine kinase, which phosphorylates endogenous substrate proteins, primarily members of the insulin receptor substrate (IRS) family (White 1997). Tyrosine phosphorylated motifs in these substrates serve as docking sites for the recruitment and activation of a number of signaling proteins, including PI3K and mitogen activated protein (MAP) kinase (Sampson and Cooper, 2009). Activation of these elements may then lead to stimulation of additional enzymes, among which are certain members of the PKC family. Recent studies implicate specific PKC isoforms in the insulin-signaling cascade (Figure 11, Acevedo-Duncan et al., 1989; Chalfant et al., 1995; Chalfant et al., 1996; Cooper et al., 1987; Cooper et al., 1992; Cooper et al., 1990; Farese et al., 1992; Ishizuka et al., 1991; Patel et al., 2001; Braiman et al., 2012; Braiman et al., 1999; Braiman et al., 2001a; Braiman et al., 2001b) (Figure 11; Miinea et al., 2005).



### Involvement of PKC in the plasma membrane proteins trafficking

Numerous studies have shown the involvement of the different PKC isoforms in the regulation of intracellular trafficking of membrane proteins. Interestingly, the final effect on membrane trafficking (endocytosis vs exocytosis) is strictly dependent on the isoform, the target, the organ or the type of cell considered. For example, in the CNS, the PKC is responsible for the insertion of new NMDA channels in hippocampal neurons via SNARE-dependent exocytosis (Lau et al., 2010), but also induces the internalization of glutamate metabotropic receptors (mGluR1-R5) or Kainate receptors in cortical presynaptic neurons (Konopacki et al., 2011). Previous studies have demonstrated that acute activation of PKC causes also a redistribution of GLT-1 from the plasma membrane to an intracellular compartment (Bala et al., 2008). This effect has been observed in stably and transiently transfected C6 glioma, in primary astrocyte cultures induced to express GLT-1, and in co-cultures of neurons and astrocytes that express GLT-1 (Kalandadze et al., 2002, Zhou and Sutherland, 2004 and Guillet et al., 2005).

In addition, each of the PKC isoforms has one or more roles in the glucose metabolism and insulin signaling cascade, if not via direct activation in response to insulin, then by activation via conditions that modify insulin-induced effects. For example, the PKC promotes the membrane translocation of glucose transport GLUT2 on the cell surface of immature enterocytes and allow them to respond to extracellular glucose (Zheng et al., 2011). It induces also the membrane exposition of the human Na<sup>+</sup>-glucose cotransporter (SGLT2), expressed mainly in the kidney proximal convoluted tubule and considered responsible for the bulk of glucose reabsorption (Ghezzi and Wright 2012). Furthermore, together with the PI3K and AKT, it takes part in the

dynamic regulation of the glucose transport GLUT4 trafficking, in skeletal muscles and adipose tissue (Dugani and Klip, 2005). The fact that so many substrates, such as the glutamate transporter GLT1 its self, components of the endocytic machinery (caveolae, clathrin adaptor complexes) and of the insulin transduction pathways (IRS, IR, Akt) are phosphorylated by PKCs, makes this kinase a good candidate to explain GLT1 regulation also in  $\beta$ -cells.

### **PI3K: phosphatidylinositol 3-kinase**

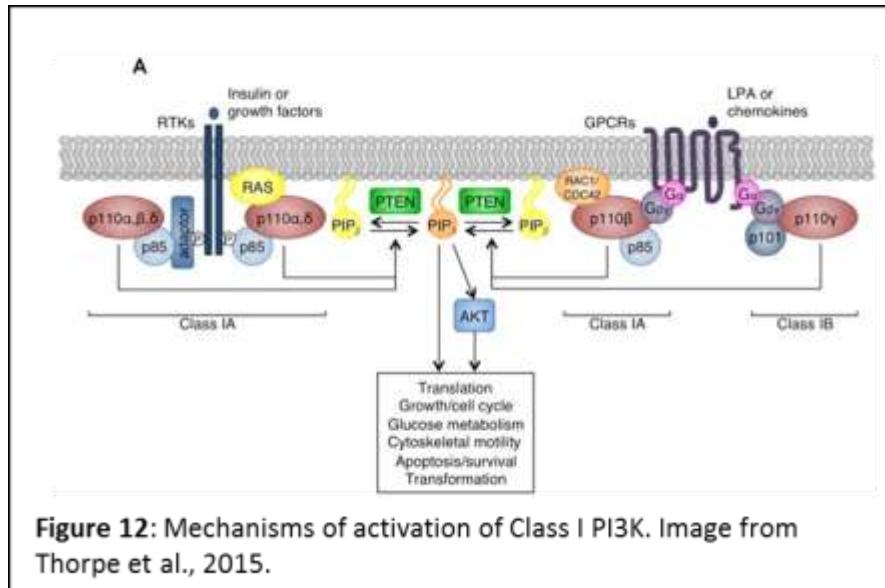
The phosphatidylinositol 3-kinase (PI3K) signaling axis impacts on cell growth, survival, motility and metabolism (Madhunapantula et al., 2011). PI3Ks are a family of intracellular lipid kinases that phosphorylate the 3' hydroxyl group of phosphatidylinositols (Pis) and phosphoinositides (Aziz et al., 2009; Franke 2008). Based on substrate specificity and structure, PI3K proteins have been categorized into class-I, class-II and class-III kinases (Franke 2008; Marone et al., 2008). Whereas activity of class-Ia PI3K is triggered by growth factor receptor tyrosine kinases, class-Ib proteins are activated by G protein-coupled receptors. Class-Ia PI3K is a heterodimer comprising a p85 regulatory and p110 catalytic subunits (Franke 2008; Marone et al., 2008). Upon growth factor stimulation class-Ia PI3Ks phosphorylates PtdIns (4,5) $P_2$  at the 3' position converting it into PtdIns(3,4,5) $P_3$ , which binds to the PH domain containing PDK1 and Akt proteins, thereby facilitating translocation of these proteins to the cell membrane. Class-I PI3Ks also exhibit protein kinase activity, but activation of each of the two class-I isoforms has differing consequences (Fruman 2010; Vogt et al., 2009). For example, class-Ia PI3K phosphorylates insulin receptor substrate-1 (IRS-1), whereas class-Ib PI3K activates the MAPK signaling cascade (Franke 2008; Marone et al., 2008).

#### **Mechanism of activation of PI3Ks**

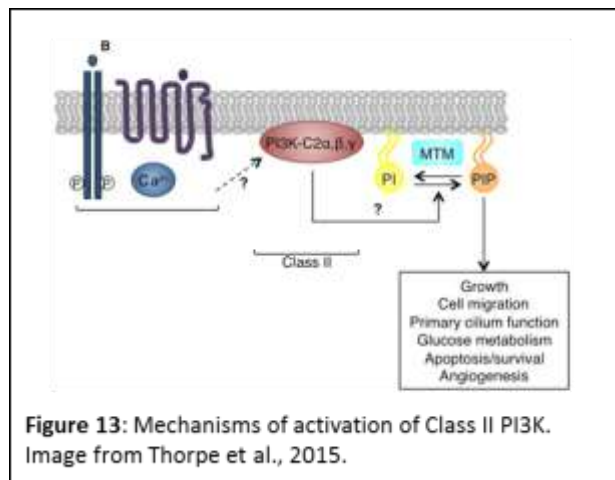
PI3Ks phosphorylate the 3'-hydroxyl group of phosphatidylinositides (PtdIns). They are divided into three classes based on their structures, their activation and substrate specificities.

#### **Signaling by class I, II, and III PI3K isoforms:**

**(A)** Upon receptor tyrosine kinase (RTK) or G-protein coupled receptor (GPCR) activation, class I PI3Ks are recruited to the plasma membrane by interaction with phosphorylated YXXM motifs on RTKs or their adaptors, or with GPCR-associated  $G_{\beta\gamma}$  subunits (Figure 12). There they phosphorylate PtdIns(4,5) $P_2$  (PIP<sub>2</sub>) to generate PtdIns(3,4,5) $P_3$  (PIP<sub>3</sub>), a second messenger which activates a number of AKT-dependent and independent downstream signaling pathways regulating diverse cellular functions including growth, metabolism, survival, and transformation. The phosphatase and tensin homolog (PTEN) lipid phosphatase removes the 3' phosphate from PtdIns(3,4,5) $P_3$  to inactivate class I PI3K signaling (Figure 12; Liu et al., 2009; Thorpe and Yuzugullu 2015).

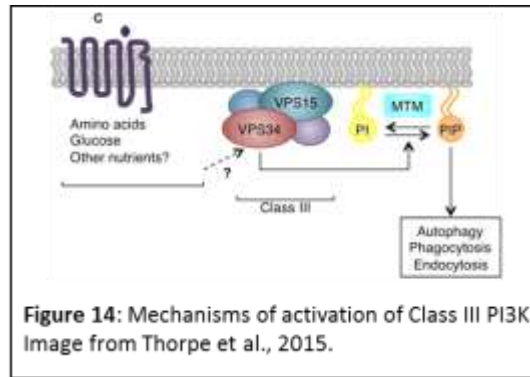


**(B)** Class II PI3Ks are not well understood, but may be activated by a number of different stimuli, including hormones, growth factors, chemokines, cytokines, phospholipids and calcium ( $Ca^{2+}$ ). Although *in vitro* class II PI3Ks can phosphorylate both PtdIns and PtdIns(4)P, *in vivo* this class may preferentially phosphorylate PtdIns (PI) to generate PtdIns(3)P (PIP) (Figure 13; Aziz et al., 2007; Maffucci et al., 2005; Yoshioka et al., 2012). Class II PI3Ks regulate cellular functions including glucose transport, endocytosis, cell migration and survival. Myotubularin (MTM) family phosphatases remove the 3' phosphate from PtdIns(3)P to inactivate class II PI3K signaling (Figure 13).



**(C)** The class III VPS34-VPS15 heterodimer is found in distinct multiprotein complexes, which perform specific cellular functions. VPS34 may be activated by stimuli including amino acids, glucose, other nutrients and

phosphorylates PtdIns (PI) to generate PtdIns(3)P (PIP) (Figure 14). It plays critical roles in autophagy, endosomal trafficking and phagocytosis. MTM family phosphatases remove the 3' phosphate from PtdIns(3)P to inactivate class III PI3K signaling (Figure 14).



### PI3K and Insulin Receptor

IRS-1 initializes the classical PI3 kinase-dependent pathway downstream of IR in the metabolic signaling cascade (Ramalingam et al., 2013). The center and C-terminus of IRS proteins act as a hub for scaffolding molecules downstream of IRS. Although IRS-1 is the primary substrate in skeletal muscle/adipose insulin signaling, six different IRS proteins serve different cellular functions, owing to their differences in tissue distribution and intrinsic activity (Sun et al., 1995). For example, both IRS-1 and IRS-2 are expressed in skeletal muscle, adipocytes and  $\beta$ -cells. In  $\beta$ -cells IRS-1 binds to its main downstream effector, PI3K, through its C-terminus, activating PI3K and propagating the IR signaling cascade (Myers et al., 1992). Importantly, decreased content of IRS-1 is associated with some cases of insulin resistance in animals and humans (Sesti et al., 2001). PI3K is a dimer composed by an 85 kDa adapter subunit and a 110 kDa catalytic subunit (Myers et al., 1992; Shepherd et al., 1998).

PI3K catalyzes the addition of a phosphate at the third position of the inositol ring of phosphoinositol to generate PIP3. p70S6 kinase, Akt and PKC are all downstream effectors of PI3K. Once phosphorylated, these substrates serve as docking molecules which bind and activate other cellular kinases, initiating divergent signaling pathways that mediate cellular insulin action (Jewel et al., 2010).

The PI3K/AKT pathway is essential for beta-cell growth and survival and it has been studied extensively in diabetes (Kotani et al., 1998).

Recently, experiments in genetically modified animal models have assessed the role of Akt1 and Akt2 in glucose homeostasis. Akt1-deficient mice exhibited impairment in organ growth with normal glucose tolerance

and insulin-stimulated glucose disposal (Cho et al., 2001a; Chen et al., 2001). In contrast, Akt2/PKB $\beta$ -deficient mice have impaired glucose disposal due to a reduction in insulin-stimulated glucose uptake in muscle and fat (Cho et al., 2001b). Ablation of Akt2 in a different background resulted in decreased adipose tissue associated with hyperglycemia and  $\beta$  cell failure in a small subset of animals, suggesting that Akt could play a role in  $\beta$  cell adaptation to insulin resistance states (Garofalo et al., 2003; Bae et al., 2003). While mice with increased Akt activity exhibit a marked increase in  $\beta$  cell mass, this does not define Akt as the physiologic mediator of the effects of the insulin/IGF pathway in  $\beta$  cell mass and function (Tuttle et al., 2001; Bernal-Mizrachi et al., 2001).

In addition, mice expressing a kinase-dead mutant of Akt in  $\beta$  cells demonstrate that the serine-threonine kinase Akt is essential for normal  $\beta$  cell function and has a novel regulatory role in the second phase of insulin secretion, at the level of the exocytotic pathway distal to Ca<sup>2+</sup> influx (Bernal-Mizrachi et al., 2004).

### **AMPK: AMP-activated protein kinase**

One of the central regulators of cellular and organismal metabolism in eukaryotes is the AMP-activated protein kinase (AMPK), which is activated when intracellular ATP levels are low. AMPK plays critical roles in regulating growth and reprogramming metabolism and recently has been connected to cellular processes including autophagy and cell polarity (Mihaylova and Shaw, 2012). AMPK is a highly conserved sensor of intracellular adenosine nucleotide levels that is activated when a modest decrease in ATP production results in an increase in AMP or ADP. In response, AMPK promotes catabolic pathways to generate more ATP and inhibits anabolic pathways to prevent the ATP consumption. AMPK plays a general role in coordinating growth and metabolism, and specialized roles in metabolic control in tissues such as the liver, muscle, fat and endocrine pancreas (Kahn et al., 2005).

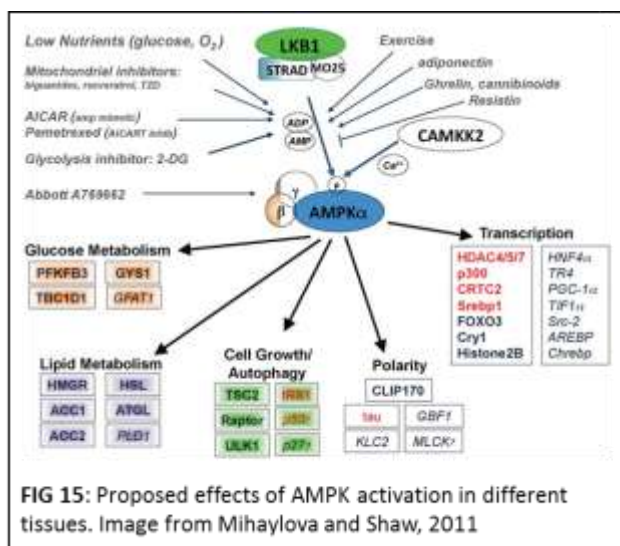
### **Mechanism of action of AMPK**

In most species, AMPK exists as an obligate heterotrimer, containing a catalytic subunit ( $\alpha$ ) and two regulatory subunits ( $\beta$  and  $\gamma$ ). AMPK is hypothesized to be activated by a two-pronged mechanism:

- 1) Under low intracellular ATP levels, AMP or ADP can directly bind to the  $\gamma$  regulatory subunits, leading to a conformational change that protects the activating phosphorylation of AMPK (Xiao et al., 2011; Oakhill et al., 2011).
- 2) Recent studies discover that ADP can also bind the nucleotide binding pockets in the AMPK  $\gamma$  and suggest that it may be the physiological nucleotide for AMPK activation under a variety of cellular stresses (Bland and Birnbaum 2011; Hawley et al., 2003; Woods et al., 2008; Shaw et al., 2004; Shackelford and Shaw 2009; Hawley et al., 2005; Hurley et al., 2005; Woods et al., 2005).

In addition to nucleotide binding, phosphorylation of Thr172 in the activation loop of AMPK is required for its activation and several groups have demonstrated that the serine/threonine kinase LKB1 directly mediates this event (Hawley et al., 2003; Woods et al., 2008; Shaw et al., 2004). Importantly, AMPK can also be phosphorylated on Thr172 in response to calcium increase, independently of LKB1, via CAMKK2 (CAMKK $\beta$ ) kinase, which is the closest mammalian kinase to LKB1 by sequence homology (Hawley et al., 2005; Hurley et al., 2005; Woods et al., 2005; Fogarty et al., 2010).

Many types of cellular stresses can lead to AMPK activation (Figure 15). In addition to physiological AMP/ADP elevation from stresses such as low nutrients or prolonged exercise, AMPK can be activated in response to several pharmacological agents such as metformin, the most widely prescribed Type 2 diabetes drug. Metformin has been shown to activate directly AMPK (Zhou et al., 2001) in an LKB1 dependent manner (Shaw et al., 2005) or indirectly, by acting as mild inhibitors of Complex I of the respiratory chain, which leads to a drop of intracellular ATP levels (Figure 15; Hawley et al., 2010; Hardie 2006).



### Role of AMPK in Glucose Metabolism and Protein Trafficking

AMPK is expressed in multiple mammalian tissues involved in the control of glucose and lipid metabolism (Hardie 2004; Carling 2004; Kemp et al., 2003; Da Silva et al., 2003). Furthermore, AMPK integrates signaling circuits between peripheral tissues and the hypothalamus to regulate food intake and whole-body energy expenditure. Active AMPK phosphorylates and inactivates a number of metabolic enzymes involved in cholesterol and fatty acid synthesis, including HMG-CoA reductase (Brown, et al., 1975) and acetyl-CoA carboxylase (Yeh et al., 1980; Carling 1987) thus reducing cellular ATP consumption (Carling 1987 and Hardie et

al., 1989) during conditions of metabolic stress (Munday, et al., 1991; Stapleton et al., 1994; Da Silva et al., 2003).

The action of AMPK is not simply restricted to activation/inhibition of enzymatic activities and more recently a role in the control in vesicle dynamics has also been proposed. In 3T3-L1 adipocytes, activators of AMPK are able to enhance GLUT4 translocation to the plasma membrane and consequently glucose transport activity in (Yamaguchi et al., 2005). Also in skeletal myocytes, AMPK activation via physiological stimulation such as muscle contraction or by pharmacological activation with AICAR (5-Aminoimidazole-4-carboxamide ribonucleotide, an analogue of adenosine monophosphate (AMP) able to stimulate AMPK) leads to a significant increase of glucose uptake, a process mediated by the GLUT4 translocation (Hayashi et al., 1998; Mu et al., 2001).

AMPK is expressed also in endocrine cells of the pancreas. AMP and ADP concentrations in  $\beta$  cells decrease in response to elevations in glucose concentration (Detimary et al., 1998; Salt et al., 1998) and this suggests that AMPK could play a role in insulin release by acting as a fuel sensor. In line with this possibility, an increase in glucose levels represses AMPK activity in  $\beta$  cell lines (Salt et al., 1998; Silva Xavier et al., 2000; Silva Xavier et al., 2003; Leclerc et al., 2004), whereas AICAR-induced activation of AMPK markedly reduced glucose-stimulated insulin release from primary pancreatic islets (Salt et al., 1998; Silva Xavier et al., 2000; Silva Xavier et al., 2003) and  $\beta$  cell lines (Silva Xavier et al., 2003; Leclerc et al., 2004; Zhang et al., 1995). Similarly, incubation of either human islets or cultured  $\beta$  cells with metformin activates AMPK and inhibits glucose-stimulated insulin secretion (Leclerc et al., 2004). Although seemingly undesirable in the treatment of T2D, AMPK-mediated suppression of insulin release may be physiologically relevant for maintaining glucose homeostasis through inhibition of insulin secretion during glucose deficiency. Furthermore, overexpression of a constitutively active form of AMPK reduces calcium influx in response to depolarizing agents and results in repressed glucose-induced insulin release from  $\beta$  cell lines (Silva-Xavier et al., 2003; Zhang and Kim 1995). Conversely, overexpression of a dominant-negative form of AMPK leads to increases in insulin release without apparent changes in glucose metabolism and calcium influx (Silva-Xavier et al., 2003).

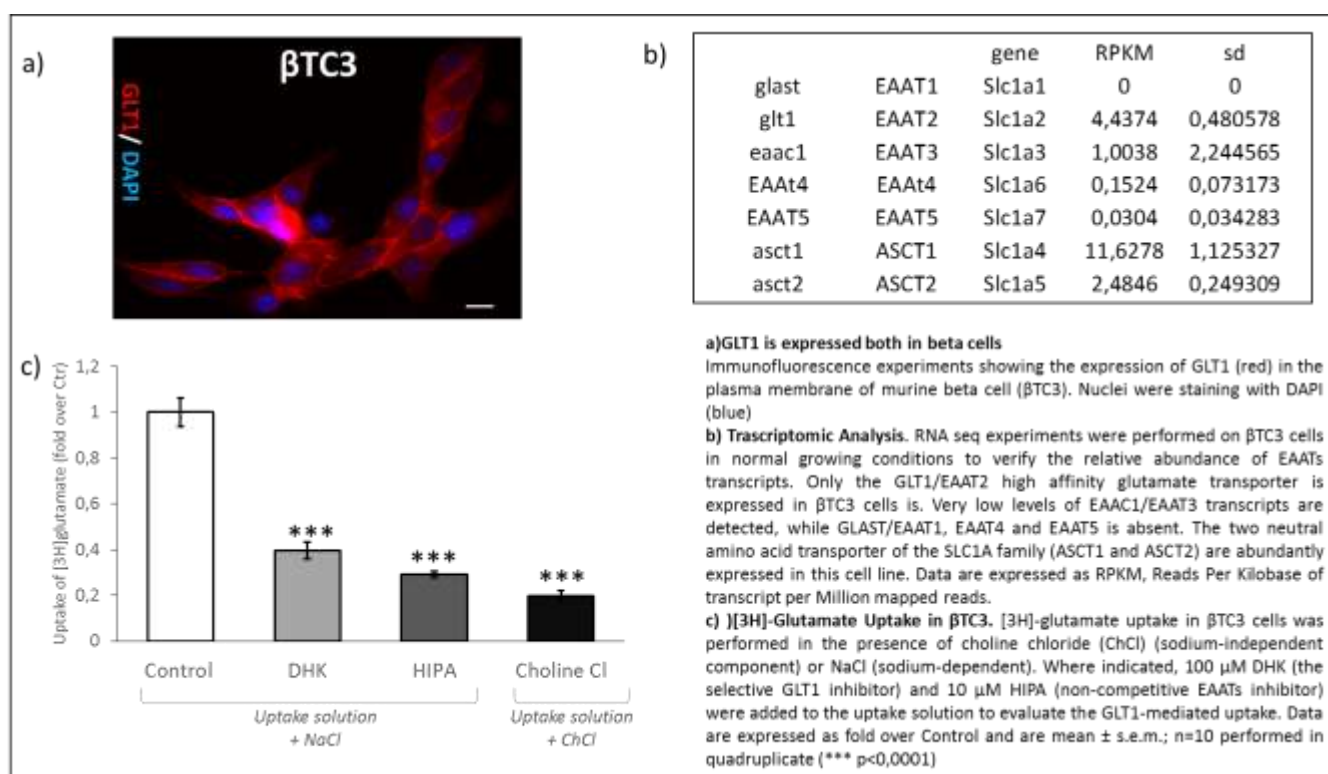
Despite its profound effects on insulin release, the role of AMPK in  $\beta$  cell vesicle trafficking is unclear and downstream targets of AMPK that mediate these physiological processes remain to be identified. The role of AMPK in the regulation of  $\beta$  cell function is clearly an unresolved question that requires further investigation.

# CHAPTER I

## Dynamic modulation of GLUT1 activity and localization in beta cell lines

### GLT1 is expressed and functional in the $\beta$ TC3-cell line

We first confirmed the expression of GLUT1 in the murine beta cell line  $\beta$ TC3 by immunofluorescence assays. As shown in Fig. 1A, in normal growing conditions, the anti-GLT1 staining was almost exclusively localized to the plasma membrane of clonal beta cells.



To test whether the transport was also functional glutamate uptake experiments were performed (figure 1b). Being GLUT1 a  $\text{Na}^+$ -dependent transporter we performed the assays in the presence of an uptake solution containing sodium chloride (NaCl). We also measured the  $\text{Na}^+$ -independent glutamate transport using an uptake solution with Cholin Chloride (ChCl). The basal sodium independent glutamate transport measured in the presence of choline chloride was increased approximately 5-fold in the presence of a sodium gradient, indicating that  $\beta$ -cells express a  $\text{Na}^+$ -dependent glutamate transport system. To verify whether the  $\text{Na}^+$ -dependent activity was only due to GLUT1 we performed the uptake experiments in the presence of two different glutamate inhibitors: HIPA (  $(\pm)$ -3-Hydroxy-4,5,6,6a-tetrahydro-3aH-pyrrolo[3,4-d]isoxazole-4-carboxylic acid) and dihydrokainate (DHK). Incubation of  $\beta$ TC3 cells with HIPA, (kind gift of Prof. De Micheli,

Dept of Pharmacology, Milan) a non-selective EAATs blocker, completely abolished the Na<sup>+</sup>-dependent component of (<sup>3</sup>H)D-glutamate uptake (IC<sub>50</sub> = 18 μM). The same rate of inhibition was obtained after exposure to DHK, a selective GLT1 inhibitor (IC<sub>50</sub>= 0.05 mM) (Arriza et al., 1994) (Fig. 1B).

Our results demonstrate that GLT1 is the main regulator of the glutamate clearance in β-cells. Data were confirmed also at the molecular level. A RNA seq experiment was performed on βTC3 cells in normal growing conditions to verify the relative abundance of EAAT transcripts. As shown in fig 1C, the only high affinity glutamate transporter expressed in βTC3 cells is GLT1/EAAT2. Very low levels of EAAC1/EAAT3 transcripts were detected, while GLAST/EAAT1, EAAT4 and EAAT5 were absent. Interestingly, the two neutral amino acid transporter of the SLC1A family (ASCT1 and ASCT2) are abundantly expressed in this cell line.

### Modifications of extracellular glucose concentrations cause alterations of GLT1 transport activity and localization

Physiologically, pancreatic beta cells are exposed to rapid changes in extracellular glucose, which primarily controls insulin secretion. Given, the involvement of GLT1 in the control of extracellular glutamate and thereby in hormone release, we evaluate possible effects of modification of glucose levels on GLT1 surface activity. βTC3 cells were incubated for 30 minutes with different glucose concentrations and the transporter activity was assessed by means of uptake experiments. βTC3 cells normally grow in the presence of 11mM glucose, we therefore tested 5,5mM glucose as low glucose condition (LG) or hypoglycaemia and 16mM and 20mM as high glucose (HG) condition or hyperglycaemia (HG).

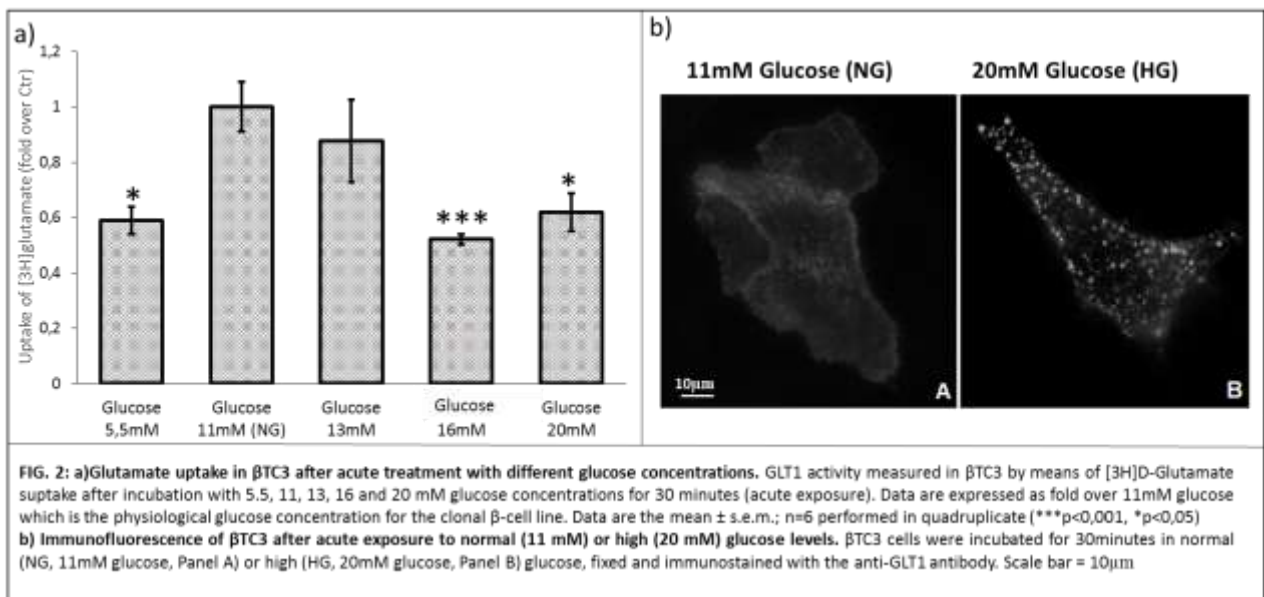


**FIG. 2:** a) Glutamate uptake in βTC3 after acute treatment with different glucose concentrations. GLT1 activity measured in βTC3 by means of [<sup>3</sup>H]D-Glutamate uptake after incubation with 5.5, 11, 13, 16 and 20 mM glucose concentrations for 30 minutes (acute exposure). Data are expressed as fold over 11mM glucose which is the physiological glucose concentration for the clonal β-cell line. Data are the mean ± s.e.m.; n=6 performed in quadruplicate (\*\*\*p<0,001, \*p<0,05) b) Immunofluorescence of βTC3 after acute exposure to normal (11 mM) or high (20 mM) glucose levels. βTC3 cells were incubated for 30minutes in normal (NG, 11mM glucose, Panel A) or high (HG, 20mM glucose, Panel B) glucose, fixed and immunostained with the anti-GLT1 antibody. Scale bar = 10 μm

As shown in figure 2A, the optimal Na<sup>+</sup>-dependent (<sup>3</sup>H)-D-glutamate uptake results reduced both in low and high glucose conditions indicating that the extracellular glucose levels regulates GLUT1 activity in β-cells. We then performed immunofluorescence experiments with anti-GLT1 antibodies on βTC3 incubated for 30 minutes under normal (11 mM) or high (20 mM) glucose conditions. As reported in the representative image (figure 2b), in the normal growing conditions GLUT1 distributed uniformly in the cell membrane where it can transport glutamate. Conversely under high glucose conditions GLUT1 prevalently localized in vesicular structures distributed in the cytoplasm. Therefore, the reduction in glutamate uptake observed under high glucose concentrations is likely due to the transporter relocalization from the plasma membrane to intracellular compartments.

To confirm this possibility, we monitored the GLUT1 plasma membrane localization under high glucose concentrations by means of Total Internal Reflection Fluorescence Microscopy (TIRFM). The TIRFM technique allows the selective excitation of fluorochromes located in or immediately below the plasma membrane (100 nm above the glass coverslip; Axelrod, 2001). This technique is particularly useful in studies of plasma membrane protein dynamics. Indeed, if a protein fused to a genetically encoded fluorescent protein like GFP, undergoes endocytosis, it progressively exit the TIRFM plane and the associated fluorescence signal decreases. Conversely, if a GFP-tagged protein undergoes exocytosis, it progressively accumulates at the plasma membrane and the associated fluorescence signal coherently increases.

For this purpose, we generated a GFP-tagged GLUT1 transporter. The tag does not interfere with the protein targeting to the plasma membrane or with its transport activity. The construct was transfected in βTC3 cells plated onto glass coverslips and, 48 hours after transfection, analysed by time lapse TIRF microscopy. Cells were maintained under normal (11 mM, NG) or high glucose concentrations (20 mM, HG) and the fluorescence signal recorded over 30 minutes. Figure 3 shows representative image sequences of the GFP-GLUT1 transporter (panel B), together with the averaged fluorescence intensity curves (panel C) recorded 20 minutes after incubation with NG or HG. The total fluorescence intensity of the GFP-transporter under NG remained almost constant during the 5-min recording, but under 20 mM glucose it markedly decreased. Quantification of the fluorescence changes indicated a  $15.92 \pm 0.31\%$  decrease in the total GFP-GLUT1 signal during 5 min recording under HG, but only a  $2.02 \pm 0.03\%$  decrease under control conditions ( $p < 0.01$ ), thus indicating that glucose controls the transporter resident time in the plasma membrane.

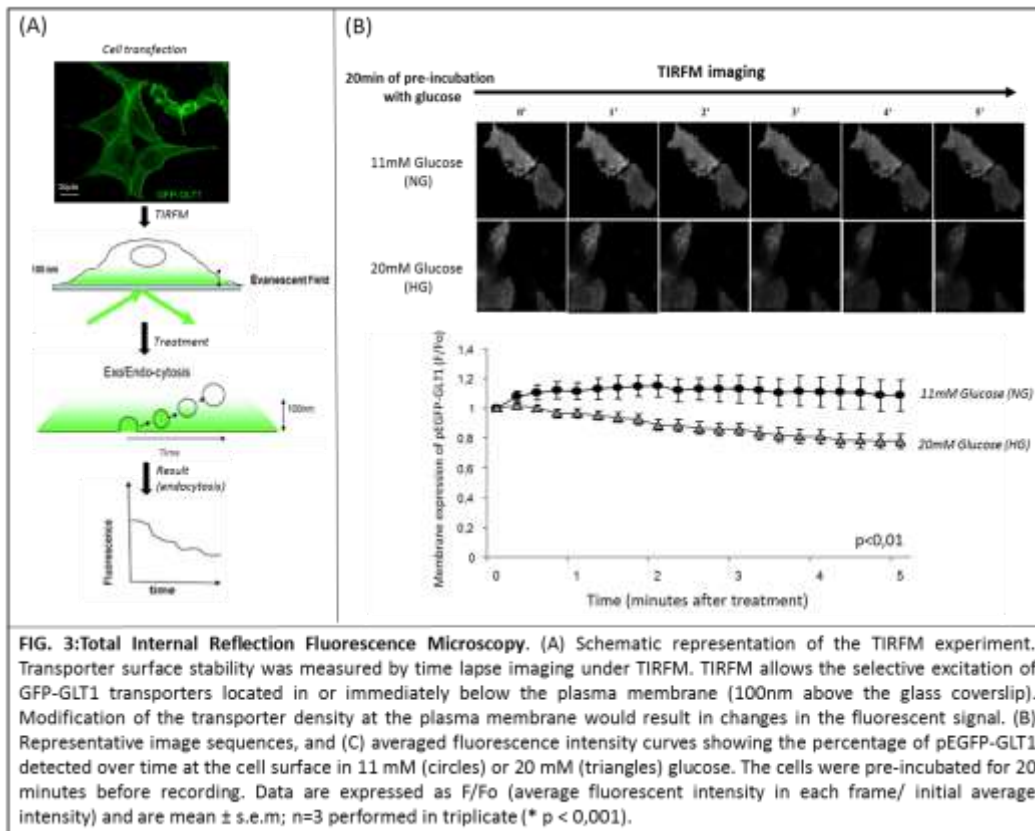


**FIG. 3: Total Internal Reflection Fluorescence Microscopy.** (A) Schematic representation of the TIRFM experiment. Transporter surface stability was measured by time lapse imaging under TIRFM. TIRFM allows the selective excitation of GFP-GLT1 transporters located in or immediately below the plasma membrane (100nm above the glass coverslip). Modification of the transporter density at the plasma membrane would result in changes in the fluorescent signal. (B) Representative image sequences, and (C) averaged fluorescence intensity curves showing the percentage of pEGFP-GLT1 detected over time at the cell surface in 11 mM (circles) or 20 mM (triangles) glucose. The cells were pre-incubated for 20 minutes before recording. Data are expressed as F/Fo (average fluorescent intensity in each frame/ initial average intensity) and are mean  $\pm$  s.e.m; n=3 performed in triplicate (\* p < 0,001).

Under resting conditions, the transporter is expressed in the plasma membrane and efficiently transports glutamate. Under high extracellular glucose concentrations, GLT1 accumulates in intracellular vesicular compartments causing a reduction in the density of transporters at the plasma membrane and in the glutamate transport activity.

### The role of intracellular pathway (PKC, PI3K and AMPK) in the GLT1 regulation

We then investigated the molecular mechanisms responsible for the glucose-mediated GLT1 relocalization. In the CNS, GLT1 localization and activity change in response to activation of different protein kinases. We first focus on protein kinases involved in vesicle trafficking and known to be modulated by glucose concentrations: PKC, PI3K and AMPK. Generally, it is thought that high glucose activates PKC and PI3K directly or indirectly, through insulin receptor activation. Conversely, AMPK is activated by decrease glucose concentrations or nutrient depletion. To verify whether these kinases are involved in the regulation of the GLT1 trafficking in  $\beta$  cell lines, we performed uptake experiments in presence of different inhibitors or activators of these pathways. To better understand the role of these enzymes, the experiments were performed in the presence of different extracellular glucose concentrations, in order to simulate the different physiological conditions under which pancreatic beta cells are normally exposed.

### **PKC mediates the glucose-driven GLT1 relocalization in $\beta$ TC3 cells**

PKC is normally active in hyperglycemic conditions and plays a role in the glucose metabolism regulation in different tissues. For example, it promotes the translocation of the glucose transporter GLUT4 to the plasma membrane in skeletal muscle and adipose tissue (Sampson and Cooper 2009; Baluch and Capco 2002). It is also expressed in  $\beta$ -cells and its activity is required to drive the first phase of insulin release. To study the possible involvement of PKC in the GLT1 regulation we performed uptake assays using radiolabeled glutamate. Indeed, GLT1 is the only  $\text{Na}^+$ -dependent glutamate transporter expressed in  $\beta$ TC3 cells (Figure 1), consequently, alteration in its transport activity or modification of its membrane localization will be detectable as changes in ( $^3\text{H}$ )-glutamate uptake.

First, we verify the involvement of PKC in the glutamate uptake in  $\beta$ TC3. The cells were grown in normal culture medium containing 11mM glucose (NG). To stimulate PKC we used PMA (Phorbol 12-myristate 13-acetate), also called TPA (12-O-Tetradecanoylphorbol 13-acetate). It is a phorbol diester and a potent tumor promoter that it is able to activate the PKC signal transduction by mimicking DAG, one of the natural activators of classic PKC isoforms. As PKC inhibitors we employed bisindolylmaleimide (Bis): a highly selective, cell-permeable and reversible PKC inhibitor, which acts as a competitive ATP binding site blocker of PKC. It shows high selectivity for PKC $\alpha$ -,  $\beta$ 1-,  $\beta$ 2-,  $\gamma$ -,  $\delta$ -, and  $\epsilon$ -isozymes. Both inhibitors require an incubation of 30 minutes before uptake experiments.

The results are reported in figure 4 as fold increase over control. In normal glucose concentrations (11 mM), inhibition of PKC by bisindolylmaleimide did not affect the glutamate uptake. Conversely, TPA treatment caused a statistically significant reduction in the glutamate uptake, indicating that PKC controls the localization and/or activity of this transporter. As expected, the pre-incubation of TPA together with bisindolylmaleimide completely abolished the effect induced by TPA, demonstrating the specific involvement of the PKC pathway.

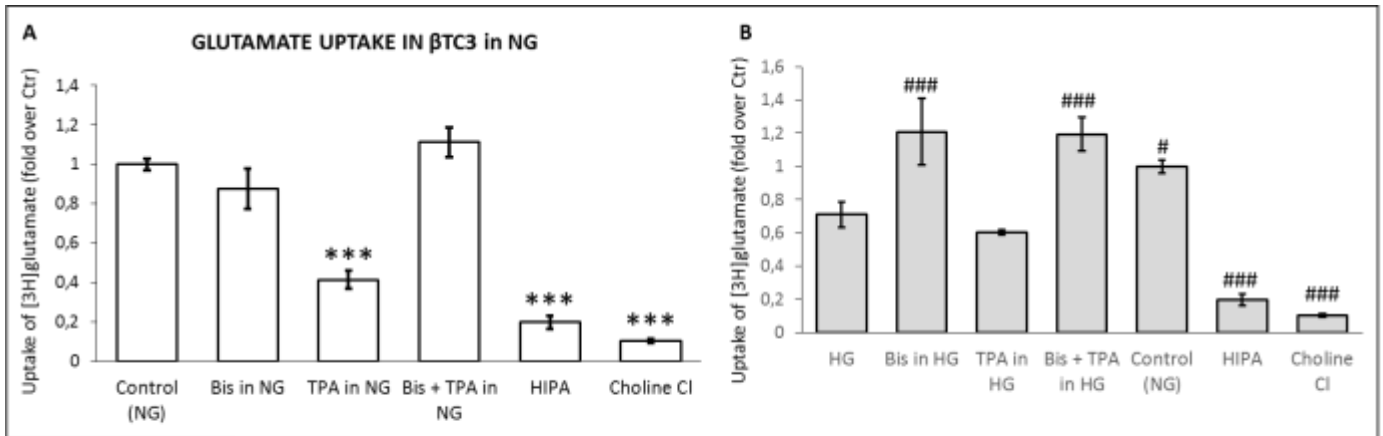


**FIG. 4: PKC-mediated modulation of glutamate uptake in  $\beta$ TC3 maintained in normal (11 mM) or high (20 mM) glucose concentrations**  
 The Na-dependent  $[3H]$ Glutamate uptake in  $\beta$ TC3 in normal (11mM Glucose; Panel A) and high (20mM Glucose; Panel B) glucose conditions was measured after 30 minutes of incubation with the indicated treatments. 10 $\mu$ M Bisindolylmaleimide (Bis, PKC inhibitor,) and 10 $\mu$ M TPA (PKC activator,). Choline chloride has been used to evaluate the Na-independent glutamate transport. The HIPA has been used to evaluate the GLUT1-mediated glutamate transport. Data are expressed as fold over control and are mean  $\pm$  s.e.m; n=3 performed in quadruplicate (Panel A\*\*\* p < 0,001 vs Control; Panel B #; p<0,05; ### p < 0,001 vs HG).

If PKC is involved in the high glucose-induced relocalization of GLUT1, we would expect that PKC inhibition would prevent the glucose-induced GLUT1 down regulation. Accordingly, we found that  $\beta$ TC3 pre-treatment with the PKC inhibitor Bisindoleymide abolished the glutamate uptake downregulation induced by 20 mM glucose incubation.

Furthermore, no additive effects were observed when  $\beta$ TC3 cells, maintained in 20 mM glucose, were incubated with the PKC activator TPA.

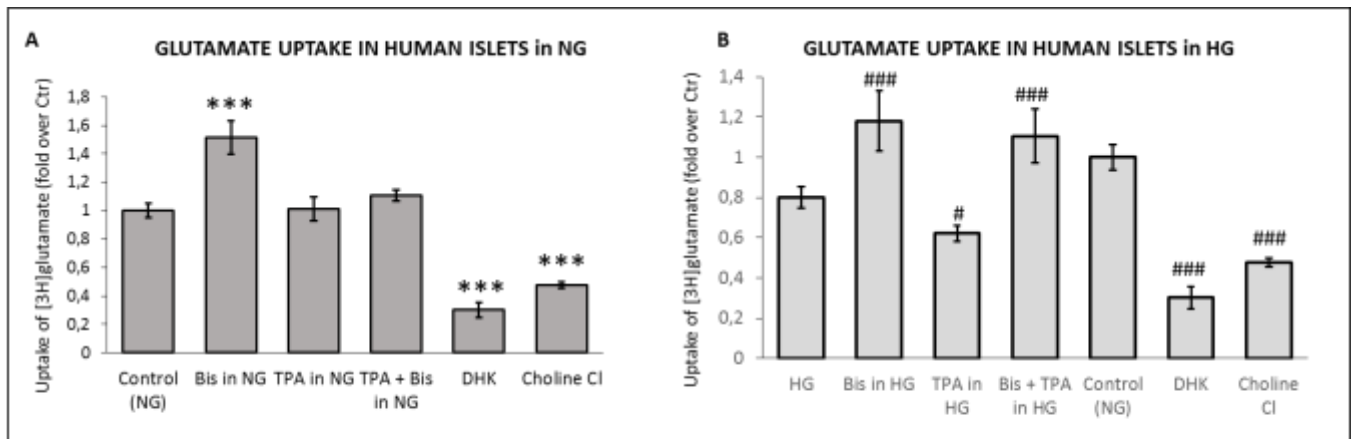


**FIG. 5: PKC-mediated modulation of glutamate uptake in human isolated islets maintained in normal (5.5 mM) or high (16.7 mM) glucose concentrations**  
 The Na-dependent  $[3H]$ Glutamate uptake in human isolated islets in normal (5.5 mM Glucose; Panel A) and high (16.7 mM Glucose; Panel B) glucose conditions was measured after 30 minutes of incubation with the indicated treatments. 10 $\mu$ M Bisindolylmaleimide (Bis, PKC inhibitor,) and 10 $\mu$ M TPA (PKC activator,). Choline chloride has been used to evaluate the Na-independent glutamate transport. The DHK has been used to evaluate the GLUT1-mediated glutamate transport. Data are expressed as fold over control and are mean  $\pm$  s.e.m; n=3 performed in quadruplicate (Panel A\*\*\* p < 0,001 vs Control; Panel B #; p<0,05; ### p < 0,001 vs HG).

We investigated also the role of the PKC in human islets of Langerhans (figure 5).

In the human isolated islets, the glucose concentration in normal growing is lower (5 mM) if compared to  $\beta$ TC3 cell line (11 mM). The analysis of acute treatment in this experimental model is more complicated because the islets are a heterogeneous population of different endocrine cell types. Accordingly, the effects observed not only rely on the treatment applied but also on the interaction between different cell sub-populations that can modulate each other intracellular pathway.

Probably for this reason, already in normal glucose conditions (figure 5a), the TPA and bisindolylmaleimide actions are different is compared with  $\beta$ TC3 cell lines. In fact, the activation of PKC by means of TPA did not induce a significant change in the levels of radio-labeled glutamate uptake (three different islet preparations); while its inhibition through the bisindolylmaleimide significantly increased the amino acid uptake.

These data suggest that PKC is probably already activated in basal conditions and for this reason uptake measurements are lower. Vice versa, blocking this kinase in human isolated islets promotes an increase in the activity of transport or in the numbers of transporters expressed on the plasma membrane.

Similarly to data observed in  $\beta$ TC3 cells, short term incubation with high glucose (16.7 mM) (figure 5b) reduced the glutamate uptake, although the statistical significance was not reached. To this point it should be considered that human islets derive from different subjects that are genetically and biochemically different, furthermore the purification process does not always give the same yield (three different islet preparations were used in this experiment with different percentage of exocrine cell contamination). TPA treatment did not show a significant effect, while incubation with the PKC inhibitor bisindolylmaleimide prevented the high glucose-induced uptake reduction. These data suggest that also in human islets, high glucose causes a relocalization of the glutamate transporter, a process mediated by PKC activation.

The consequences of this relocalization are not completely understood. In the context of the islet physiology, glutamate is an important paracrine signal that positively modulate the somatostatin secretion. Being GLUT1 the main regulator of extracellular glutamate concentration, its relocalization in intracellular compartments would potentiate the activation of glutamate receptors on  $\delta$ -cells, thus overstimulating the somatostatin release.

## **The role of the PI3K in the GLUT1 regulation**

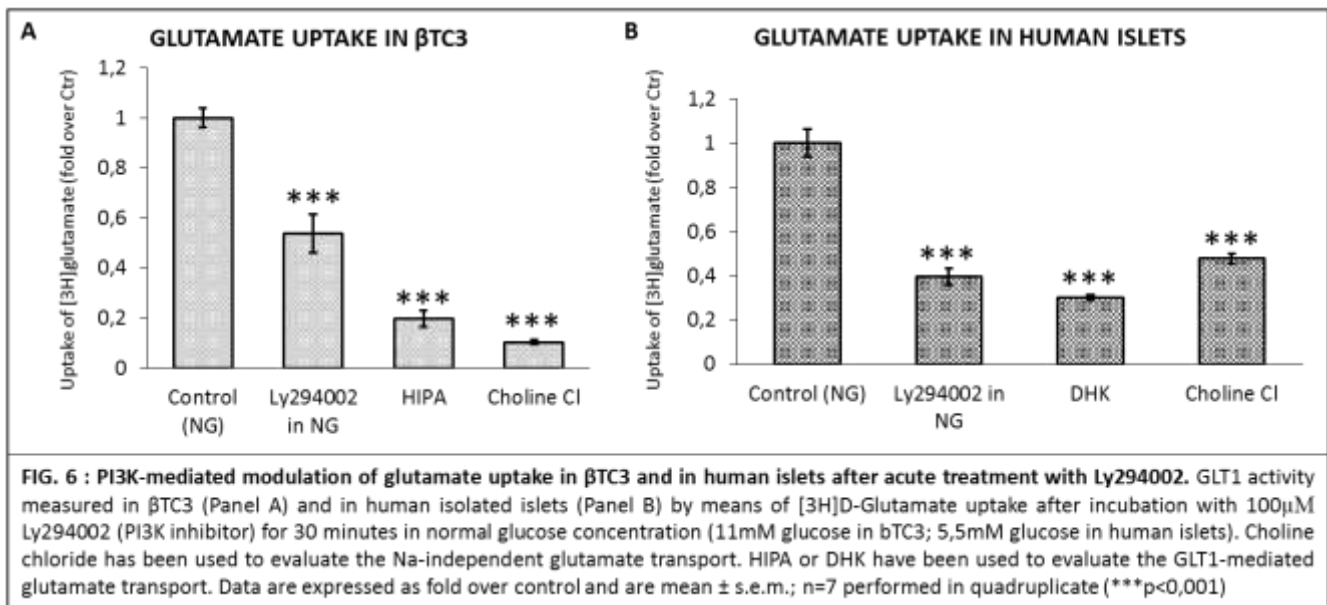
### **PI3K inhibits GLUT1 activity in a dose- and time-dependent manner**

The PI3K (Phosphatidylinositol-4,5-bisphosphate 3-kinase) is an important signalling molecule in beta cells. Indeed, this enzyme is activated by the signal transduction cascade of the insulin receptor (IR), which is also

expressed by pancreatic beta cells (Cho et al., 2001a; Cho et al., 2001b; Chen et al., 2001; Garofalo et al., 2003) Through the the PI3K-mediated phosphorylation of AKT, this kinase is involved in the regulation of membrane trafficking of various proteins, among these is the glucose transporter GLUT4 which translocates on the membrane of skeletal muscle and adipose tissue after activation of the insulin receptor (IR/PI3K/AKT pathway) (Franke 2008; Marone et al., 2008; Thorpe et al., 2015). Therefore, also this kinase has a key role in modulating glucose metabolism and may be involved in the GLT1 regulation.

To verify the potential involvement of this kinase in GLT1 modulation, the uptake experiments were performed in the presence of LY294002, a selective PI3K inhibitor which prevents Akt phosphorylation.

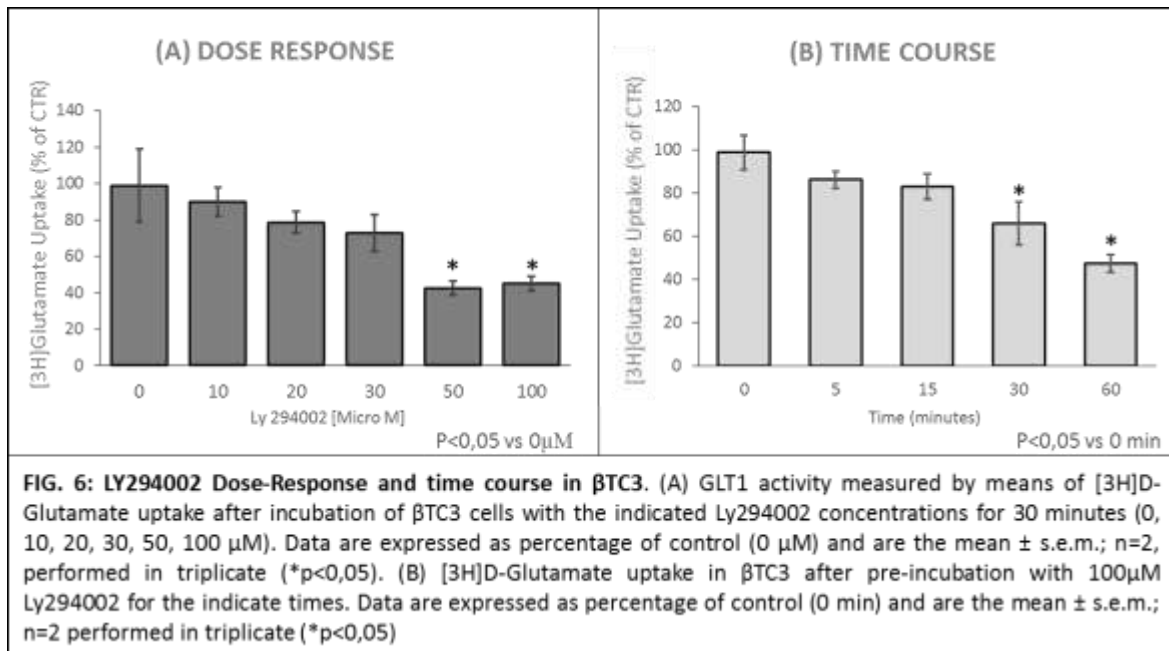
The inhibition of the PI3K/AKT pathway had a very strong effect on the glutamate uptake both in murine beta cell line ( $\beta$ TC3) and in human islets of Langerhans. Indeed, LY294 treatment resulted in a 50% decrease of glutamate uptake. The effect was even more pronounced in human islets (80% reduction compared to the control sample). Incubation with the selective GLT1 inhibitor DHK allowed us to demonstrate that GLT1 is the main glutamate transporter expressed by  $\beta$ TC3 and islets of Langerhans (Wang et al., 1998). Furthermore, in human islets the uptake value obtained in the presence of LY294002 was almost comparable to that obtained with the DHK, indicating that inhibition of the PI3K pathway completely inhibited GLT1-mediated glutamate uptake in islets.



We then performed dose-response and time course experiments. In dose-dependent experiments, cells were pre-treated with different concentration of LY294002, for 30 minutes and then the uptake experiment was

performed. As shown in figure 8A, the progressive increase in LY294002 concentration caused a parallel decrease in glutamate transport activity that reached the statistical significance at a 50  $\mu\text{M}$  concentration.

In time-course experiments, cells were incubated with 100  $\mu\text{M}$  LY294002 for 0', 5', 15', 20', 30' and 60' and then the uptake experiment performed (Figure 8B). Inhibition of the transport activity became appreciable after 15 minutes of incubation and reached the statistical significance difference after 30 minutes. The effect reached the maximal activity after 60 minutes, thus indicating that the phenomenon is also time-dependent.

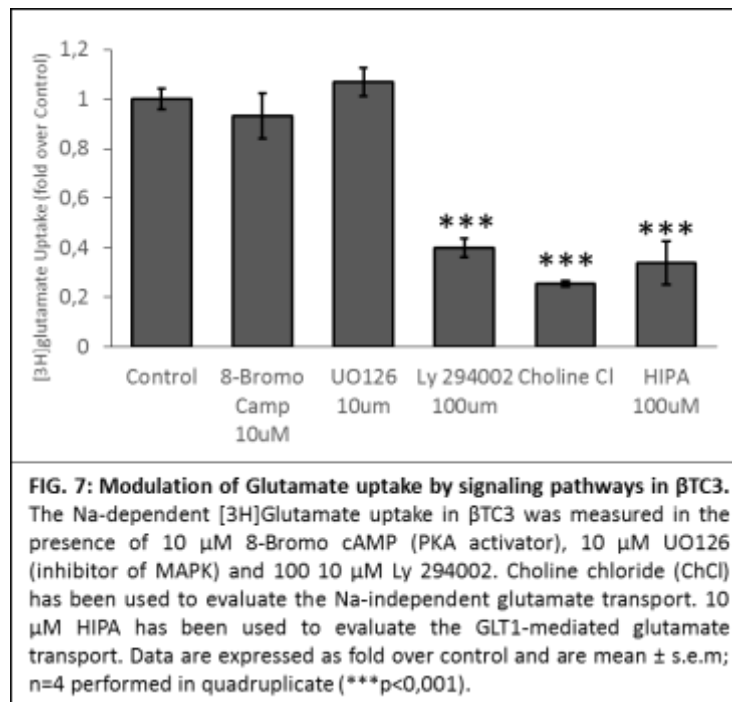


### The effect on GLT1 is specific of the PI3K/AKT pathway

To demonstrate that modifications of GLT1 activity was due to activation of the selective PI3K/AKT pathway, uptake experiments were also performed in the presence of inhibitors of other important intracellular pathways, such as PKA and MAPK signalling. In particular we used 8-Bromo camp (8-Bromoadenosine 3',5'-cyclic monophosphate, 10  $\mu\text{M}$ ) for the PKA signalling and UO126 for the MAPK inhibition. Also in this case, cells were pre-incubated for 30 minutes with the relative compounds before the uptake assay with radiolabeled glutamate.

As shown in figure 9, neither 8BrcAMP nor UO126 significantly modified glutamate uptake. Conversely, LY294002 completely abolished the transport activity. A similar decrease in glutamate uptake was detected in the absence of a  $\text{Na}^+$  gradient (Choline chloride) and in the presence of HIPA, the non-selective inhibitor of

sodium-dependent transporters, thus further confirming that GLT1 is the only Na<sup>+</sup>-dependent glutamate transport system for the pancreatic βTC3 cell line.



### The downregulation of PI3K/AKT pathway causes the relocalization of GLT1 in intracellular compartments

To verify whether the glutamate uptake downregulation observed after LY294002 treatment was due to a GLT1 relocalization time-lapse immunofluorescence experiments were performed. The GFP-GLT1 construct was transfected in βTC3 cells and 48 hours after transfection, the cells were recorded under epifluorescence or TIRF microscopy.

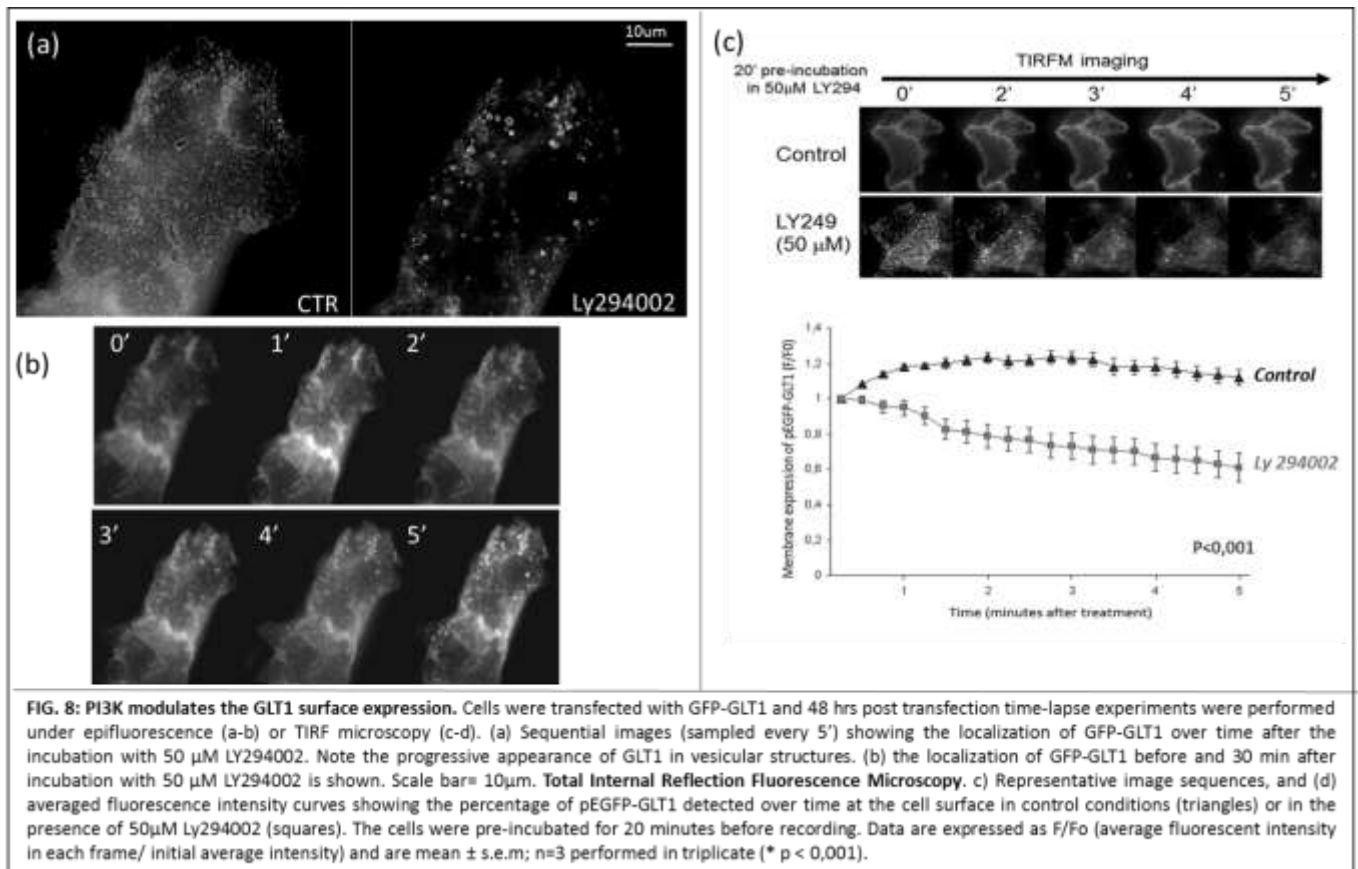
#### 1) Video microscopy on βTC3 transfected with pEGFP-GLT1

We first recorded GFP-GLT1 transfected βTC3 cells in vivo, under epifluorescence. GFP-GLT1 localization was monitored every 15 seconds, for a total period of 30 minutes.

As shown in the representative images of figure 10a, in normal medium, no modifications in the surface distribution of GLT1 were detected. Conversely, incubation with 100 μM LY294002 caused a progressive redistribution of GLT1 from the plasma membrane to intracellular vesicular compartments. It is possible to appreciate the observed effects in the temporal sequence of images reported in the Figure 10b. At time 0, GLT1 was homogeneously distributed over the cell surface; 5 minutes after LY294002 exposure, the transporter was still uniformly distributed on the cell surface, although formation of sporadic intracellular vesicles was already appreciable.

After 10 minutes, the number and size of GLT1 containing vesicles increased. After 20 minutes, the phenomenon became increasingly evident and after 25 minutes the transporter was virtually absent at the level of the plasma membrane and localized almost exclusively to intracellular vesicles.

The rapid relocalization of the GLT1 transporter and its appearance of in cytoplasmic vesicular structures confirm that the pathway PI3K/AKT modulates GLT1 trafficking  $\beta$ -cell lines.



## 2) Total internal reflection microscopy (TIRFM) on $\beta$ TC3 transfected with pEGFP-GLT1

To evaluate the progressive GLT1 disappearance from the plasma membrane, we performed time lapse TIRFM experiments.

48 hours after transfection, GFP-GLT1 transfected cells were recorded under TIRF microscopy, in the presence of LY294002 or in control conditions. Five consecutive video of 5 minutes were recorded and images were sampled every 15 seconds. No evident modifications of plasma membrane GLT1 localization were detected within the first 15 minutes of LY294002 incubation, then the surface signal abruptly decrease in LY treated cells but not in control conditions. The temporal sequence shown in figure 10b reported the images acquired 20 minutes after LY treatment.

In the images is possible to appreciate, in a qualitative manner, the progressive decrease of the fluorescence signal at the plasma membrane only in the sample incubated with the LY294002 inhibitor.

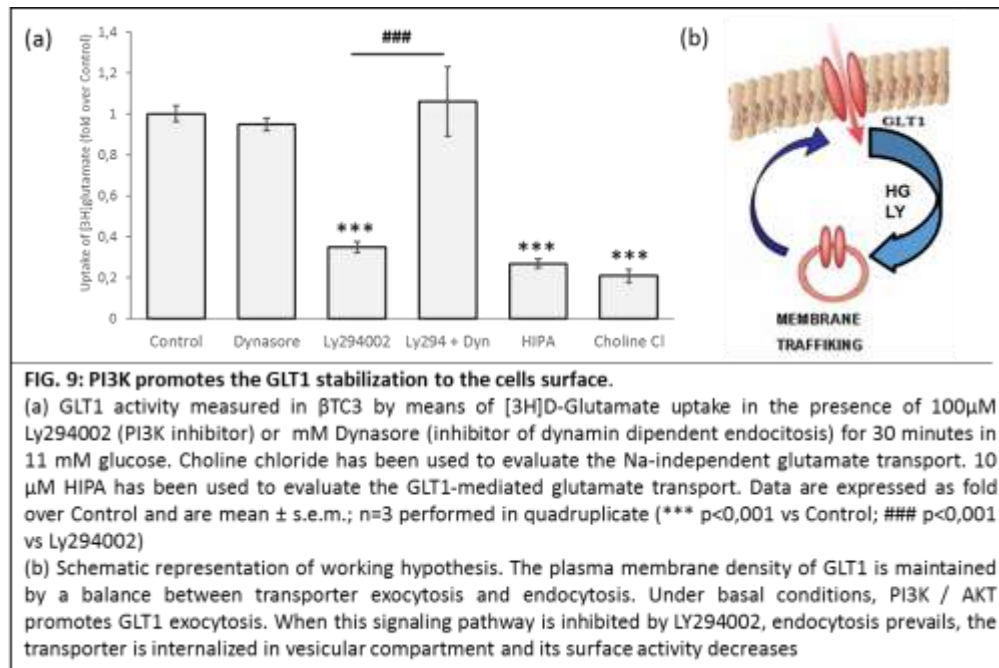
By means of the Image Pro Plus software we performed the quantitative analysis of the immunofluorescence signal. As reported in details in the material and method section, different areas of the cell membrane were selected, and the associated averaged fluorescence intensity measured in each frame (F). The value was normalized to the initial fluorescence intensity (F<sub>0</sub>) and F / F<sub>0</sub> ratio was evaluated and plotted in the graph versus the incubation time, expressed in minutes.

As shown in the figure 11c, in control conditions no significant changes in the fluorescent intensity signal were detected. On the contrary, following LY294002 treatment the fluorescence signal progressively decreased (40% of reduction compared to the control). Because the fluorescence signal is due to the presence of the GFP-GLT1 protein on the cell surface, this means that the incubation with LY294002 resulted in a progressive reduction of GLT1 from the plasma membrane, further confirming our hypothesis.

#### **The causative mechanism responsible for the GLT1 intracellular accumulation is a decrease of endocytosis**

In astrocytes and in epithelial cells, the surface expression of glutamate transporters is controlled through rapid constitutive cycling between the plasma membrane and intracellular compartments, with the proportions at the cell surface and in endosomal compartments depending on the relative rates of transporter insertion or removal from the plasma membrane (D'Amico et al, 2007). Consequently, the decreased GLT1 expression at the plasma membrane after LY treatment may be due to increased endocytosis (excessive removal of GLT1 from the cell membrane) or decrease exocytosis (decrease GLT1 delivery to the plasma membrane). In order to distinguish between these two possibilities, we performed uptake experiments in the presence of dynasore, an inhibitor of the clatrin-dependent endocytosis.

As shown in figure 9, in agreement with previous experiments, the incubation with LY294002 alone induced a strong reduction of glutamate uptake, but if this drug is associated with the inhibitor of the endocytosis, the dynasore, there is a complete recovery of the glutamate uptake levels. No appreciable effects were detected in the presence of the dynasore alone.



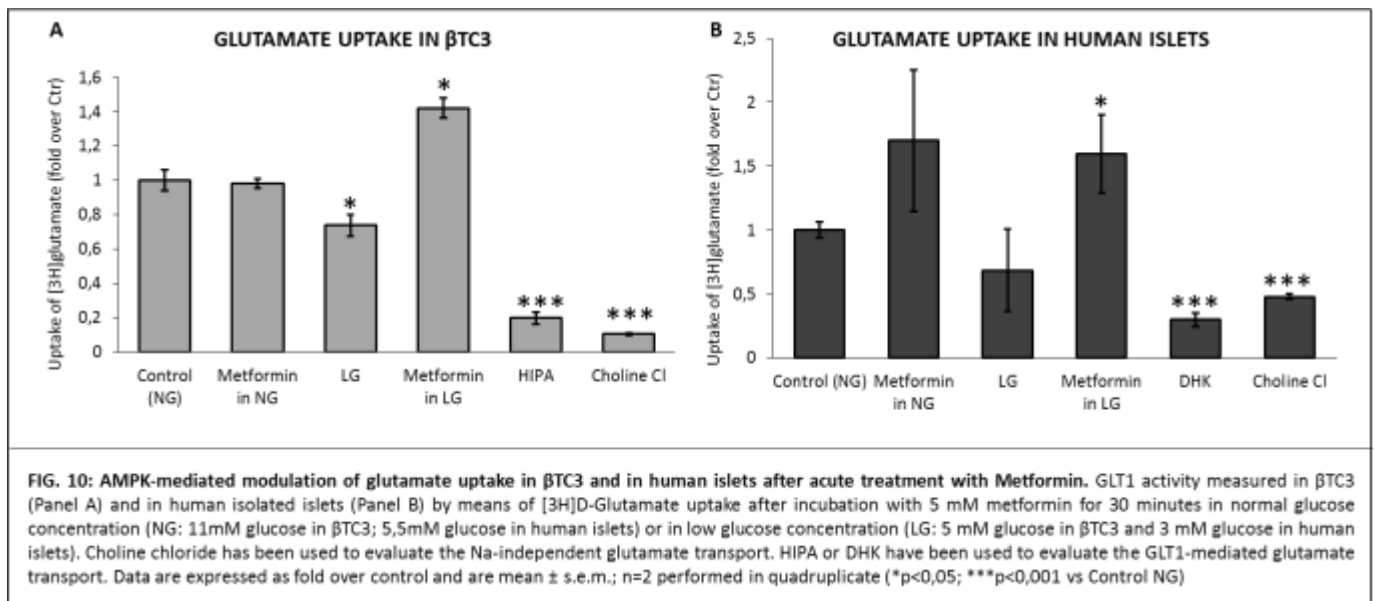
Our data are in agreement with the hypothesis that the surface density of GLT1 is maintained by a dynamic transporter recycling between the plasma membrane and intracellular vesicular pool. The PI3K/AKT pathway normally promotes the delivery of GLT1 to the plasma membrane. If this pathway is downregulated by pharmacological inhibition (LY treatment), the GLT1 protein is constitutively removed, consequently the surface GLT1 localization progressively decreased.

### The role of the AMPK in the GLT1 regulation (Normal and Low Glucose condition)

We finally analyzed the possible mechanisms responsible for glutamate down-regulation in low glucose conditions. We focus on AMPK, a kinase activated in response to stress conditions resulting in ATP depletion such as those observed under low glucose, hypoxia, ischemia and heat shock. As a cellular energy sensor responding to low ATP levels, generally, AMPK activation positively regulates signaling pathways regenerating ATP. It is possible to activate this kinase pharmacologically using molecules such as AICAR and Metformin. Metformin is an anti-diabetic drugs and decreases hyperglycemia primarily by suppressing hepatic gluconeogenesis (Kirpichnikov et al., 2002; Hundal 2000). The molecular mechanism of metformin action is incompletely understood but a direct effect on AMPK activation has been reported (Rena et al., 2013; Burcelin et al., 2013; Foretz et al., 2010).

Therefore in order to verify a possible AMPK-mediated modulation of GLT1, we performed uptake experiments in normal (11 mM) and low (5 mM) glucose conditions and in presence of the anti diabetic and AMPK activator metformin (Met).

The results of uptake experiments are reported in figure 5 as fold increase over control. 30 minutes treatment with low glucose (5 mM) induced a decrease of glutamate uptake in both  $\beta$ TC3 cells and in human isolated islets of Langerhans, but only for the clonal beta cell line, the results were statistically different. In normal growing conditions, no significant modification in glutamate uptake was detected, thus indicating that either AMPK does not play a major role in the control of GLUT1 trafficking and/or activity. Conversely, in low glucose conditions, metformin significantly increased the glutamate uptake, thus suggesting that metformin potentially controls GLUT1 trafficking and/or activity but it can exert its function only in low glucose conditions. Furthermore, given that opposite effects of low glucose (decrease) and metformin (increase) alone on glutamate uptake, it is possible that signalling pathways in addition to AMPK may be active under low glucose concentrations. Similar results were obtained after incubation of human islets of Langerhans (figure 10b). Certainly, other experiments are necessary to understand the complexity of metformin action and the exact molecular target of this drug.



## CHAPTER II

# Regulation of GLUT1 activity and localization in conditions of chronic hyperglycemia

Our data on acute regulation of GLUT1 suggest that alteration in glucose concentrations may alter the GLUT1 activity. Given that diabetes is characterized by hyperglycaemia, the aim of the research presented in Chapter II is to evaluate the activity, expression and localization of GLUT1 in the presence of chronic glucose concentrations and to verify whether dysfunction of GLUT1 may be involved in diabetes pathogenesis.

### INTRODUCTION:

#### ***Glutamate Toxicity in endocrine cells of pancreas***

Glutamate is an important signalling molecule both in the CNS and in the islet of Langerhans, but if its extracellular concentration reaches high levels, the glutamate exerts a potent cytotoxic effect, acting on the same receptors system involved in the normal signalling transmission (excitotoxicity) (Hermanussen et al., 2003; Heywood et al., 1972). Indeed, it has been clearly demonstrated that an excessive activation of iGlu and mGlu receptors in the CNS induces a massive calcium influx, which in turn led to caspase pathway activation and cell death (Guemez-gamboa et al., 2011).

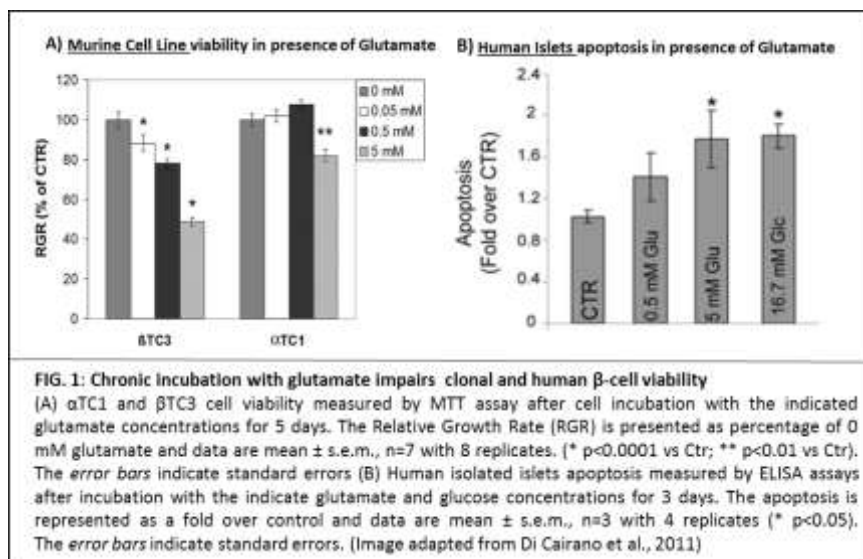
As reported in the general introduction, islet cells express a glutamate signalling system composed of receptors (Weaver et al., 1996; Brice et al., 2002; Molnar et al., 1995; Muroyama et al., 2004), plasma membrane and vesicular glutamate transporters (Bai et al., 2003), therefore also islet cells may be potentially vulnerable to glutamate toxicity. This may be particularly relevant, given that islets are not protected by a blood brain barrier; therefore, they may be potentially exposed to excessive glutamate concentrations derived from islet dysfunction but also from general glutamate metabolism or food consumption.

#### ***Glutamate induced toxicity in pancreatic $\beta$ -cells***

Pancreatic beta cells have many similarities with the neurons, for example the expression of similar transcription factors, specialized proteins involved in synaptic transmissions and neurotransmitters, such as GABA and glutamate (Turque et al., 1994; Furuta et al., 1997; Molnar et al., 1995).

Studies from our laboratory on  $\alpha$  and  $\beta$  cells have shown that an excess of extracellular glutamate concentration (0.5-5 mM glutamate) is toxic selectively for  $\beta$  cells, while it does not induce apoptosis in  $\alpha$  cells

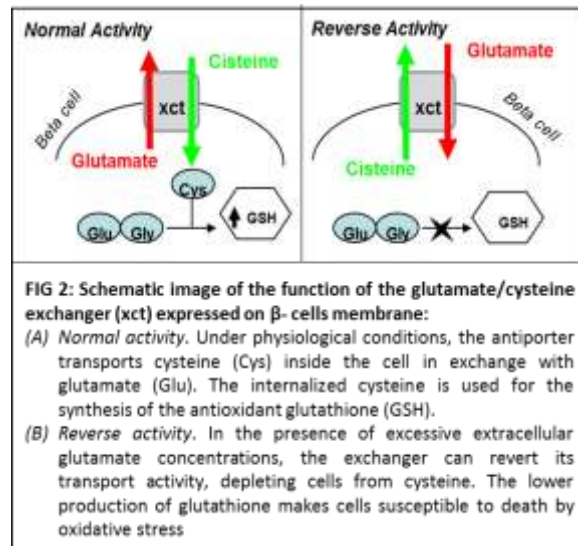
(Figure 1A)(Di Cairano et al., 2011). A similar effect has been observed in human isolated islets after prolonged exposure to glutamate (0.5-5 mM glutamate), (Figure 1B).



Indeed, 3-day exposure of human islets to glutamate induces a progressive β-cell dysfunction characterized by increased insulin secretion under basal conditions, increased proinsulin-to-insulin ratio, typically observed in human islets damaged by chronic exposure to high glucose concentrations. Glutamate also induced a dose-dependent increase of apoptosis that was statistically significant at 5 mmol/L glutamate and quantitatively similar to that observed at high glucose concentrations (16.7 mmol/L) (Di Cairano et al., 2011) (Figure 1B). Glutamate-induced apoptosis was restricted to the β-cells as confirmed by a quantitative electron microscopy analysis: 75% of β-cells of islets exposed to 5 mmol/L glutamate showed severe degenerative features including condensed apoptotic nuclei and numerous cytoplasmic vacuoles, some of which contained dark bodies. Interestingly, α-cells of glutamate-exposed islets were well preserved (Di Cairano et al., 2011).

The mechanisms of cytotoxicity induced by glutamate on the pancreatic beta cells seems however different from that observed in the CNS. Indeed, at least in human islets, it is not prevalently mediated by activation of glutamate receptors but it rather relies on increased oxidative-stress (Gomez-Gamboa et al., 2011). We demonstrated, in fact, that β cell express also a glutamate/cysteine exchanger  $X_{ct}$  (Di Cairano et al, 2011). In physiological conditions, the exchanger transports cysteine inside the cell and glutamate outside the cell (Figure 2, Normal activity),(Albrecht et al., 2010; Lenzen et al., 1996). Excess extracellular glutamate, reverts the direction of the glutamate/cysteine antiporter system  $X_{ct}$ , thus depleting the cells of cysteine, a building block of the antioxidant glutathione (Figure 2, reverse activity). In support of this hypothesis, we observe reduced intracellular glutathione levels in βTC3 cells exposed to high glutamate levels (Bachelor thesis of

Stefania Moretti, “Functional interaction between the glutamate/cysteine exchanger and high-affinity glutamate transporters in the endocrine cells of pancreas”).



The control of glutamate concentration in the intercellular spaces is therefore of crucial importance also in islets of Langerhans. The glutamate levels in the islet depend on:

- a) Plasma glutamate concentrations
- b) Release of glutamate by pancreatic  $\alpha$ -cells
- c) Activity of the glutamate clearance systems

Interestingly, these mechanisms seem to be modified in diabetic and pre-diabetic conditions, thus suggesting that abnormal glutamate homeostasis may play a role in diabetes development.

### A) PLASMA GLUTAMATE CONCENTRATION:

Unlike the CNS, the islet cells are not protected by the presence of a blood brain barrier, therefore the extracellular glutamate concentration in the islet is probably identical to the plasma concentration. The plasma level of this amino acid is the result of glutamate intake via food, and glutamate metabolism in different organs.

The glutamic acid is present in foods as a free form or a polymeric form. It constitutes 22% of animal proteins and approximately 40% of vegetal proteins. Despite glutamate is very abundant in food, its hematic concentration is generally very low because i) it is extensively oxidized by the small intestine to meet the high energy demand of the epithelium and ii) it is rapidly excreted by the kidney (Blachier et al., 2009). In healthy volunteers, nearly all of the enterically delivered glutamate is removed by the splanchnic bed/liver on the first

pass. As a result, the glutamate concentration in the blood, in fasting-state condition, is approximately 50µmol/L, while the glutamine concentration reaches approximately 0,7mmol/L. The circulating glutamine penetrates into the cells where it may be enzymatically converted to glutamate by the glutaminase enzyme. Consequently, the glutamate is more abundant in intracellular environment where it may rise to 20mmol/L. Inside the cells the glutamate is used as energy source after oxidative reactions and is central to numerous transamination and deamination reactions. It has an important role as antioxidant associated with the glutathione synthesis.

The plasma level of glutamate may increase with food. There are food traditionally enriched in glutamate like sauces (soy; Worcestershire), cheese (especially Parmesan), tomatoes, mushrooms, or meat, fish and vegetable stocks and all have the effect of increasing glutamate levels (Yamaguchi and Ninomiya 2000; Yamaguchi 1991; Yamaguchi and Takahashi 1984a,b).

Glutamate is also an important flavor-enhancing compound which provides the “umami” taste to food. Since early 1900s, monosodium L-glutamate (MSG) has been commercially manufactured as a flavor enhancer, and there is ample evidence that adding MSG to suitable foods increases their palatability (Bellisle et al., 1991; Yamaguchi and Takahashi, 1984 a,b) and consumption (Bellisle, 1998; Rogers and Blundell, 1990; Schiffman, 1998). The MSG consumption is increased in recent years (Figure 6) and it is found in significant amounts in a wide variety of foods habitually consumed also by very young children (Prescott, 2004) such as chips and fast food products.

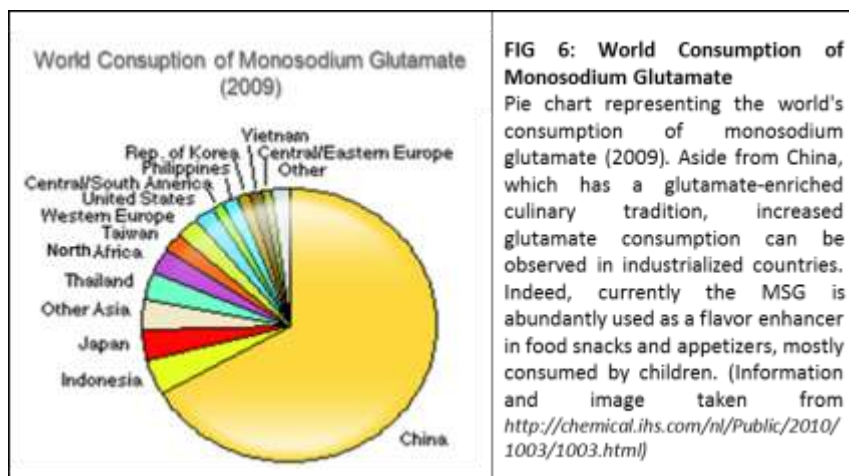
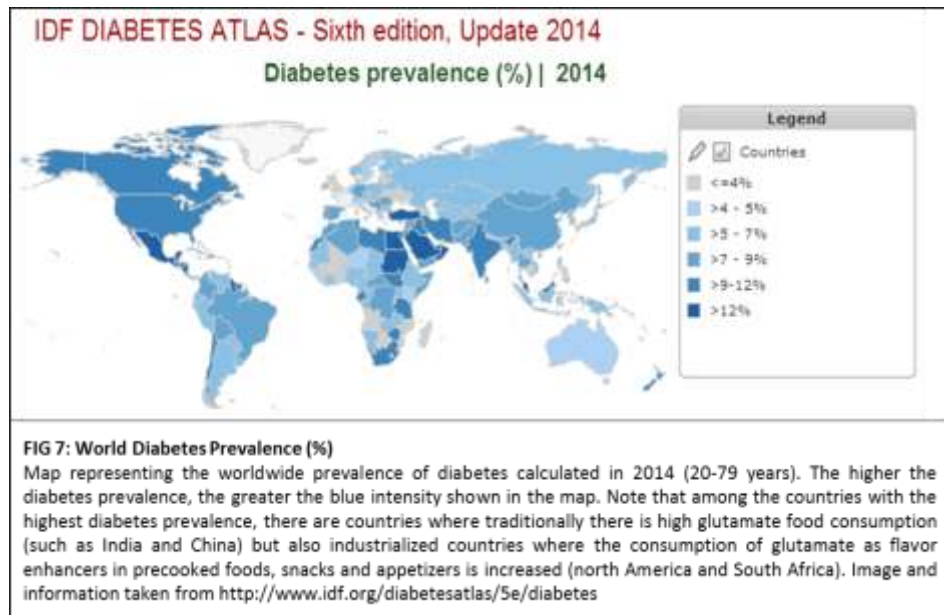


**FIG 6: World Consumption of Monosodium Glutamate**  
 Pie chart representing the world's consumption of monosodium glutamate (2009). Aside from China, which has a glutamate-enriched culinary tradition, increased glutamate consumption can be observed in industrialized countries. Indeed, currently the MSG is abundantly used as a flavor enhancer in food snacks and appetizers, mostly consumed by children. (Information and image taken from <http://chemical.ihs.com/nl/Public/2010/1003/1003.html>)

The comparison of the map of the global consumption of monosodium glutamate (Figure 6) with that of worldwide prevalence of diabetes (Figure 7) shows that the largest number of subjects with diabetes live in countries where cuisine is traditionally rich in glutamate, such as India and China, or in developing countries, where it is well known and documented the increased consumption of snacks, particularly in children and young adults.



It has been demonstrated that an excessive of glutamate consumption with food, mainly in the form of MSG supplementation, may cause obesity and insulin resistance. It is presently unclear whether, under certain circumstances, glutamate-enriched foods may actually increase plasma glutamate to toxic levels and if that in turn may induce  $\beta$ -cell death.

Interestingly, high systemic level of glutamate has been observed also in several pathologies, characterized by inflammation and oxidative stress. In particular, hyperglutatememia has been identified in liver disorders (Fujinami et al., 1990; Vannucchi et al., 1985), obesity (Jeevanadam et al., 1991) in some cancers (Holm et al., 1997; Eck et al., 1989a; Eck et al., 1989b; Droge et al., 1988) patients with HIV (Eck et al., 1989a; Eck et al., 1989b; Droge et al., 1987) and in several neurodegenerative diseases.

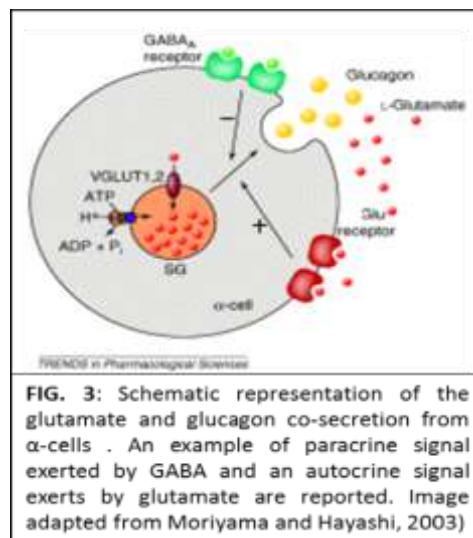
Although the causes responsible for the hyperglutatememia may vary in the different diseases, it is worth mentioning that increased oxidative stress and inflammation are common features of all these conditions and also of T1D and T2D. Platelet activation is present in obesity, metabolic syndrome, T1D, and T2D (Anfossi et al., 2009; Nieuwdorp et al., 2005; Davi et al., 2003; Hu et al., 2004) and it might cause hyperglutatememia in these conditions.

Studies in the last years indicated increased plasmatic glutamate levels also in insulin-resistant non-obese subjects (Tai et al., 2010) in gestational diabetes (Butte et al., 1999) and type 2 diabetic patients (Bao *et al.*, 2009). Analysis of serum metabolite profiles between children who eventually developed T1D and those who remained healthy and autoantibody-free showed a dramatic increase (\*32-fold above normal) in glutamate

levels only in the children who later developed T1D (Oresic et al., 2008). It is presently unknown how these changes might have occurred and how higher levels of circulating glutamate may interfere with T1D initiation.

## B) RELEASE OF GLUTAMATE IN THE ISLET OF LANGERHANS:

Pancreatic  $\alpha$ -cells co-secrete glucagon together with glutamate that, in turn, modulates the secretion of glucagon, insulin, and somatostatin (Bertrand et al., 1993; Brice et al., 2002; Cho et al., 2010; Cabrera et al., 2008; Uehara et al., 2004). In human islets, the glutamate released by  $\alpha$ -cells is a positive autocrine signal for glucagon secretion (Cabrera et al., 2008) and, consequently, for glutamate itself (Figure 3).



$\alpha$ -cell dysfunction and hyperactivity may thus trigger a vicious cycle that maintains and further increases the release of both glucagon and glutamate. The possible role of  $\alpha$ -cells dysfunction in the pathogenesis of diabetes, and in particular of hyperglutamatemia in the islet, is supported by a series of evidences. Plasma glucagon levels are abnormally elevated in T2D subjects, indicating that  $\alpha$ -cell hypersecretion is a common diabetic feature (Mu¨ller et al., 1973; Baron et al., 1987; Reaven et al., 1987; Dunning and Gerich, 2007). Abnormally high fasting glucagon levels, suggestive of  $\alpha$ -cell hypersecretion, have been found also in normoglycemic insulin-resistant obese adults and adolescents (Starke et al., 1984; Solerte et al., 1999; Weiss et al., 2011; Ferranini et al., 2007; Asano et al., 1989). The correlation between body weight and  $\alpha$ -cell mass has never been studied in detail; however, a progressive increase in the  $\alpha$ -cell number, leading to an imbalance between  $\beta$ - and  $\alpha$ -cell mass, is expected to occur in obesity. Recently, a retrospective analysis has been performed in a large baboon population and it has been demonstrated that diabetes development was associated not only with increased  $\beta$ -cell apoptosis and decreased relative  $\beta$ -cell volume but also with significant  $\alpha$ -cell replication and hypertrophy and increased relative  $\alpha$ -cell volume. In baboons,  $\alpha$ -cell proliferation correlated with both hyperglucagonemia and hyperglycemia (Guardado-Mendoza et al., 2009).

Unfortunately, they did not measure plasma glutamate levels therefore we do not know whether they were also hyperglutamemic.

Interleukin-6 (IL6) is a pleiotropic cytokine with metabolic effects (Kamimura et al., 2003) and its levels are chronically elevated in obesity and predictive of T2D development (Spranger et al., 2003; Herder et al., 2005). IL6 is also a potent regulator of cellular proliferation (Kamimura et al., 2003), and the pancreatic  $\alpha$ -cell is a primary target of IL6 function that increases glucagon secretion and stimulates  $\alpha$ -cell proliferation (Ellingsgaard et al., 2008).

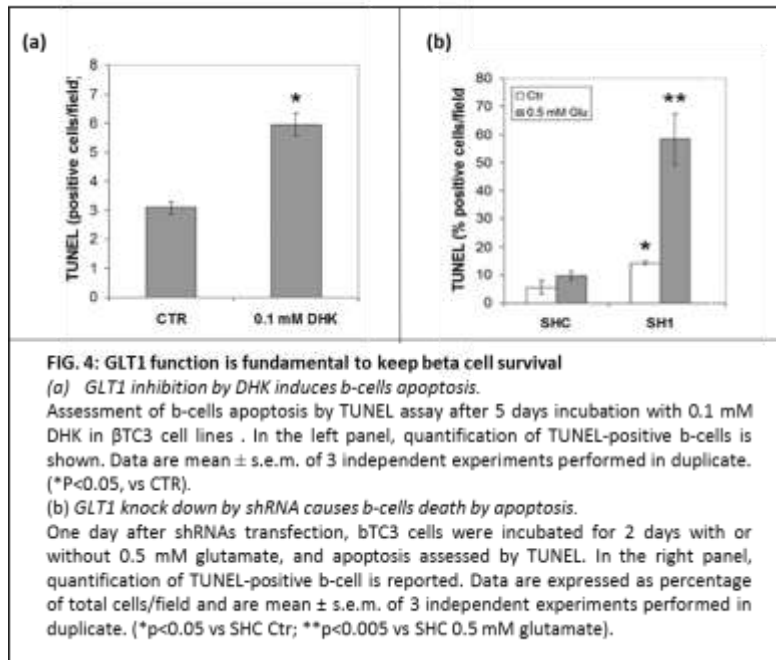
The raising evidence that  $\alpha$ -cells dysregulation is present not only in diabetes, but also in obesity and insulin resistance suggests that hyperglutamemia described in these conditions (Chevalier et al., 2005; Felig et al., 1969; Gougeon et al., 2008; Marliss and Gougeon 2002, Pereira et al., 2008; Tai et al., 2010) may be causally related also to  $\alpha$ -cell hyperactivity.

### **C) GLUTAMATE CLEARANCE IN THE ISLETS: the Glutamate Transporter 1 (GLT1)**

The likely elevated glutamate concentrations in the islet microenvironment, together with the demonstrated vulnerability of human  $\beta$ -cells to this amino acid, justify the presence in the islets of a glutamate clearance system. In fact, also in the islet, the glutamate-mediated cellular responses may be controlled, directly or indirectly, by regulating the amino acid transport across the plasma membrane.

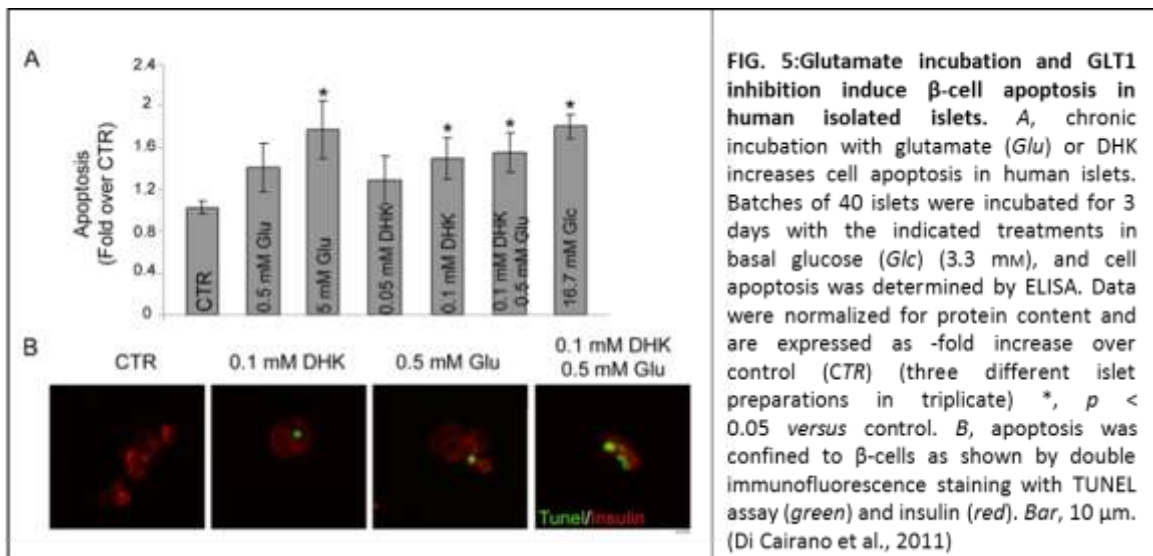
As described in Chapter I, the high-affinity,  $\text{Na}^+$ -dependent GLT1 glutamate transporter is the principal and the most important transporter responsible for glutamate clearance in islets of Langerhans. In both human and monkey pancreas, GLT1 staining was almost exclusively localized to the cell membrane, at cell-cell boundaries of insulin-positive cells. In contrast, we did not observe colocalization of GLT1 with both glucagon and somatostatin, suggesting that  $\alpha$ - and  $\delta$ -cells do not express GLT1 or that, if expressed, it is under the level of detection (Di Cairano et al., 2011).

GLT1 is functional in isolated human islets and is the main regulator of the glutamate clearance in the islets. In fact, selective GLT1 inhibition with the specific inhibitor dihydrokainate (DHK) almost completely blocked the glutamate uptake in human islets (Di Cairano et al., 2011).



GLT1 exerts a key role in the preservation of the  $\beta$  cell survival (and therefore  $\beta$  cell mass) and is essential to prevent the  $\beta$ -cell specific toxicity induced by glutamate (Di Cairano et al., 2011).

Indeed, pharmacological inhibition of GLT1 activity with DHK in  $\beta$ TC3 cell lines and in human islets significantly increased the concentration of extracellular glutamate in the medium and caused a parallel increase in  $\beta$ -cell apoptosis (Di Cairano et al., 2011) (Figure 4 and 5). Similar results were obtained when GLT1 expression was downregulated in  $\beta$ TC3 by means of a short hairpin RNA (shRNA) (Figure 4b). Interestingly, the shRNA constructs increased  $\beta$ TC3 apoptosis also in the absence of glutamate supplementation, suggesting that impaired GLT1 activity “per se” is sufficient to induce  $\beta$ TC3 cell death (Di Cairano et al., 2011).



These data confirm that the GLUT1 function in the islet is to control the extracellular glutamate concentration and to preserve  $\beta$ -cell survival. They also suggest that abnormal function, expression or localization of this transporter may directly cause  $\beta$  cell death.

Our data on acute regulation of GLUT1 suggest that alteration in glucose concentrations may alter the GLUT1 activity. Given that diabetes is characterized by hyperglycaemia, the aim of the research presented in Chapter II was to evaluate the activity, expression and localization of GLUT1 in the presence of chronic glucose concentrations and to verify whether dysfunction of GLUT1 may be involved in diabetes pathogenesis.

Our hypothesis is that that abnormal glutamate homeostasis in the islet due to increased plasma levels but also altered GLUT1 expression and/or activity could cause elevated extracellular glutamate concentrations in the islets that, in turn, may contribute to  $\beta$ -cell death.

The study has been performed in human isolated islets (collaboration with Dr Bertuzzi, Niguarda hospital, Milan). They currently represent the best model to study islet physiopathology. Indeed, they are more physiological if compared with immortalized cell lines, and more suitable than murine islets for studies on paracrine interactions. Furthermore, human islets have a peculiar arrangement of endocrine cells, a specific repertoire of channels and receptors and it is becoming increasingly evident that our knowledge on rodent islet cannot be automatically translated in humans.

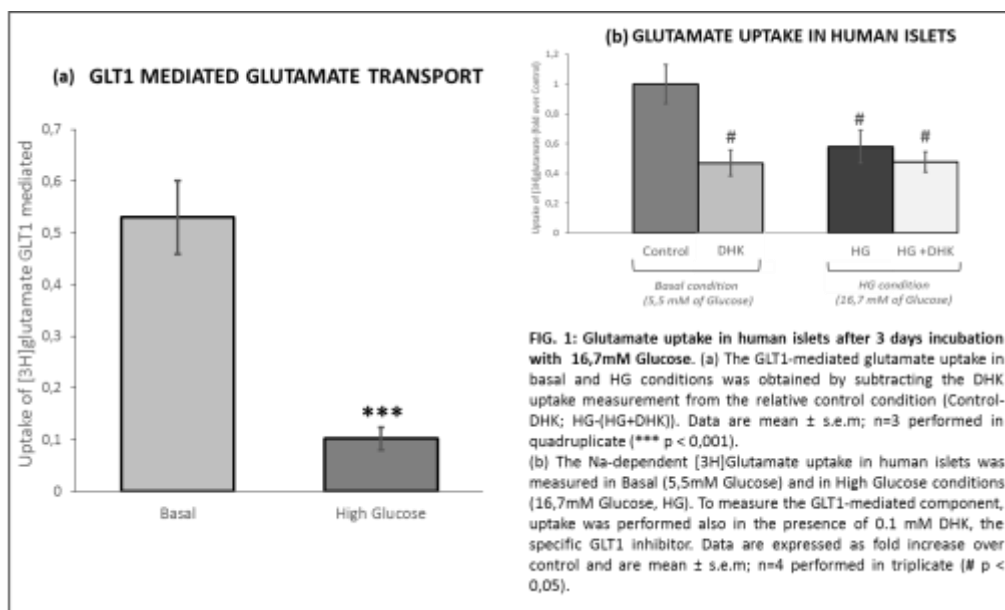
## RESULTS

In Chapter I we have shown that rapid alterations of extracellular glucose concentrations modulate the surface activity of GLUT1. In diabetes mellitus there is a chronic alteration of blood glucose levels. Given the susceptibility of  $\beta$  cells to glutamate and given the key role of GLUT1 in maintaining glutamate homeostasis in the islet, in this chapter we evaluate the effects of long-term exposure to high glucose concentrations on GLUT1 activity and localization.

We exposed human islets for three days to 16.7 mM glucose (a concentration that mimic hyperglycaemic conditions (Davalli et al, 1991)) in normal growing medium and then we evaluated the effects on GLUT1 expression and activity by means of functional experiments and immunolocalization assays.

### **3 days treatment with high glucose drastically reduces glutamate uptake in human islets**

Functional experiments, by means of uptake assays using radiolabel glutamate were performed to test the possible effects of long term exposure to glucose on GLUT1 activity. As shown in figure 1b, in human islets we measured a  $\text{Na}^+$ -dependent glutamate uptake that was drastically inhibited (> 50% reduction,  $p < 0.05$ ) by DHK, the selective GLUT1 inhibitor, indicating that also in the islet, GLUT1 represents the principal glutamate clearance system. The long-term exposure of human islets to hyperglycaemic conditions (16.7 mM glucose, HG) resulted in a significant reduction of glutamate uptake. No further reduction was observed in the presence of DHK, thus indicating that chronic hyperglycaemia abolished the GLUT1-mediated glutamate transport in the islet (Figure 1a b).

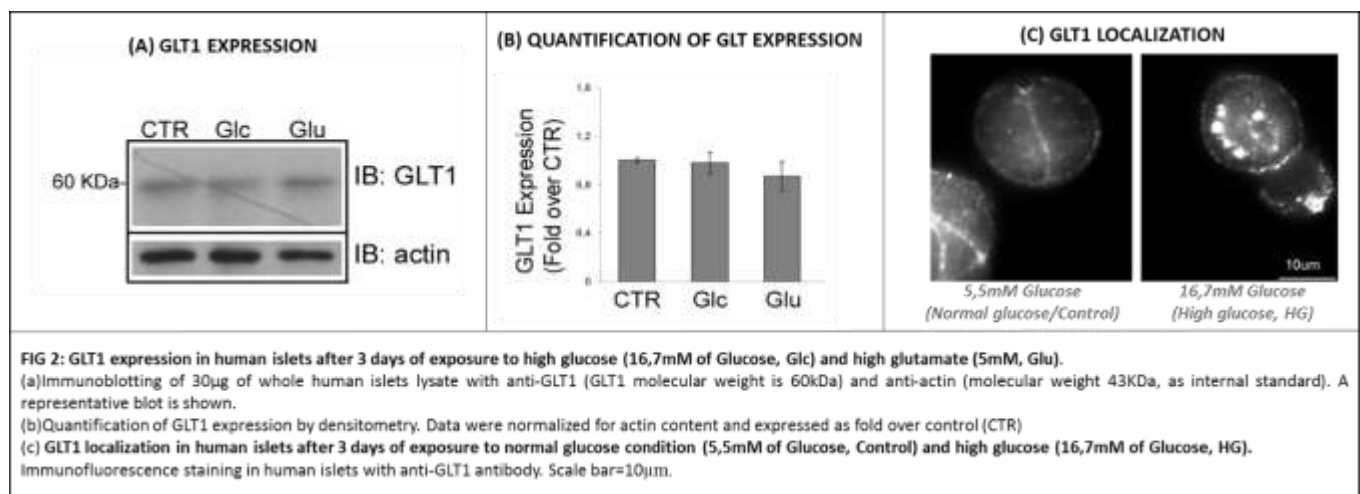


**The chronic incubation with high glucose does not affect the total expression of GLUT1 but induces its relocalization in vesicular compartments**

The reduction of GLUT1-mediated transport activity revealed by uptake experiments, may be due to changes in the total GLUT1 expression (for increased protein degradation or decreased transcription) or to modifications of GLUT1 trafficking, as observed in acute glucose treatments. To discriminate between these two mechanisms we evaluated the GLUT1 expression and localization in normal and high glucose.

Western blot experiments were performed to verify the expression of GLUT1 after chronic glucose treatments (Figure 2A and B). The human isolated islets were incubated for three days with 16,7mM glucose and then, after lysis, lysates were loaded and immunoblotted with an anti-GLUT1 specific antibody (Perego et al, 2000). We used actin as a control of correct protein loading. Figure 2A showed that the chronic treatment with high glucose did not affect the total expression of GLUT1, which was comparable to that obtained in control conditions (5.5 mM glucose) (figure 2B).

We then evaluated the GLUT1 localization to investigate the possible implications of traffic mechanisms (Figure 2C). Three days after incubation in 16.7 mM glucose, islets were fixed and the localization of GLUT1 detected by means of the anti-GLUT1 specific antibody. While in normal conditions (5,5mM of glucose) the transporter well localized on the cell surface, 3 days incubation with high glucose determined an evident accumulation of GLUT1 in intracellular compartments (Figure 2C). These data suggest that the hyperglycaemia does not act on the GLUT1 synthesis or degradation but probably induces changes of the transporter trafficking between the plasma membrane and intracellular pool, resulting in its cytoplasmic accumulation.

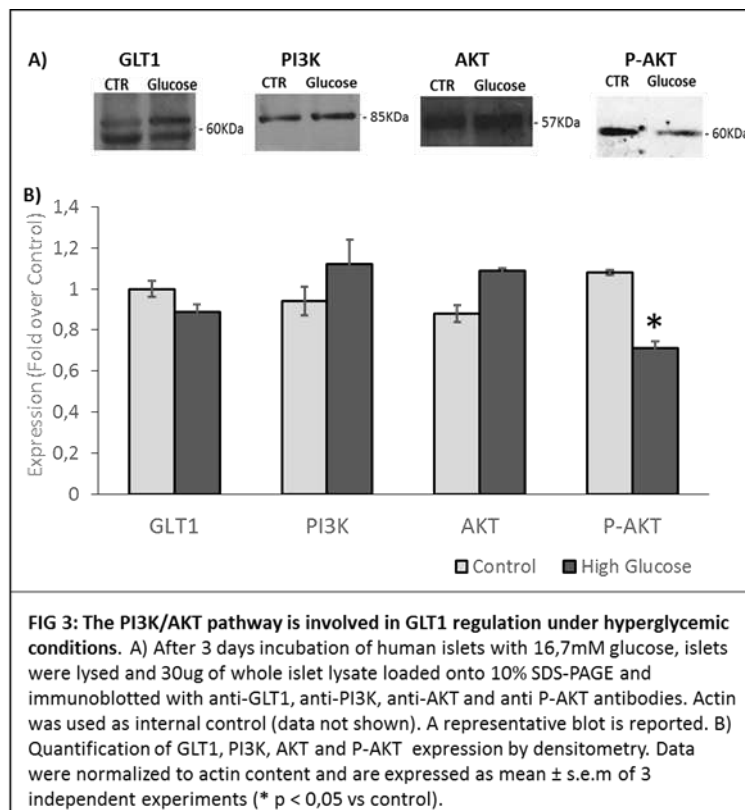


### **The PI3K/ AKT pathway is involved in the regulation of GLUT1 membrane trafficking after 3 days incubation in 16.7 mM glucose**

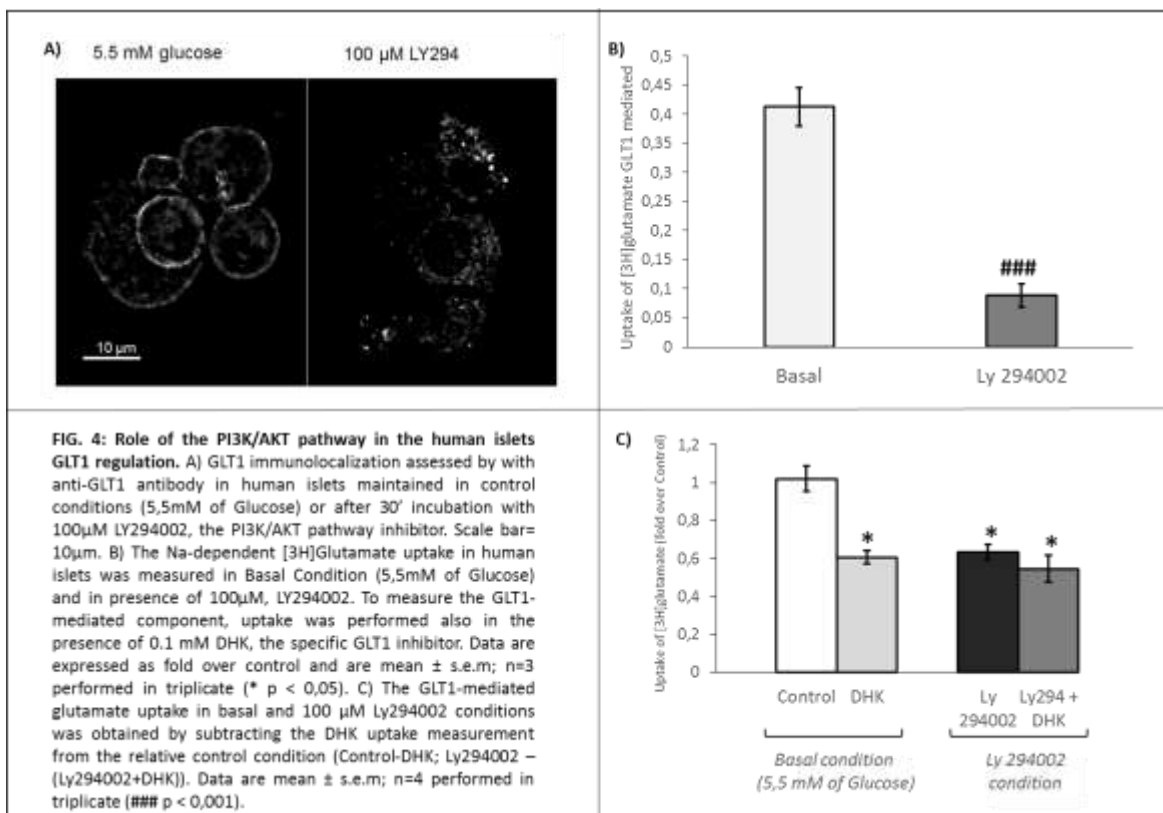
We then studied the molecular mechanisms responsible for this downregulation. In particular, we focused on the PI3K/AKT pathway because:

- 1) it is known to regulate GLUT1 trafficking in the CNS (Davis et al., 1998; Duan et al., 1999; Nieoullon et al., 2006) and in  $\beta$ TC3 cells (Chapter 1)
- 2) this pathway is severely downregulated in  $\beta$ -cells lines exposed to high glucose and in patients with type 2 diabetes mellitus (T2DM) (Hribal et al., 2003; Folli et al., 2011).

To verify the involvement of this pathway in GLUT1 membrane relocalization we first analyzed the expression of proteins involved in the PI3K/AKT cascade (Figure 3). In particular, we analyzed the total expression of PI3K, AKT and the phosphorylated form of AKT (Threonin 308) (Figure 3A), which represents the active form of this enzyme. The expression was evaluated by means of western blot experiments after 3 days of incubation with 16,7 mM glucose (Figure 3A). The results are reported in figure 3. As shown in panel B, hyperglycaemic conditions did not affect GLUT1, AKT or PI3K total expression, but induced a significant reduction of phospho-AKT, indicating that this pathway is strongly downregulated in chronic high glucose conditions.



To confirm the possibility that PI3K may be involved in the GLUT1 relocalization, we evaluated the activity and localization of GLUT1 in human islets after incubation with LY249002, a blocker of the PI3K cascade (Figure 4). After 30 minutes of treatment with the LY294002 blocker, we obtained an analogous relocalization of GLUT1 to that obtained with the chronic high glucose treatment (Figure 4A). The GLUT1 transporters accumulated in intracellular vesicular compartments similar to those observed in chronic hyperglycaemic conditions. The accumulation of GLUT1 in cytoplasmic compartments may be associated to a decrease in the transporters density at the plasma membrane and consequently, a reduction in the glutamate transport activity. To test this hypothesis, we performed functional assays (Figure 4B and 4C). Isolated islets were pre-incubated for 30 minutes with the LY294002 inhibitor, and glutamate uptake experiments were performed in the presence of a Na-gradient. The inhibition of PI3K/AKT pathway caused a significant reduction of radiolabelled glutamate accumulated within the islets (Figure 4B).



To verify whether the effect of LY29400 on glutamate uptake was mediated by GLUT1 or other transporter systems, we performed the experiments also in the presence of the selective GLUT1 inhibitor DHK (0.1 mM). As shown in panel C, LY294002 completely abolished the GLUT1-mediated glutamate uptake, thus indicating that GLUT1 is the main target of PI3K inhibition (Figure 4C).

Taken together, these data indicate that relocalization of GLUT1 transporter in intracellular compartments and inhibition of glutamate uptake observed in hyperglycaemic conditions is likely caused by inhibition of the PI3K pathway in human islets.

**Altered GLUT1 localization in islet of Langerhans of Type 2 diabetic patients**

Our previous data demonstrated that the chronic exposure of human islets to high glucose caused a reduction of GLUT1 density and activity at the cell membrane. Chronic hyperglycaemia is a characteristic feature of both type 1 and type 2 of diabetes, to verify whether this relocalization may occur also *in vivo* we analysed the localization of GLUT1 in the pancreas of type 2 diabetic patients (collaboration with Dr. La Rosa Stefano, Ospedale di Circolo, Varese).

We carried out immunohistochemistry experiments on pancreases from 5 normal subjects and 10 T2D patients using the specific anti-GLUT1 antibody. The personal and clinical characteristic of the different subjects are reported in figure 5a.

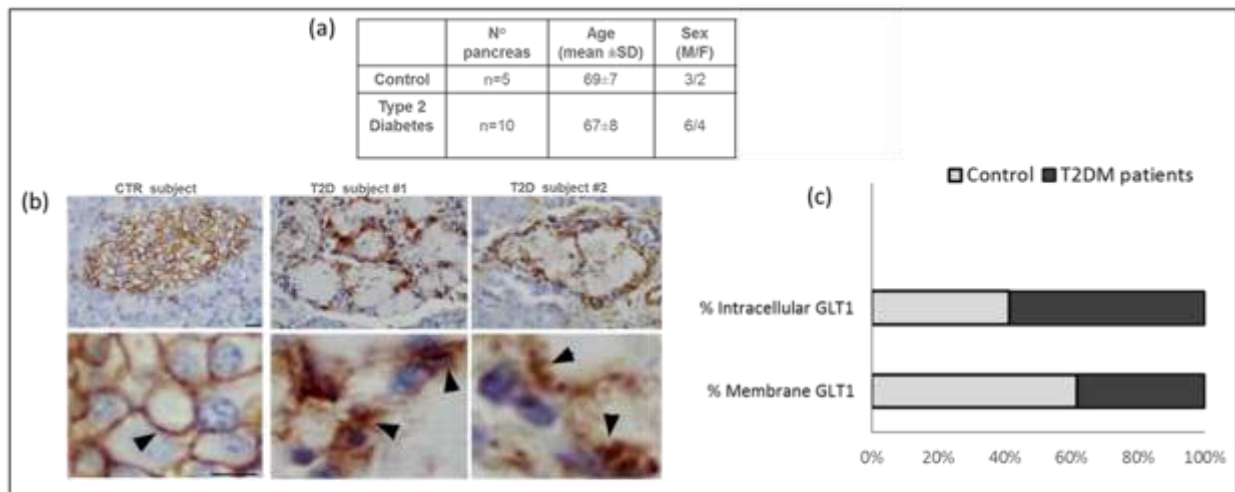


**FIG. 5: GLUT1 expression and localization in pancreas sections from healthy subjects and T2DM patients.**  
 (a) Characteristic of Control and Diabetic subjects (Age and Gender)  
 (b) Personal and clinical average characteristics of controls and T2DM patients studied. Data are given as mean value ± SD; b) Immunohistochemistry staining of human pancreas sections from controls and T2D subjects with a selective anti-GLUT1 antibody. Sections were counterstained with Mayer’s haemalum, to stain cytoplasm and nuclei. The 40x (upper panels) and 100x (lower panels) image magnifications are shown. In the 100x images, arrows indicate the plasma membrane localization and arrowheads the clustered intracellular localization of GLUT1.  
 (c) Quantification of the localization of GLUT1 in pancreas section. The histogram shows the % of GLUT1 at the cell membrane and the % of GLUT1 in intracellular compartments in control and in T2DM pancreas

Pancreases from normal subjects confirmed GLUT1 expression selectively in the islet, at the cell membrane, as indicated by the brown colour accumulated at cell-cell boundaries in the majority of the islet cells (Figure 5b, CTR subject). In contrast, type 2 diabetic pancreases revealed an altered expression of GLUT1. In particular, in the representative images of figure 5b (T2D subjects) it is evident that GLUT1 was not exclusively expressed at

the plasma membrane but it was also present in intracellular compartments (Figure 5b). For each subject, we examined at least 30 different islets, and we counted the number of cells within the islet with GLT1 staining at the plasma membrane over the total number of cells positive for GLT1 (Figure 5c). The percentage of cells having GLT1 staining at the plasma membrane [number of cell with membrane GLT1/ total number of cell in the islet expressing GLT1] or in intracellular compartments [number of cell with intracellular GLT1/ total number of cell in the islet expressing GLT1] in control and diabetic subjects is reported in 5C. We found that the 52 % of GLT1 positive cells in control subjects have GLT1 at the cell surface (and 47% intracellular GLT1) while in the type 2 diabetic subjects the percentage of membrane GLT1 is reduced to 32.4% (the remaining 67,6% is intracellular).

As only plasma membrane GLT1 can be functional for glutamate clearance, this suggests that the glutamate clearance activity is impaired in the islets of a subset of T2D patients and may contribute to the progressive  $\beta$ -cell dysfunction.

#### ***Ceftriaxone treatment causes GLT1 upregulation in human isolated islets***

Having demonstrated the relocalization of GLT1 in pancreas sections from diabetic patients, we evaluated the possibility of considering GLT1 as a pharmacological target to preserve  $\beta$ -cell mass in diabetes mellitus.

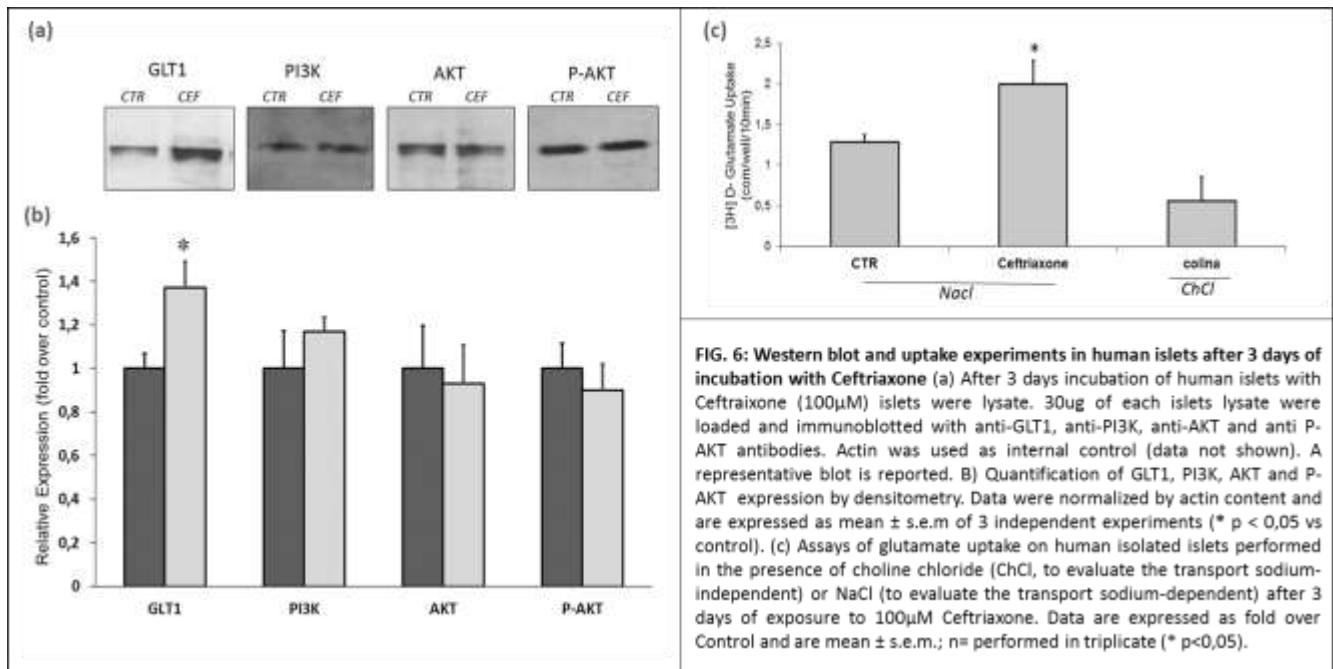
Given the role of GLT1 in preserving the  $\beta$ -cell viability and the evident downregulation of GLT1 activity induced by hyperglycaemia, we reasoned that up-regulating GLT1 expression could represent a good strategy to prevent glutamate toxicity and  $\beta$ -cell death. A well known up regulator of GLT1 expression in the CNS is ceftriaxone (Rothstein et al., 2005; Lipski et al., 2007; Miller et al., 2008; Nicholson et al., 2014). Ceftriaxone is commonly used as third-generation cephalosporin antibiotic ( $\beta$ -lactam antibiotic), but is also able to increase brain GLT1/EAAT2 expression and activity. Different papers have shown the efficacy of this molecule in inducing neuro-protection in models of ischemic injury, radicular pain, Huntington's disease and motor neuron degeneration, by protecting the nervous system from excitotoxicity (Rothstein et al., 2005; Lipski et al., 2007; Miller et al., 2008; Nicholson et al., 2014).

Therefore, we first verify the effects of chronic treatment with Ceftriaxone on GLT1 expression and activity in human islets (Figure 6). The human islets were incubated for three days with 100uM Ceftriaxone and then we evaluated the GLT1 expression by means of western blot experiments and the GLT1 activity by means of uptake experiments.

As reported in figures 6a and 6b, western blot experiments revealed that also in the islets, the  $\beta$ -lactamic antibiotic treatment induced a statistically significant increase of GLT1 expression (Figure 6b). The increase was

GLT1 specific and was not detected on other proteins involved in the PI3K/AKT signalling cascade: PI3K, AKT and P-AKT.

We then performed uptake experiments in the same experimental conditions (Figure 6c). The uptake experiments confirmed the GLT1 upregulation, because increased glutamate uptake was detected after long-term incubation with 100µM of ceftriaxone (Figure 6c).



### ***β cell death can be pharmacologically prevented by treatment with Ceftriaxone***

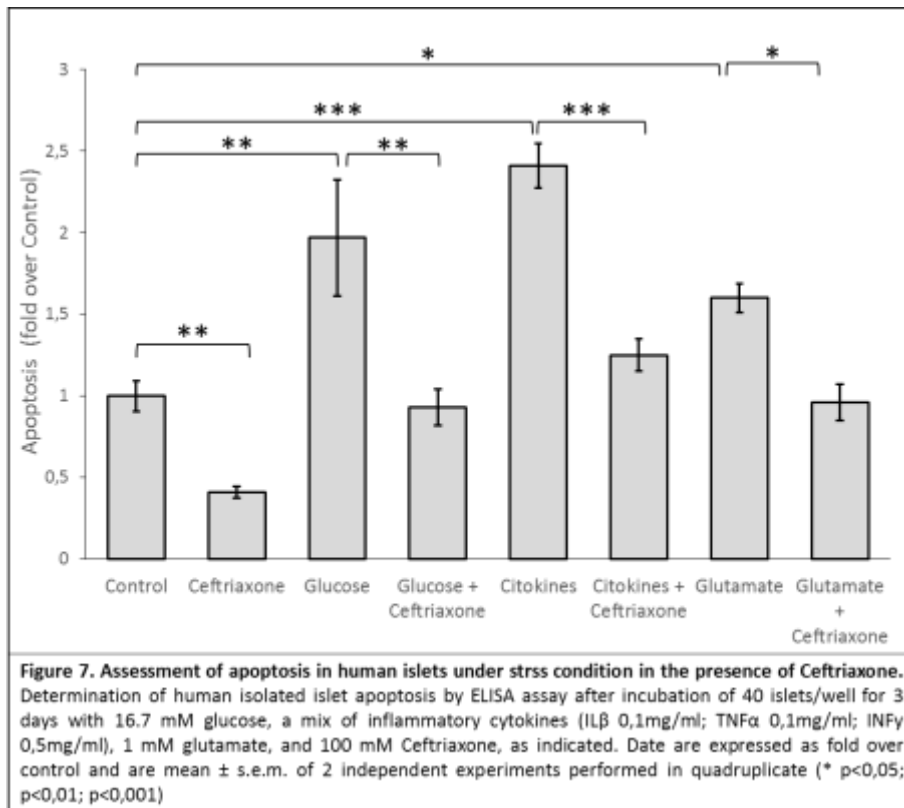
Having demonstrated the upregulation of GLT1 in human islets after ceftriaxone treatment, we evaluated also the effects on pancreatic cells apoptosis. We evaluated cell apoptosis by ELISA assay in human islets incubated for 3 days with 100µM ceftriaxone in the presence or absence of known β-cell insults: high glucose (16.7 mM), inflammatory cytokines (a mix of inflammatory cytokines: ILβ 0,1mg/ml; TNFα 0,1mg/ml; INFγ 0,5mg/ml) and glutamate (1 mM). Data are reported in figure 7. As expected, the exposure to glucose, glutamate or a mix of inflammatory cytokines dramatically increased apoptosis compared to the control sample.

Co-incubation with ceftriaxone reduced the cell apoptosis induced by the presence of chronic high glucose, glutamate and a mix of inflammatory cytokines. We achieved a statistically significant difference in all the experimental conditions tested (Figure 7).

Of note, ceftriaxone was able to reduce cell death also in normal growing conditions, thus indicating that alteration of glutamate homeostasis can be a common component of islet stress.

Although islet cells are a heterogeneous population, we have already shown that apoptosis in this model is almost exclusively due to  $\beta$ -cell death (Federici et al, 1999; Di Cairano et al, 2011), therefore our data can be considered in good approximation due to modification of  $\beta$ -cell apoptosis.

Taken together our data confirm that GLT1 is a key protein to control beta cell viability and a promising therapeutic target to prevent  $\beta$  cell death in diabetes.



# CHAPTER I and CHAPTER II

## DISCUSSION

Endocrine cells of the islet use a sophisticated system of endocrine, paracrine and autocrine signals to synchronize their activities, among these is glutamate. There are two main reasons that attracted us in the study of glutamate signalling within islets of Langerhans:

- 1) It modulates hormone secretion, therefore it is required to fine tune islet function in response to the body demand
- 2) It controls  $\beta$ -cell viability, therefore it may be implicated in islet of Langerhans pathology.

Although glutamate-mediated signalling has been recognised as a modulator of islet function the characterization of proteins involved in its signalling pathway is still incomplete. In particular, our knowledge of the clearance system is still poor.

In a previous study, the high affinity plasma membrane glutamate transporter GLUT1 was identified as the main regulator of the extracellular glutamate clearance in the islet, and here we investigated the molecular mechanisms responsible for its regulation and function. In particular, given the key role of glutamate in controlling hormones release and  $\beta$ -cell viability, we first verify the impact of physiological acute changes of glucose concentrations on the GLUT1 transporter localization and function, and then we focus on the pathological state when the islet is chronically exposed to hyperglycaemia.

### ***Short-term glucose treatments (chapter 1).***

We demonstrated that the GLUT1 transport activity is finely tuned by short-term changes in extracellular glucose concentrations.

By means of uptake assays using [ $^3$ H]D-glutamate, in chapter 1 figure 2A, we show that GLUT1 activity is modified by alterations of glucose concentrations in the medium.

This modification does not involve the change in GLUT1 expression, but rather the alteration of GLUT1 trafficking. Indeed, experiments of immunofluorescence staining and time lapse TIRF microscopy demonstrate that the progressive disappearance of GLUT1 from the cells surface is concomitant to the transporter recruitment in intracellular compartments (figure 2B and 3).

We investigate the mechanisms responsible for such as modification and we found the involvement of PKC PI3K/AKT and AMPK pathways.

In particular, the results reported in chapter 1, figures 4 and 5, indicate that PKC controls the surface activity of GLT1. Indeed, PKC activation by TPA decreases the glutamate uptake in  $\beta$ TC3 cells.

It is known that PKC is expressed in  $\beta$ -cells and its activation is required to drive the first phase of insulin release under glucose stimulations. PKC seems to be involved also in the high glucose-induced relocalization of GLT1. Indeed, PKC inhibition by Bisindoleamide pre-treatment prevents the glutamate uptake downregulation induced by 20 mM glucose incubation.

Taken together these data indicate that high glucose activates PKC and this in turn induces GLT1 downregulation via inhibition of GLT1 activity and/or promotion of GLT1 endocytosis.

Our data show that also the PI3K/AKT pathway controls GLT1 activity. Functional, pharmacological and cellular approaches suggest that the PI3K/AKT pathway is involved in GLT1 exocytosis (Figures 6-9).

Indeed, the PI3K inhibition with the selective inhibitor LY294002 results in a time and dose-dependent reduction of GLT1 activity, measured by means of uptake experiments. As for the glucose treatment, we evaluated the pEGFP-GLT1 localization in transfected  $\beta$ TC3 by means of time lapse experiments under epifluorescence and TIRFM microscopy. In agreement with uptake experiments, we found that 100 $\mu$ M LY294002 causes the progressive reduction of the GLT1 fluorescent signal at the plasma membrane and its concomitant appearance in intracellular vesicular compartments.

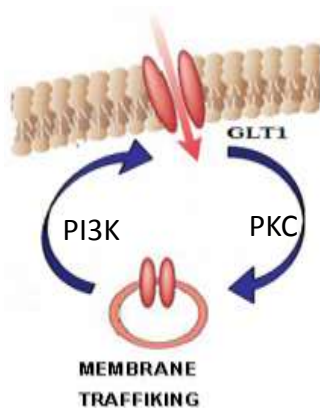
The decreased GLT1 expression at the plasma membrane observed after LY294002 treatment may be due to excessive removal of GLT1 from the cell membrane or decrease GLT1 delivery. By uptake experiments, we found that dynasore, the specific inhibitor of the clathrin-dependent endocytosis, prevents the LY294002-induced decrease in GLT1 surface activity.

Although these experiments are not conclusive, we favour the hypothesis that the PI3K/AKT pathway normally promotes the delivery of GLT1 to the plasma membrane. If this pathway is downregulated by LY294002 treatment, the GLT1 protein is progressively removed from the cell surface and accumulates in recycling compartments. In the presence of dynasore, also the endocytosis is inhibited and the density of GLT1 at the plasma membrane remains constant.

### ***Dynamic modulation of GLT1 localization and activity***

Based on these data, we propose that the surface density of GLT1 is controlled by cycling between the plasma membrane and intracellular compartments, with the proportions at the cell surface and in endosomal

compartments depending on the relative rates of transporter insertion or removal from the plasma membrane (Robinson et al., 1999; Bala et al., 2007). Our data indicate that modification of glucose concentrations in the extracellular medium may rapidly modify the density of transporter at the plasma membrane, by changing the rate of GLUT1 exocytosis or endocytosis. The process is mediated by activation of signalling pathways, namely PI3K/AKT, PKC and AMPK. This fine modulation is necessary to allow the glutamate to act as autocrine and paracrine messenger in the islets but also serves to prevent the excessive permanence of this amino acid in the islets extracellular microenvironment, where it may reach toxic concentrations for the pancreatic  $\beta$ -cells.



In particular, in  $\beta$ TC3 cells, PI3K/AKT activation promotes GLUT1 exocytosis, while PKC activation its endocytosis. In physiological conditions, the action of PI3K prevails, and the transporter is mainly localized on the plasma membrane where it can transport glutamate and control its extracellular concentration. When the extracellular glucose concentration rises, PKC is activated, and the transporter internalized in intracellular compartments.

The consequences of this relocalization are not completely understood. In the context of the islet physiology, glutamate is an important paracrine signals that positively modulates the somatostatin secretion via ionotropic glutamate receptors. Being GLUT1 the main regulator of extracellular glutamate concentration, its relocalization in intracellular compartments would potentiate the activation of glutamate receptors on  $\delta$ -cells, thus stimulating the somatostatin release.

### ***Long-term glucose treatments (Chapter II)***

In chapter II we evaluated the localization and activity of GLUT1 in human islets, after 3 days treatments with 16.7 mM glucose, a state of long-term hyperglycaemia that simulates diabetic conditions. In these experiments, we used the human islets of Langerhans that we consider the best model to study islets physiopathology.

Our data show that 3 days incubation with high glucose (16,7mM) determines an almost complete reduction of GLUT1 surface activity measured by [ $^3$ H]D-glutamate uptake, in human islets (figure 1). Again, we did not find modification of GLUT1 expression (evaluated by means of western blot experiments) (figure 2). Similarly to the acute high glucose treatment, we observed a relocalization of GLUT1 in intracellular compartments. We investigate the mechanisms of this relocalization and we focus on the PI3K/AKT pathway. Indeed, it is well known that this pathway is severely downregulated in  $\beta$ -cells lines exposed to high glucose and in patients with type 2 diabetes mellitus (T2DM) (Hribal et al., 2003; Folli et al.,2011).

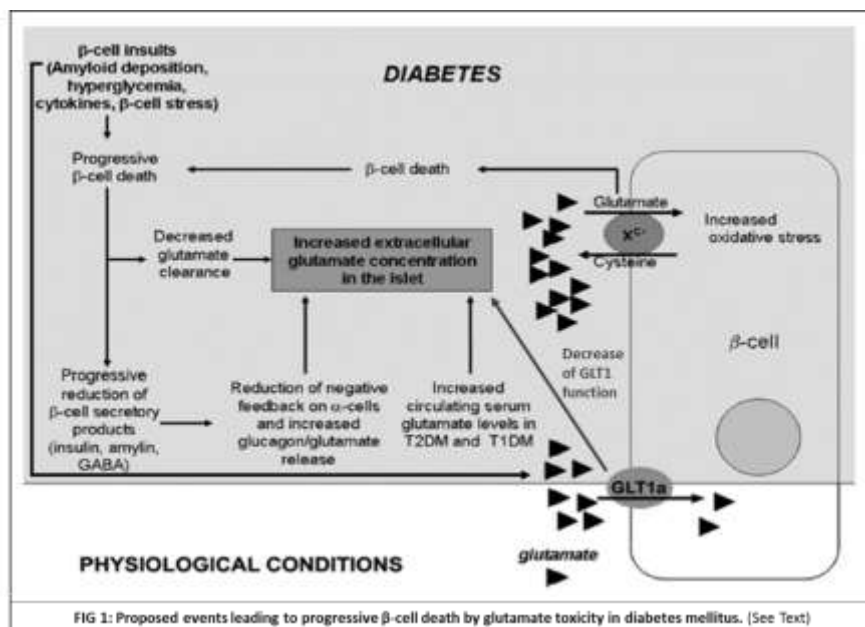
By means of western blot assays we were able to demonstrate that the PI3K/AKT pathway is indeed downregulated in chronic hyperglycaemic conditions. Furthermore, inhibition of PI3K with LY249002 caused a relocalization of GLUT1 very similar to that observed in chronic hyperglycaemia also in human islets.

In conclusion, these data confirm that long-term exposure to glucose severely down regulated the PI3K/AKT pathway. As a consequence, the GLUT1 surface activity decreases and the extracellular glutamate concentration progressively raises. This may perturb glutamate homeostasis within the islet inducing  $\beta$ -cell death.

Chronic hyperglycaemia is a typical feature of both type 1 and type 2 diabetes, two diseases characterized by progressive  $\beta$ -cell dysfunction and death. Given the key role of GLUT1 in the control of  $\beta$ -cell viability, we hypothesised that its expression may be altered in patients with diabetes, and this in turn may contribute to  $\beta$ -cell death.

Coherently with this hypothesis, we found that GLUT1 localisation is altered also in pancreases of type 2 diabetic patients. In particular, the plasma membrane localisation of GLUT1 in the majority of islet cells is lost and the transporter accumulated in intracellular compartments, where it can not accomplish its function. In the microenvironment of the islets, this would probably results in alteration of glutamate homeostasis. Although these evidences need further support, they certainly suggest that the GLUT1 transporter may play a role in diabetes.

### ***The possible role of an altered glutamate homeostasis in Diabetes pathology***



Our hypothesis is that in physiological condition, the extracellular glutamate concentration in the islet of Langerhans is controlled by the activity of GLUT1 (Figure 1, *white part*). Early, in the progression of T2DM (Figure

1, *grey part*) islet's  $\beta$ - to  $\alpha$ -cell ratio changes in favour of  $\alpha$ -cell and this may perturb islets glutamate homeostasis. In diabetes mellitus in particular, a combination of insults (inflammatory cytokines, hyperglycaemia, etc.) may decrease the glutamate clearance in the islet (directly, targeting GLUT1, or indirectly by triggering  $\beta$ -cell death). Consequently, the extracellular glutamate concentration in the islet is modified because increases its release via  $\alpha$ -cells and decreases its clearance via GLUT1 and  $\beta$ -cells. Increased glutamate levels may cause  $\beta$ -cell death, thus triggering a vicious cycle that further increases the glutamate levels in the islet of Langerhans and  $\beta$ -cell death (Figure 1, *grey part*). Also an excessive consumption of glutamate-enriched food can help in increasing the amino acid concentration in the islets microenvironment and in triggering the vicious circle.

The hyperglutamatemia described in diabetic and obese subjects is generally ascribed to abnormal proteins metabolism in liver and muscle and excessive glutamate release by activated platelets. However, accumulating data in favour of the presence of  $\alpha$ -cell dysfunction and hyper-secretion in diabetes, obesity, and insulin resistance, together with our evidence that the glutamate clearance mediated by GLUT1 is reduced under hyperglycaemia suggest that also an alteration of the glutamate signalling in the islets microenvironment may contribute to hyperglutamatemia.

Our data highlight that hyperglutamatemia might be considered a novel  $\beta$ -cell insult, and its toxic effects may be more devastating on genetically fragile  $\beta$ -cells. Moreover, as hyperglutamatemia influences the immune system in genetically predisposed subjects, it might also foster  $\beta$ -cell autoimmunity.

### ***GLT1 as a pharmacological target to prevent $\beta$ -cell death***

We provide evidence that GLUT1 may be also an important pharmacological target to prevent  $\beta$ -cell death. In our study we used Ceftriaxone, a  $\beta$ -lactamic known for its ability to increase GLUT1 expression in neurons and to provide neuroprotection against excitotoxicity in the CNS (Rothstein et al., 2005; Lipski et al., 2007; Miller et al., 2008; Nicholson et al., 2014).

We provide evidence that this compound is active also in human islets where it upregulates GLUT1 expression and activity. Interestingly, Ceftriaxone significantly reduces  $\beta$ -cell death induced by long-term exposure to high glucose, inflammatory cytokines or excessive glutamate; all of them characteristics of diabetes mellitus. Of note, ceftriaxone was able to reduce cell death also in normal growing conditions, thus indicating that alteration of glutamate homeostasis can be a common component of islet stress.

Ceftriaxone and other compounds capable to increase GLUT1 expression or/and activity, may represent novel therapeutic strategies to achieve  $\beta$ -cell cytoprotection.

Interestingly, all the antidiabetic drugs with known  $\beta$ -cell cytoprotective effects such as GLP-1, exenatide, and glitazones (Cunha et al., 2009; Tsunekawa et al., 2007; Walter et al., 2005) show also significant neuroprotective activity (Perry et al., 2007; Harkavyi and Whitton, 2010; White and Murphy, 2010) against glutamate-induced cytotoxicity (Perry et al., 2002). Further, glitazones-mediated neuroprotection is associated with increased GLT1 expression (Romera et al., 2007; Thal et al., 2011).

Therefore, prevention of glutamate toxicity may be an additional mechanism by which these drugs exert their beneficial effect on the  $\beta$ -cells. Similar conclusions can be drawn by considering the case of topiramate, an antiepileptic agent that provides neuroprotection by counteracting glutamate toxicity (Angehagen et al., 2003; Follett et al., 2004) but it has also significant antidiabetic and  $\beta$ -cell cytoprotective effects (Toplak et al., 2007; Stenlof et al., 2007; Rosenstock et al., 2007). In rodent models of T2D, topiramate improves glucose-stimulated insulin release and increases islet insulin content (Liang et al., 2005), and in vitro exposure of rodent  $\beta$ -cells to topiramate prevents lipotoxicity (Frigerio et al., 2006). Recently has been described also a long-lasting remission (>of 5 years) of T1D after treatment with topiramate for generalized seizures (Davalli et al., 2011).

Altogether, these data suggest that drugs acting on the glutamate-induced toxicity and in particular on the glutamate transporter GLT1 may be helpful in the treatment of diabetes.

## MATERIAL AND METHODS

### 1.1 Cell line

Cell lines represent a useful model to study the peculiar characteristics of each cell type present in the islet of Langerhans. Moreover, they can be grown in vitro for a considerable number of passages, maintaining their characteristic and their similarity to the native cells.

Mouse  $\beta$ TC3 cells were kindly provided by Prof. Douglas Hanahan (Department of Biochemistry and Biophysics, University of California, San Francisco, CA).  $\beta$ TC3 cells derive from pancreas of transgenic mice generated with a fusion gene between SV40 large T antigen and insulin promoters [Powers 1990; Efrat 1988]. The cells were grown in RPMI 1640 (from the name of the institute where the media was developed: Roswell Park Memorial Institute) 11 mM glucose (normal glucose condition), supplemented with 10% heat inactivated foetal bovine serum, 2 mM L-glutamine, and 100 IU/ml streptomycin/penicillin, at 37°C in a humidified atmosphere of 5% CO<sub>2</sub>.

### 1.2 Human Isolated Islets

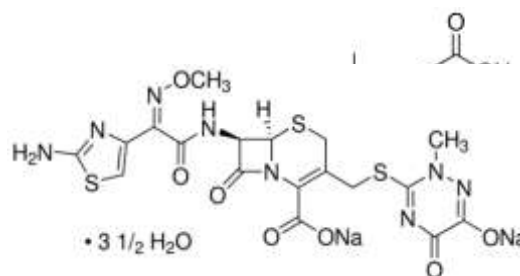
The islets used in this study were kindly provided by Ospedale Niguarda Ca' Granda. The islets were isolated from cadaveric multiorgan donors by using the procedure already described by Ricordi [Ricordi et al., 1988] in conformity to the ethical requirements approved by the Niguarda Cà Granda Ethics Board.

The purified islets were incubated in RPMI 1640 medium (Sigma Aldrich) containing 10% fetal bovine serum (FBS), 1% Glutamine and 1% Streptomycin-Penicillin in the presence of 5.5 mmol/l glucose (normal glucose condition) or 3 days in the presence of glucose 16.7 mmol/l (high glucose condition) as described [Marchetti *et al.*, 2002]. Some purified islets were incubated with mannitol 16,7 mmol/l for 3 days for osmotic control. The experiments of acute treatment were performed after 30 minutes of incubation with different molecules as reported in the treatments section. All incubations were performed at 37°C/5% CO<sub>2</sub>.

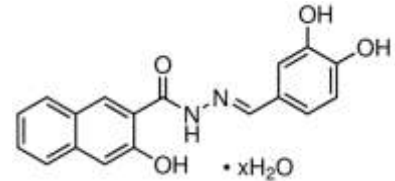
### 1.3 Treatments

The following treatments were used:

- **Ceftriaxone** (100nM). It is a third-generation cephalosporin antibiotic. Ceftriaxone increases EAAT2 expression in the central nervous system and reduce glutamatergic toxicity. (Sigma Aldrich)

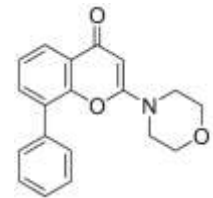


- **Dihydro Kainic acid** (DHK 0,1mM). The selective inhibitor of glutamate transporter GLT1/EAAT2 ( $K_i = 23 \mu\text{M}$ ). 130-fold selective over EAAT1 and EAAT3 ( $K_i > 3 \text{ mM}$ ). (Sigma Aldrich)
- **3-hydroxy-4,5,6,6a-tetrahydro-3aH-pyrrolo[3,4-d]isoxazole-4-carboxylic acid** (HIP-A 10uM). Potent, non-competitive excitatory amino acid transporter (EAAT) blocker. Preferentially inhibits glutamate release ( $\text{IC}_{50} = 1.6 \mu\text{M}$ ) rather than glutamate uptake ( $\text{IC}_{50} = 18 \mu\text{M}$ ). Moderately selective; displays no affinity for NMDA and metabotropic glutamate receptors, and low affinity for AMPA and kainate receptors ( $\text{IC}_{50}$  values are 43 and  $8 \mu\text{M}$  respectively). (Sigma Aldrich).
- **Dynasore** (Dyn, 30mM). The inhibitor of clathrin-dependent endocytosis. It is a small molecule, GTPase inhibitor that targets dynamin-1, dynamin-2 and Drp1 (mitochondrial). Dynasore blocks dynamin-dependent endocytosis, scission of endocytic vesicles (Sigma Aldrich)

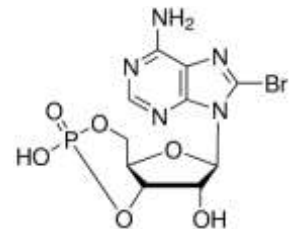


Signaling Pathways Inhibitors or activators:

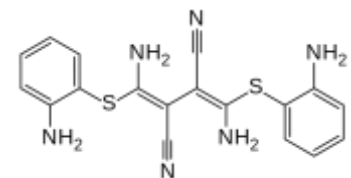
- **LY294002** (PI3K inhibitor, 50-100 $\mu\text{M}$ ): 2-Morpholin-4-yl-8-phenylchromen-4-one is a morpholine-containing chemical compound that is a potent inhibitor of numerous proteins, and a strong inhibitor of phosphoinositide 3-kinases (PI3Ks). (Sigma Aldrich).



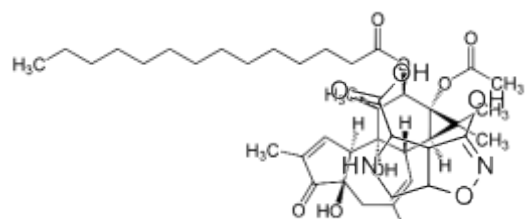
- **8-Bromoadenosine 3',5'-cyclic monophosphate** (8-Br-cAMP, PKA Activator, 10 $\mu\text{M}$ ): it is a brominated derivative of cyclic adenosine monophosphate (cAMP). 8-Br-cAMP is an activator of cyclic AMP-dependent protein kinase, and it is a cell-permeable cAMP analog having greater resistance to hydrolysis by phosphodiesterases than cAMP. 8-Bromoadenosine 3',5'-cyclic monophosphate activates protein kinase A (Sigma Aldrich).



- **UO126** (MAPK Inhibitor, ERK1/2, 10uM). It is MEK Inhibitor that is a chemically synthesized organic compound that inhibits activation of MAPK (ERK 1/2) by inhibiting the kinase activity of MAP Kinase Kinase (MAPKK or MEK 1/2). UO126 inhibits MEK1 with an  $\text{IC}_{50}$  of  $0.5 \mu\text{M}$  (in vitro) (Sigma Aldrich).

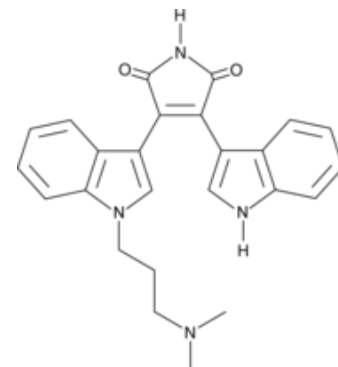


- **Phorbol 12-myristate 13-acetate** (PMA or TPA, PKC activator, 1 $\mu\text{M}$ ). Potent nanomolar activator of protein kinase C in vivo and in vitro. Binds to C1 domain of protein

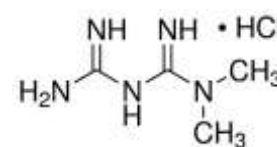


kinase C, induces membrane translocation and enzyme activation. Also reported to have actions on non-kinase proteins including chimaerins, RasGRP and Unc-13/Munc-13. Phorbol esters, such as PMA, affect PKCs by mimicking diacylglycerol, a natural ligand and activator of PKCs. A common alternative name for PMA is 12-O-tetradecanoylphorbol 13-acetate (TPA). (Sigma Aldrich)

- **Bisindolylmaleimide** (BIM, PKC inhibitor, 10 $\mu$ M) is a highly selective, cell-permeable, and reversible protein kinase C (PKC) inhibitor ( $K_i = 14$  nM). It acts as a competitive inhibitor for the ATP binding site of PKC and shows high selectivity for PKC $\alpha$ -,  $\beta$ 1-,  $\beta$ 2-,  $\gamma$ -,  $\delta$ -, and  $\epsilon$ -isozymes. Bisindolylmaleimide indirectly inhibits GSK3 in primary adipocyte lysates ( $IC_{50} = 360$  nM). This compound also competitively antagonizes the 5-HT<sub>3</sub> receptor with a  $K_i$  value of 61 nM. (Sigma Aldrich).



- **Metformin** (AMPK activator, 5mM). An antidiabetic agent reduces blood glucose levels and improves insulin sensitivity. Its metabolic effects, including the inhibition of hepatic gluconeogenesis, are mediated at least in part by activation of the LKB1-AMPK (AMP-activated protein kinase) pathway. Activation of this pathway also appears to be involved in the antiproliferative and proapoptotic actions of metformin in cancer cell lines. (Sigma Aldrich)



Pro apoptotic / toxic treatments:

- **Glucose:** the basal glucose condition is 5,5mM Glucose for human islets and 11mM Glucose for beta cell lines. As high Glucose condition we used 16,7mM Glucose for human islets and 20mM Glucose for beta cell line. (Sigma Aldrich)
- **Glutamate:** we used 1mM of Glutamate concentration as a toxic stimulus for beta cells. (Sigma Aldrich)
- Inflammatory cytokine **Interleukin  $\beta$**  (0,1mg/ml): IL-1 $\beta$  is a proinflammatory cytokine produced in a variety of cells including monocytes, tissue macrophages, keratinocytes and other epithelial cells. Both IL-1 $\alpha$  and IL-1 $\beta$  bind to the same receptor and have similar if not identical biological properties. Recombinant human IL-1b is a 17.3 kDa protein containing 153 amino acid residues. (Sigma Aldrich)
- Inflammatory cytokine **TNF  $\alpha$**  (0,1mg/ml ): TNF- $\alpha$  is a pleiotropic pro-inflammatory cytokine secreted by various cells including adipocytes, activated monocytes, macrophages, B cells, T cells and fibroblasts. It belongs to the TNF family of ligands and signals through two receptors, TNFR1 and TNFR2. TNF- $\alpha$  is cytotoxic to a wide variety of tumor cells and is an essential factor in mediating the immune response against bacterial infections. TNF- $\alpha$  also plays a role in the induction of septic shock, auto immune diseases, rheumatoid arthritis, inflammation, and diabetes. Recombinant human TNF- $\alpha$  is a soluble 157

amino acid protein (17.4 kDa) which corresponds to C-terminal extracellular domain of the full length transmembrane protein. (Sigma Aldrich)

- Inflammatory cytokine **Interferon  $\gamma$**  (0,5mg/ml). It is produced by T-lymphocytes stimulated by antigen or by T-cell mitogens. A broad range of biological activities has been attributed to IFN- $\gamma$  (e.g., the establishment of the antiviral state, immunoregulatory functions, antiproliferative effects and inhibition of cell growth). The anti-proliferative effects of IFN- $\gamma$  are superior to those of either IFN- $\alpha$  or IFN- $\beta$ . Growth inhibition is dependent on cell type, dose, and length of exposure. (Sigma Aldrich)

The substances were added to the uptake solution or to RPMI medium at the indicated concentrations. DHK and HIPA must be present in the solution during the uptake assays, the other treatments were incubated for 30 minutes (for the acute treatment) or 3 days (for the long-term treatment) in RPMI medium, at 37°C, 5% CO<sub>2</sub> before the experiment. The PMA, Bisindoleimide and the Dynasore require 1 hour of cell starving (medium RPMI 1640 1%Glutammine, 1% Penicillin-Streptomycin without 10% FBS) before their introduction in the medium. The treatment with Ceftriaxone was performed incubating the human islets for three days with 100 $\mu$ M of Ceftriaxone diluted in the complete RPMI medium

#### **1.4 Cell and Islets Lysis and Western Blotting**

$\beta$ TC3 cells were seeded onto 6-cm tissue culture plates and allowed to attach and grow until confluence. Cells or 1500 isolated human islets were harvested and lysed in 100  $\mu$ l lysis buffer (150 mM NaCl, 30 mM Tris-HCl, 1 mM MgCl<sub>2</sub>, 1% Triton X-100, 1 mM phenylmethylsulfonylfluoride, and 1  $\mu$ g/ml aprotinin and leupeptin). as described [Perego et al., 2000]. After 1 h at 4° C, nuclei and insoluble material were separated from soluble proteins by centrifuging the samples at 10,000 rpm for 10 min at 4°C. After protein assay with Bradford reagent (Sigma), 30  $\mu$ g of protein were resolved by western blot. We used 9% SDS-polyacrylamide gel running gel in denaturing condition (1%SDS): the extracted proteins were solubilised with denaturing  $\beta$ -mix (5% SDS, 20% Glycerol, 0.3M  $\beta$ -mercaptoethanol, blue bromophenol) and separated by SDS-PAGE (Tris-Gly/ SDS buffer: 25 mM Tris-Base, 192 mM Glycine, 0.1% SDS). Finally, proteins were transferred to a nitrocellulose membrane (Transfer buffer: 25 mM Tris-Base, 192 mM Glycine, 20% Methanol). After membrane incubation with blocking buffer (5% non-fat milk, 0.1% Tween 20, 20 mM tris HCl pH 7, 150 mM NaCl), the blots were probed with specific antibodies as a primary reagents in the blocking solution. Antibodies HRP-conjugated IgG (80 ng/ml; Amersham, GE Healthcare) followed this incubation. The primary antibodies were dissolved in a block solution with 5% of non-fat milk and were applied for 2h at room temperature. Then the nitrocellulose membranes were washed three times with blocking solution (milk 5%, TS 1X and Tween 0,1% p/v). Next, the anti-rabbit horseradish peroxidase was

added as a secondary antibody, followed by incubation for 1h at room temperature in the same blocking buffer. The nitrocellulose membrane were washed three times with the blocking solution without milk and visualised by ECL (EuroClone, LiteAblot EXTENDED). The reaction products were visualized after peroxidase activation by chemiluminescence substrate ECL and imposed on photographic plates (Kodak).

Band quantification was performed using Scion-image software and results were normalised for actin content and shown in bar graphs.

### **1.5 Antibodies for Western Blotting**

The protein expression was detected immunohistochemically with rabbit anti-GLT1 (1:75, Alpha Diagnostic), an affinity purified rabbit anti-GLT1 (1:250, kindly provided by Dr. Grazia Pietrini [Perego *et al.*, 2000], PI3K (1:1000; rabbit polyclonal antibody; Cell Signalling), AKT(1:2000; rabbit polyclonal antibody; Cell Signalling) and p-Akt Th 308 (1:1000; rabbit polyclonal antibody; Cell Signalling) or anti-actin (Sigma) antibodies as a primary reagents in the blocking solution. As secondary reagents we used an anti-rabbit HRP-conjugated IgG (80 ng/ml; Amersham, GE Healthcare) or an anti-mouse HRP-conjugated IgG (80 ng/ml; Amersham, GE Healthcare).

### **1.6 Immunofluorescence**

20 hand-picked islets were seeded onto sterile glass coverslips covered with gelatine (Sigma-Aldrich) to facilitate adhesion and cultured in RPMI medium. The  $\beta$ TC3 cells were seeded onto sterile glass coverslips (without gelatine) and cultured in RPMI medium. After 24 hours, islets and cells were fixed with 4% paraformaldehyde. Fixed cells were then incubated with primary antibody for 2 hours at room temperature in GDB solution (150 mM NaCl, 10 mM Phosphate Buffer pH 7.4, 0.2% Triton, 0.2% gelatine). Following incubation, cells were washed in PBS LS (PBS Low Salts: NaCl 150mM and PO<sub>4</sub> buffer 10mM pH 7,4) and then incubated in GDB with the appropriate fluorochrome-conjugated secondary antibodies (Jackson) for 1 hour at room temperature, in dark. The cover glasses were washed three times with PBS LS and then were mounted on glass slides with Phenilendiammine (1 mg/ml in Glycerol-PBS; Sigma-Aldrich) as antifade reagent and sealed with nail-polish.

The control samples are represented by the cells or the islets incubated with complete RPMI in normal/physiological glucose condition (11mM of glucose for Beta TC3 and 5,5mM of glucose for Human isolated Islets). The high glucose treatment corresponds to three days/thirty minutes of exposure to 20mM glucose for Beta cell line (bTC3) and 16,7mM glucose for human islets (37°C, 5% CO<sub>2</sub>).

### **1.7 Antibodies for Immunofluorescence**

The following primary antibodies were used: rabbit anti-GLT1 [Perego et al., 2000] and Alpha Diagnostic International), guinea pig anti-insulin (Roche Applied Science), mouse anti-glucagon (R&D Systems), mouse anti-somatostatin (Biomedica), mouse anti-chromogranin (Biogenex). The following secondary antibodies were used: FITC-conjugated anti-mouse and anti-rabbit IgG, biotin-conjugated anti-rabbit IgG, rhodamine-conjugated anti-mouse IgG, and rhodamine-conjugated anti-guinea pig IgG (Jackson ImmunoResearch Laboratories, West Grove, PA).

### **1.8 Immunohistochemistry**

Immunohistochemistry has been performed in formalin fixed human pancreas paraffin embedded sections. The ABC immune complex served for the identification of GLT1. After removal of paraffin and rehydration of tissue, the pancreas sections were first treated with an hydrogen peroxide solution to suppress possible endogenous peroxidase activity and then heated in citrate buffer 10 mM pH 6 using a microwave oven to expose antigens. This was followed by permeabilization with TBS-Triton 0,2% (150 mM NaCl, 50 mM Tris-HCl pH 7.4, 0.2% Triton X-100) and by an incubation with normal serum to quench nonspecific protein binding; finally the sections were incubated with a primary antibody, o/n at 4°C. Unbound antibodies were washed with TBS-Triton 0,2% and then the signal was amplified using secondary antibodies biotin conjugated, incubated at room temperature for 2 hours, followed by an incubation with Peroxidase conjugated-streptavidin (Chemicon). The reaction was performed with freshly activated 40% DAB (Diaminobenzidine, Sigma-Aldrich). The colour development was stopped by washing the slides thoroughly in tap water. To stain cytoplasm and nuclei, the sections were then counterstained with Mayer's haemalum, turned with tap water and dishydrated. Coverslips were mounted with an hydrophobic mounting medium (Dako Corp.).

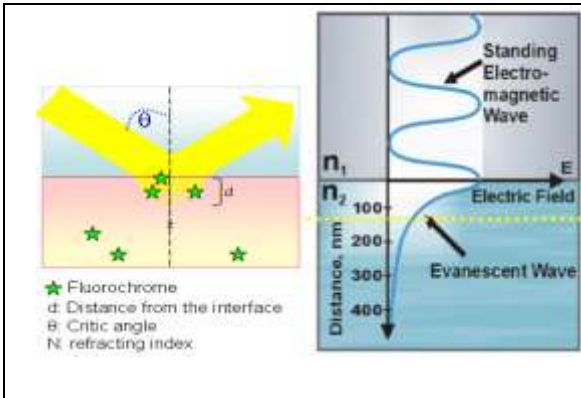
### **1.9 Antibodies for Immunohistochemistry**

We used as a primary antibody a rabbit anti-GLT1 [Perego *et al.*, 2000] and Alpha Diagnostic. Secondary antibodies: biotin-conjugated anti-rabbit IgG; Rhodamine-conjugated anti guinea pig (Jackson ImmunoResearch: West Grove, PA); Peroxidase conjugated-streptavidin (Chemicon). .

### **1.10 [<sup>3</sup>H]-Glutamate Uptake**

The transport of [<sup>3</sup>H]-glutamate assays were performed in 96 wells plate using 40 human Islets/well or 8000 βtc3 cells/well. Cells and islets were cultured in 100ul/well of RPMI medium, supplemented with 10% fetal bovine serum, 1% of Glutamine and 1% of Penicillin -Streptomycin. Three days or 30 minutes before the experiments, in some well, the treatments were added in the medium. The day of the experiment the





Seventy-two hours after transfection, the mouse  $\beta$ TC3 cells plated onto glass coverslips were imaged through a TIRF microscope (Axiovert; Carlo Zeiss, Inc.) equipped with an Argon laser at 37°C using a 100 × 1.45 numerical aperture (NA) oil immersion objective. Green fluorescence was excited using the 488 nm laser line and imaged through a band-pass filter (Zeiss) onto a Retiga SRV CCD camera [D'Amico et al., 2010]. For the time-lapse experiments, single-cell imaging under TIRF illumination was carried out at 3 frames/min for 7 min before and after incubation at 37°C with 50 $\mu$ M-100 $\mu$ m LY294002. Up to five cells were imaged on each coverslip, in three independent experiments

### 1.14 Videomicroscopy

The use of a high-quality video camera or attached to a research-quality light microscope is useful to obtaining real-time or high-speed imaging of biological samples. These images are recorded at regular intervals, and the time-lapse sequence can be played back in the form of a movie. Video microscopy for rapid time-lapse imaging techniques is used frequently to image small structures that move rapidly within cells such as to study the protein trafficking . For our videomicroscopy experiments have been used beta cell (Beta TC3) transfected with the glutamate transporter 1 (GLT1) tagged with the green fluorescence protein (GFP). This system allows us to follow in vivo the localization of glt1 and its changes or movements after specific treatment.

### 1.15 Image processing

For each recorded cell image, eight 50 × 50-pixel regions were randomly selected within the cell, and the average fluorescence intensity and its associated standard deviation in each frame were calculated using the Image-ProPlus software (Media Cybernetics, Bethesda, MD). The fluorescence intensities in the various frames were normalized to their respective initial average intensities ( $F_0 = 100\%$ ) and plotted against time. Fluorescence intensities were corrected for bleaching during the acquisition of serial images (bleaching was estimated by imaging outside transfected cells).

### **1.16 Apoptosis**

The apoptosis in human islets were evaluated with a kit based on a photometric enzyme-immunoassay Cell Death Detection ELISA plus (*Version 11.0, Cell Death human ELISA kit, Roche*) that allows to quantify spectrophotometrically the histone-complexed DNA fragment out of cytoplasm after the introduction of potentially apoptosis agents. 40 human islets/well were seeded on 96well plates and after three days of treatment (5,5mM Glucose, 16,7mM Glucose or 100µM of Ceftriaxone) in complete RPMI 1640 medium were lysate in 100µl of lysis buffer equipped in the kit. Data were expressed as -fold increase over control samples.

### **1.17 Apoptosis Treatments**

The treatments were added in complete RPMI medium for three days. The basal glucose condition was obtained using 5,5mM of Glucose, while we used 16,7mM of Glucose to simulate long-term high glucose exposition. We used also Ceftriaxone (final concentration 100nM) and a mix of inflammatory cytokines (Interleukinβ 0,1mg/ml; TNFα 0,1mg/ml and Interferonγ 0,5mg/ml)

### **1.18 Statistical Analysis**

Statistical significance of difference between groups was determined by unpaired Student's *t*-test. Differences were considered significant at  $P \leq 0.05$ . Data are presented as means  $\pm$  S.E. of at least three independent experiments. The number of replicates for each experiment is reported. Statistical comparisons were performed by unpaired Student's *t* test or analysis of variance followed by multiple post hoc comparison analysis performed with Tukey's test. The difference was considered statistically significant when the *p* value was  $\leq 0.05$ .

## **Reference:**

1. Axelrod D. (2001) Total internal reflection fluorescence microscopy in cell biology. *Traffic*. 2:764-774.
2. D' Amico A, Soragna A, Di Cairano E, Panzeri N, Anzai N, Vellea Sacchi F, Perego C. (2010) The Surface Density of the Glutamate Transporter EAAC1 is Controlled by Interactions with PDZK1 and AP2 Adaptor Complexes. *Traffic*. Aug 17. doi: 10.1111/j.1600-0854.2010.01110.x. [Epub ahead of print].
3. Efrat S, Linde S, Kofod H, Spector D, Delannoy M, Grant S, Hanahan D, Baekkeskov S. (1988) Beta-cell lines derived from transgenic mice expressing a hybrid insulin gene-oncogene. *Proc Natl Acad Sci U S A* 85(23): 9037-41.
4. Marchetti P, Lupi R, Federici M, Marselli L, Masini M, Boggi U, Del Guerra S, Patanè G, Piro S, Anello M, Bergamini E, Purrello F, Lauro R, Mosca F, Sesti G, Del Prato S. (2002) Insulin secretory function is impaired in isolated human islets carrying the Gly(972)-->Arg IRS-1 polymorphism. *Diabetes*. 51(5):1419-24
5. Perego C, Vanoni C, Bossi M, Massari S, Basudev H, et al. (2000) The GLT-1 and GLAST glutamate transporters are expressed on morphologically distinct astrocytes and regulated by neuronal activity in primary hippocampal cocultures. *J Neurochem*, 75:1076-1084.
6. Powers AC, Efrat S, Mojsov S, Spector D, Habener JF, Hanahan D (1990) Proglucagon processing similar to normal islets in pancreatic alpha-like cell line derived from transgenic mouse tumor. *Diabetes.*, 39(4): 406-14.
7. Ricordi C, Lacy PE, Finke EH, Olack BJ, Sharp DW (1988) Automated method for isolation of human pancreatic islets. *Diabetes* 37:413-420.

## Bibliography Chapter 1

1. Acevedo-Duncan M, Cooper DR, Standaert ML, Farese RV (1989). Immunological evidence that insulin activates protein kinase C in BC3H-1 myocytes. *FEBS Lett.* 1989;244:174–176.
2. Ahren B (2000) Autonomic regulation of islet hormone secretion. Implications for health and disease. *Diabetologia* 43:393–410. [PubMed: 10819232]
3. Ahren B (2009). Islet G protein-coupled receptors as potential targets for treatment of type 2 diabetes. *Nat Rev Drug Discov* 8:369–385.
4. Alenghat F. J. and David E. Golan D. E (2013). Membrane Protein Dynamics and Functional Implications in Mammalian Cells Published in final edited form as: *Curr Top Membr.* 2013; 72: 89–120. PMID: PMC4193470 NIHMSID: NIHMS632147 doi: [10.1016/B978-0-12-417027-8.00003-9](https://doi.org/10.1016/B978-0-12-417027-8.00003-9).
5. Allan BB, Balch WE. (1999) Protein sorting by directed maturation of Golgi compartments. *Science.* 285(5424):63-6.
6. Aridor M, Balch WE. (1996) Principles of selective transport: coat complexes hold the key. *Trends Cell Biol* 6(8):315-20.
7. Arriza JL, Eliasof S, Kavanaugh MP, Amara SG. (1997) Excitatory amino acid transporter 5, a retinal glutamate transporter coupled to a chloride conductance. *Proc Natl Acad Sci U S A.* 94(8):4155-60.
8. Arriza JL, Fairman WA, Wadiche JI, Murdoch GH, Kavanaugh MP, et al. (1994) Functional comparisons of three glutamate transporter subtypes cloned from human motor cortex. *J Neurosci,* 14:5559-5569.
9. Ashcroft FM, Rorsman P. (1989). Electrophysiology of the pancreatic beta-cell. *Prog Biophys Mol Biol.* 1989;54:87–143.
10. Ashcroft FM, Rorsman P.(2004) Molecular defects in insulin secretion in type-2 diabetes. *Rev Endocr Metab Disord.* 2004;5:135–142.
11. Ashcroft SJ, Sugden MC, Williams IH (1980). Carbohydrate metabolism and the glucoreceptor mechanism. *Horm Metab Res.* 1980;(Suppl 10):1–7.
12. Aspinwall CA, Qian WJ, Roper MG, Kulkarni RN, Kahn CR, Kennedy RT (2000) Roles of insulin receptor substrate-1, phosphatidylinositol 3-kinase, and release of intracellular Ca<sup>2+</sup> stores in insulin-stimulated insulin secretion in beta-cells. *J Biol Chem* 275:22331–22338
13. Axelrod D. (2001) Total internal reflection fluorescence microscopy in cell biology. *Traffic.* 2:764-774
14. Aziz SA, Davies M, Pick E, Zito C, Jilaveanu L, Camp RL, Rimm DL, Kluger Y, Kluger HM.(2009). Phosphatidylinositol-3-kinase as a therapeutic target in melanoma. *Clin Cancer Res.* 2009;15:3029–3036. doi: 10.1158/1078-0432.CCR-08-2768.
15. Aziz SA, Davies M, Pick E, Zito C, Jilaveanu L, Camp RL, Rimm DL, Kluger Y, Kluger HM. (2007) The role of phosphoinositide 3-kinase C2alpha in insulin signaling. *J Biol Chem.* 2007;282:28226–36.
16. Bae SS, Cho H, Mu J, Birnbaum MJ. (2003) Isoform-specific regulation of insulin-dependent glucose uptake by Akt/protein kinase B. *J Biol Chem.* 2003;278:49530–49536.
17. Bai L, Zhang X, Ghishan FK (2003) Characterization of vesicular glutamate transporter in pancreatic alpha—and beta—cells and its regulation by glucose. *Am J Physiol Gastrointest Liver Physiol* 284(5):G808–G814
18. Bala T.S. Susarla, Michael B. Robinson (2007) Internalization and degradation of the glutamate transporter GLT-1 in response to phorbol ester. *Neurochemistry International Volume Neurosteroids.* 52, Issues 4–5, March–April 2008, Pages 709–722. doi:10.1016/j.neuint.2007.08.020
19. Balasubramanian R, Ruiz de Azua I, Wess J, Jacobson KA. (2010). Activation of distinct P2Y receptor subtypes stimulates insulin secretion in MIN6 mouse pancreatic beta cells. *Biochem Pharmacol* 79:1317-1326.
20. Baluch DP, Capco DG (2002) Cellular scaffolds in mammalian eggs. *Front Biosci* 7:d1653–d1661,2002
21. Barlowe, C., Orci, L., Yeung, T., Hosobuchi, M., Hamamoto, S., Salama, N., Rexach, M.F., Ravazzola, M., Amherdt, M., and Schekman, R. (1994). COPII: a membrane coat formed by Sec proteins that drive vesicle budding from the endoplasmic reticulum. *Cell* 77, 895–907.
22. Beart PM, O'Shea RD (2007). Transporters for l-glutamate: an update on their molecular pharmacology and pathological involvement. *Br. J. Pharmacol.,* 150 (2007), pp. 5–17

23. Bernal-Mizrachi E, Fatrai S, Johnson JD, Ohsugi M, Otani K, Han Z, Polonsky KS, Permutt MA (2004) Defective insulin secretion and increased susceptibility to experimental diabetes are induced by reduced Akt activity in pancreatic islet beta cells. *J Clin Invest.*114:928–936
24. Bernal-Mizrachi E, Wen W, Stahlhut S, Welling C, Permutt MA. (2001). Islet  $\beta$  cell expression of constitutively active Akt1/PKB induces striking hypertrophy, hyperplasia, and hyperinsulinemia. *J. Clin. Invest.*2001;108:1631–1638. doi:10.1172/JCI200113785.
25. Bertrand G, Gross R, Puech R, Loubatier`res-Mariani MM, Bockaert J (1992) Evidence for a glutamate receptor of the AMPA subtype which mediates insulin release from rat perfused pancreas. *Br J Pharmacol* 106(2):354–359
26. Bertrand G, Gross R, Puech R, Loubatier`res-Mariani MM, Bockaert J (1993) Glutamate stimulates glucagon secretion via an excitatory amino acid receptor of the AMPA subtype in rat pancreas. *Eur J Pharmacol* 237(1):45–50
27. Bertrand G, Puech R, Loubatier`res-Mariani MM, Bockaert J. (1995) Glutamate stimulates insulin secretion and improves glucose tolerance in rats. *Am J Physiol.* 269(3 Pt 1):E551–6.
28. Bland ML, Birnbaum MJ. (2011) Cell biology. ADApting to energetic stress. *Science.* 2011;332:1387–1388.
29. Bonaventura MM, Catalano PN, Chamson-Reig A, Arany E, Hill D, Bettler B, Saravia F, Libertun C, Lux-Lantos VA. (2008). GABAB receptors and glucose homeostasis: evaluation in GABAB receptor knockout mice. *Am J Physiol Endocrinol Metab* 294:E157-167.
30. Bonifacino, J.S., and Glick, B.S. (2004). The mechanisms of vesicle budding and fusion. *Cell* 116, 153–166.
31. Bosco D, Armanet M, Morel P, Niclauss N, Sgroi A, Muller YD, Giovannoni L, Parnaud G, Berney T. (2010). Unique arrangement of  $\alpha$ -and $\beta$ -cells in human islets of Langerhans. *Diabetes* 59:1202–10
32. Braiman L, Alt A, Kuroki T, Ohba M, Bak A, Tennenbaum T, Sampson SR. (2012)Protein kinase Cdelta mediates insulin-induced glucose transport in primary cultures of rat skeletal muscle. *Mol Endocrinol.*1999;13:2002–2012.
33. Braiman L, Alt A, Kuroki T, Ohba M, Bak A, Tennenbaum T, Sampson SR.(2001a) Insulin induces specific interaction between insulin receptor and PKC in primary cultured skeletal muscle. *Mol Endocrinol.*2001;15:565–574.
34. Braiman L, Alt A, Kuroki T, Ohba M, Bak A, Tennenbaum T, Sampson SR (2001b). Activation of protein kinase C zeta induces serine phosphorylation of VAMP2 in the GLUT4 compartment and increases glucose transport in skeletal muscle. *Mol Cell Biol.* 2001;21:7852–7861.
35. Braiman L, Sheffi-Friedman L, Bak A, Tennenbaum T, Sampson SR.(1999) Tyrosine phosphorylation of specific protein kinase C isoenzymes participates in insulin stimulation of glucose transport in primary cultures of rat skeletal muscle. *Diabetes.* 1999;48:1922–1929.
36. Braun M, Ramracheya R, Bengtsson M, Clark A, Walker JN, Johnson PR, Rorsman P. (2010). Gamma-aminobutyric acid (GABA) is an autocrine excitatory transmitter in human pancreatic beta-cells. *Diabetes* 59:1694-701.
37. Braun M, Ramracheya R, Bengtsson M, Zhang Q, Karanauskaite J, Partridge C, Johnson PR, Rorsman P.(2008). Voltage-gated ion channels in human pancreatic beta-cells: electrophysiological characterization and role in insulin secretion. *Diabetes.* 2008;57:1618–28.
38. Braun M, Wendt A, Birnir B, Broman J, Eliasson L, Galvanovskis J, Gromada J, Mulder H, Rorsman P. (2004). Regulated Exocytosis of GABA-containing Synaptic-like Microvesicles in Pancreatic  $\beta$ -cells. *J Gen Physiol* 123:191–204.
39. Braun M, Wendt A, Karanauskaite J, Galvanovskis J, Clark A, MacDonald PE, Rorsman P. (2007). Corelease and Differential Exit via the Fusion Pore of GABA, Serotonin, and ATP from LDCV in Rat Pancreatic  $\beta$  Cells. *J Gen Physiol* 129:221-231.
40. Brice NL, Varadi A, Ashcroft SJ, Molnar E (2002) Metabotropic glutamate and GABA(B) receptors contribute to the modulation of glucose-stimulated insulin secretion in pancreatic beta cells.*Diabetologia* 45:242–252
41. Brown D, Stow JL. (1996) Protein trafficking and polarity in kidney epithelium: from cell biology to physiology. *Physiol Rev.* 76(1):245-97.
42. Brown, M. S., Brunschede, G. Y. and Goldstein, J. L. (1975) Inactivation of 3-hydroxy- 3-methylglutaryl coenzyme A reductase in vitro. An adenine nucleotide-dependent reaction catalyzed by a factor in human fibroblasts. *J. Biol. Chem.* 250, 2502–2509
43. Buchner K. (1995) Protein kinase C in the transduction of signals toward and within the cell nucleus. *Eur J Biochem.* 1995;228:211–221.
44. Burcelin R (2013). "The antidiabetic gutsy role of metformin uncovered?".*Gut* 63 (5): 706–707. doi:10.1136/gutjnl-2013-305370. PMID 23840042.

45. Burnstock G and Novak I. (2012). Purinergic signaling in the pancreas in health and disease. *J Endocrinol* 213:123-141.
46. Burnstock G. (2008). Dual control of vascular tone and remodelling by ATP released from nerves and endothelial cells. *Pharmacol Rep.* 60(1):12-20.
47. Butchbach ME, Tian G., Guo H, Lin C.L (2004). Association of excitatory amino acid transporters, especially EAAT2, with cholesterol-rich lipid raft microdomains: importance for excitatory amino acid transporter localization and function. *J. Biol. Chem.*, 279 (2004), pp. 34388–34396
48. Buteau J, Foisy S, Rhodes CJ, Carpenter L, Biden TJ, Prentki M (2001) Protein kinase C $\zeta$  activation mediates glucagon-like peptide-1–induced pancreatic  $\beta$ -cell proliferation. *Diabetes* 50 :2237 –2243,2001
49. Cabrera O, Berman DM, Kenyon NS, Ricordi C, Berggren PO, Caicedo A. (2006). The unique cytoarchitecture of human pancreatic islets has implications for islet cell function. *Proc. Natl. Acad. Sci. USA* 103:2334–39
50. Cabrera O, Berman DM, Kenyon NS, Ricordi C, Berggren PO, Caicedo A. (2005). The unique cytoarchitecture of human pancreatic islets has implications for islet cell function. *Proc Natl Acad Sci U S A.* 2006 Feb 14;103(7):2334-9. Epub 2006 Feb 6. PMID: 16461897 [PubMed - indexed for MEDLINE] PMCID: PMC1413730
51. Cabrera O, Jacques-Silva C, Speier S, Yang SN, Kohler M, Fachado A, Vieira E, Zierath JR, Kibbey R, Berman DM, Kenyon NS, Ricordi C, Caicedo A, Berggren PO (2008) Glutamate is a positive autocrine signal for glucagon release. *Cell Metab* 7:545–554.
52. Cai H, Reinisch K, Ferro-Novick S. (2007) Coats, tethers, Rab, and SNAREs work together to mediate the intracellular destination of a transport vesicle. *Dev Cell.* 12(5):671-82.
53. Caicedo A. (2012). Paracrine and autocrine interactions in the human islet: More than meets the eye. *journal homepage: www.elsevier.com/locate/semcdb*
54. Carling D (2004) The AMP-activated protein kinase cascade: a unifying system for energy control. *Trends Biochem. Sci.* 2004;29:18–24.
55. Carling, D., Zammit, V. A. and Hardie, D. G. (1987) A common bicyclic protein kinase cascade inactivates the regulatory enzymes of fatty acid and cholesterol biosynthesis. *FEBS Lett.* 223, 217–222
56. Carrick V, Dunlop J (1999). Protein kinase C modulation of the human excitatory amino acid transporter 2 subtype of glutamate transporter. *Soc. Neurosci. Abs.*, 25 (1999), p. 426
57. Chalfant CE, Mischak H, Watson JE, Winkler BC, Goodnight J, Farese RV, Cooper DR.(1995) Regulation of alternative splicing of protein kinase C beta by insulin. *J Biol Chem.* 1995;270:13326–13332.
58. Chalfant CE, Ohno S, Konno Y, Fisher AA, Bisnauth LD, Watson JE, Cooper DR. (1996) A carboxy-terminal deletion mutant of protein kinase C beta II inhibits insulin-stimulated 2-deoxyglucose uptake in L6 rat skeletal muscle cells. *Mol Endocrinol.* 1996;10:273–1281.
59. Chan CB, De Leo D, Joseph JW, McQuaid TS, Ha XF, Xu F, Tsushima RG, Pennefather PS, Salapatek AM, Wheeler MB.(2001). Increased uncoupling protein-2 levels in beta-cells are associated with impaired glucose-stimulated insulin secretion: Mechanism of action. *Diabetes.* 2001;50:1302–1310.
60. Chen WS, Xu PZ, Gottlob K, Chen ML, Sokol K, Shiyanova T, Roninson I, Weng W, Suzuki R, Tobe K, Kadowaki T, Hay N (2001). Growth retardation and increased apoptosis in mice with homozygous disruption of the Akt1 gene. *Genes Dev.* 2001;15:2203–2208.
61. Cho H, Mu J, Kim JK, Thorvaldsen JL, Chu Q, Crenshaw EB 3rd, Kaestner KH, Bartolomei MS, Shulman GI, Birnbaum MJ. (2001b). Insulin resistance and a diabetes mellitus-like syndrome in mice lacking the protein kinase Akt2 (PKB beta) *Science.* 2001;292:1728–1731.
62. Cho H, Thorvaldsen JL, Chu Q, Feng F, Birnbaum MJ.(2001a) Akt1/PKBalpha is required for normal growth but dispensable for maintenance of glucose homeostasis in mice. *J. Biol. Chem.* 2001;276:38349–38352.
63. Cho W. (2001). Membrane targeting by C1 and C2 domains. *J Biol Chem.* 2001;276:32407–32410.
64. Cooper DR, Hernandez H, Kuo JY, Farese RV. (1990) Insulin increases the synthesis of phospholipid and diacylglycerol and protein kinase C activity in rat hepatocytes. *Arch Biochem Biophys.* 1990;276:486–494.
65. Cooper DR, Konda TS, Standaert ML, Davis JS, Pollet RJ, Farese RV.(1987) Insulin increases membrane and cytosolic protein kinase C activity in BC3H-1 myocytes. *J Biol Chem.* 1987;262:3633–3639.
66. Cooper DR, Watson JE, Hernandez H, Yu B, Standaert ML, Ways DK, Arnold TT, Ishizuka T, Farese RV. (1992) Direct evidence for protein kinase C involvement in insulin-stimulated hexose uptake. *Biochem Biophys Res Commun.* 1992;188:142–148.
67. Cooperberg BA, Cryer PE (2010) Insulin reciprocally regulates glucagon secretion in humans. *Diabetes* 59:2936–2940

68. Curry DL, Bennett LL, Grodsky GM (1968). Requirement for calcium ion in insulin secretion by the perfused rat pancreas. *Am J Physiol.* 1968;214:174–178.
69. D’Amico A, Soragna A, Panzeri N, Di Cairano ES, Anzai N, Sacchi VF and Perego C. (2007). PDZ-domain interactions control the surface stability and degradation of the EAAC1 glutamate transporter. *FEBS Journal.* 2007 274, supp.1, B4-44- 351
70. Da Silva Xavier G, Leclerc I, Varadi A, Tsuboi T, Moule Sk And Rutter Ga.(2003) Role for AMP-activated protein kinase in glucose-stimulated insulin secretion and preproinsulin gene expression *Biochem. J.* (2003) 371, 761–774. (Hardie 2004; Carling 2004; Kemp et al., 2003)
71. Danbolt NC (2001) Glutamate uptake. *Prog. Neurobiol.*, 65 (2001), pp. 1–105
72. Dean PM, Matthews EK. (1968). Electrical activity in pancreatic islet cells. *Nature.* 1968;219:389–390.
73. Deeney JT, Cunningham BA, Chheda S, Bokvist K, Juntti-Berggren L, Lam K, Korchak HM, Corkey BE, Berggren PO (1996). Reversible Ca<sup>2+</sup>-dependent translocation of protein kinase C and glucose-induced insulin release. *J Biol Chem* 271 :18154 –18160,1996
74. Defronzo RA. (2011). Bromocriptine: a sympatholytic, D2-dopamine agonist for the treatment of type 2 diabetes. *Diabetes Care* 34:789-794.
75. Detimary P., Gilon P., Henquin J.C.(1998) Interplay between cytoplasmic Ca<sup>2+</sup> and the ATP/ADP ratio: a feedback control mechanism in mouse pancreatic islets. *Biochem. J.* 1998;333:269–274.
76. Di Cairano ES, Davalli AM, Perego L, Sala S, Sacchi VF, La Rosa S, Finzi G, Placidi C, Capella C, Conti P, Centonze VE, Casiraghi F, Bertuzzi F, Folli F, Perego C (2011). The glial glutamate transporter 1 (GLT1) is expressed by pancreatic betacells and prevents glutamate-induced beta-cell death. *J Biol Chem* 286(16):14007–14018 *Diabetologia* 49(12):2824–2827
77. Doliba NM, Qin W, Najafi H, Liu C, Buettger CW, Sotiris J, Collins HW, Li C, Stanley CA, Wilson DF, Grimsby J, Sarabu R, Naji A, Matschinsky FM. (2012). Glucokinase activation repairs and defective bioenergetics of islets of Langerhans isolated from type 2 diabetics. *Am. J. Physiol.. Endocrinol. Metab.* 302:E87–102
78. Dugani CB and Klip A (2005) Glucose transporter 4: cycling, compartments and controversies Third in the Cycles Review Series *EMBO Rep.* 2005 Dec; 6(12): 1137–1142. doi: 10.1038/sj.embor.7400584 PMID: PMC1369215
79. Ekholm R, Ericson LE, Lundquist I. (1971). Monoamines in the pancreatic islets of the mouse. *Diabetologia* 7:339-348.
80. Farese RV, Standaert ML, Arnold T, Yu B, Ishizuka T, Hoffman J, Vila M, Cooper DR. 1992 The role of protein kinase C in insulin action. *Cell Signal.* 1992;4:133–143.
81. Feliciello A, Gottesman ME, Avvedimento EV (2001). The biological functions of A-kinase anchor proteins. *J Mol Biol* 308 :99 –114,2001
82. Fernandez-Alvarez J, Hillaire-Buys D, Loubatières-Mariani MM, Gomis R, Petit P. (2001). P2 receptor agonists stimulate insulin release from human pancreatic islets. *Pancreas* 22:69-71.
83. Fogarty S, Hawley SA, Green KA, Saner N, Mustard KJ, Hardie DG.(2010). Calmodulin-dependent protein kinase kinase-beta activates AMPK without forming a stable complex: synergistic effects of Ca<sup>2+</sup> and AMP. *Biochem J.* 2010;426:109–118.
84. Foretz M, Hébrard S, Leclerc J, Zarrinpashneh E, Soty M, Mithieux G, Sakamoto K, Andreelli F, Viollet B.(2010). Metformin inhibits hepatic gluconeogenesis in mice independently of the LKB1/AMPK pathway via a decrease in hepatic energy state. *J Clin Invest.* 2010;120:2355–2369.
85. Franke TF (2008). PI3K/Akt: getting it right matters. *Oncogene.* 2008;27:6473–6488. doi: 10.1038/onc.2008.313. (Franke 2008; Marone et al., 2008)
86. Franklin I, Gromada J, Gjinovci A, Theander S, Wollheim CB (2005) Beta-cell secretory products activate alpha-cell ATP-dependent potassium channels to inhibit glucagon release *Diabetes* 54:1808–1815
87. Frayn KN. 2010. *Metabolic Regulation: A Human Perspective.* Oxford, UK:Wiley-Blackwell. 384 pp.
88. Fruman DA. (2010) Regulatory subunits of class IA PI3K. *Curr Top Microbiol Immunol.* 2010;346:225–244. doi: 10.1007/82\_2010\_39. (Fruman 2010; Vogt et al., 2009)
89. Gammelsaeter R, Froyland M, Aragon C, Danbolt NC, Fortin D, Storm-Mathisen J, Davanger S, Gundersen V (2004) Glycine, GABA and their transporters in pancreatic islets of Langerhans: evidence for a paracrine transmitter interplay. *J Cell Sci* 117:3749–3758
90. Ganel R, Crosson CE (1998) Modulation of human glutamate transporter activity by phorbol ester. *J. Neurochem.*, 70 (1998), pp. 993–1000

91. Gao ZY, Gilon P, Henquin JC (1994) The role of protein kinase-C in signal transduction through vasopressin and acetylcholine receptors in pancreatic B-cells from normal mouse. *Endocrinology* 135 :191 –199,1994 CrossRefMedline
92. Garcia Barrado MJ, Iglesias Osma MC, Blanco EJ, Carretero Hernández M, Sánchez Robledo V, Catalano Iniesta L, Carrero S, Carretero J. (2015). Dopamine modulates insulin release and is involved in the survival of rat pancreatic beta cells. *PLoS One*. 10(4):e0123197.
93. Garofalo RS, Orena SJ, Rafidi K, Torchia AJ, Stock JL, Hildebrandt AL, Coskran T, Black SC, Brees DJ, Wicks JR, McNeish JD, Coleman KG. (2003). Severe diabetes, age-dependent loss of adipose tissue, and mild growth deficiency in mice lacking Akt2/PKB $\beta$ . *J. Clin. Invest.* 2003;112:197–208.
94. Ghezzi C and Wright EM (2012). Regulation of the human Na<sup>+</sup>-dependent glucose cotransporter hSGLT2 *Am J Physiol Cell Physiol.* 2012 Aug 1; 303(3): C348–C354. Published online 2012 Jun 6. doi: 10.1152/ajpcell.00115.2012 PMID: PMC342302
95. Glas R, Sauter NS, Schulthess FT, Shu L, Oberholzer J, Maedler K. (2009). Purinergic P2X7 receptors regulate secretion of interleukin-1 receptor antagonist and beta cell function and survival. *Diabetologia* 52:1579-1588.
96. Gloyn AL, Odili S, Zelent D, Buettger C, Castleden HA, Steele AM, Stride A, Shiota C, Magnuson MA, Lorini R, d'Annunzio G, Stanley CA, Kwagh J, van Schaftingen E, Veiga-da-Cunha M, Barbetti F, Dunten P, Han Y, Grimsby J, Taub R, Ellard S, Hattersley AT, Matschinsky FM. 2005. Insights into the structure and regulation of glucokinase from a novel mutation (V62M), which causes maturity-onset diabetes of the young. *J. Biol. Chem.* 280:14105–13
97. Gonoï T, Mizuno N, Inagaki N, Kuromi H, Seino Y, Miyazaki J, Seino S. (1994) Functional neuronal ionotropic glutamate receptors are expressed in the non-neuronal cell line MIN6. *J Biol Chem.* 269(25): 16989-92.
98. González MI, Robinson MB (2003) Interaction of PICK1 and the glutamate transporter, EAAC1 [abstract]. Society for Neuroscience 33rd Annual Meeting, November 8–12 2003, New Orleans. [Program number 372.7; URL:<http://web.sfn.org>]
99. Gonzalez MI, Susarla B.T, Robinson M.B (2005). Evidence that protein kinase Calpha interacts with and regulates the glial glutamate transporter GLT-1. *J. Neurochem.*, 94 (2005), pp. 1180–1188
100. González, M.B. Robinson (2004) Neurotransmitter transporters: why dance with so many partners. *Curr. Opin. Pharmacol.*, 4 (2004), pp. 30–35
101. Gromada J, Franklin I, Wollheim C. (2007) Alpha-cells of the endocrine pancreas: 35 years of research but the enigma remains. *Endocr Rev.* 2007;28:84–116.
102. Guigas B, de Leeuw van Weenen JE, van Leeuwen N, Simonis-Bik AM, van Haften TW, Nijpels G, Houwing-Duistermaat JJ, Beekman M, Deelen J, Havekes LM, Penninx BW, Vogelzangs N, van 't Riet E, Dehghan A, Hofman A, Witteman JC, Uitterlinden AG, Grarup N, Jørgensen T, Witte DR, Lauritzen T, Hansen T, Pedersen O, Hottenga J, Romijn JA, Diamant M, Kramer MH, Heine RJ, Willemsen G, Dekker JM, Eekhoff EM, Pijl H, de Geus EJ, Slagboom PE, 't Hart LM. (2014). Sex-specific effects of naturally occurring variants in the dopamine receptor D2 locus on insulin secretion and type 2 diabetes susceptibility. *Diabet Med.* 31(8):1001-1008.
103. Guillet J, Velly L.J., Canolle B., Masméjean F.M., Nieoullon A.L., Pisano P.(2005). Differential regulation by protein kinases of activity and cell surface expression of glutamate transporters in neuron-enriched culture. *Neurochem. Int.*, 46 (2005), pp. 337–346
104. Hales CN, Milner RD. (1968) Cations and the secretion of insulin from rabbit pancreas in vitro. *J Physiol.* 1968;199:177–187.
105. Hammerton RW, Krzeminski KA, Mays RW, Ryan TA, Wollner DA, Nelson WJ. (1991) Mechanism for regulating cell surface distribution of Na<sup>+</sup>,K<sup>(+)</sup>-ATPase in polarized epithelial cells. *Science.* 254(5033):847-50.
106. Hardie DG (2004). The AMP-activated protein kinase pathway: new players upstream and downstream. *J. Cell Sci.* 2004;117:5479–5487.
107. Hardie DG (2006). Neither LKB1 nor AMPK are the direct targets of metformin. *Gastroenterology.* 2006;131:973. author reply 974-975.
108. Hardie, D. G., Carling, D. and Sim, A. T. R. (1989) The AMP-activated protein kinase : a multisubstrate regulator of lipid metabolism. *Trends Biochem. Sci.* 14, 20–23
109. Hauge-Evans AC, Reers C, Kerby A, Franklin Z, Amisten S, King AJ, Hassan Z, Vilches-Flores A, Tippu Z, Persaud SJ, Jones PM.(2014). Effect of hyperglycaemia on muscarinic M3 receptor expression and secretory sensitivity to cholinergic receptor activation in islets. *Diabetes Obes Metab* 16:947-956.
110. Havel PJ, Veith RC, Dunning BE, Taborsky GJ Jr.(1988) Pancreatic noradrenergic nerves are activated by neuroglucopenia but not by hypotension or hypoxia in the dog. Evidence for stress-specific and regionally

- selective activation of the sympathetic nervous system (1988). *Nov*;82(5):1538-45. *J Clin Invest*. 1988; 82:1538–1545. [PubMed: 3183052]
111. Hawley SA, Boudeau J, Reid JL, Mustard KJ, Udd L, Mäkelä TP, Alessi DR, Hardie DG.(2003). Complexes between the LKB1 tumor suppressor, STRADalpha/beta and MO25alpha/beta are upstream kinases in the AMP-activated protein kinase cascade. *J Biol*. 2003;2:28.
  112. Hawley SA, Pan DA, Mustard KJ, Ross L, Bain J, Edelman AM, Frenguelli BG, Hardie DG. (2005). Calmodulin-dependent protein kinase kinase-beta is an alternative upstream kinase for AMP-activated protein kinase. *Cell Metab*. 2005;2:9–19.
  113. Hawley SA, Ross FA, Chevtzoff C, Green KA, Evans A, Fogarty S, Towler MC, Brown LJ, Ogunbayo OA, Evans AM, Hardie DG.(2010) Use of cells expressing gamma subunit variants to identify diverse mechanisms of AMPK activation. *Cell Metab*. 2010;11:554–565.
  114. Hayashi M, Morimoto R, Yamamoto A, Moriyama Y (2003a) Expression and localization of vesicular glutamate transporters in pancreatic islets, upper gastrointestinal tract, and testis. *J Histochem Cytochem* 51:1375–1390
  115. Hayashi M, Yamada H, Uehara S, Morimoto R, Muroyama A, Yatsushiro S, Takeda J, Yamamoto A, Moriyama Y (2003b) Secretory granule-mediated co-secretion of L-glutamate and glucagon triggers glutamatergic signal transmission in islets of Langerhans. *J Biol Chem* 278(3):1966–1974
  116. Hayashi T, Hirshman MF, Kurth EJ, Winder WW, and Goodyear LJ. (1998) Evidence of 5' AMP-activated protein kinase mediation of the effect of muscle contraction on glucose transport. *Diabetes* 47: 1369–1373,1998.
  117. Heller RS, Kieffer TJ, Habener JF (1997) Insulinotropic glucagon-like peptide I receptor expression in glucagon-producing alpha-cells of the rat endocrine pancreas. *Diabetes* 46:785–791
  118. Hellman B. (1959). The frequency distribution of the number and volume of the islets of Langerhans in man. I. Studies on non-diabetic adults. *Acta Soc. Med. Ups*. 64:432–60
  119. Henquin J.(2009) Regulation of insulin secretion: a matter of phase control and amplitude modulation. *Diabetologia*. 2009;52:739–51.
  120. Henquin JC, Meissner HP. (1984) Significance of ionic fluxes and changes in membrane potential for stimulus-secretion coupling in pancreatic  $\beta$ -cells. *Experientia*. 1984;40:1043–1052.
  121. Hille B (2001) Ion channels of excitable membranes. Neuroscience, Biophysics. Sinauer associate.
  122. Hundal RS, Krssak M, Dufour S, Laurent D, Lebon V, Chandramouli V, Inzucchi SE, Schumann WC, Petersen KF, Landau BR, Shulman GI.(2000). Mechanism by which metformin reduces glucose production in type 2 diabetes. *Diabetes*. 2000;49:2063–2069.
  123. Hurley JH, Misra S. (2000) Signaling and subcellular targeting by membrane-binding domains. *Annu Rev Biophys Biomol Struct*. 2000;29:49–79.
  124. Hurley RL, Anderson KA, Franzone JM, Kemp BE, Means AR, Witters LA.(2005). The  $Ca^{2+}$ /calmodulin-dependent protein kinase kinases are AMP-activated protein kinase kinases. *J Biol Chem*. 2005;280:29060–29066.
  125. Iismaa TP, Kerr EA, Wilson JR, Carpenter L, Sims N, Biden TJ. (2000). Quantitative and functional characterization of muscarinic receptor subtypes in insulin-secreting cell lines and rat pancreatic islets. *Diabetes* 49:392-398.
  126. Inagaki N, Kuromi H, Gonoi T, Okamoto Y, Ishida H, Seino Y, Kaneko T, Iwanaga T, Seino S (1995) Expression and role of ionotropic glutamate receptors in pancreatic islet cells. *FASEB J* 9(8):686–691.
  127. Ishizuka T, Cooper DR, Arnold T, Hernandez H, Farese RV.(1991) Downregulation of protein kinase C and insulin-stimulated 2-deoxyglucose uptake in rat adipocytes by phorbol esters, glucose, and insulin. *Diabetes*.1991;40:1274–1281.
  128. Jacques-Silva MC, Correa-Medina M, Cabrera O, Rodriguez-Diaz R, Makeeva N, Fachado A, Diez J, Berman DM, Kenyon NS, Ricordi C, Pileggi A, Molano RD, Berggren PO, Caicedo A. (2010). ATP-gated P2X3 receptors constitute a positive autocrine signal for insulin release in the human pancreatic beta cell. *Proc Natl Acad Sci USA* 107:6465-6470.
  129. Jansson L, Hellerstrom C. (1986). Glucose-induced changes in pancreatic islet blood flow mediated by central nervous system. *Am. J. Physiol. Endocrinol. Metab*. 251:E644–47
  130. Jewell JL, Oh E, Thurmond DC (2010). Exocytosis mechanisms underlying insulin release and glucose uptake: conserved roles for Munc18c and syntaxin 4 *Am J Physiol Regul Integr Comp Physiol*. 2010 Mar; 298(3): R517–R531. Published online 2010 Jan 6. PMID: PMC2838661. doi: 10.1152/ajpregu.00597.2009
  131. Jing X, Li DQ, Olofsson CS, Salehi A, Surve VV, Caballero J, Ivarsson R, Lundquist I, Pereverzev A, Schneider T, Rorsman P, Renström E.(2005). Cav2.3 calcium channels control second-phase insulin release. *J Clin Invest*. 2005;115:146–154.

132. Junger WG. (2011). Immune cell regulation by autocrine purinergic signalling. *Nat Rev Immunol.* 11:201-212.
133. Kahn BB, Alquier T, Carling D, Hardie DG. (2005) AMP-activated protein kinase: ancient energy gauge provides clues to modern understanding of metabolism. *Cell Metab.* 2005;1:15–25.
134. Kahn SE. (2003). The relative contributions of insulin resistance and  $\beta$ -cell dysfunction to the pathophysiology of type 2 diabetes. *Diabetologia* 46:3–19
135. Kalandadze A, Wu Y, Robinson M.B. (2002) Protein kinase C activation decreases cell surface expression of the GLT-1 subtype of glutamate transporter. Requirement of a carboxyl-terminal domain and partial dependence on serine 486. *J. Biol. Chem.*, 277 (2002), pp. 45741–45750
136. Kanai Y and Hediger MA. (2003) The glutamate/neutral amino acid transporter family SLC1: molecular, physiological and pharmacological aspects. *Pflügers Archiv European Journal of Physiology* (2003) 447:1146 DOI: 10.1007/s00424-003-1146-4
137. Karlsson S, Scheurink AJ, Steffens AB, Ahren B (1994) Involvement of capsaicin-sensitive nerves in regulation of insulin secretion and glucose tolerance in conscious mice. *Am J Physiol* 267:R1071–R1077
138. Katz LE, Bhala A, Camron E, Nunn SE, Hintz RL, Cohen P (1997) IGF-II, IGF-binding proteins and IGF receptors in pancreatic beta-cell lines. *J Endocrinol* 152:455–464
139. Kemp BE, Stapleton D, Campbell DJ, Chen ZP, Murthy S, Walter M, Gupta A, Adams JJ, Katsis F, van Denderen B, Jennings IG, Iseli T, Michell BJ, Witters LA. (2003) AMP-activated protein kinase, super metabolic regulator. *Biochem. Soc. Trans.* 2003;31:162–168
140. Kirpichnikov D, McFarlane SI, Sowers JR. (2002) [Metformin: an update.](#) *Ann Intern Med.* 2002;137(1):25–33. doi:10.7326/0003-4819-137-1-200207020-00009. PMID 12093242.
141. Kojima M, Hosoda H, Date Y, Nakazato M, Matsuo H, Kangawa K (1999) Ghrelin is a growth-hormone-releasing acylated peptide from stomach. *Nature* 402:656–660
142. Konopacki FA, Jaafari N, Rocca DL, Wilkinson KA, Chamberlain S, Rubin P, Kantamneni S, Mellor JR, Henley JM Agonist-induced PKC phosphorylation regulates GluK2 SUMOylation and kainate receptor endocytosis. 2011, Nov 16 Neuroscience. *Proc Natl Acad Sci U S A.* 2011 Dec 6; 108(49): 19772–19777. PMID: PMC3241814 doi: 10.1073/pnas.1111575108
143. Kotani K, Ogawa W, Matsumoto M, Kitamura T, Sakaue H, Hino Y, Miyake K, Sano W, Akimoto K, Ohno S, Kasuga M. (1998) Requirement of Atypical Protein Kinase C for Insulin Stimulation of Glucose Uptake but Not for Akt Activation in 3T3-L1 Adipocytes. *Mol Cell Biol.* 1998;18:6971–6982.
144. Lau CG, Takayasu Y, Rodenas-Ruano A, Paternain AV, Lerma J, Bennett MVL, and Zukin RS. (2010) SNAP-25 Is a Target of Protein Kinase C Phosphorylation Critical to NMDA Receptor Trafficking *J Neurosci.* 2010 Jan 6; 30(1): 242–254 PMID: PMC3397691 NIHMSID: NIHMS382594 doi: 10.1523/JNEUROSCI.4933-08.2010.
145. Leclerc I, Woltersdorf WW, da Silva Xavier G, Rowe RL, Cross SE, Korbitt GS, Rajotte RV, Smith R, Rutter GA. (2004). Metformin, but not leptin, regulates AMP-activated protein kinase in pancreatic islets: impact on glucose-stimulated insulin secretion. *Am. J. Physiol. Endocrinol. Metab.* 2004;286:E1023–E1031.
146. Leibiger B, Leibiger IB, Moede T, Kemper S, Kulkarni RN, Kahn CR, de Vargas LM, Berggren PO (2001) Selective insulin signalling through A and B insulin receptors regulates transcription of insulin and glucokinase genes in pancreatic beta cells. *Mol Cell* 7:559–570.
147. Leibiger IB, Leibiger B, Berggren PO (2008). Insulin signaling in the pancreatic beta-cell. *Annu Rev Nutr* 28:233–251.
148. Letourneur F., Gaynor E.C., Hennecke, S., Demolliere, C., Duden, R., Emr, S.D., Riezman, H., and Cosson, P. (1994). Coatamer is essential for retrieval of dilysine-tagged proteins to the endoplasmic reticulum. *Cell* 79, 1199–1207.
149. Leung YM, Ahmed I, Sheu L, Gao X, Hara M, Tsushima RG, Diamant NE, Gaisano HY (2006) Insulin regulates islet alpha-cell function by reducing KATP channel sensitivity to adenosine 5'-triphosphate inhibition. *Endocrinology* 147:2155–2162.
150. Ligon B, Yang J, Morin SB, Ruberti MF, Steer ML. (2007). Regulation of pancreatic islet cell survival and replication by gamma-aminobutyric acid. *Diabetologia* 50:764-773
151. Lindström P. (1986). Aromatic-L-amino-acid decarboxylase activity in mouse pancreatic islets. *Biochim Biophys Acta* 884:276-281.
152. Liu P, Cheng H, Roberts TM, Zhao JJ. (2009) Targeting the phosphoinositide 3-kinase pathway in cancer. *Nat Rev Drug Discov.* 2009;8:627–44.
153. Lundquist I, Panagiotidis G, Stenström A. (1991). Effect of L-dopa administration on islet monoamine oxidase activity and glucose-induced insulin release in the mouse. *Pancreas* 6:522-527.

154. MacDonald MJ, Longacre MJ, Stoker SW, Kendrick M, Thonpho A, Brown LJ, Hasan NM, Jitrapakdee S, Fukao T, Hanson MS, Fernandez LA, Odorico J. (2011). Differences between human and rodent pancreatic islets: low pyruvate carboxylase, ATP citrate lyase, and pyruvate carboxylation and high glucose-stimulated acetoacetate in human pancreatic islets. *J. Biol. Chem.* 286:18383–96
155. MacDonald P, Braun M, Galvanovskis J, Rorsman P. (2006). Release of small transmitters through kiss-and-run fusion pores in rat pancreatic  $\beta$  cells. *Cell Metabolism* 4:283–290.
156. Madhunapantula SV, Mosca PJ, Robertson GP. (2011). [The Akt signaling pathway: an emerging therapeutic target in malignant melanoma \(2011\). \*Cancer Biol Ther.\* 2011 Dec 15; 12\(12\): 1032–1049. PMID: PMC3335938. doi: 10.4161/cbt.12.12.18442](#)
157. Maffucci T, Cooke FT, Foster FM, Traer CJ, Fry MJ, Falasca M. (2005). Class II phosphoinositide 3-kinase defines a novel signaling pathway in cell migration. *J Cell Biol.* 2005;169:789–99.
158. Malaisse WJ, Boschero AC. (1977) Calcium antagonists and islet function. XI. Effect of nifedipine (1977). *Horm Res.* 1977;8:203–209.
159. Malsam J, Satoh A, Pelletier L, Warren G. (2005) Golgin tethers define subpopulations of COPI vesicles. *Science.* 307(5712):1095–8.
160. Marone R, Cmiljanovic V, Giese B, Wymann MP. (2008) Targeting phosphoinositide 3-kinase: moving towards therapy. *Biochim Biophys Acta.* 2008;1784:159–185.
161. Matthews EK, Sakamoto Y (1975). Electrical characteristics of pancreatic islet cells. *J Physiol.* 1975;246:421–437.
162. McCulloch LJ, Van de Bunt M, Braun M, Frayn KN, Clark A, Gloyn AL. (2011). GLUT2 (SLC2A2) is not the principal glucose transporter in human pancreatic  $\beta$  cells: implications for understanding genetic association signals at this locus. *Mol. Genet. Metab.* 104:648–53
163. Meier JJ, Nauck MA (2006) Incretins and the development of type 2 diabetes. *Curr Diab Rep* 6:194–201
164. Mezey E, Eisenhofer G, Harta G, Hansson S, Gould L, Hunyady B, Hoffman BJ. (1996). A novel non neuronal catecholaminergic system: exocrine pancreas synthesizes and releases dopamine. *Proc Natl Acad Sci USA.* 93:10377–10382.
165. Mihaylova MM and Shaw RJ. The AMPK signaling pathway coordinates cell growth, autophagy and metabolism. *Nat Cell Biol.* Author manuscript; available in PMC 2012 Mar 2. Published in final edited form as: *Nat Cell Biol.* 2011 Sep 2; 13(9): 1016–1023. Published online 2011 Sep 2. doi: 10.1038/ncb2329
166. Mīinea CP, Sano H, Kane S, Sano E, Fukuda M, Peränen J, Lane WS, Lienhard GE. (2005). AS160, the Akt substrate regulating GLUT4 translocation, has a functional Rab GTPase-activating protein domain. *Biochem J.* 2005;391:87–93.
167. Mochly-Rosen D, Gordon AS (1998). Anchoring proteins for protein kinase C: a means for isozyme selectivity. *FASEB J* 12 :35 –42,1998.
168. Moens K, Heimberg H, Flamez D, Huypens P, Quartier E, Ling Z, Pipeleers D, Gremlich S, Thorens B, Schuit F (1996) Expression and functional activity of glucagon, glucagon-like peptide I, and glucose-dependent insulinotropic peptide receptors in rat pancreatic islet cells. *Diabetes* 45:257–261.
169. Molina J, Rodriguez-Diaz R, Fachado A, Jacques-Silva MC, Berggren PO, Caicedo A. (2014). Control of insulin secretion by cholinergic signaling in the human pancreatic islet. *Diabetes* 63:2714–2726.
170. Molnar E, Varadi A, McIlhinney RA, Ashcroft SJ (1995) Identification of functional ionotropic glutamate receptor proteins in pancreatic beta-cells and in islets of Langerhans. *FEBS Lett* 371:253–257.
171. Moriyama and Omote (2008) Vesicular Glutamate Transporter Acts as a Metabolic Regulator. *Biol. Pharm. Bull.* 31(10) 1844:1846
172. Moriyama Y, Hayashi M (2003) Glutamate-mediated signaling in the islets of Langerhans: a thread entangled. *Trends Pharmacol Sci* 24:511–517
173. Morley P, MacLean S, Gendron TF, Small DL, Tremblay R, et al. (2000) Pharmacological and molecular characterization of glutamate receptors in the MIN6 pancreatic beta-cell line. *Neurol Res*, 22:379–385.
174. Mu J, Brozinick JT, Valladares O, Bucan M, and Birnbaum MJ. (2001) A role for AMP-activated protein kinase in contraction- and hypoxia-regulated glucose transport in skeletal muscle. *Mol Cell* 7: 1085–1094, 2001.
175. Muller D, Huang GC, Amiel S, Jones PM, Persaud SJ (2006) Identification of insulin signaling elements in human beta-cells: autocrine regulation of insulin gene expression. *Diabetes* 55:2835–2842
176. Munday, M. R., Milic, M. R., Takhar, S., Holness, M. J. and Sugden, M. C. (1991) The short-term regulation of hepatic acetyl-CoA carboxylase during starvation and re-feeding in the rat. *Biochem. J.* 280, 733–737

177. Muroyama A, Uehara S, Yatsushiro S, Echigo N, Morimoto R, Morita M, Hayashi M, Yamamoto A, Koh DS, Moriyama Y (2004) A novel variant of ionotropic glutamate receptor regulates somatostatin secretion from delta-cells of islets of Langerhans. *Diabetes* 53(7):1743–1753
178. Myers MG Jr, Backer JM, Sun XJ, Shoelson S, Hu P, Schlessinger J, Yoakim M, Schaffhausen B, White MF. (1992). IRS-1 activates phosphatidylinositol 3'-kinase by associating with src homology 2 domains of p85. *Proc Natl Acad Sci USA*. 1992;89:10350–10354.
179. Neshler R, Cerasi E (1987) Biphasic insulin release as the expression of combined inhibitory and potentiating effects of glucose. *Endocrinology* 121 :1017–1024, 1987
180. Nishizuka Y (1989). The family of protein kinase C for signal transduction. *JAMA*. 1989;262:1826–1833.
181. Nishizuka Y. (1984) The role of protein kinase C in cell surface signal transduction and tumor promotion. *Nature*. 1984;308:693–698.
182. Nishizuka Y. (1986). Studies and perspectives of protein kinase C. *Science*. 1986;233:305–312.
183. Nishizuka Y. (1988) The molecular heterogeneity of PKC and its implications for cellular regulation. *Nature*. 1988;334:661–665.
184. [Oakhill JS](#), [Steel R](#), [Chen ZP](#), [Scott JW](#), [Ling N](#), [Tam S](#), [Kemp BE](#). AMPK is a direct adenylate charge-regulated protein kinase. *Science*. 2011;332:1433–1435.
185. Oh CM, Namkung J, Go Y, Shong KE, Kim K, Kim H, Park BY, Lee HW, Jeon YH, Song J, Shong M, Yadav VK, Karsenty G, Kajimura S, Lee IK, Park S, Kim H. (2015). Regulation of systemic energy homeostasis by serotonin in adipose tissues. *Nat Commun*. 6:6794
186. Ohta Y, Kosaka Y, Kishimoto N, Wang J, Smith SB, Honig G, Kim H, Gasa RM, Neubauer N, Liou A, Tecott LH, Deneris ES, German MS. (2011). Convergence of the Insulin and Serotonin Programs in the Pancreatic  $\beta$ -Cell. *Diabetes* 60:3208–3216.
187. Orci L, Malaisse-Lagae F, Ravazzola M, Rouiller D, Renold AE, Perrelet A, Unger R (1975) A morphological basis for intercellular communication between alpha- and beta-cells in the endocrine pancreas. *J Clin Invest* 56:1066–1070
188. Owen, D.J., Collins, B.M., and Evans, P.R. (2004). Adaptors for clathrin coats: structure and function. *Annu. Rev. Cell Dev. Biol.* 20, 153–191.
189. Patel NA, Chalfant CE, Watson JE, Wyatt JR, Dean NM, Eichler DC, Cooper DR. (2001). Insulin regulates alternative splicing of protein kinase C beta II through a phosphatidylinositol 3-kinase-dependent pathway involving the nuclear serine/arginine-rich splicing factor, SRp40, in skeletal muscle cells. *J Biol Chem*. 2001;276:22648–22654.
190. Paulmann N, Grohmann M, Voigt J-P, Bert B, Vowinckel J, Bader M, Skelin M, Jevšek M, Fink H, Rupnik M, Walther DJ. (2009). Intracellular serotonin modulates insulin secretion from pancreatic  $\beta$ -cells by protein serotonylation. *PLoS Biol* 7:e1000229.
191. Pearse, B.M. (1975). Coated vesicles from pig brain: purification and biochemical characterization. *J. Mol. Biol.* 97, 93–98.
192. Petit P, Lajoix AD, Gross R. (2009). P2 purinergic signaling in the pancreatic beta-cell: control of insulin secretion and pharmacology. *Eur J Pharm Sci* 37:67–75.
193. Pochini L, Scalise M, Galluccio M, and Indiveri C. (2014) Membrane transporters for the special amino acid glutamine: structure/function relationships and relevance to human health. *Front Chem*. 2014; 2: 61. Published online 2014 Aug 11. doi: 10.3389/fchem.2014.00061. PMID: PMC4127817.
194. Pouyssegur J, Volmat V, Lenormand P: Fidelity and spatio-temporal control in MAP kinase (ERKs) signaling (2002). *Biochem Pharmacol* 64 :755–763, 2002 .
195. Quesada I, Tuduri E, Ripoll C, Nadal A (2008) Physiology of the pancreatic alpha-cell and glucagon secretion: role in glucose homeostasis and diabetes. *J Endocrinol* 199:5–19.
196. Raffo A, Hancock K, Polito T, Xie Y, Andan G, Witkowski P, Hardy M, Barba P, Ferrara C, Maffei A, Freeby M, Goland R, Leibel RL, Sweet IR, Harris PE. (2008). Role of vesicular monoamine transporter type 2 in rodent insulin secretion and glucose metabolism revealed by its specific antagonist tetrabenazine. *J Endocrinol* 198:41–49.
197. Ramalingam L, Oh E, Thurmond DC (2013). [Novel roles for insulin receptor \(ir\) in adipocytes and skeletal muscle cells via new and unexpected substrates](#). *Cell Mol Life Sci*. 2013 Aug; 70(16): 2815–2834. PMID: PMC3556358. NIHMSID: NIHMS413940. doi: 10.1007/s00018-012-1176-1
198. Ramracheya R, Ward C, Shigeto M, Walker JN, Amisten S, Zhang Q, Johnson PR, Rorsman P, Braun M. (2010) Membrane potential-dependent inactivation of voltage-gated ion channels in alpha-cells inhibits glucagon secretion from human islets. *Diabetes*. 2010;59:2198–208.

199. Rebelato E, Abdulkader F, Curi R, Carpinelli AR. (2011). Control of the intracellular redox state by glucose participates in the insulin secretion mechanism. *PLoS ONE* 6:e24507.
200. Reetz A, Solimena M, Matteoli M, Folli F, Takei K, De Camilli P. (1991). GABA and pancreatic beta-cells: colocalization of glutamic acid decarboxylase (GAD) and GABA with synaptic-like microvesicles suggests their role in GABA storage and secretion. *EMBO J* 10:1275-1284
201. Rena G, Pearson ER, Sakamoto K (2013). "Molecular mechanism of action of metformin: old or new insights?". *Diabetologia* 56 (9): 1898–906. doi:10.1007/s00125-013-2991-0. PMC 3737434. PMID 23835523.
202. Robinson MB (1999) The family of sodium-dependent glutamate transporters: A focus on the GLT-1/EAAT2 subtype. *Neurochem Int* 33:479–491.
203. Robinson MB and Dowd LA (1997) Heterogeneity and functional properties of subtypes of sodium-dependent glutamate transporters in the mammalian central nervous system. *Adv Pharmacol* 37:69–115
204. Rodriguez-Diaz R, Abdulreda MH, Formoso AL, Gans I, Ricordi C, Berggren PO, Caicedo A. (2011a). Innervation patterns of autonomic axons in the human endocrine pancreas. *Cell Metab.* 14:45–54
205. Rodriguez-Diaz R, Dando R, Jacques-Silva MC, Fachado A, Molina J, Abdulreda MH, Ricordi C, Roper SD, Berggren PO, Caicedo A. (2011b). Alpha cells secrete acetylcholine as a non-neuronal paracrine signal priming beta cell function in humans. *Nat Med* 17:888-892.
206. Rogers SL, Gelfand VI. (1998) Myosin cooperates with microtubule motors during organelle transport in melanophores. *Curr Biol.* 8(3):161-4.
207. Rorsman P, Berggren PO, Bokvist K, Ericson H, Möhler H, Ostenson CG, Smith PA. (1989). Glucose-inhibition of glucagon secretion involves activation of GABA<sub>A</sub>-receptor chloride channels. *Nature* 341:233-236.
208. Rorsman P, Braun M. (2013). Regulation of Insulin Secretion in Human Pancreatic Islets . *Annu Rev Physiol.* 2013;75:155-79. doi: 10.1146/annurev-physiol-030212-183754. Epub 2012 Sep 4.
209. Rorsman P, Renstrom E (2003). Insulin granule dynamics in pancreatic beta cells. *Diabetologia.* (2003);46:1029–1045.
210. Rorsman P, Trube G. Glucose dependent K<sup>+</sup>-channels in pancreatic beta-cells are regulated by intracellular ATP (1985). *Pflugers Arch.* 1985;405:305–309.
211. Rosenzweig T, Braiman L, Bak A, Alt A, Kuroki T, Sampson SR.(2002). Differential effects of tumor necrosis factor- $\alpha$  on protein kinase C isoforms  $\alpha$  and  $\delta$  mediate inhibition of insulin receptor signaling. *Diabetes.* (2002);51:1921–1930.
212. Rossowski WJ, Coy DH (1994) Specific inhibition of rat pancreatic insulin or glucagon release by receptor-selective somatostatin analogs. *Biochem Biophys Res Commun* 205:341–346
213. Rothman JE (1994) Mechanisms of intracellular protein transport. *Nature* 372:55-63
214. Rubí B, Ljubicic S, Pournourmohammadi S, Carobbio S, Armanet M, Bartley C, Maechler P. (2005). Dopamine D<sub>2</sub>-like receptors are expressed in pancreatic beta cells and mediate inhibition of insulin secretion. *J Biol Chem* 280:36824-36832.
215. Salt I.P., Johnson G., Ashcroft S.J., Hardie D.G. AMP-activated protein kinase is activated by low glucose in cell lines derived from pancreatic beta cells, and may regulate insulin release. *Biochem. J.* 1998;335:533–539.
216. Sampson RS, and Cooper DR. (2006). Specific protein kinase C isoforms as transducers and modulators of insulin signaling. *Mol Genet Metab.* 2006; 89(1-2): 32–47 NIHMSID: NIHMS97655. PMCID: PMC2664304. doi: 10.1016/j.ymgme.2006.04.017
217. Sano H, Kane S, Sano E, Miinea CP, Asara JM, et al. Insulin-stimulated phosphorylation of a Rab GTPase-activating protein regulates GLUT4 translocation (2003). *J Biol Chem.* 2003;278:14599–14602.
218. Schroer TA, Sheetz MP. (1991) Functions of microtubule-based motors. *Annu Rev Physiol.* 53:629-52.
219. Schuit F, De Vos A, Farfari S, Moens K, Pipeleers D, Brun T, Prentki M. (1997). Metabolic fate of glucose in purified islet cells. Glucose-regulated anaplerosis in  $\beta$  cells. *J. Biol. Chem.* 272:18572–79.
220. Schulla V, Renström E, Feil R, Feil S, Franklin I, Gjinovci A, Jing XJ, Laux D, Lundquist I, Magnuson MA, Obermüller S, Olofsson CS, Salehi A, Wendt A, Klugbauer N, Wollheim CB, Rorsman P, Hofmann F.(2003). Impaired insulin secretion and glucose tolerance in  $\beta$  cell-selective Cav1.2 Ca<sup>2+</sup> channel null mice(2003). *EMBO J.* 2003;22:3844–3854.
221. Schwartz TW, Holst JJ, Fahrenkrug J, Jensen SL, Nielsen OV, Rehfeld JF, de Muckadell OB, Stadil F. (1978) Vagal, cholinergic regulation of pancreatic polypeptide secretion. *J Clin Invest.* 1978; 61:781–789. [PubMed: 641155]
222. Sesti G, Federici M, Hribal ML, Lauro D, Sbraccia P, Lauro R. (2001). Defects of the insulin receptor substrate (IRS) system in human metabolic disorders. *FASEB J.* 2001;15:2099–2111.

223. Shackelford DB and Shaw RJ. (2009). The LKB1-AMPK pathway: metabolism and growth control in tumour suppression. *Nat Rev Cancer*. 2009;9:563–575.
224. Shankar E, Santhosh KT, Paulose CS. (2006) Dopaminergic regulation of glucose-induced insulin secretion through dopamine D2 receptors in the pancreatic islets in vitro. *IUBMB Life*. 2006 58(3):157-163.
225. Shaw RJ, Kosmatka M, Bardeesy N, Hurley RL, Witters LA, DePinho RA, Cantley LC. (2004) The tumor suppressor LKB1 kinase directly activates AMP-activated kinase and regulates apoptosis in response to energy stress. *Proc Natl Acad Sci U S A*. 2004;101:3329–3335.
226. Shaw RJ, Lamia KA, Vasquez D, Koo SH, Bardeesy N, Depinho RA, Montminy M, Cantley LC. (2005). The kinase LKB1 mediates glucose homeostasis in liver and therapeutic effects of metformin. *Science*. 2005;310:1642–1646.
227. Shepherd PR, Withers DJ, Siddle K. (1998) Phosphoinositide 3-kinase: the key switch mechanism in insulin signalling. *Biochem J*. 1998;333(Pt 3):471–490.
228. Shorter J, Beard MB, Seemann J, Dirac-Svejstrup AB, Warren G. (2002). Sequential tethering of Golgins and catalysis of SNAREpin assembly by the vesicle-tethering protein p115. *J Cell Biol*. 157(1):45-62
229. Silva Xavier G, Leclerc I, Salt IP, Doiron B, Hardie DG, Kahn A, Rutter GA. (2000). Role of AMP-activated protein kinase in the regulation by glucose of islet beta cell gene expression. *Proc. Natl. Acad. Sci. U. S. A.* . 2000;97:4023–4028.
230. Silva Xavier G, Leclerc I, Varadi A, Tsuboi T, Moule SK, Rutter GA. (2003). Role for AMP-activated protein kinase in glucose-stimulated insulin secretion and preproinsulin gene expression. *Biochem. J*. 2003;371:761–774.
231. Silverthorn DU, (2000) *Physiology, CEA*
232. Simpson N, Maffei A, Freeby M, Burroughs S, Freyberg Z, Javitch J, Leibel RL, Harris PE. (2012). Dopamine-mediated autocrine inhibitory circuit regulating human insulin secretion in vitro. *Mol Endocrinol*. 26(10):1757-1772.
233. Söllner T, Whiteheart SW, Brunner M, Erdjument-Bromage H, Geromanos S, Tempst P, Rothman JE. (1993) SNAP receptors implicated in vesicle targeting and fusion. *Nature*. 362(6418):318-24.
234. Soltani N, Qiu H, Aleksic M, Glinka Y, Zhao F, Liu R, Li Y, Zhang N, Chakrabarti R, Ng T, Jin T, Zhang H, Lu WY, Feng ZP, Prud'homme GJ, Wang Q. (2011). GABA exerts protective and regenerative effects on islet beta cells and reverses diabetes. *Proc Natl Acad Sci USA* 108:11692-11697.
235. Spanswick D, Smith MA, Mirshamsi S, Routh VH, Ashford ML (2000) Insulin activates ATP-sensitive K<sup>+</sup> channels in hypothalamic neurons of lean, but not obese rats. *Nat Neurosci* 3:757–758.
236. Stagner JI & Samols E (1992). The vascular order of islet cellular perfusion in the human pancreas. *Diabetes* 41, 93–97.
237. Stapleton, D., Gao, G., Michell, B. J., Widmer, J., Mitchelhill, K., Teh, T., House, C. M., Witters, L. A. and Kemp, B. E. (1994) Mammalian 5 $\alpha$ -AMP-activated protein kinase non-catalytic subunits are homologs of proteins that interact with yeast Snf1 protein kinase. *J. Biol. Chem*. 269, 29343–29346.
238. Steinman RM, Mellman IS, Muller WA, Cohn ZA. Endocytosis and the recycling of plasma membrane. (1983) *J Cell Biol*. 1983;96:1–27.
239. Storto M, Capobianco L, Battaglia G, Molinaro G, Gradini R, Rizzo B, Di Mambro A, Mitchell KJ, Bruno V, Vairetti MP, Rutter GA, Nicoletti F (2006) Insulin secretion is controlled by mGlu5 metabotropic glutamate receptors. *Mol Pharmacol* 69:1234–1241.
240. Straub SG and Sharp GW. (2002). Glucose-stimulated signaling pathways in biphasic insulin secretion. *Diabetes Metab Res Rev*. 2002 Nov-Dec;18(6):451-63. PMID: 12469359
241. Strowski MZ, Cashen DE, Birzin ET, Yang L, Singh V, Jacks TM, Nowak KW, Rohrer SP, Patchett AA, Smith RG et al (2006) Antidiabetic activity of a highly potent and selective non-peptide somatostatin receptor subtype-2 agonist. *Endocrinology* 147:4664–4673.
242. Sun XJ, Wang LM, Zhang Y, Yenush L, Myers MG Jr, Glasheen E, Lane WS, Pierce JH, White MF. Role of IRS-2 in insulin and cytokine signalling. *Nature*. (1995);377:173–177.
243. Sun Y, Asnicar M, Saha PK, Chan L, Smith RG. (2006). Ablation of ghrelin improves the diabetic but not obese phenotype of ob/ob mice. *Cell Metab*. 2006 May;3(5):379-86. PMID: 16679295
244. Swanson RA, Liu J, Miller JW, Rothstein JD, Farrell K, Stein BA, and Longuemare MC (1997) Neuronal regulation of glutamate transporter subtype expression in astrocytes. *J Neurosci* 17:932–940.
245. Taborsky GJ Jr, Ahrén B, Havel PJ. (1998) *Diabetes*. 1998; 47:995–1005. Autonomic mediation of glucagon secretion during hypoglycemia: implications for impaired alpha-cell responses in type 1 diabetes. [PubMed: 9648820]

246. Tang SH, Sharp GW (1998) Atypical protein kinase C isozyme  $\zeta$  mediates carbachol-stimulated insulin secretion in RINm5F cells. *Diabetes* 47:905–912, 1998
247. Thomas-Reetz A, Hell JW, Doring MJ, Walch-Solimena C, Jahn R, De Camilli P. (1993). A gamma-aminobutyric acid transporter driven by a proton pump is present in synaptic-like microvesicles of pancreatic beta cells. *Proc Natl Acad Sci USA* 90:5317–5321.
248. Thorpe LM, Yuzugullu H, Zhao JJ. (2015) PI3K in cancer: divergent roles of isoforms, modes of activation and therapeutic targeting. *Nat Rev Cancer*. 2015 Jan;15(1):7–24. doi: 10.1038/nrc3860
249. Tian J, Dang H, Chen Z, Guan A, Jin Y, Atkinson MA, Kaufman DL. (2013).  $\gamma$ -Aminobutyric acid regulates both the survival and replication of human  $\beta$ -cells. *Diabetes* 62:3760–3765.
250. Tong Q, Ouedraogo R, Kirchgessner AL (2002) Localization and function of group III metabotropic glutamate receptors in rat pancreatic islets. *Am J Physiol Endocrinol Metab* 282:E1324–E1333.
251. Torres G, Amara SG (2007) Glutamate and monoamine transporters: new visions of form and function. Elsevier, volume 17, Issue 3, June 2007, Pages 304–312. Signalling mechanisms.
252. Tuttle RL, Gill NS, Pugh W, Lee JP, Koeberlein B, Furth EE, Polonsky KS, Naji A, Birnbaum MJ. (2001). Regulation of pancreatic beta-cell growth and survival by the serine/threonine protein kinase Akt1/PKB $\alpha$ . *Nat. Med.* 2001;7:1133–1137.
253. Uehara S, Muroyama A, Echigo N, Morimoto R, Otsuka M, Yatsushiro S, Moriyama Y (2004) Metabotropic glutamate receptor type 4 is involved in autoinhibitory cascade for glucagons secretion by alpha-cells of islet of Langerhans. *Diabetes* 53(4):998–1006.
254. Uhles S, Moede T, Leibiger B, Berggren PO, Leibiger IB (2003) Isoform-specific insulin receptor signaling involves different plasma membrane domains. *J Cell Biol* 163:1327–1337.
255. Ustione A, Piston DW. (2012). Dopamine synthesis and D3 receptor activation in pancreatic  $\beta$ -cells regulates insulin secretion and intracellular [Ca<sup>2+</sup>] oscillations. *Mol Endocrinol.* (11):1928–1940.
256. Van Schravendijk CF, Fורים A, Van den Brande JL, Pipeleers DG (1987) Evidence for the presence of type I insulin-like growth factor receptors on rat pancreatic A and B cells. *Endocrinology* 121:1784–1788
257. Vetterli L., Carobbio S., Pournourmohammadi S., Martin-Del-Rio R., Skytt D.M., Waagepetersen H.S., Tamarit-Rodriguez J., Maechler P. Delineation of glutamate pathways and secretory responses in pancreatic islets with  $\beta$ -cell-specific abrogation of the glutamate dehydrogenase. *Mol. Biol. Cell.* 2012;23:3851–3862
258. Vogt PK, Gymnopoulos M, Hart PI. (2009) Jr 3-kinase and cancer: changing accents. *Curr Opin Genet Dev.* 2009;19:12–17. doi: 10.1016/j.gde.2008.11.011.
259. Wang C, Ling Z, Pipeleers D. (2005). Comparison of cellular and medium insulin and GABA content as markers for living beta-cells. *Am J Physiol Endocrinol Metab.* 288(2):E307–13.
260. Wang GJ, Chung HJ, Schnuer J, Lea E, Robinson MB, Potthoff WK, Aizenman E, Rosenberg PA. (1998) Dihydrokainate-sensitive neuronal glutamate transport is required for protection of rat cortical neurons in culture against synaptically released glutamate. *Eur J Neurosci.* 10(8):2523–31.
261. Wang Y, et al. 1997 AMPA receptor-mediated regulation of a Gi-protein in cortical neurons *Nature*, 389 (1997), pp. 502–504.
262. Wang Z, Thurmond DC. (2009) Mechanisms of biphasic insulin-granule exocytosis - roles of the cytoskeleton, small GTPases and SNARE proteins. *J Cell Sci.* 2009;122:893–903.
263. Waters, M.G., Serafini, T., and Rothman, J.E. (1991). ‘Coatamer’: a cytosolic protein complex containing subunits of non-clathrin-coated Golgi transport vesicles. *Nature* 349, 248–251
264. Weaver CD, Gundersen V, Verdoorn TA (1998) A high affinity glutamate/aspartate transport system in pancreatic islets of Langerhans modulates glucose-stimulated insulin secretion. *J Biol Chem* 273(3):1647–1653
265. Weaver CD, Yao TL, Powers AC, Verdoorn TA (1996) Differential expression of glutamate receptor subtypes in rat pancreatic islets. *J Biol Chem* 271(22):12977–12984
266. Wessler IK, Kirkpatrick CJ. (2012). Activation of muscarinic receptors by non-neuronal acetylcholine. *Handb Exp Pharmacol* 208:469–491.
267. White MF. The insulin signalling system and the IRS proteins (1997). *Diabetologia.* 1997;40(Suppl 2):2–17.
268. Woods A, Dickerson K, Heath R, Hong SP, Momcilovic M, Johnstone SR, Carlson M, Carling D. (2005). (Ca<sup>2+</sup>)/calmodulin-dependent protein kinase kinase-beta acts upstream of AMP-activated protein kinase in mammalian cells. *Cell Metab.* 2005;2:21–33.

269. Woods A, Johnstone SR, Dickerson K, Leiper FC, Fryer LG, Neumann D, Schlattner U, Wallimann T, Carlson M, Carling D. (2008) LKB1 is the upstream kinase in the AMP-activated protein kinase cascade. *Curr Biol.* 2003;13:2004–2008.
270. Wu H, MacFarlane WM, Tadayyon M, Arch JR, James RF, Docherty K (1999) Insulin stimulates pancreatic-duodenal homoeobox factor-1 (PDX1) DNA-binding activity and insulin promoter activity in pancreatic beta cells. *Biochem J* 344:813–818.
271. Xiao B, Sanders MJ, Underwood E, Heath R, Mayer FV, Carmena D, Jing C, Walker PA, Eccleston JF, Haire LF, Saiu P, Howell SA, Aasland R, Martin SR, Carling D, Gamblin SJ. (2011). Structure of mammalian AMPK and its regulation by ADP. *Nature.* 2011;472:230–233.
272. Xu E, Kumar M, Zhang Y, Ju W, Obata T, Zhang N, Liu S, Wendt A, Deng S, Ebina Y et al (2006) Intra-islet insulin suppresses glucagons release via GABA–GABAA receptor system. *Cell Metab* 3:47–58.
273. Yamaguchi S, Katahira H, Ozawa S, Nakamichi Y, Tanaka T, Shimoyama T, Takahashi K, Yoshimoto K, Imaizumi MO, Nagamatsu S, Ishida H. (2005) Activators of AMP-activated protein kinase enhance GLUT4 translocation and its glucose transport activity in 3T3-L1 adipocytes. *American Journal of Physiology - Endocrinology and Metabolism* 2005 Vol. 289 no. 4, E643-E649 DOI: 10.1152/ajpendo.00456.2004
274. Yaney GC, Fairbanks JM, Deeney JT, Korchak HM, Tornheim K, Corkey BE (2002) Potentiation of insulin secretion by phorbol esters is mediated by PKC- $\alpha$  and nPKC isoforms. *Am J Physiol Endocrinol Metab* 283 :E880 – E888, 2002
275. Yarden Y, Ullrich A (1988) Growth factor receptor tyrosine kinases. *Annu Rev Biochem.* 57:443–478
276. Yedovitzky M, Mochly-Rosen D, Johnson JA, Gray MO, Ron D, Abramovitch E, Cerasi E, Neshler R: Translocation inhibitors define specificity of protein kinase C isoenzymes in pancreatic beta-cells. *J Biol Chem* 272 :1417 – 1420, 1997
277. Yeh, L. A., Lee, K. H. and Kim, K. H. (1980) Regulation of rat liver acetyl-CoA carboxylase. Regulation of phosphorylation and inactivation of acetyl-CoA carboxylase by the adenylate energy charge. *J. Biol. Chem.* 255, 2308–2314
278. Yernool D, Boudker O, Jin Y, Gouaux E. (2004) Structure of a glutamate transporter homologue from *Pyrococcus horikoshii*. *Nature* 431(7010):811-8.
279. Yoshikawa H, Hellström-Lindahl E, Grill V. (2005). Evidence for functional nicotinic receptors on pancreatic beta cells. *Metabolism* 54:247-254.
280. Yoshioka K, Yoshida K, Cui H, Wakayama T, Takuwa N, Okamoto Y, Du W, Qi X, Asanuma K, Sugihara K, Aki S, Miyazawa H, Biswas K, Nagakura C, Ueno M, Iseki S, Schwartz RJ, Okamoto H, Sasaki T, Matsui O, Asano M, Adams RH, Takakura N, Takuwa Y. (2012). Endothelial PI3K-C2 $\alpha$ , a class II PI3K, has an essential role in angiogenesis and vascular barrier function. *Nat Med.* 2012;18:1560–9.
281. Zang M, Zuccollo A, Hou X, Nagata D, Walsh K, Herscovitz H, Brecher P, Ruderman NB, Cohen RA (2004). AMP-activated protein kinase is required for the lipid-lowering effect of metformin in insulin-resistant human HepG2 cells. *J Biol Chem.* 2004;279:47898–47905.
282. Zelenia O, Schlag BD, Gochenauer GE, Ganel R, Song W, Beesley JS, Grinspan JB, Rothstein JD, Robinson MB. (2000) Epidermal growth factor receptor agonists increase expression of glutamate transporter GLT-1 in astrocytes through pathways dependent on phosphatidylinositol 3-kinase and transcription factor NF- $\kappa$ B. *Mol Pharmacol.* 2000 Apr;57(4):667-78. PMID: 10727511
283. Zhang CY, Baffy G, Perret P, Krauss S, Peroni O, Grujic D, Hagen T, Vidal-Puig AJ, Boss O, Kim YB, Zheng XX, Wheeler MB, Shulman GI, Chan CB, Lowell BB (2001). Uncoupling protein-2 negatively regulates insulin secretion and is a major link between obesity, beta cell dysfunction and type 2 diabetes. *Cell.* 2001;105:745–755.
284. Zhang Q, Zhu Y, Zhou W, Gao L, Yuan L, Han X. (2013). Serotonin receptor 2C and insulin secretion *PLoS One* 8:e54250.
285. Zhang S. and Kim K.H. (1995) Glucose activation of acetyl-CoA carboxylase in association with insulin secretion in a pancreatic beta-cell line. *J. Endocrinol.* 1995;147:33–41.
286. Zhang Y, Zheng R, Meng X, Wang L, Liu L, Gao Y. (2015). Pancreatic Endocrine Effects of Dopamine Receptors in Human Islet Cells. *Pancreas* 44(6):925-929.
287. Zheng Ye and Sarr Mg. (2011) Translocation of Transfected GLUT2 to the Apical Membrane in Rat Intestinal IEC-6 Cells Published online 2011 Nov 25. *Dig Dis Sci.* 2012 May; 57(5): 1203–1212. PMID: PMC3331913 NIHMSID: NIHMS344640. doi: 10.1007/s10620-011-1984-4

288. Zhou G, Myers R, Li Y, Chen Y, Shen X, Fenyk-Melody J, Wu M, Ventre J, Doebber T, Fujii N, Musi N, Hirshman MF, Goodyear LJ, Moller DE (2001). Role of AMP-activated protein kinase in mechanism of metformin action. *J Clin Invest.* 2001;108:1167–1174.
289. Zhou J, Sutherland ML (2004) Glutamate transporter cluster formation in astrocytic processes regulates glutamate uptake activity. *J. Neurosci.*, 24 (2004), pp. 6301–6306

## Bibliography Chapter II

- Albrecht P, Lewerenz J, Dittmer S, Noack R, Maher P, Methner A (2010) Mechanisms of oxidative glutamate toxicity: the glutamate/ cystine antiporter system xc<sup>-</sup> as a neuroprotective drug target. *CNS Neurol Disord Drug Targets* 9(3):373–382.
- Aliprandi A, Longoni M, Stanzani L, Tremolizzo L, Vaccaro M, Begni B, Galimberti G, Garofolo R, Ferrarese C (2005) Increased plasma glutamate in stroke patients might be linked to altered platelet release and uptake. *J Cereb Blood Flow Metab* 25(4):513–519.
- Anfossi G, Russo I, Trovati M (2009) Platelet dysfunction in central obesity. *Nutr Metab Cardiovasc Dis* 19(6):440–449.
- Asano T, Ninomiya H, Kan K, Yamamoto T, Okumura M (1989) Plasma glucagon response to intravenous alanine in obese and non-obese subjects. *Endocrinol Jpn* 36(5):767–773.
- Bai L, Zhang X, Ghishan FK (2003) Characterization of vesicular glutamate transporter in pancreatic alpha—and beta—cells and its regulation by glucose. *Am J Physiol Gastrointest Liver Physiol* 284(5):G808–G814
- Baron AD, Schaeffer L, Shragg P, Kolterman OG (1987) Role of hyperglucagonemia in maintenance of increased rates of hepatic glucose output in type II diabetics. *Diabetes* 36(3):274–283.
- Bellisle F, Monneuse MO, Chabert M, Larue-Achagiots C, Lanteaume MT, Louis-Sylvestre J (1991) Monosodium glutamate as a palatability enhancer in the European diet. *Physiol Behav* 49(5):869–873.
- Bertrand G, Gross R, Puech R, Loubatière-Mariani MM, Bockaert J (1993) Glutamate stimulates glucagon secretion via an excitatory amino acid receptor of the AMPA subtype in rat pancreas. *Eur J Pharmacol* 237(1):45–50.
- Blachier F, Boutry C, Bos C, Tome D (2009) Metabolism and functions of L-glutamate in the epithelial cells of the small and large intestines. *Am J Clin Nutr* 90(3):814S–821S
- Brice NL, Varadi A, Ashcroft SJ, Molnar E (2002) Metabotropic glutamate and GABA(B) receptors contribute to the modulation of glucose-stimulated insulin secretion in pancreatic beta cells. *Diabetologia* 45:242–252.
- Butte NF, Hsu HW, Thotathuchery M, Wong WW, Khoury J, Reeds P (1999) Protein metabolism in insulin-treated gestational diabetes. *Diabetes Care* 22(5):806–811
- Cabrera O, Jacques-Silva MC, Speier S, Yang SN, Köhler M, Fachado A, Vieira E, Zierath JR, Kibbey R, Berman DM, Kenyon NS, Ricordi C, Caicedo A, Berggren PO (2008) Glutamate is a positive autocrine signal for glucagon release. *Cell Metab* 7(6):545–554
- Castellanos M, Sobrino T, Pedraza S, Moldes O, Pumar JM, Silva Y, Serena J, García-Gil M, Castillo J, Dávalos A (2008) High plasma glutamate concentrations are associated with infarct growth in acute ischemic stroke. *Neurology* 71(23):1862–1868
- Chevalier S, Marliss EB, Morais JA, Lamarche M, Gougeon R (2005) Whole-body protein anabolic response is resistant to the action of insulin in obese women. *Am J Clin Nutr* 82(2):355–365.
- Cho JH, Chen L, Kim MH, Chow RH, Hille B, Koh DS (2010) Characteristics and functions of {alpha}-amino-3-hydroxy-5-methyl-4-isoxazolepropionate receptors expressed in mouse pancreatic {alpha}-cells. *Endocrinology* 151(4):1541–1550
- Davalli AM, Ricordi C, Socci C, Braghi S, Bertuzzi F, Fattor B, Di Carlo V, Pontiroli AE, Pozza G. Abnormal sensitivity to glucose of human islets cultured in a high glucose medium: partial reversibility after an additional culture in a normal glucose medium. *J Clin Endocrinol Metab.* 1991 Jan;72(1):202-8.
- Davi G, Chiarelli F, Santilli F, Pomilio M, Vigneri S, Falco A, Basili S, Ciabattini G, Patrono C (2003) Enhanced lipid peroxidation and platelet activation in the early phase of type 1 diabetes mellitus: role of interleukin-6 and disease duration. *Circulation* 107(25):3199–3203
- Davis RE. (1998). Action of excitatory amino acids on hypodermis and the motor nervous system of *Ascaris suum*: pharmacological evidence for a glutamate transporter. *Parasitology.* 1998 May;116 ( Pt 5):487-500.
- Di Cairano ES, Davalli AM, Perego L, Sala S, Sacchi VF, La Rosa S, Finzi G, Placidi C, Capella C, Conti P, Centonze VE, Casiraghi F, Bertuzzi F, Folli F, Perego C (2011). The glial glutamate transporter 1 (GLT1) is expressed by pancreatic beta cells and prevents glutamate-induced beta-cell death. *J Biol Chem* 286(16):14007–14018 *Diabetologia* 49(12):2824–2827.
- Droge W, Eck HP, Betzler M, Naether H (1987) Elevated plasma glutamate levels in colorectal carcinoma patients and in patients with acquired immunodeficiency syndrome (AIDS). *Immunobiology* 174(4–5):473–479
- Droge W, Eck HP, Betzler M, Schlag P, Drings P, Ebert W (1988) Plasma glutamate concentration and lymphocyte activity. *J Cancer Res Clin Oncol* 114(2):124–128

23. Duan S, Christopher M. Anderson, Becky A. Stein, and Raymond A. Swanson (1999). Glutamate Induces Rapid Upregulation of Astrocyte Glutamate Transport and Cell-Surface Expression of GLAST. *The Journal of Neuroscience*, December 1, 1999, 19(23):10193–10200.
24. Dunning BE, Gerich JE (2007) The role of alpha-cell dysregulation in fasting and postprandial hyperglycemia in type 2 diabetes and therapeutic implications. *Endocr Rev* 28(3):253–283
25. Eck HP, Drings P, Droëge W (1989a) Plasma glutamate levels, lymphocyte reactivity and death rate in patients with bronchial carcinoma. *J Cancer Res Clin Oncol* 115(6):571–574 59.
26. Eck HP, Frey H, Droëge W (1989b) Elevated plasma glutamate concentrations in HIV-1 infected patients may contribute to loss of macrophage and lymphocyte functions. *Int Immunoll* (4):367–372.
27. Ellingsgaard H, Ehses JA, Hammar EB, Van Lommel L, Quintens R, Martens G, Kerr-Conte J, Pattou F, Berney T, Pipeleers D, Halban PA, Schuit FC, Donath MY (2008) Interleukin-6 regulates pancreatic alpha-cell mass expansion. *Proc Natl Acad Sci USA* 105(35):13163–13168
28. Federici M, Hribal M, Perego L, Ranalli M, Caradonna Z, Perego C, Usellini L, Nano R, Bonini P, Bertuzzi F, Marlier LN, Davalli AM, Carandente O, Pontiroli AE, Melino G, Marchetti F, Ferrannini E, Muscelli E, Natali A, Gabriel R, Mitrakou A, Flyvbjerg A, Golay A, Hojlund K (2007) The relationship between insulin sensitivity and cardiovascular disease risk (RISC) project Investigators. Association of fasting glucagons and proinsulin concentrations with insulin resistance. *Diabetologia* 50(11):2342–2347.
29. Felig P, Marliss E, Cahill GF Jr (1969) Plasma amino acid levels and insulin secretion in obesity. *N Engl J Med* 281(15):811–816.
30. Ferrannini E, Muscelli E, Natali A, Gabriel R, Mitrakou A, Flyvbjerg A, Golay A, Hojlund K (2007) The relationship between insulin sensitivity and cardiovascular disease risk (RISC) project Investigators. Association of fasting glucagons and proinsulin concentrations with insulin resistance. *Diabetologia* 50(11):2342–2347.
31. Folli F, Terumasa Okada, Carla Perego, Jenny Gunton, Chong Wee Liew, Masaru Akiyama, Anna D'Amico, Stefano La Rosa, Claudia Placidi, Roberto Lupi, Piero Marchetti, Giorgio Sesti, Marc Hellerstein, Lucia Perego, and Rohit N. Kulkarni (2011). Altered Insulin Receptor Signalling and  $\beta$ -Cell Cycle Dynamics in Type 2 Diabetes Mellitus. *PLoS One*. 2011; 6(11): e28050. Published online 2011 Nov 30. doi: 10.1371/journal.pone.0028050 PMID: PMC3227614.
32. Fujinami S, Hijikata Y, Shiozaki Y, Sameshima Y (1990) Profiles of plasma amino acids in fasted patients with various liver diseases. *Hepatogastroenterology* 37(suppl 2):81–84.
33. Furuta M, Yano H, Zhou A, Rouille Y, Holst JJ, Carroll R, Ravazzola M, Orci L, Furuta H, Steiner DF (1997) Defective prohormone processing and altered pancreatic islet morphology in mice lacking active SPC2. *Proc Natl Acad Sci U S A* 94(13):6646–6651
34. Gougeon R, Morais JA, Chevalier S, Pereira S, Lamarche M, Marliss EB (2008) Determinants of whole-body protein metabolism in subjects with and without type 2 diabetes. *Diabetes Care* 31(1):128–133
35. Guardado-Mendoza R, Davalli AM, Chavez AO, Hubbard GB, Dick EJ, et al. (2009) Pancreatic islet amyloidosis, beta-cell apoptosis, and alpha-cell proliferation are determinants of islet remodeling in type-2 diabetic baboons. *Proc Natl Acad Sci U S A*. 106:13992-13997.
36. Guemez-Gamboa A, Estrada-Sánchez AM, Montiel T, Páramo B, Massieu L, Morán J (2011) Activation of NOX2 by the stimulation of ionotropic and metabotropic glutamate receptors contributes to glutamate neurotoxicity in vivo through the production of reactive oxygen species and calpain activation. *J Neuropathol Exp Neurol* 70(11):1020–1035
37. Hawkins RA (2009) The blood-brain barrier and glutamate. *Am J Clin Nutr* 90(3):867S–874S
38. Herder C, Haastert B, Müller-Scholze S, Koenig W, Thorand B, Holle R, Wichmann HE, Scherbaum WA, Martin S, Kolb H (2005) Association of systemic chemokine concentrations with impaired glucose tolerance and type 2 diabetes: results from the Cooperative health research in the region of Augsburg survey S4 (KORA S4). *Diabetes* 54(suppl 2):S11–S17.
39. Holm E, Hack V, Tokus M, Breitreutz R, Babylon A, Droëge W (1997) Linkage between postabsorptive amino acid release and glutamate uptake in skeletal muscle tissue of healthy young subjects, cancer patients, and the elderly. *J Mol Med* 75(6):454–461.
40. Hribal ML, Perego L, Lovari S, Andreozzi F, Menghini R, Perego C, Finzi G, Usellini L, Placidi C, Capella C, Guzzi V, Lauro D, Bertuzzi F, Davalli A, Pozza G, Pontiroli A, Federici M, Lauro R, Brunetti A, Folli F, Sesti G. (2003). Chronic hyperglycemia impairs insulin secretion by affecting insulin receptor expression, splicing, and signaling in RIN beta cell line and human islets of Langerhans. *FASEB J*. 2003 Jul;17(10):1340-2.

41. Hu H, Johansson BL, Hjemdahl P, Li N (2004) Exercise-induced platelet and leucocyte activation is not enhanced in well-controlled Type 1 diabetes, despite increased activity at rest. *Diabetologia* 47(5):853–859 156.
42. Jeevanandam M, Ramias L, Schiller WR (1991) Altered plasma free amino acid levels in obese traumatized man. *Metabolism* 40(4):385–390.
43. Kamimura D, Ishihara K, Hirano T (2003) IL-6 signal transduction and its physiological roles: the signal orchestration model. *Rev Physiol Biochem Pharmacol* 149:1–38
44. Lenzen S, Drinkgern J, Tiedge M (1996) Low antioxidant enzyme gene expression in pancreatic islets compared with various other mouse tissues. *Free Radic Biol Med* 20(3):463– 466.
45. Lipski J, Wan CK, Bai JZ, Pi R, Li D, Donnelly D. (2007)Neuroprotective potential of ceftriaxone in in vitro models of stroke. *Neuroscience*. 2007 May 11;146(2):617-29.
46. Marliss EB, Gougeon R (2002) Diabetes mellitus, lipidus et proteinus! *Diabetes Care* 25(8):1474–1476
47. Matthews DE, Marano MA, Campbell RG. (1993). Splanchnic bed utilization of glutamine and glutamic acid in humans. *Am J Physiol*. 1993 Jun;264(6 Pt 1):E848-54.
48. Miller BR, Dorner JL, Shou M, Sari Y, Barton SJ, Sengelau DR, Kennedy RT, Rebec GV.(2008)Up-regulation of GLT1 expression increases glutamate uptake and attenuates the Huntington's disease phenotype in the R6/2 mouse. *Neuroscience*. 2008 Apr 22;153(1):329-37. doi: 10.1016/j.neuroscience.2008.02.004.
49. Molnar E, Varadi A, McIlhinney RA, Ashcroft SJ (1995) Identification of functional ionotropic glutamate receptor proteins in pancreatic beta-cells and in islets of Langerhans. *FEBS Lett* 371:253–257.
50. Moriyama Y and Hayashi M (2003). Glutamate-mediated signaling in the islets of Langerhans: a thread entangled. *Trend in pharmacological sciences*. Volume 24, Issue 10, October 2003, Pages 511–517doi:10.1016/j.tips.2003.08.002.
51. Mu¨ller WA, Falona GR, Unger RH (1973) Hyperglucagonemia in diabetic ketoacidosis. Its prevalence and significance. *Am J Med* 54(1):52–57.
52. Muroyama A, Uehara S, Yatsushiro S, Echigo N, Morimoto R, Morita M, Hayashi M, Yamamoto A, Koh DS, Moriyama Y (2004) A novel variant of ionotropic glutamate receptor regulates somatostatin secretion from delta-cells of islets of Langerhans. *Diabetes* 53(7):1743– 1753.
53. Nicholson KJ, Gilliland TM, Winkelstein BA. (2014)Upregulation of GLT-1 by treatment with ceftriaxone alleviates radicular pain by reducing spinal astrocyte activation and neuronal hyperexcitability. *J Neurosci Res*. 2014 Jan;92(1):116-29. doi: 10.1002/jnr.23295.
54. Nieoullon A, Canolle B, Masméjean F, Guillet B, Pisano P, Lortet S. (2006). The neuronal excitatory amino acid transporter EAAC1/EAAT3: does it represent a major actor at the brain excitatory synapse? *J Neurochem*. 2006 Aug;98(4):1007-18.
55. Nieuwdorp M, Stroes ES, Meijers JC, Büller H (2005) Hypercoagulability in the metabolic syndrome. *Curr Opin Pharmacol* 5(2):155–159.
56. Oresic M, Simell S, Sysi-Aho M, Na¨ntö¨-Salonen K, Seppä¨nen- Laakso T, Parikka V, 161. Katajamaa M, Hekkala A, Mattila I, Keskinen P, Yetukuri L, Reinikainen A, La¨hde J, Suortti T, Hakalax J, Simell T, Hyo¨ty H, Veijola R, Ilonen J, Lahesmaa R, Knip M, Simell O (2008) Dysregulation of lipid and amino acid metabolism precedes islet autoimmunity in children who later progress to type 1 diabetes. *J Exp Med* 205(13):2975–2984.
57. Perego C, Vanoni C, Bossi M, Massari S, Basudev H, Longhi R, Pietrini G.(2000).M The GLT-1 and GLAST glutamate transporters are expressed on morphologically distinct astrocytes and regulated by neuronal activity in primary hippocampal cocultures. *J Neurochem*. 2000 Sep;75(3):1076-84.
58. Pereira S, Marliss EB, Morais JA, Chevalier S, Gougeon R (2008) Insulin resistance of protein metabolism in type 2 diabetes. *Diabetes* 57(1):56–63.
59. Prescott J (2004). Effects of added glutamate on liking for novel food flavors. *Appetite*. 2004 Apr;42(2):143-50.
60. Reaven GM, Chen YD, Golay A, Swislocki AL, Jaspan JB (1987) Documentation of hyperglucagonemia throughout the day in non-obese and obese patients with noninsulin- dependent diabetes mellitus. *J Clin Endocrinol Metab* 64(1):106–110
61. Rothstein JD, Patel S, Regan MR, Haenggeli C, Huang YH, Bergles DE, Jin L, Dykes Hoberg M, Vidensky S, Chung DS, Toan SV, Bruijn LI, Su ZZ, Gupta P, Fisher PB. (2005). Beta-lactam antibiotics offer neuroprotection by increasing glutamate transporter expression. *Nature*. 2005 Jan 6;433(7021):73-7.
62. Schiffman SS (2000) Intensification of sensory properties of foods for the elderly. *J Nutr* 130(4S suppl):927S–930S.

63. Solerte SB, Rondanelli M, Giaccherio R, Stabile M, Lovati E, Cravello L, Pontiggia B, Vignati G, Ferrari E, Fioravanti M (1999) Serum glucagon concentration and hyperinsulinemia influence renal haemodynamics and urinary protein loss in normotensive patients with central obesity. In *J Obes Relat Metab Disord* 23(9):997–1003.
64. Spranger J, Kroke A, Möhlig M, Hoffmann K, Bergmann MM, Ristow M, Boeing H, Pfeiffer AF (2003) Inflammatory cytokines and the risk to develop type 2 diabetes: results of the prospective population-based European prospective investigation into cancer and nutrition (EPIC)-Potsdam Study. *Diabetes* 52(3):812–817.
65. Starke AA, Erhardt G, Berger M, Zimmermann H (1984) Elevated pancreatic glucagon in obesity. *Diabetes* 33(3):277–280.
66. Tai ES, Tan ML, Stevens RD, Low YL, Muehlbauer MJ, Goh DL, Ilkayeva OR, Wenner BR, Bain JR, Lee JJ, Lim SC, Khoo CM, Shah SH, Newgard CB (2010) Insulin resistance is associated with a metabolic profile of altered protein metabolism in Chinese and Asian-Indian men. *Diabetologia* 53(4):757–767.
67. Tolosa L, Caraballo-Miralles V, Olmos G, Llado´ J (2011) TNF- $\alpha$  potentiates glutamate-induced spinal cord motoneuron death via NF- $\kappa$ B. *Mol Cell Neurosci* 46(1):176–186.
68. Tremolizzo L, DiFrancesco JC, Rodriguez-Menendez V, Sirtori E, Longoni M, Cassetti A, Bossi M, El Mestikawy S, Cavaletti G, Ferrarese C (2006) Human platelets express the synaptic markers VGLUT1 and 2 and release glutamate following aggregation. *Neurosci Lett* 404(3):262–265.
69. Turque N, Plaza S, Radvanyi F, Carriere C, Saule S (1994) Pax- QNR/Pax-6, a paired box- and 210. homeobox-containing gene expressed in neurons, is also expressed in pancreatic endocrine cells. *Mol Endocrinol* 8(7):929–938.
70. Vannucchi H, Marchini JS, Padovan GJ, dos-Santos JE, Dutra- Oliveira JE (1985) Amino acid patterns in the plasma and ascitic fluid of cirrhotic patients. *Braz J Med Biol Res* 18(4): 465–470
71. Weaver CD, Yao TL, Powers AC, Verdoorn TA (1996) Differential expression of glutamate receptor subtypes in rat pancreatic islets. *J Biol Chem* 271(22):12977–12984.
72. Weiss R, D’Adamo E, Santoro N, Hershkop K, Caprio S (2011) Basal  $\alpha$ -cell up-regulation in 225. obese insulin-resistant adolescents. *J Clin Endocrinol Metab* 96(1):91–97.
73. Yamaguchi S (1991) Basic properties of umami and effects on humans. *Physiol Behav* 49(5):833–841
- Bellisle F, Monneuse MO, Chabert M, Larue-Achagiotis C, Lanteaume MT, Louis-Sylvestre J (1991) Monosodium glutamate as a palatability enhancer in the European diet. *Physiol Behav* 49(5):869–873.
74. Yamaguchi S and Ninomiya K (2000) Umami and food palatability. *J Nutr* 130(4S suppl):921S–926S.

## Bibliography of Discussion (Chapter I and II)

1. Angehagen M1, Ben-Menachem E, Rönnbäck L, Hansson E (2003). Topiramate protects against glutamate- and kainate-induced neurotoxicity in primary neuronal-astroglial cultures. *Epilepsy Res.* 2003 Apr;54(1):63-71.
2. Bala T.S. Susarla, Michael B. Robinson (2007) Internalization and degradation of the glutamate transporter GLT-1 in response to phorbol ester. *Neurochemistry International Volume Neurosteroids.* 52, Issues 4–5, March–April 2008, Pages 709–722. doi:10.1016/j.neuint.2007.08.020
3. Cunha DA, Ladrière L, Ortis F, Igoillo-Esteve M, Gurzov EN, Lupi R, Marchetti P, Eizirik DL, Cnop M. (2009). Glucagon-like peptide-1 agonists protect pancreatic beta-cells from lipotoxic endoplasmic reticulum stress through upregulation of BiP and JunB. *Diabetes.* 2009 Dec;58(12):2851-62. doi: 10.2337/db09-0685.
4. Davalli AM, Perego C, Folli FB, Bosi E.(2012). Long-lasting remission of type 1 diabetes following treatment with topiramate for generalized seizures. *Acta Diabetol.* 2012 Feb;49(1):75-9. doi: 10.1007/s00592-011-0268-y.
5. Follett PL, Deng W, Dai W, Talos DM, Massillon LJ, Rosenberg PA, Volpe JJ, Jensen FE. (2004). Glutamate receptor-mediated oligodendrocyte toxicity in periventricular leukomalacia: a protective role for topiramate. *J Neurosci.* 2004 May 5;24(18):4412-20.
6. Folli F, Terumasa Okada, Carla Perego, Jenny Gunton, Chong Wee Liew, Masaru Akiyama, Anna D'Amico, Stefano La Rosa, Claudia Placidi, Roberto Lupi, Piero Marchetti, Giorgio Sesti, Marc Hellerstein, Lucia Perego, and Rohit N. Kulkarni (2011). Altered Insulin Receptor Signalling and  $\beta$ -Cell Cycle Dynamics in Type 2 Diabetes Mellitus. *PLoS One.* 2011; 6(11): e28050. Published online 2011 Nov 30. doi: 10.1371/journal.pone.0028050 PMID: PMC3227614.
7. Frigerio F, Chaffard G, Berwaer M, Maechler P. (2006). The antiepileptic drug topiramate preserves metabolism-secretion coupling in insulin secreting cells chronically exposed to the fatty acid oleate. *Biochem Pharmacol.* 2006 Oct 16;72(8):965-73.
8. Harkavyi A and Whitton PS. (2010). Glucagon-like peptide 1 receptor stimulation as a means of neuroprotection. *Br J Pharmacol.* 2010 Feb 1;159(3):495-501. doi: 10.1111/j.1476-5381.2009.00486.x.
9. Hribal ML, Perego L, Lovari S, Andreozzi F, Menghini R, Perego C, Finzi G, Usellini L, Placidi C, Capella C, Guzzi V, Lauro D, Bertuzzi F, Davalli A, Pozza G, Pontiroli A, Federici M, Lauro R, Brunetti A, Folli F, Sesti G. (2003). Chronic hyperglycemia impairs insulin secretion by affecting insulin receptor expression, splicing, and signaling in RIN beta cell line and human islets of Langerhans. *FASEB J.* 2003 Jul;17(10):1340-2.
10. Liang Y, Chen X, Osborne M, DeCarlo SO, Jetton TL, Demarest K. (2005) Topiramate ameliorates hyperglycaemia and improves glucose-stimulated insulin release in ZDF rats and db/db mice. *Diabetes Obes Metab.* 2005 Jul;7(4):360-9.
11. Lipski J, Wan CK, Bai JZ, Pi R, Li D, Donnelly D. (2007) Neuroprotective potential of ceftriaxone in in vitro models of stroke. *Neuroscience.* 2007 May 11;146(2):617-29.
12. Miller BR, Dorner JL, Shou M, Sari Y, Barton SJ, Sengelaub DR, Kennedy RT, Rebec GV.(2008) Up-regulation of GLT1 expression increases glutamate uptake and attenuates the Huntington's disease phenotype in the R6/2 mouse. *Neuroscience.* 2008 Apr 22;153(1):329-37. doi: 10.1016/j.neuroscience.2008.02.004.
13. Nicholson KJ, Gilliland TM, Winkelstein BA. (2014) Upregulation of GLT-1 by treatment with ceftriaxone alleviates radicular pain by reducing spinal astrocyte activation and neuronal hyperexcitability. *J Neurosci Res.* 2014 Jan;92(1):116-29. doi: 10.1002/jnr.23295.
14. Perry T, Haughey NJ, Mattson MP, Egan JM, Greig NH.(2002) Protection and reversal of excitotoxic neuronal damage by glucagon-like peptide-1 and exendin-4. *J Pharmacol Exp Ther.* 2002 Sep;302(3):881-8.
15. Perry T, Holloway HW, Weerasuriya A, Mouton PR, Duffy K, Mattison JA, Greig NH.(2007). Evidence of GLP-1-mediated neuroprotection in an animal model of pyridoxine-induced peripheral sensory neuropathy. *Exp Neurol.* 2007 Feb;203(2):293-301
16. Robinson MB (1999) The family of sodium-dependent glutamate transporters: A focus on the GLT-1/EAAT2 subtype. *Neurochem Int* 33:479–491.
17. Romera C, Hurtado O, Mallolas J, Pereira MP, Morales JR, Romera A, Serena J, Vivancos J, Nombela F, Lorenzo P, Lizasoain I, Moro MA (2007). Ischemic preconditioning reveals that GLT1/EAAT2 glutamate transporter is a novel PPAR $\gamma$  target gene involved in neuroprotection. *J Cereb Blood Flow Metab.* 2007 Jul;27(7):1327-38.
18. Rosenstock J, Foley JE, Rendell M, Landin-Olsson M, Holst JJ, Deacon CF, Rochotte E, Baron MA. Effects of the dipeptidyl peptidase-IV inhibitor vildagliptin on incretin hormones, islet function, and postprandial glycemia in subjects with impaired glucose tolerance. *Diabetes Care.* 2008 Jan;31(1):30-5. Epub 2007 Oct 18.

19. Rothstein JD, Patel S, Regan MR, Haenggeli C, Huang YH, Bergles DE, Jin L, Dykes Hoberg M, Vidensky S, Chung DS, Toan SV, Buijij LI, Su ZZ, Gupta P, Fisher PB. (2005). Beta-lactam antibiotics offer neuroprotection by increasing glutamate transporter expression. *Nature*. 2005 Jan 6;433(7021):73-7.
20. Thal SC, Heinemann M, Luh C, Pieter D, Werner C, Engelhard K.(2010). Pioglitazone reduces secondary brain damage after experimental brain trauma by PPAR- $\gamma$ -independent mechanisms. *J Neurotrauma*. 2011 Jun;28(6):983-93. doi: 10.1089/neu.2010. 1685.
21. Toplak H, Hamann A, Moore R, Masson E, Gorska M, Vercruysse F, Sun X, Fitchet M.Efficacy and safety of topiramate in combination with metformin in the treatment of obese subjects with type 2 diabetes: a randomized, double-blind, placebo-controlled study. *Int J Obes (Lond)*. 2007 Jan;31(1):138-46.
22. Tsunekawa S, Yamamoto N, Tsukamoto K, Itoh Y, Kaneko Y, Kimura T, Ariyoshi Y, Miura Y, Oiso Y, Niki I. (2007)Protection of pancreatic beta-cells by exendin-4 may involve the reduction of endoplasmic reticulum stress; in vivo and in vitro studies. *J Endocrinol*. 2007 Apr;193(1):65-74.
23. Walter H, Lübben G.(2005). Potential role of oral thiazolidinedione therapy in preserving beta-cell function in type 2 diabetes mellitus. *Drugs*. 2005;65(1):1-13.
24. White AT, Murphy A (2010). Administration of thiazolidinediones for neuroprotection in ischemic stroke: A pre-clinical systematic review. *Journal of Neurochemistry (Impact Factor: 4.28)*. 11/2010; 115(4):845-53. DOI: 10.1111/j.1471-4159.2010.06999.x.

# CHAPTER III:

## CYTOTOXIC AUTOANTIBODIES AGAINST THE GLIAL GLUTAMATE TRANSPORTER GLT1 IN TYPE 1 DIABETES MELLITUS

### INTRODUCTION

#### DIABETES MELLITUS

Metabolic syndrome are characterized by hyperglycaemia caused by an absolute deficiency of insulin secretion or the reduction of its biological effectiveness (or both defects).

Traditionally, diabetes mellitus was classified according to age of the patient at the onset of symptoms (juvenile or adult). The current classification is:

- Type 1 of Diabetes mellitus (T1DM): syndrome characterized by the destruction of pancreatic  $\beta$  cells. In 95% of cases it is of autoimmune origin, in the remaining 5%, is idiopathic.
- Type 2 of Diabetes Mellitus (T2DM): heterogeneous syndrome that includes a set of defects characterized by insulin resistance accompanied by alteration of insulin secretion (the body's attempt to compensate for the failure response of target tissues). (Genuth et al., 2003; Expert Committee on the Diagnosis of Diabetes Mellitus and classification)

#### ***Diabetes Mellitus Type 1 (T1DM) and auto-immunogenicity***

Type 1 diabetes is a form of immune-mediated diabetes. It is caused by the selective and progressive destruction of  $\beta$ -cells of the islets of Langerhans due to the loss of tolerance to  $\beta$ -cell antigens in genetically predisposed subjects (Atkinson et al., 2011; Rossini et al., 2004; Kukreja et al., 2002). It is commonly believed that type 1 diabetes autoimmunity is initiated by  $\beta$ -cell insults, leading to abnormal  $\beta$ -cell immunogenicity and consequent activation of autoreactive T- and B-lymphocytes. The nature of the primary insult to the  $\beta$ -cells is unclear, although viral infection and endoplasmic reticulum stress have been implicated (Roep et al., 2010). T1DM a catabolic disease where circulating insulin is absent, glucagon is high and the  $\beta$  cells are not able to

respond to insulinogenic stimuli. In absence of insulin, the three main target tissues: liver, muscle and fat tissue, not only are not able to use absorbed nutrients, but they continue to release into circulation glucose, amino acids and fatty acids derived from the intracellular stores. In addition, the alteration of the fatty acids metabolism leads to production and accumulation of ketone bodies that can lead to ketoacidosis and diabetic coma (Polonsky et al., 1995).

The onset of this type of diabetes may relate to any age, but usually appears in child and young adult and the risk of developing diabetes later in life is higher in family members of the diabetic proband. The possibility of a destruction of pancreatic  $\beta$  cells to selective loss of immune tolerance (autoimmune death) is supported by evidence that a proportion of patients with newly diagnosed type 1 diabetes treated with immunosuppressive therapy, showed an interruption of progression to insulin deficiency. Also in the Islets of Langerhans of diabetic child is observed a strong and widespread infiltration of lymphocytes T helper and cytotoxic lymphocytes associated with the presence in their serum of autoantibodies against structural and secretory proteins of pancreatic  $\beta$  cells (Genuth et al., 2003; Dedov et al., 2015; Taplin et al., 2008). Based on the evidence described above, it has been proposed that the autoimmune destruction of pancreatic  $\beta$ -cells mediated by the immune system that recognizes as foreign  $\beta$  cell proteins. This could be due to the partial homology between  $\beta$ -cell proteins and viral peptides or other foreign peptides identified as potentially pathologic.

The efficiency in presenting endogenous proteins to the immune system depends on the composition of the class II antigens on the surface of the cells responsible for antigen presentation (antigen presenting cells, macrophages) and appear to affect significantly the deletion of thymus self-reactive cells. At the time of diagnosis, the majority of patients with type 1 diabetes have circulating antibodies (Herold, et al., 2002; Dedov et al., 2015):

- Antibodies directed against intracellular protein of islets of Langerhans (ICA) (Dedov et al., 2015),
- Autoantibodies against insulin (IAA) (Taplin et al., 2008),
- Antibodies for tyrosine phosphatase (IA-2 or ICA-512) (Umpaichitra et al., 2002; Hypponen et al., 2000),
- Antibodies for the enzyme responsible for glutamic acid decarboxylation (GAD 65) (Hathout et al., 2001). The GAD is localized within the pancreatic  $\beta$ -cells as well as at the level of the inhibitory neurons of the central nervous system that secrete GABA.
- Antibodies directed against the zinc transporter 8 (ZnT8) (Libman et al., 2003)

The diagnostic sensitivity and specificity of some of these autoimmune markers in patients with type 1 diabetes is shown in the following table:

<b><i>Antibodies Identified</i></b>	<b><i>Sensitivity</i></b>	<b><i>Specificity</i></b>
Glutamic acid decarboxylase (GAD 65)	70-90%	99%
Insulin (IAA)	40-70%	99%
Tyrosine phosphatase (IA-2)	50-70%	99%

However is important to highlight that none of these antibodies appear to be pathogenic since they are all intracellular antigens. Therefore, their presence seems an index of pancreatic  $\beta$ -cell destruction and immune reaction in progress. As already suggested in the past, the existence of other antigens, localized on the plasma membrane (ICSA: islet cell surface antibodies) and directly responsible of  $\beta$ -cytotoxicity has been proposed and observed (Fourlanos et al., 2004; Donath et al., 2011; Sanda et al., 2010; Wilkin 2001) in about 50% of the sera with T1DM, but the antigen recognized by the ICSA has never been identified.

*The glutamate transporter GLT1 could be an ideal target for T1D autoantibodies. Indeed:*

- 1) GLT1 is mainly present in pancreatic  $\beta$ -cells
- 2) It is a plasma membrane protein. The membrane topology of the glutamate transporter has been studied extensively and the model includes eight  $\alpha$ -helix transmembrane domains, connected by intra and extracellular loops, two of which only partially cross the plasma membrane and regulate transport activity (Hairpins loops HP1 and HP2; Slotboom et al, 2001). The N- and C-terminal regions localize in the intracellular side. Particularly interesting could be the extracellular loops because exposed to recognition by circulating autoantibodies.
- 3) GLT1 is the main transporter responsible for extracellular glutamate removal in islets of Langerhans, therefore, alterations of its cell surface localization or transport activity may result in an increase of extracellular glutamate concentrations to levels toxic selectively for the insulin-secreting cells.

Several evidence support the possibility that glutamate may increase to toxic levels in the islets of T1D subjects: glutamate is a major secretory product of the  $\alpha$ -cells (Baekkeskov et al., 1990) which are over secreting in T1D islets as the result of the decreased negative feedback exerted by insulin on the  $\alpha$ -cells (Bonifacio et al., 1995; Wenzlau et al., 2007). Extracellular glutamate may increase further with the progression of the disease, when the islets are characterized by an inverted  $\beta$ -cell/ $\alpha$ -cell ratio. Moreover, glutamate is released also by T lymphocytes (Stadinski et al., 2010), activates T-cells and stimulates adhesion and

chemotaxis (Dobersen et al., 1980). Islet lymphocytes infiltration (insulinitis) may thus contribute to increase extracellular glutamate that, in turn, might foster T cell migration, insulinitis and  $\beta$ -cell death.

Interestingly, in children who later progress to type 1 diabetes, alterations in the metabolic profile characterize the early pathogenesis of the disease, suggesting a role in its progression. The appearance of insulin and glutamic acid decarboxylase autoantibodies (IAA and GADA) in the serum is preceded by abnormally high glutamic acid (13-fold increase) (Oresic *et al.*, 2008). These data support the hypothesis that glutamate-induced  $\beta$ -cell toxicity might participate to T1D onset and progression.

Since immunoglobulins (IgG and IgM), targeting membrane proteins, are potentially pathogenic, we hypothesized that GLT1 could be a putative immune target in subjects with type 1 diabetes.

We tested this hypothesis by searching for the presence of autoantibodies against GLT1 in the sera of individuals with type 1 diabetes.

During the project of my master thesis we collect sera from 45 T1D patients and 35 healthy controls (Collaboration with dr. Davalli, San Raffaele, Milan and Prof Folli, Texas, USA) and we performed immunoprecipitation and immunofluorescence experiments to verify the presence of antibodies against GLT1 in the sera of type 1 diabetic patients.

We were able to demonstrate that 9 out of the 18 sera tested from subjects with type 1 diabetes immunoprecipitated a protein of the same molecular weight as that of GLT1 (Figure 1) that was recognized by rabbit anti-GLT1 antibodies from brain, pancreatic human islets, and GLT1-transfected COS7-cell extracts. This immunoreactivity was not detected in the 11 healthy controls (Fig. 1a).

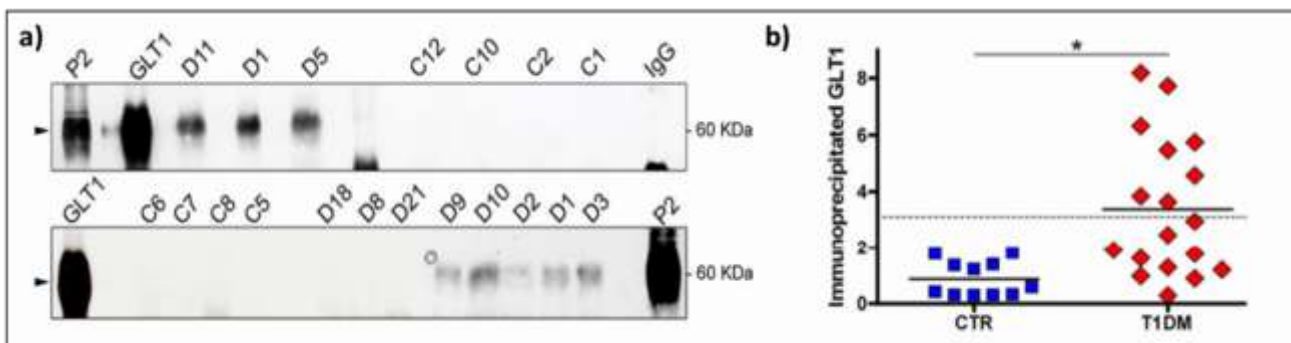


**FIG 1: IDENTIFICATION OF GLT1 AS A TARGET OF SERUM IgGs IN A SUBSET OF TYPE 1 DIABETIC PATIENTS**  
 Image a) shows GLT1 detection by western blot analysis in immunoprecipitation assays. 20 mg of P2 brain membrane fraction were immunoprecipitated with a rabbit anti-GLT1 antibody (GLT1, positive control), a rabbit serum (IgG, negative control) and sera from healthy subjects (Cn) or type 1 diabetic patients (Dn). Representative blots immunostained with the rabbit anti-GLT1 antibody are shown. 5  $\mu$ g of P2 extracts (Lys) were immunoblotted in the same gel. Protein markers are indicated on the right. Arrows indicate GLT1. Serum characteristics are reported in Supplementary Table II.  
 Image b) shows the quantification of immunoprecipitated GLT1 by densitometric analysis. Band intensity is expressed as Arbitrary Units. The horizontal line represents the cut-off (mean + 3SD of healthy controls) above which the results are considered positive. The median values are shown for each group. Frequency differences between control and type 1 diabetes groups are statistically significant (P = 0.0005, unpaired t-test).

To confirm the specificity of GLUT1 as a target of serum IgG from subjects with type 1 diabetes, we performed immunofluorescence assays on GLUT1 transfected COS7 cells, an example is reported in Figure 2.

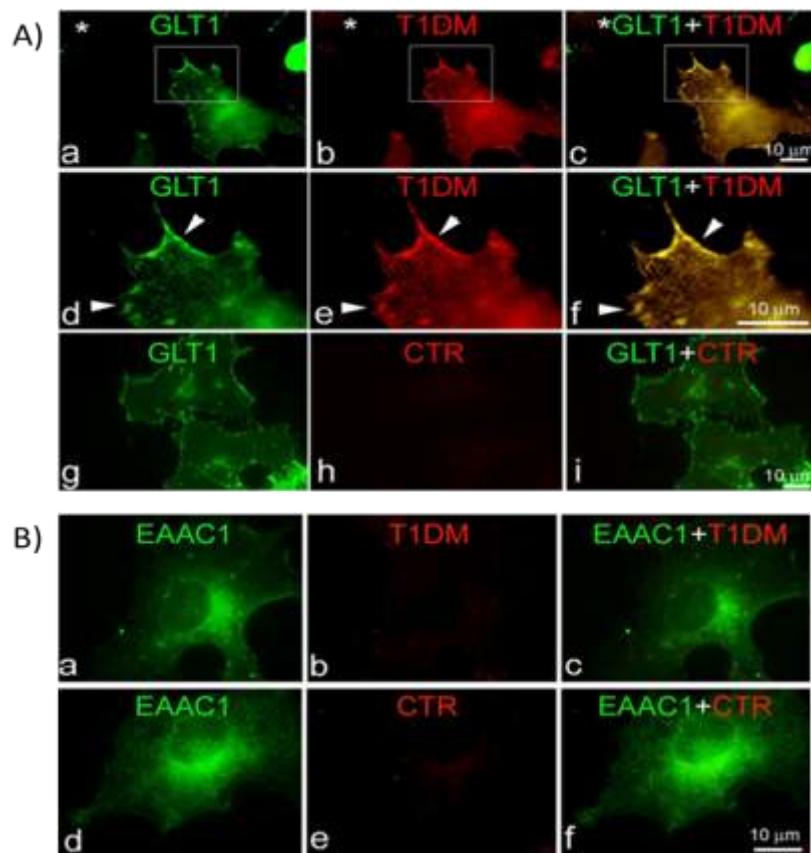


**FIG 2: IDENTIFICATION OF GLUT1 AS A TARGET OF SERUM IgGs IN A SUBSET OF TYPE 1 DIABETIC PATIENTS**  
 Image A), Panels a-f show immunofluorescence labelling of COS7 cells transfected with GFP-GLUT1 (green) with a type 1 diabetes serum (red). The yellow staining in the overlay reveals colocalization between GLUT1 and human IgGs from type 1 diabetes serum. \* indicates a non-transfected cell. The higher magnification (2.5x, A, d-f) highlights colocalization between the two labellings at the cell surface and in terminal tips (arrowheads). Staining with serum of a healthy subject is shown as control (E, g-i).  
 Image B) shows immunofluorescence labelling of GFP-EAAC1 transfected COS7 cells (green) with type 1 diabetes (B, panel a-c) or control (B, panel d-f) sera (red). IgGs from type 1 diabetes did not recognizes GFP-EAAC1, a different glutamate transporter. Representative images obtained with the C5 control and D4 Type 1 diabetes sera are shown

The type 1 diabetes serum selectively labelled the cell surface of GFP-GLUT1 transfected COS7-cells (Fig. 2Aa-f). Staining was specific for GLUT1, since it was undetectable in cells expressing EAAC1, a different glutamate transporter subtype. No staining was observed in GFP-GLUT1 and GFP-EAAC1 transfected COS cells incubated with the serum of a control subject (Figura 2Ba-f).

We used the cell-based immunofluorescence assay to screen the sera from 35 control and 43 diabetic subjects. Twenty of 43 type 1 diabetes sera (47%) specifically labelled GLUT1-transfected COS7 cells with a plasma

membrane and intracellular vesicular staining ( $P < 0.0005$ , data not shown). Altogether, our data indicate that GLT1 is a novel autoantigen and GLT1 autoantibodies are present in  $\sim 50\%$  of patients with type 1 diabetes.

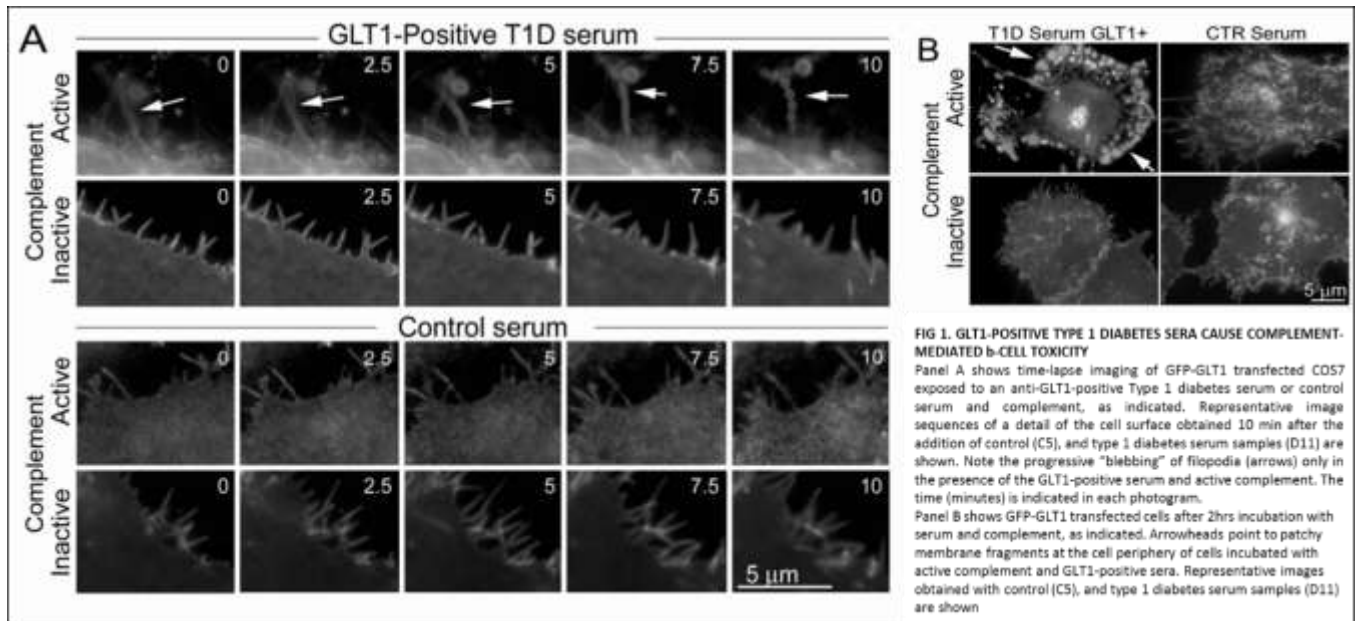
Having demonstrated the presence of anti-GLT1 antibodies in a cohort of T1D subjects, the goal of the project was to verify whether these autoantibodies could be also cytotoxic for  $\beta$ -cells.

## RESULTS CHAPTER III

### Cytotoxic autoantibodies against the glial glutamate transporter GLT1 in type 1 diabetes mellitus

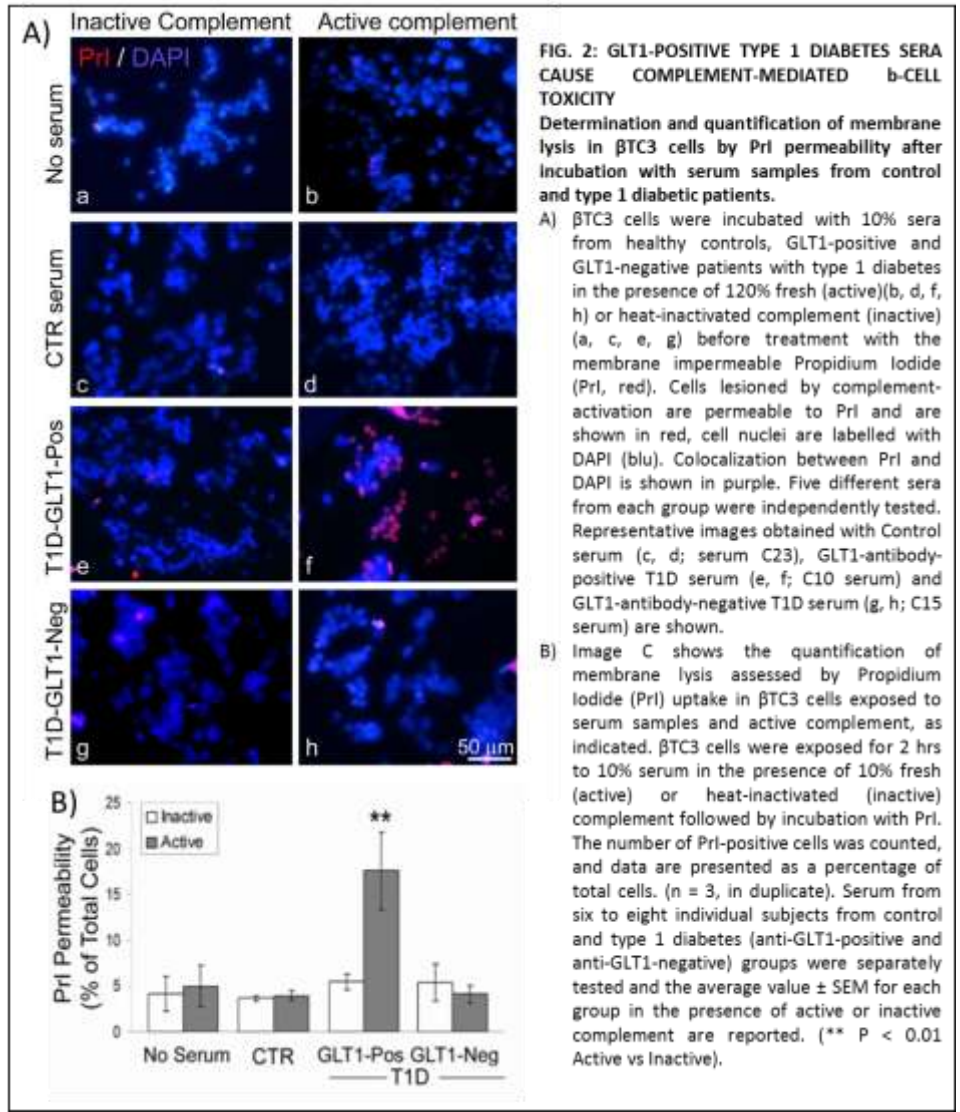
Complement-fixing islet cell autoantibodies, which should be able to activate the terminal complement complex cascade and cause cell damage, have been observed previously in type 1 diabetic subjects as well as in individuals at high risk for developing it (Bottazzo et al 1980; Tarn et al., 1988; Radillo et al., 1996).

To test the possibility that GLT1 could be this previously unidentified autoantigen, we explored the biological effects of anti-GLT1 IgGs on cells expressing the transporter by *in vivo* cell-imaging. When exposed to the type 1 diabetes serum and active complement, GLT1-expressing cells underwent progressive membrane damage and swelling, this process was particularly evident at the cell periphery, in filopodia structures (Fig. 1A). After 2 hours, several cells expressing GLT1 were lysed and/or severely injured (Fig. 1B). No visible changes were detected in the presence of inactive complement or after exposure to control serum (Fig. 1A and 1B).

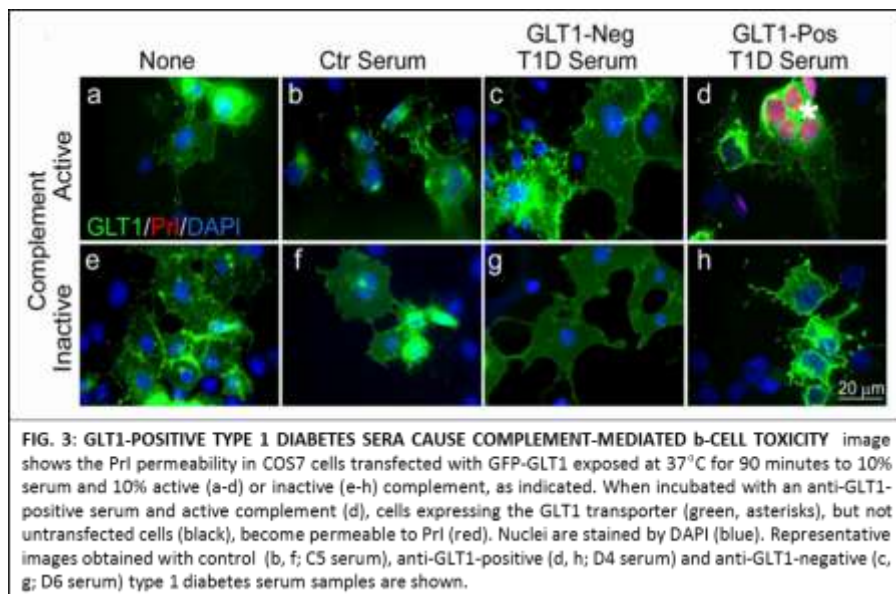


To verify the membrane integrity of  $\beta$ -cells exposed to diabetic sera in the presence of active complement, we quantified the number of cells permeable to the viability dye propidium iodide (PrI) (Fig. 2A and B). The exposure of  $\beta$ TC3 cells to GLT1-positive sera supplemented with active complement significantly increased the PrI uptake, indicating the disruption of membrane integrity ( $3.7 \pm 0.7$  fold increase; damaged  $\beta$ -cells,  $17 \pm 5\%$  and  $3.6 \pm 0.2\%$  in GLT1-positive and control sera, respectively;  $P < 0.05$ ; Figure 2B). No change in PrI

permeability was detected after incubation with heat-inactivated complement or GLT1 negative sera (Figure 2A and B).



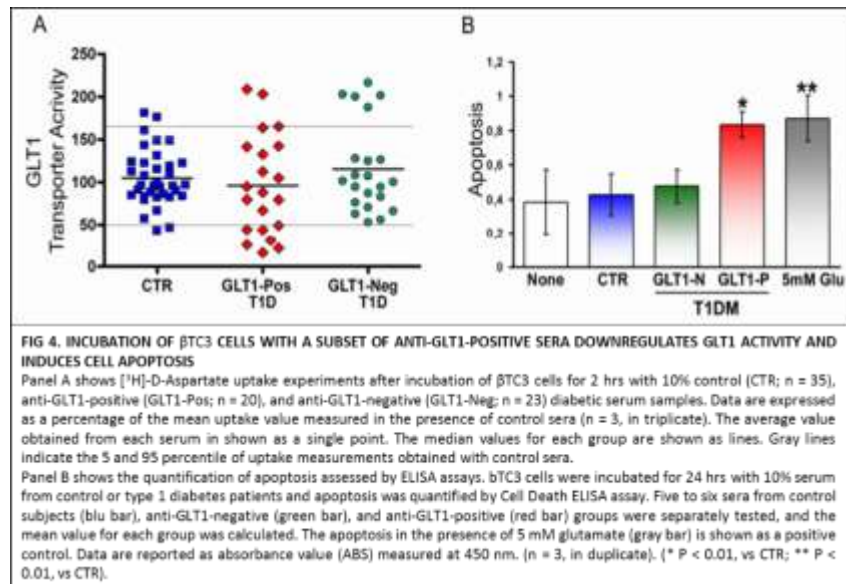
The change in permeability was mediated by the selective binding of IgGs to GLT1, because Pri uptake was detected only in GLT1-expressing cells exposed to GLT1-positive serum and active complement (Fig. 3d) but not with control or GLT1-negative type 1 diabetes sera (Fig. 3a-c and 3e-h).



**A subset of type 1 Diabetes sera with GLT1 autoantibodies downregulates GLT1 surface activity and increases  $\beta$ -cell death in the absence of complement**

To test the possibility that autoantibodies directed against GLT1 could have also an inhibitory effect on its function, we measured the uptake of [ $^3$ H]D-aspartate, a non-metabolizable GLT1 transporter substrate (Arriza et al., 1994), in  $\beta$ TC3 cells incubated with control and type 1 diabetes sera, in the absence of active complement (Fig. 4A). The mean GLT1 activity measured in the presence of different sera did not significantly change among groups, but an analysis of variance indicated a significant difference between the GLT1-positive and the control groups ( $P < 0.05$ , F test). More interestingly, considering as a normal GLT1 activity the 5 to 95 percentile of [ $^3$ H]D-aspartate uptake values measured in the presence of control sera (equivalent to the 50-160% of uptake activity), we found that 7 of 20 (35%) GLT1-positive diabetic sera drastically inhibited the uptake of [ $^3$ H]D-aspartate (below 50% of control activity), in contrast to only 2 of 35 (6%) and 1 of 23 (4%) in control and GLT1-negative groups, respectively.

Within the islet, the physiological function of GLT1 is to control the extracellular glutamate concentration, thereby preventing glutamate-induced  $\beta$ -cell death (Hayashi et al., 2003; Di Cairano et al., 2011).



We therefore tested the effects of autoantibody-mediated GLT1 inhibition on  $\beta$ -cell integrity. In the absence of active complement, a 24 hr incubation of  $\beta$ TC3 cells with 20% of GLT1-positive diabetic sera significantly increased cell apoptosis in comparison to control and GLT1-negative diabetic sera (Fig. 4B) (2.66 fold increase;  $P < 0.001$ ).

Finally, we evaluated the molecular mechanisms responsible for the downregulation of [ $^3$ H]D-aspartate uptake and  $\beta$ -cell death. *In vivo* incubation of  $\beta$ -cells with GLT1-positive diabetic sera with inhibitory activity caused the disappearance of GLT1 expression from the plasma membrane and its concomitant accumulation in intracellular vesicular structures (Fig. 5Ad-f, insets). In contrast, GLT1 retained its plasma membrane distribution when cells were incubated in the same conditions with control sera or GLT1-negative diabetic sera (Fig. 5a-c).

Double immunofluorescence experiments indicated that anti-GLT1 autoantibodies caused the GLT1 internalization into endocytic compartments, positive for the Early Endosome Antigen 1 (EEA1), and the subsequent translocation to Cathepsin D-positive lysosomes, where GLT1 is probably degraded (Fig. 5B). Altogether, these data show that a subgroup of type 1 diabetes sera binds to GLT1 and can interfere with its normal localization and function, possibly by enhancing its intracellular lysosomal degradation.

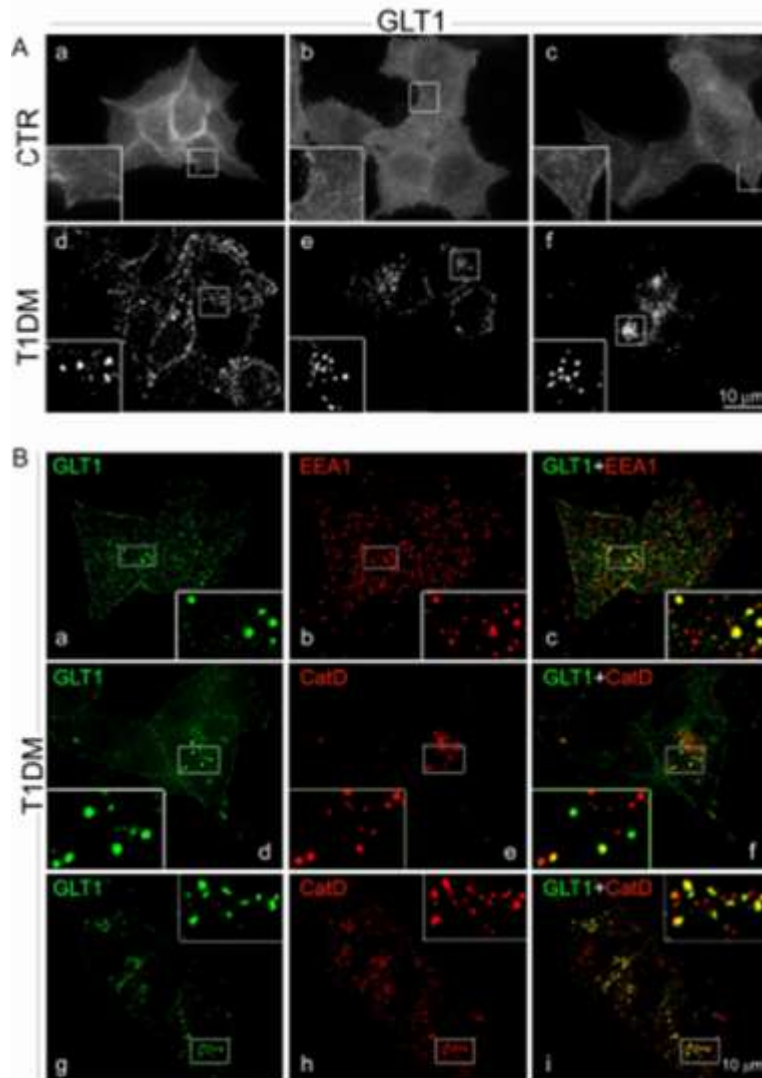


**Figure 5. GLUT1 DOWNREGULATION IS DUE TO THE TRANSPORTER INTERNALIZATION INTO ENDOCYTIC-DEGRADATIVE COMPARTMENTS.**

Panel A shows the immunolocalization of GLUT1 after incubation of  $\beta$ TC3 cells with 10% control or type 1 diabetes serum samples at 20°C for 2 hrs, before fixation and staining. Representative images obtained with control serum (a), anti-GLT1 negative sera (b,c), and anti-GLT1 positive sera (d-f) are shown. The GLUT1 internalization in intracellular vesicular compartments is induced after incubation with anti-GLT1 positive Type 1 diabetic sera (d-f) but not with control sera (a-c). Inset, X2.5 magnification of the particular indicated in the figure.

Panel B shows double immunofluorescence staining revealing colocalization (yellow colour in the overlay) between internalised GLUT1 (red) and markers of the endocytic pathway (Early Endosome Antigen 1, EEA1) (a-c) or lysosomes (Cathepsin D, CatD) (d-i).  $\beta$ TC3 cells were incubated for 2 hrs at 37°C with 10% anti-GLT1 positive sera, fixed and double stained with GLUT1 and EEA1 or Cathepsin D. Inset is a X3 magnification of the particular indicated in the figure.

## DISCUSSION Chapter III

After the discovery of islet cell autoantibodies (ICAs) in subjects with type 1 diabetes mellitus, several of their target proteins subsequently have been identified (Baekkeskov et al., 1990; 8. Bonifacio et al., 1995; Wenzlau et al., 2007; Stadinski et al., 2011). Of note, none of these autoantigens reside on the plasma membrane of the  $\beta$ -cell as GAD65 is primarily located in the cytosol while IA-2 and ZnT8 on the insulin secretory granule. Our data show that GLT1 is the first plasma cell membrane autoantigen identified in type 1 diabetes and that antibodies directed against it are pathogenic. Our findings clarify previous reports, which described the presence of cytotoxic islet cell surface autoantibodies (ICSAs) in these subjects (Stadinski et al., 2011; Dobersen et al., 1980; Toguchi et al., 1985; Van De Winkel et al., 1982), thereby challenging the prevailing belief that  $\beta$ -cell loss in subjects with type 1 diabetes is entirely caused by autoreactive T-cells (Baekkeskov et al., 1990; Bonifacio et al., 1995; Wenzlau et al., 2007; Stadinski et al., 2010).

In our patient cohort, autoantibodies against GLT1 were detected in 47% of patients with type 1 diabetes and in none of healthy control subjects. The identification of this new autoantigen provides an important predictive biomarker for the underlying autoimmunity.

The identification of a new target of type 1 diabetes autoimmunity provides a new instrument for the development of antigen-specific immunotherapies; this is of particular interest, since anti-GLT1 antibodies exert a cytotoxic effect on  $\beta$ -cells.

Pathogenic autoantibodies have already been demonstrated in endocrine (Kahn et al., 1976; Rees et al., 1988; Iorio and Lennon 2012; Lindstrom et al., 1976; Lucchinetti et al., 2002) and neurologic diseases (Iorio and Lennon 2012), in which they bind to cell-surface proteins, such as receptors and channels, and impair their function directly or indirectly by inducing endocytosis and degradation (Iorio and Lennon 2012). Examples of pathogenic autoantibodies are those present in type B insulin resistance syndromes (Kahn et al., 1976). In this syndrome autoantibodies to the insulin receptor block insulin action, with resultant severe hyperglycemia, hypercatabolism, acanthosis nigricans, and hyperandrogenism in women. Pathogenic autoantibodies also may induce complement-mediated inflammation and cytotoxicity (Iorio and Lennon 2012) as those directed against the skeletal muscle nicotinic acetylcholine receptor (AChR) responsible for acquired myasthenia gravis (Lindstrom et al., 1976; Lucchinetti et al., 2002), and those against the aquaporin-4 water channel that contribute to the pathogenesis of neuromyelitis optica (Lindstrom et al., 1976; Lucchinetti et al., 2002). Immunoglobulins against ionotropic glutamate and metabotropic

glutamate receptors also participate to the pathological process of diverse myelopathies and encephalopathies through both complement-dependent and independent mechanisms (Iorio and Lennon 2012).

Our data provide direct experimental evidence that the sera from subjects with type 1 diabetes containing GLT1 autoantibodies cause  $\beta$ -cell death. Cell-based assays demonstrate the selective binding of type 1 diabetes IgGs to GLT1, a process that, in the presence of active complement, initiates complement activation and induces the rapid loss of membrane integrity. Interestingly, GLT1-immunoreactivity was detected in approximately half of ICA-positive sera, which is consistent with previous reports on complement-fixing ICAs (Bottazzo et al., 1980; Tarn et al., 1988; Radillo et al., 1996). Furthermore, we found that complement-mediated cell death is not the only mechanism: a subset of anti-GLT1 antibody positive sera induce  $\beta$ -cell apoptosis in the absence of complement, through the inhibition of GLT1 activity and its downregulation through endocytosis and lysosomal-mediated intracellular degradation (Figure 4 and 5). Through both these mechanisms, extracellular glutamate concentrations in the islet microenvironment may rise to a concentration which is toxic to  $\beta$ -cells (Di Cairano et al., 2011). Thus, the anti-GLT1 autoantibodies may act similarly to the autoantibodies against the potassium channel KIR4.1 recently described in individuals with multiple sclerosis, which contribute to the pathogenesis of the disease through complement activation but also by interfering with the channel function (Srivastava et al., 2012). In conclusion, our data provide evidence that GLT1 is a novel immune target in subjects with type 1 diabetes mellitus. Most importantly, autoantibodies to GLT1 are pathogenic by complement-mediated  $\beta$ -cell membrane lysis and death and also by downregulating GLT1 protein and function. Future studies should address the predictive value of humoral and cellular autoreactivity against GLT1 and the correlation with the  $\beta$ -cell secretory reserve in subjects with new onset and long lasting type 1 diabetes as well as in those who are at high risk of developing the disease.

## MATERIAL and METHODS

### **Cell lines.**

The mouse  $\beta$ TC3 cell line was originally provided by Prof. Douglas Hanahan (University of California, San Francisco, CA).  $\beta$ TC3 were grown in RPMI 1640, 11 mM glucose supplemented with 10% heat inactivated foetal bovine serum, 2 mM L-glutamine, and 100 IU/ml streptomycin/penicillin.

COS7 cells were cultured in DMEM supplemented with 10% fetal calf serum, 2 mM L-glutamine, and 100 IU/ml streptomycin/penicillin. Cultures were performed under standard humidified conditions of 5% CO<sub>2</sub> at 37° C. All media were supplied by Sigma-Aldrich.

### **Cell transfection**

About  $2.5 \times 10^5$  COS7 cells were seeded onto glass coverslips or on 6 cm Petri dishes and 24 hours after plating, they were transfected with 1  $\mu$ g or 6  $\mu$ g of plasmids by means of lipofection (Promega). 48 hours later, they were processed for immunoprecipitation or immunofluorescence assays.

### **Time-lapse imaging**

48 hrs after transfection, GFP-GLT1 expressing COS7 cells were exposed to 10% serum samples in Krebs solution for 15 minutes before incubation with 10% active or heat inactivated complement. Then cells were imaged using a Zeiss Axiovert inverted microscope equipped with a Retiga SRV CCD camera at 37°C using a 100 $\times$  1.45 numerical aperture (NA) oil immersion objective. Single-cell imaging under fluorescence illumination was carried out at 4 frames per minute for 30 min in the continuous presence of serum and complement at 37°C. Up to three cells were imaged on each coverslip in three independent experiments.

**Apoptosis** After serum incubation, cells were transferred in normal growing medium for 24 hours, then they were fixed in ice-cold methanol and apoptosis was estimated by ELISA assay (La Roche).

**Image analysis:** Immunofluorescence cell images and in vivo imaging were obtained using a Zeiss Axiovert inverted microscope equipped with a Retiga SRV CCD camera.

### **Patients**

The diabetic group comprised 43 subjects with a diagnosis of type 1 diabetes mellitus who were seen at the Ospedale San Raffaele (OSR), Milan, Italy, according to the 2006 American Diabetes Association criteria (25). Serum samples were obtained from these individuals after written informed consent was obtained, according

to the guidelines of the OSR ethical board. The control group consisted of 35 healthy donors. Details of the subjects in both groups are provided in Tables 1.

	Type 1 diabetes	Control
Samples	(n=43)	(n=35)
Age (years)		
Mean	28.25 ± 2.96	29.25 ± 5.56
Range	(2-65)	(7-68)
Gender (n)		
Male : Female	20 : 23	19 : 16
Disease Duration (years)		
Mean	3.30	-
Range	(1-20)	-
Glycated haemoglobin (%)		
Mean	9.36 ± 0.5	-
Range	(7-16.3)	-
ICA Positive (%)	89.76	0
GADA Positive (%)	89.76	0
IA-2A Positive (%)	34.88	0
IAA Positive (%)	53.48	0

**Table 1: Summary of Demographic and Clinical Characteristics of control subjects and persons with type 1 diabetes.** Age and Disease duration at sampling; ICA = Islet Cell Antibodies; GADA = Glutamic Acid Decarboxylase Antibodies (Normal Range: 0-3 UA); IA2A = Insulinoma Antigen 2 (Normal Range: 0-1 UA); IAA = Insulin AutoAntibodies (Normal Range: 0-5 UA). Details of the type 1 diabetes serie are displayed in Table 2.

### Cell-Based ELISA Assay.

Elisa Assay was performed by testing type 1 diabetes and control sera on MDCK cells expressing the GFP-GLT1 construct or mock cells.  $6 \times 10^4$  MDCK mock cells or expressing GFP-GLT1 were plated in 96 well plate and 24 hrs later, they were incubated with 5  $\mu$ l of serum samples from healthy controls, T1DM patients, anti-GLT1 rabbit serum (3) or an anti-GFP antibody (Invitrogen) at RT for 2 hrs. After 1 hr incubation with HRP-conjugated anti-human or anti-rabbit IgG, they were incubated for 30 min with the substrate (Pierce). Data were corrected for background (ABS values measured in MDCK mock cells) and expressed as a mean  $\pm$  S.D. of three independent experiments performed in triplicate.

### Immunoglobulin and Complement Mediated Cell Lysis Assay

Forty-eight hours after plating, GLT1-transfected COS7 cells or  $\beta$ TC3 cells (15, 25) were incubated in Krebs' buffer with 10% serum from healthy controls or type 1 diabetic subjects at 4°C for 30 minutes, followed by 90 minutes of incubation at 37°C in the same solution supplemented with 10% fresh or heat-inactivated human complement (Sigma). To quantify complement-mediated cell lysis, the cells were then incubated for 15 minutes in a buffer containing 0.5  $\mu$ g of Propidium iodide (Pri) (Sigma), fixed in ice-cold methanol, and counterstained with DAPI (Sigma). Pri-positive cells were counted by three independent blinded observers, using a 20X objective from 10 randomly selected fields per coverslip.

### [<sup>3</sup>H]D-Aspartic Acid Uptake

Glutamate transport uptake was assessed by measuring the uptake of [<sup>3</sup>H]D-aspartic acid. After incubation of βTC3 cells with 10% serum from healthy controls or type 1 diabetic subjects at 37°C for 2 hours in Kreb's buffer, the cells were maintained for 10 minutes in 200 μl of Na<sup>+</sup>-dependent (150 mM NaCl 2 mM KCl, 1 mM CaCl<sub>2</sub>, 1 mM MgCl<sub>2</sub>, 10 mM Hepes pH 7.5) uptake solution containing 5 μCi/ml of [<sup>3</sup>H]D-Aspartic acid (specific activity 37 Ci/mmol; Amersham Biosciences). The amino acid uptake was stopped by washing the cells twice in ice-cold sodium-free solution. Cells were dissolved in 150 μl of SDS 1% for liquid scintillation counting.

### **Statistical Analyses**

Statistical analysis software GraphPad Prism 4.00 (San Diego) was used for all statistical analyses. Comparison between two groups was determined by unpaired, two tailed, Student's t-test or by two-sided Fisher's exact test. Comparison among groups was determined by one way ANOVA, followed by Tukey's test. P values of less than 0.05 were considered to indicate statistical significance.

## Bibliography chapter III

1. Arriza JL, Fairman WA, Wadiche JI, Murdoch GH, Kavanaugh MP, Amara SG. Functional comparisons of three glutamate transporter subtypes cloned from human motor cortex. *J Neurosci* 1994;14(9):5559-69.
2. Atkinson MA, Bluestone JA, Eisenbarth GS, Hebrok M, Herold KC, Accili D, Pietropaolo M, Arvan PR, Von Herrath M, Markel DS, Rhodes CJ.(2011). How does type 1 diabetes develop?: the notion of homicide or  $\beta$ -cell suicide revisited. PMID: 21525508 PMCID: PMC3292309.
3. Baekkeskov S, Aanstoot HJ, Christgau S, Reetz A, Solimena M, et al. Identification of the 64K autoantigen in insulin-dependent diabetes as the GABA-synthesizing enzyme glutamic acid decarboxylase. *Nature* 1990; 347:151-56.
4. Bonifacio E, Lampasona V, Genovese S, Ferrari M, Bosi E. Identification of protein tyrosine phosphatase-like IA2 (islet cell antigen 512) as the insulin-dependent diabetes-related 37/40K autoantigen and a target of islet-cell antibodies. *J Immunol* 1995;155:5419-26.
5. Bottazzo GF, Dean BM, Gorsuch AN, Cudworth AG, Doniach D. Complement-fixing islet-cell antibodies in type-1 diabetes: possible monitors of active beta-cell damage. *Lancet*. 1980;1(8170):668-72.
6. Dedov II, Shestakova MV, Kuraeva TL, Titovich EV, Nikonova TV. Nozological Heterogeneity, Molecular Genetics and Immunology of Autoimmune Diabetes Mellitus. *Vestn Ross Akad Med Nauk*. 2015;(2):132-8.
7. Di Cairano ES, Davalli AM, Perego L, Sala S, Sacchi VF, et al. The glial glutamate transporter 1 (GLT1) is expressed by pancreatic  $\beta$ -cells and prevents glutamate-induced  $\beta$ -cell death. *J Biol Chem*. 2011;286 (16):14007-018.
8. Dobersen MJ, Scharff JE, Ginsberg-Fellner F, Notkins AL. Cytotoxic autoantibodies to beta cells in the serum of patients with insulin-dependent diabetes mellitus. *N Engl J Med*. 1980;303(26):1493-98.
9. Donath MY, Shoelson SE (2011) Type 2 diabetes as an inflammatory disease. *Nat Rev Immunol* 11(2):98–107.
10. Fournanos S, Narendran P, Byrnes GB, Colman PG, Harrison LC (2004) Insulin resistance is a risk factor for progression to type 1 diabetes. *Diabetologia* 47(10):1661–1667.
11. Genuth S (2003) Lowering the criterion for impaired fasting glucose is in order. *Diabetes Care* 26:3331–3332.
12. Hathout EH, Thomas W, El-Shahawy M, Nahab F, Mace JW.(2001)Diabetic autoimmune markers in children and adolescents with type 2 diabetes. *Pediatrics*. 2001 Jun;107(6):E102.
13. Hayashi M, Yamada H, Uehara S, Morimoto R, Muroyama A, et al. Secretory granule-mediated co-secretion of L-glutamate and glucagon triggers glutamatergic signal transmission in islets of Langerhans. *J Biol Chem*. 2003;278(3):1966-74.
14. Herold KC, Hagopian W, Auger JA, Poumian-Ruiz E, Taylor L, Donaldson D, Gitelman SE, Harlan DM, Xu D, Zivin RA, Bluestone JA (2002).Anti-CD3 monoclonal antibody in new-onset type 1 diabetes mellitus. *N Engl J Med*. 2002 May 30;346(22):1692-8.
15. Hyppönen E, Virtanen SM, Kenward MG, Knip M, Akerblom HK. (2000) Childhood Diabetes in Finland Study Group.Obesity, increased linear growth, and risk of type 1 diabetes in children. *Diabetes Care*. 2000 Dec;23(12):1755-60.
16. Iorio R, Lennon VA. Neural antigen-specific autoimmune disorders. *Immunol Rev*. 2012 Jul;248(1):104-21.
17. Kahn CR, Flier JS, Bar RS, Archer JA, Gorden P, Martin MM, Roth J. The syndromes of insulin resistance and acanthosis nigricans. Insulin-receptor disorders in man. *N Engl J Med*. 1976;294(14):739-45.
18. Kukreja A, Cost G, Marker J, Zhang C, Sun Z, et al. Multiple immuno-regulatory defects in type-1 diabetes. *J Clin Invest*. 2002;109(1):131-40.
19. Libman IM1, Pietropaolo M, Arslanian SA, LaPorte RE, Becker DJ (2003) Evidence for heterogeneous pathogenesis of insulin-treated diabetes in black and white children. *Diabetes Care*. 2003 Oct;26(10):2876-82.
20. Lindstrom JM, Seybold ME, Lennon VA, Whittingham S, Duane DD. Antibody to acetylcholine receptor in myasthenia gravis. Prevalence, clinical correlates, and diagnostic value. *Neurology*. 1976;26(11):1054-9.
21. Lucchinetti CF, Mandler RN, McGavern D, Bruck W, Gleich G, et al. A role for humoral mechanisms in the pathogenesis of Devic's neuromyelitis optica. *Brain*. 2002;125(Pt 7):1450-61.
22. Oresic M, Simell S, Sysi-Aho M, Na<sup>o</sup>nto<sup>o</sup>-Salonen K, Seppa<sup>o</sup>nen- Laakso T, Parikka V, Katajamaa M, Hekkala A, Mattila I, Keskinen P, Yetukuri L, Reinikainen A, La<sup>o</sup>hde J, Suortti T, Hakalax J, Simell T, Hyo<sup>o</sup>ty H, Veijola R, Ilonen J, Lahesmaa R, Knip M, Simell O (2008) Dysregulation of lipid and amino acid metabolism precedes islet autoimmunity in children who later progress to type 1 diabetes. *J Exp Med* 205(13):2975–2984.
23. Polonsky KS1.(1995) Lilly Lecture 1994. The beta-cell in diabetes: from molecular genetics to clinical research. *Diabetes*. 1995 Jun;44(6):705-17.

24. Radillo O, Nocera A, Leprini A, Barocci S, Mollnes TE, et al. Complement-fixing islet cell antibodies in type-1 diabetes can trigger the assembly of the terminal complement complex on human islet cells and are potentially cytotoxic. *Clin Immunol Immunopathol.* 1996;79(3):217-23.
25. Rees Smith B, McLachlan SM, Furmaniak J. Autoantibodies to the thyrotropin receptor. *Endocr Rev.* 1988;9(1):106-21.
26. Roep BO, Kleijwegt FS, van Halteren AG, Bonato V, Boggi U, Vendrame F, Marchetti P, Dotta F. Islet inflammation and CXCL10 in recent-onset type 1 diabetes. *Clin Exp Immunol.* 2010;159(3):338-43.
27. Rossini AA. Autoimmune diabetes and the circle of tolerance. *Diabetes* 2004;53:267-75.
28. Sanda S, Bollyky J, Standifer N, Nepom G, Hamerman JA, Greenbaum C (2010) Short-term IL-1beta blockade reduces monocyte CD11b integrin expression in an IL-8 dependent fashion in patients with type 1 diabetes. *Clin Immunol* 136(2):170–173.
29. Slotboom DJ1, Konings WN, Lolkema JS.(2001)Glutamate transporters combine transporter- and channel-like features. *Trends Biochem Sci.* 2001 Sep;26(9):534-9.
30. Srivastava R, Aslam M, Kalluri SR, Schirmer L, Buck D, et al. Potassium channel KIR4.1 as an immune target in multiple sclerosis. *N Engl J Med.* 2012;367(2):115-23.
31. Stadinski BD, DeLong T, Reisdorph N, Reisdorph R, Powell RL, et al. Chromogranin A is an autoantigen in type 1 diabetes. *Nat Immunol.* 2010;11(3):225-31.
32. Taplin CE1, Barker JM. (2008). Autoantibodies in type 1 diabetes. *Autoimmunity.* 2008 Feb;41(1):11-8. doi: 10.1080/08916930701619169.
33. Tarn AC, Thomas JM, Dean BM, Ingram D, Schwarz G, Bottazzo GF, Gale EA. Predicting insulin-dependent diabetes. *Lancet.* 1988;1(8590):845-50.
34. The Expert Committee on the diagnosis and classification of diabetes mellitus (1997) Report of the Expert Committee on the diagnosis and classification of diabetes mellitus. *Diabetes Care* 20:1183–1197.
35. Toguchi Y, Ginsberg-Fellner F, Rubinstein P. Cytotoxic islet cell surface antibodies (ICSA) in patients with type I diabetes and their first-degree relatives. *Diabetes* 1985;34(9):855-60.
36. Umpaichitra V1, Banerji MA, Castells S (2002). Autoantibodies in children with type 2 diabetes mellitus. *J Pediatr Endocrinol Metab.* 2002 Apr;15 Suppl 1:525-30.
37. Van De Winkel M, Smets G, Gepts W, Pipeleers D. Islet cell surface antibodies from insulin-dependent diabetics bind specifically to pancreatic B cells. *J Clin Invest* 1982;70(1):41-49.
38. Wenzlau JM, Juhl K, Yu L, Moua O, Sarkar SA, et al. The cation efflux transporter ZnT8 (Slc30A8) is a major autoantigen in human type 1 diabetes. *Proc Natl Acad Sci U SA* 2007;104:17040-045.
39. Wilkin TJ (2001). The Accelerator hypothesis: weight gain as the missing link between Type I and Type II diabetes. *Diabetologia* 44(7):914–922.

## Chapter IV

This chapter is dedicated to two secondary projects of this three-year doctoral activity.

I here report a brief introduction describing the project aims and the main findings, the methods and results relative to my contribution to the work and the related articles.

### **1) Delta cell death in the islet of Langerhans and the progression from normal glucose tolerance to type 2 diabetes in non-human primates (baboon, *Papio hamadryas*).**

Published on Diabetologia, August 2015

#### **AIM**

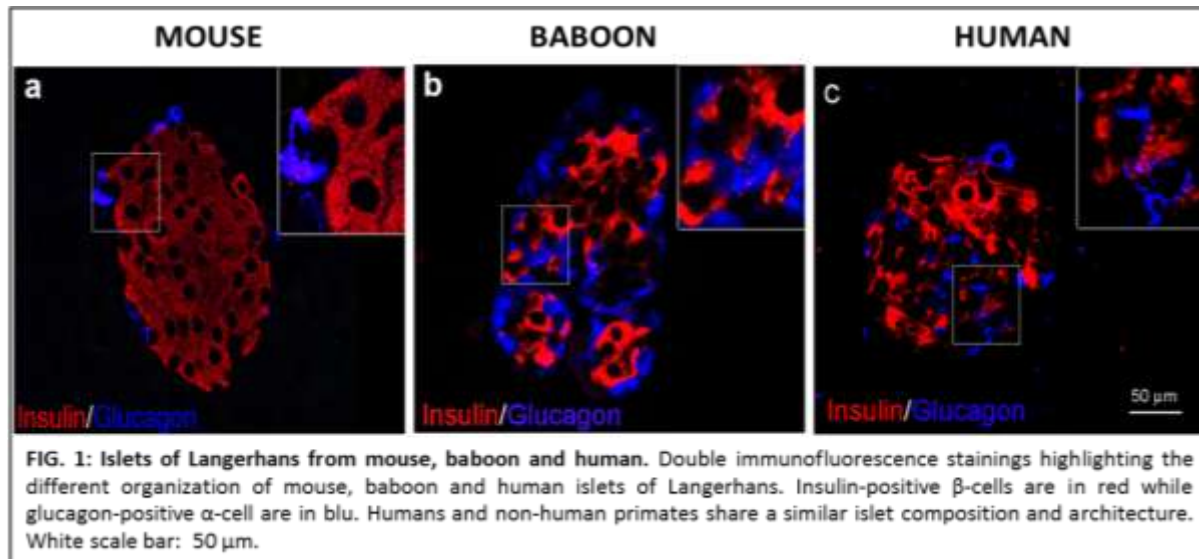
The work is the result of collaboration with Professor Folli Franco from Department of Medicine, Diabetes Division, University of Texas, Health Science Center at San Antonio.

Physiological interactions between the different pancreatic endocrine cell types ( $\alpha$ ,  $\beta$ ,  $\delta$ , F and PP cells) are essential to guarantee appropriate islet function and modifications in islet architecture have functional implications (Gannon et al., 2000; Orci and Unger 1975; Samols and Stragner 1990; Unger and Orci 2010; Gromada et al., 2007; Bonner-Weir and Orci 1982; Unger and Orci 1977).

Studies in the last years indicate that during type 2 diabetes progressions there is a progressive remodeling of the islet architecture. The consequences of these modifications are only partially understood.

Therefore, the aim of the work was to characterize further this islet remodeling and to correlate modification in islet composition with fasting glucose plasma (FGP), metabolic and hormonal parameters. We focus in particular on  $\delta$  cells. Information about the  $\delta$ -cell number and function in diabetes is limited and whether these cells are also involved in diabetes pathogenesis remains unclear. Yet, several evidences support this hypothesis (Ludvigsen et al., 2004; Hauge-Evans et al., 2009; Patel et al., 1985; Vieira et al., 2007).

Given the anatomical and functional differences existing between human and rodent islets, the study was performed on baboons (*Papio hamadryad*). Humans and non-human primates share important physiological



and pathological similarities (comprising a similar islet composition and architecture, fig1) and baboons are an interesting model of spontaneous obesity, insulin resistance and T2D (Chavez et al., 2009; Chavez et al., 2008; Guardado-Mendoza et al., 2009; Kamath et al., 2011).

In the present study, islet cell composition was analysed in 40 baboons obtained from a large cohort of animals that had FPG concentrations measured in the last year of their lives. Baboons were stratified in 4 groups according to their FPG levels, ranging from normal glucose tolerance (Group 1 or G1) to T2DM (Group 4 or G4) and the relative volumes of islet of Langerhans'  $\beta$ -,  $\alpha$ -  $\delta$ -cell component and amyloid deposits were measured in pancreases. The relationships between changes in islet cell composition and FPG, clinical, biochemical and metabolic parameters were investigated.

## INTRODUCTION

FPG increased linearly from G1 to G4, however, only baboons of G4 showed the classic diabetic phenotype characterized by *i*) increased plasma glucagon, FFA and cholesterol levels; *ii*) decreased fasting plasma insulin levels and *iii*) dramatically impaired  $\beta$ -cell function as calculated by HOMA-B. Islet volume/size did not vary significantly from G1 to G3, while it showed a significant increase in G4. Relative to islet remodelling, it was found that amyloidosis preceded the decrease in  $\beta$ -cell volume (50% in G4). As detected in human diabetic subjects,  $\alpha$ -cell volume increased ~50% in G3 and G4 ( $p < 0.05$ ), while  $\delta$ -cell volume decreased in these groups by 31 and 39%, respectively ( $p < 0.05$ ). Coherently with this islet remodelling, in the G4 group, glucagon levels were higher, while insulin were lower than in the other groups.

These data indicate for the first time a reduction in  $\delta$ -cell mass, the objective of my work was to verify whether this reduction was due to delta cell death. We focus on apoptosis, the prevalent mechanism of islet of Langerhans cell death in rodent models of diabetes and in human diabetic subjects.

## **METHODS**

To identify apoptotic cells we performed triple immunostainings of pancreatic sections derived from baboon with exert diabetes (G4) and from control animals (G1). Two different markers of apoptosis were used: TUNEL (DeadEnd™ Fluorometric TUNEL, Promega) assay; anti-cleaved caspase 3 (Asp175, CC-3). The DeadEnd™ Fluorometric TUNEL System measures the fragmented DNA of apoptotic cells by catalytically incorporating fluorescein-12-dUTP at 3'-OH DNA ends using the Terminal Deoxynucleotidyl Transferase, Recombinant, enzyme (rTdT), which forms a polymeric tail using the principle of the TUNEL (TdT-mediated dUTP Nick-End Labeling) assay. The fluorescein-12-dUTP-labeled DNA then can be visualized directly by fluorescence microscopy or quantitated by flow cytometry. Cleaved Caspase-3 (Asp175) Antibody detects endogenous levels of apoptosis revealing the large fragment (17/19 kDa) of activated caspase-3 resulting from cleavage adjacent to Asp175. This antibody does not recognize full length caspase-3 or other cleaved caspases.

To identify  $\beta$  and  $\delta$ -cells, sections were co-stained with antibodies against insulin and somatostatin, respectively.

Confocal analysis Images were acquired at the confocal microscope. Islets were imaged with the confocal LSM510 Meta system (Zeiss) with a  $\times 40$  objective. To reduce the bleed through, confocal images were acquired with a sequential acquisition setting, at  $1024 \times 1024$  pixel resolution. The fluorophores (FITC, TRITC, and Cy5) are all commonly used for triple immune-stainings and the bleed-through for these fluorophores is negligible when sequential scanning is used. Background signal caused by nonspecific binding was subtracted from "test" images.

*Apoptosis quantification.* To quantify the % of apoptotic cells in each section, the number of CC3-positive and TUNEL-positive delta or beta cells was counted in a total of 100 somatostatin-immunoreactive  $\delta$ -cells and 100 insulin-immunoreactive  $\beta$ -cells in three different animals from each group, on two different pancreas sections. Cells were counted in sequence, in different islets, until the number of 100 beta and 100 delta cells was reached. Statistical evaluation was performed using the unpaired *t* test.

## **RESULTS AND DISCUSSION**

In G4 diabetic pancreas, the number of  $\delta$ -cells is greatly reduced as compared to G1 control pancreas. To explore the possibility that  $\delta$ -cell reduction was due to apoptosis we triple stained G1 and G4 sections with TUNEL and hormones (insulin and somatostatin). In triple immunofluorescence experiments, several TUNEL-positive apoptotic cells were identified in G4 diabetic pancreas but not in normal control pancreas (Figure 5 of the paper). Co-staining with hormones revealed that they were insulin positive but also somatostatin positive.

To further confirm the presence of apoptotic  $\delta$ -cells, we also performed triple immunofluorescence stainings with a different marker of apoptosis, the anti-cleaved caspase 3 antibodies, in G1 and G4 pancreas. In diabetic pancreas, we could detect the presence of caspase-3 positive/insulin positive cells as well as caspase-3 positive/somatostatin positive cells, i.e. apoptotic somatostatin producing  $\delta$ -cells (Figure 2). Apoptosis of beta and delta cells was also confirmed by immuno-electron microscopy using an anti-somatostatin antibody.

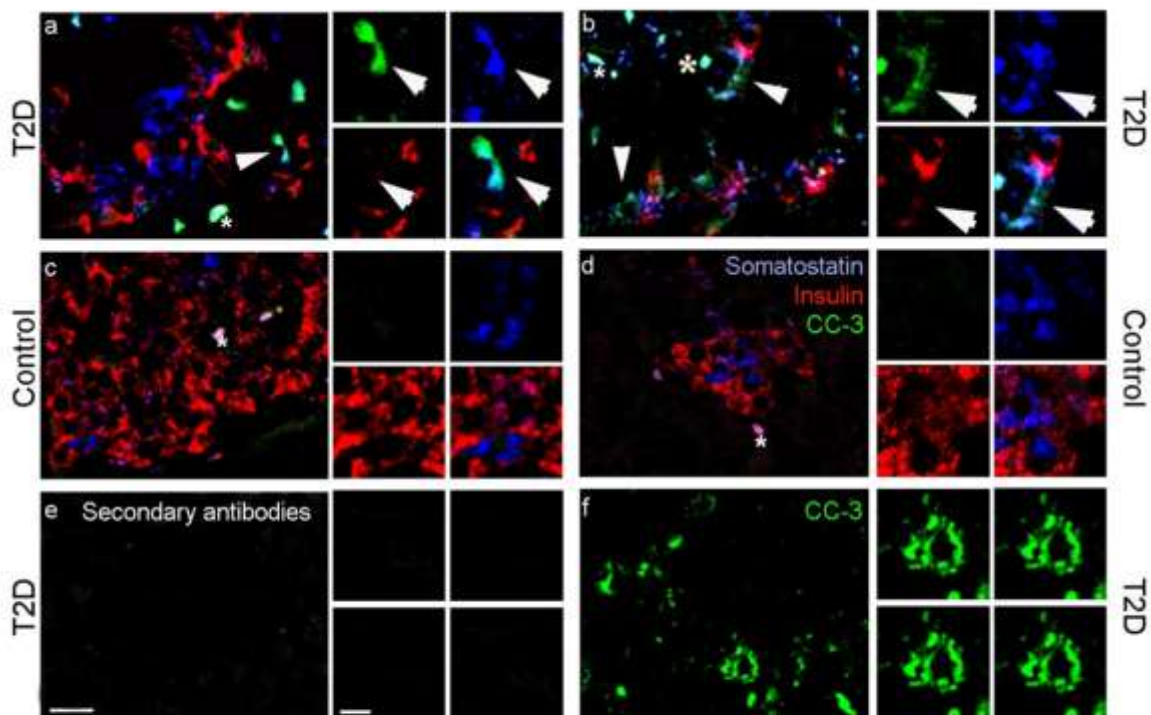


**Fig 2: Delta cells in pancreas section from T2DM baboon are positive for the apoptotic marker anti-cleaved caspase 3 (CC-3).** Triple immunofluorescence staining showing apoptotic beta and delta cells in control (c, d) or T2D (a, b) baboons. Apoptotic cells were stained with anti-cleaved caspase 3 (CC-3) antibody. To discriminate between beta and delta cells, islets were stained with anti-insulin (red) and anti-somatostatin (blue) antibodies. (e) Negative control (secondary antibodies only). (f) T2D pancreas section stained with anti-CC-3 antibody only. Representative somatostatin and insulin cells are shown at high magnification (x 2,5). Arrowheads indicates CC-3 positive cells present in pancreas of T2D baboons; \* indicates non-specific staining (scale bar= 30 $\mu$ m a-f, bar = 10  $\mu$ m in the particular shown at high magnification)

Overall, our data reinforce the evidence that amyloid deposition is an early event in islet pathology in baboons. In particular, given that amyloidosis starts before the reduction in  $\beta$ -cell volume, our data suggest that it is an

important cause of beta cell death in non-human primates, as well as in humans (Butler et al., 2003; Guardado-Mendoza et al., 2009; Jurgens et al., 2011; Westermark and Westermark 2013).

In diabetic baboons, changes in islet composition correlate also with increased alpha cells and decreased  $\delta$ -cell volume. The decrease in  $\delta$ -cell volume was due to  $\delta$ -cell death by apoptosis as showed by immunostaining with TUNEL and caspase 3.

This indicate that in baboons alpha cells are resistant to various conditions of beta cell stress, and that delta cells are also involved in the islet remodelling that occurs in type 2 diabetes (Ludvigsen et al., 2004; Hauge-Evans et al., 2009 Di Cairano et al., 2011; Federici et al., 2001; Fontès et al., 2010; Soejima and Landing 1986; Menge et al., 2011)

. The decrease in  $\delta$  cell volume and number, together with our data revealing apoptosis not only in  $\beta$  cells but also in  $\delta$  cells, allowed us to provide for the first time the direct evidence of ongoing  $\delta$ - cell death in type 2 diabetes.

## Delta cell death in the islet of Langerhans and the progression from normal glucose tolerance to type 2 diabetes in non-human primates (baboon, *Papio hamadryas*)

Rodolfo Guardado Mendoza<sup>1,2,3</sup> · Carla Perego<sup>4</sup> · Giovanna Finzi<sup>5,6</sup> · Stefano La Rosa<sup>5,6</sup> · Carlo Capella<sup>5,6</sup> · Lilia M. Jimenez-Ceja<sup>1,3</sup> · Licio A. Velloso<sup>7</sup> · Mario J. A. Saad<sup>7</sup> · Fausto Sessa<sup>5,6</sup> · Federico Bertuzzi<sup>8</sup> · Stefania Moretti<sup>4</sup> · Edward J. Dick Jr.<sup>9</sup> · Alberto M. Davalli<sup>10</sup> · Franco Folli<sup>1,7,11</sup>

Received: 5 February 2015 / Accepted: 21 April 2015 / Published online: 7 June 2015  
© Springer-Verlag Berlin Heidelberg 2015

### Abstract

**Aims/hypothesis** The cellular composition of the islet of Langerhans is essential to ensure its physiological function. Morphophysiological islet abnormalities are present in type 2 diabetes but the relationship between fasting plasma glucose (FPG) and islet cell composition, particularly the role of delta cells, is unknown. We explored these questions in pancreases from baboons (*Papio hamadryas*) with FPG ranging from normal to type 2 diabetic values.

**Methods** We measured the volumes of alpha, beta and delta cells and amyloid in pancreatic islets of 40 baboons (Group 1 [G1]: FPG < 4.44 mmol/l [*n* = 10]; G2: FPG = 4.44–5.26 mmol/l [*n* = 9]; G3: FPG = 5.27–6.94 mmol/l [*n* = 9]; G4: FPG > 6.94 mmol/l [*n* = 12]) and correlated islet composition with metabolic and hormonal variables. We also performed confo-

cal microscopy including TUNEL, caspase-3, and anti-caspase cleavage product of cytokeratin 18 (M30) immunostaining, electron microscopy, and immuno-electron microscopy with anti-somatostatin antibodies in baboon pancreases.

**Results** Amyloidosis preceded the decrease in beta cell volume. Alpha cell volume increased ~50% in G3 and G4 (*p* < 0.05), while delta cell volume decreased in these groups by 31% and 39%, respectively (*p* < 0.05). In G4, glucagon levels were higher, while insulin and HOMA index of beta cell function were lower than in the other groups. Immunostaining of G4 pancreatic sections with TUNEL, caspase-3 and M30 showed apoptosis of beta and delta cells, which was also confirmed by immuno-electron microscopy with anti-somatostatin antibodies. **Conclusions/interpretation** In diabetic baboons, changes in islet composition correlate with amyloid deposition, with in-

**Electronic supplementary material** The online version of this article (doi:10.1007/s00125-015-3625-5) contains peer-reviewed but unedited supplementary material, which is available to authorised users.

✉ Franco Folli  
folli@uthscsa.edu

<sup>1</sup> Department of Medicine, Diabetes Division, University of Texas Health Science Center at San Antonio, 7703 Floyd Curl Drive, San Antonio, TX 78229-3900, USA

<sup>2</sup> Research Department, Hospital Regional de Alta Especialidad del Bajío, León, Guanajuato, Mexico

<sup>3</sup> Department of Medicine and Nutrition, Division of Health Sciences, University of Guanajuato, León, Guanajuato, Mexico

<sup>4</sup> Dipartimento di Scienze Farmacologiche e Biomolecolari, Università degli Studi di Milano, Milan, Italy

<sup>5</sup> Department of Pathology, Ospedale di Circolo, University of Insubria, Varese, Italy

<sup>6</sup> Department of Surgical and Morphological Sciences, University of Insubria, Varese, Italy

<sup>7</sup> Department of Medicine, Obesity and Comorbidities Research Center (OCRC), University of Campinas, Campinas, São Paulo State, Brazil

<sup>8</sup> Ospedale Niguarda, Milan, Italy

<sup>9</sup> Southwest National Primate Research Center, Texas Biomedical Research Institute, San Antonio, TX, USA

<sup>10</sup> Department of Medicine and Endocrinology, Ospedale San Raffaele, Milan, Italy

<sup>11</sup> Department of Genetics, Texas Biomedical Research Institute, San Antonio, TX, USA

creased alpha cell and decreased beta and delta cell volume and number due to apoptosis. These data argue for an important role of delta cells in type 2 diabetes.

**Keywords** Alpha cell · Amyloid · Apoptosis · Baboon · Beta cell · Delta cell · Islet of Langerhans · Islet remodelling · Non-human primates · *Papio hamadryas* · Type 2 diabetes mellitus

### Abbreviations

CAST	Computer assisted stereology toolbox
CC-3	Anti-cleaved caspase 3 (Asp175) immunostaining
FPG	Fasting plasma glucose
FPI	Fasting plasma insulin
IFG	Impaired fasting glucose
M30	Anti-caspase cleavage product of cytokeratin 18
NGT	Normal glucose tolerance

### Introduction

Plasma glucose levels are tightly regulated by the islets of Langerhans in concert with insulin target tissues. Islets have a complex multi-cellular structure, containing insulin-secreting beta cells, glucagon-secreting alpha cells, somatostatin-secreting delta cells, pancreatic-polypeptide-secreting PP cells and grehlin-secreting epsilon cells. Physiological interactions between these different cell types are essential to ensure appropriate islet function, and changes in islet architecture have functional implications [1–7]. Compared with rodent islets, human and baboon islets contain proportionally fewer beta cells and more alpha cells [8–11]. In rodents, endocrine non-beta cells are confined to the islet periphery (mantle) while beta cells are concentrated in the centre (core) [12]. In sharp contrast, the vast majority of human and baboon islets do not have a core-mantle structure, as the beta cells are intermingled with alpha and delta cells throughout the islet and all the endocrine cells have equivalent access to blood vessels [8–10]. Therefore, human and baboon alpha and delta cells may exert a stronger paracrine control of the adjacent beta cells than those of rodents.

Islet composition undergoes profound changes in humans and non-human primates with type 2 diabetes, with a 50–70% reduction in beta cell mass and a variable absolute or relative increase in alpha cell numbers [13, 14], which account for the defective insulin secretion and the hyperglucagonaemia that are distinctive features of the disease [15–17]. However, studies of islet cell composition in humans have the following limitations: (1) they are necessarily performed on autoptic pancreases obtained 48–72 h post mortem when autolysis causes cell damage; (2) the vast majority of studies have compared non-diabetic vs diabetic subjects and have not examined islet composition in different stages of glucose intolerance; (3)

the different glucose-lowering regimens represent an additional confounding factor [18, 19]; and (4) most of the studies do not show correlations between morphometric and biochemical/functional variable parameters.

Delta cell fate in the diabetic pancreas is presently unknown, even though these cells may be more important than commonly thought [2–4]. A heterocellular region in which alpha, delta and beta cells are in close proximity has been described in the islets of all species and is believed to function as a pacemaker for the entire islet under the control of the delta cells [2, 3, 20]. However, information about delta cell number and function in diabetes is limited and whether these cells are also involved in the pathogenesis of diabetes remains unclear. Nevertheless, several lines of evidence support a role of delta cells in the pathogenesis of diabetes. Somatostatin receptors are present on both alpha and beta cells [21], and somatostatin secreted by delta cells paracrinally controls alpha and beta cell function [22, 23]. Major physiological insulin secretagogues such as glucose, arginine and glucagon-like peptide-1 (GLP-1) also regulate somatostatin release [22–28]. Finally, transgenic mice depleted of delta cells (*Sst*<sup>-/-</sup> mice) show enhanced insulin and glucagon release in response to nutrient stimuli [22], suggesting that delta cells exert a tonic inhibitory influence on insulin and glucagon secretion and are implicated in nutrient-induced suppression of glucagon secretion.

Baboons are an interesting model of spontaneous obesity, insulin resistance and type 2 diabetes in humans [29–33]. In the present study, we analysed the islet cell composition of 40 baboons obtained from a large cohort. The fasting plasma glucose (FPG) concentrations of the baboons were measured in the last year of their lives and the volumes of the islets of Langerhans, beta, alpha and delta cells and amyloid deposits were measured in pancreases. The relationships between changes in islet cell composition and FPG, clinical, biochemical and metabolic variables were investigated.

### Methods

**Study population** The study was conducted in accordance with the Principles of Laboratory Care in baboons that died from natural causes, with similar age and weight and different levels of FPG, (Group 1 [G1]: FPG < 4.44 mmol/l [*n* = 10]; G2: FPG = 4.44–5.26 mmol/l [*n* = 9]; G3: FPG = 5.27–6.94 mmol/l [*n* = 9]; G4: FPG > 6.94 mmol/l [*n* = 12]) selected from a large cohort followed during the past 14 years (from 1994 to 2007) at the Texas Biomedical Research Institute. Inclusion criteria were: (1) older than 8 years; and (2) availability of pancreatic tissue and clinical, anthropometric and laboratory measurements. Forty baboons were included in the present work (Table 1). Animals were fed ad libitum with a standard monkey chow (diet 5038, Purina, St Louis, MO, USA) and housed in corrals where they performed unrestrained physical activity.

**Table 1** Clinical, biochemical and morphological characteristics of the different groups according to glucose levels

Variable	Group 1 (FPG: <4.44 mmol/l)	Group 2 (FPG: 4.44–5.26 mmol/l)	Group 3 (FPG: 5.27–6.94 mmol/l)	Group 4 (FPG: >6.94 mmol/l)	<i>p</i> value
Baboons ( <i>n</i> ) (total <i>N</i> =40)	10	9	9	12	
Age (years)	21.9±1.0	19.8±0.9	22.0±1.4	21.2±0.9	0.469
Sex (F/M)	6/4	6/3	6/3	10/2	0.252
Weight (kg)					
Females	17.8±2.1	15.5±0.7	19.5±2.5	19.6±2.1	0.523
Males	26.4±2.0	28.5±1.2	27.7±0.7	25.8±3.0	0.755
FPG (mmol/l)	3.98±0.11	4.72±0.07	5.78±0.16	13.10±1.62*	<0.001
NEFA (mmol/l)	0.43±0.1	0.52±0.1	0.73±0.1	1.2±0.3*	0.001
Log <sub>e</sub> insulin (pmol/l)	11.2±0.2	11.5±0.4	11.8±0.5	9.8±0.6 <sup>†</sup>	0.024
Log <sub>e</sub> glucagon (ng/l)	11.0±0.1	11.0±0.1	11.1±0.1	11.6±0.2 <sup>†,‡</sup>	0.002
Cholesterol (mmol/l)	2.0±0.2	2.6±0.2	2.7±0.2	3.5±0.5*	0.003
Log <sub>e</sub> HOMA-B	6.3±0.3	5.5±0.4	5.1±0.5	2.6±0.4 <sup>*,‡,‡</sup>	<0.001
Log <sub>e</sub> HOMA-IR	7.6±0.3	8.0±0.3	8.5±0.4	8.3±0.3	0.064
Islets volume %/pancreas	3.2±0.3	3.3±0.4	3.9±1.1	4.4±0.6 <sup>*,‡,‡</sup>	0.002
Amyloid volume %/islets	12.9±4.6	19.1±6.3 <sup>†</sup>	33.6±7.5 <sup>†,†</sup>	70.2±5.2 <sup>†,‡,‡</sup>	0.001
Islet size (μm <sup>2</sup> )	9,287±590	9,294±960	11,709±2,511	11,135±923 <sup>*,‡,‡</sup>	0.002
Beta cell volume/pancreas vol (%)	2.1±0.2	1.9±0.2	1.9±0.4	1.0±0.3 <sup>*</sup>	0.022
Beta cell volume/islet volume (%)	60.0±3.7	60.4±5.6	50.2±6.5	23.7±4.9 <sup>†,‡,‡</sup>	0.001
Alpha cell volume/pancreas volume (%)	0.58±0.1	0.57±0.1	0.90±0.3	0.80±0.1	0.190
Alpha cell volume/islet volume (%)	16.7±1.0	18.3±2.8	26.9±5.0 <sup>†,†</sup>	24.0±1.9 <sup>*</sup>	0.018
Delta cell volume/pancreas volume (%)	0.14±0.01	0.12±0.01	0.08±0.02	0.09±0.02	0.210
Delta cell volume/islet volume (%)	4.7±0.6	4.4±0.8	2.8±0.7	2.8±0.5 <sup>*</sup>	0.050

\**p*<0.05 vs group 1<sup>†</sup>*p*<0.05 vs group 2<sup>‡</sup>*p*<0.05 vs group 3

F, female; M, male

**Tissue processing** Complete necropsies were performed on all the baboons, approximately 6–18 h post mortem. Pancreatic tissue from the body-tail region was fixed in 10% neutral-buffered formalin, processed conventionally and embedded in paraffin blocks. Sequential 5 μm sections for each baboon were stained with haematoxylin and eosin and Congo red and immunostained with antibodies for insulin, glucagon and somatostatin for evaluation of islets, amyloid deposits, and beta, alpha and delta cell morphometry, respectively. The detailed description of the automated immunohistochemistry, electron microscopy and immuno-electron microscopy is available in the electronic supplementary material (ESM) Methods section.

**Morphological measurements** The Computer Assisted Stereology Toolbox (CAST) 2.0 system (Olympus, Ballerup, Denmark) was used to perform all the microscopic measurements of beta, alpha and delta cell and amyloid deposit volume using the stereology fundamentals previously described and validated [31, 33–35]. The person who performed the

microscopic measurements (RGM) was blinded to the metabolic status of each baboon and the reproducibility of the CAST measurements was estimated twice in five specimens with a coefficient of variation <5%.

**Apoptosis assessment** To identify apoptotic cells we analysed pancreas sections derived from a total of eight G1 (normal glucose tolerant [NGT]) and eight G4 (type 2 diabetic) baboons, and three different methods were employed: (1) TUNEL; (2) anti-cleaved caspase 3 (Asp175) immunostaining (CC-3); and (3) anti-caspase cleavage product of cytokeratin 18 (M30). The detailed description of immunofluorescence and confocal microscopy methods is available in ESM Methods.

**Apoptosis quantification in beta and delta cells** To quantify the percentage of apoptotic cells in each section, the number of M30-positive and TUNEL-positive delta or beta cells was counted in a total of 100 somatostatin-immunoreactive delta cells and 100 insulin-immunoreactive beta cells in three

different animals from each group, blind, by two different observers (SL and CP). Cells were counted in sequence, in different islets, until the number of 100 beta and 100 delta cells was reached. Statistical evaluation was performed using the unpaired *t* test.

**Analytical measurements** Blood glucose was measured by the glucose oxidase method with the SYNCHRON CX System (Beckman Coulter, Brea CA, USA), insulin levels by RIA (Linco Research, St Louis, MO, USA), glucagon by RIA (Euro-Diagnostica AB, Malmö,

Sweden) and NEFA concentrations were determined using the fluorometric method.

**Calculations** Insulin resistance (HOMA-IR) and beta cell function (HOMA-B) were measured as previously described [36].

**Statistical analysis** Data are presented as means  $\pm$  SEM. ANOVA with Bonferroni correction was used as a post hoc test for comparisons between more than two groups when normal distribution was confirmed and Kruskal–Wallis or

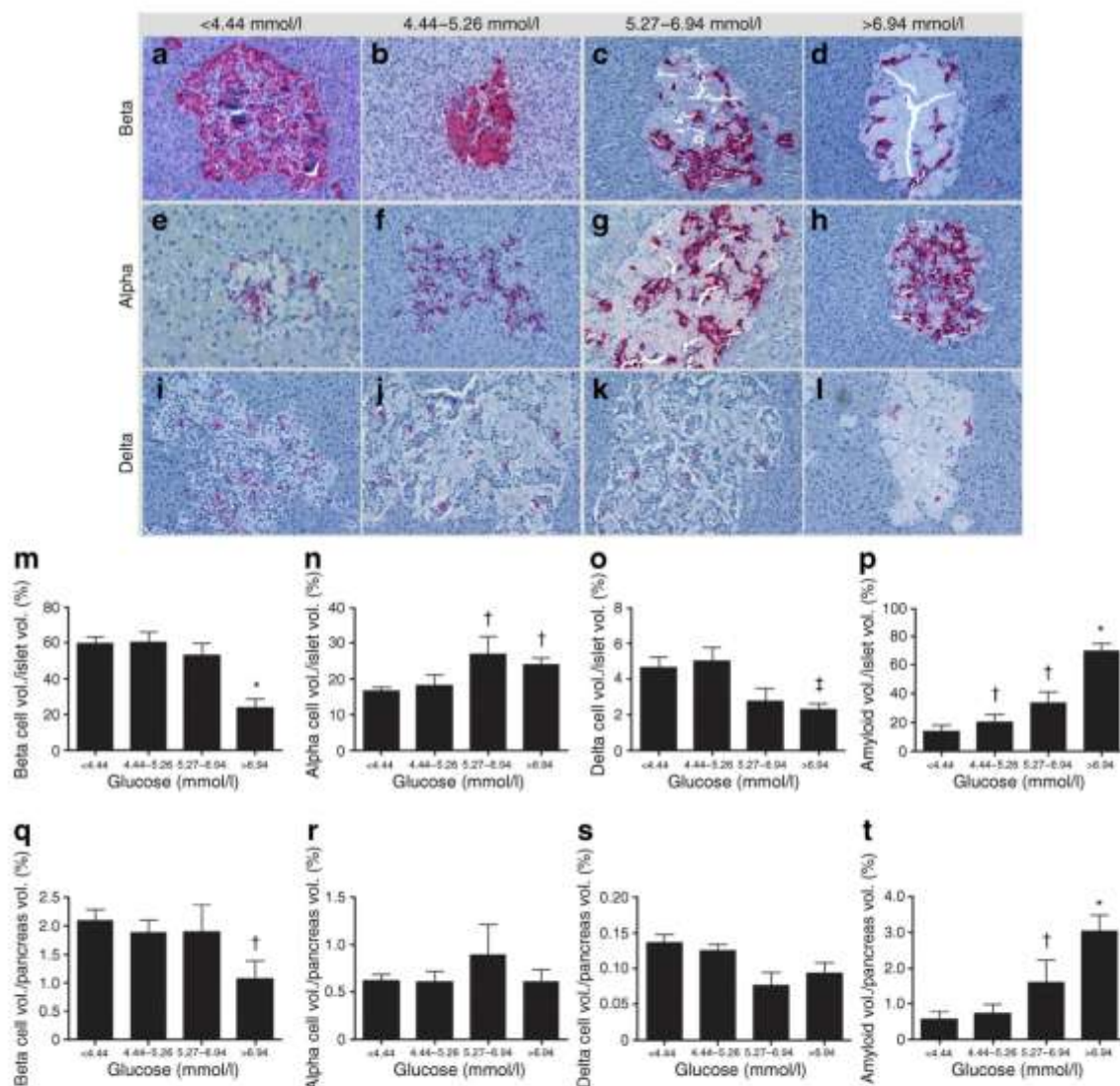


**Fig. 1** Morphological islet abnormalities in baboons with progressive increases in glucose levels. (a–d) Progressive decrease in beta cell volume (insulin immunohistochemistry); (e–h) progressive increase in alpha cell volume (glucagon immunohistochemistry); and (i–l) slight decrease in delta cell volume (somatostatin immunohistochemistry). All micrographs show a progressive increase in amyloid severity according to

glucose levels (final magnification  $\times 40$ ). Quantitative representation of the dysfunctional islet remodelling in the progression to type 2 diabetes: beta, alpha and delta cell and amyloid volumes per islet (m–p) and per pancreas (q–t) according to glucose levels in baboons. \* $p < 0.05$  vs G1, † $p < 0.05$  G3 vs G1, † $p < 0.05$  vs all groups

log transformed values were used for those with a skewed distribution, confirming a normal distribution after the log transformation. Bivariable correlations were evaluated with Pearson's correlation coefficient. A  $p$  value of  $<0.05$  was considered statistically significant.

## Results

**Clinical, biochemical and metabolic characteristics** Clinical, anthropometric, biochemical and metabolic data, as well as islet volumes, in the four groups are shown in Table 1. FPG increased linearly from G1 to G4; however, only baboons in the G4 group showed the classic diabetic phenotype characterised by: (1) increased plasma glucagon, NEFA and cholesterol levels; (2) decreased FPI levels; and (3) dramatically impaired beta cell function as calculated by HOMA-B. NEFA, cholesterol and HOMA-IR levels tended to increase from G1 to G3, while HOMA-B tended to decline even though these changes were not statistically significant. In addition, islet volume and size did not vary significantly from G1 to G3, while they showed a significant increase in G4.

**Islet cell composition and amyloid deposition** Islet cell composition and architecture in the four groups is shown in Fig. 1. Figure 1a–l are representative islets in pancreatic sections stained for insulin (a–d), glucagon (e–h) and somatostatin (i–l). Figure 1m–p are the volumes per islet of beta (m), alpha (n), delta cells (o) and amyloid deposits (p); the same data expressed as the percentage of the entire pancreatic area

are shown in Fig. 1q–t. Amyloid volume showed a striking linear increase from G1 to G4 (Fig. 1p, t). The progressive increases in amyloid deposits were not paralleled by significant changes in beta cell volumes that were in fact similar in G1 and G2, slightly decreased in G3 and dramatically reduced only in G4. Alpha cell volumes increased from G1 to G3 where they reached high statistical significance, but did not increase further in G4 (Fig. 1n, r). The volume of somatostatin-secreting delta cells was similar in G1 and G2 but showed a remarkable decrease (~41%) in G3 and G4 (Fig. 1o, s).

### Correlation between severity of amyloid deposition, FPG and islet cell composition

The analysis of the correlation between the severity of amyloid deposition, FPG levels and volumes of the three islet cell types is shown in Fig. 2. As expected, amyloid severity showed a linear positive correlation with FPG (Fig. 2a,  $R^2$  0.5275,  $p<0.001$ ) and an inverse correlation with beta cell volume (Fig. 2b,  $R^2$  0.7679,  $p<0.001$ ). By contrast, amyloid deposition and alpha cell volume showed a positive correlation (Fig. 2c,  $R^2$  0.1416,  $p<0.05$ ). Finally, the correlation between amyloid deposits and delta cell volume was, similarly to the beta cells, also negative (Fig. 2d,  $R^2$  0.1493,  $p<0.05$ ).

### Correlation between beta cell volume and biochemical and metabolic variables

The relationship between FPG levels and beta cell volume was negative and hyperbolic (Fig. 3a,  $R^2$  0.5428,  $p<0.001$ ). Beta cell volume also correlated inversely with NEFA levels (Fig. 3b,  $R^2$  0.2351,  $p<0.001$ ) and positively with FPI levels and beta cell function calculated

**Fig. 2** Correlations between (a) amyloid severity and plasma glucose level ( $R^2$  0.5275,  $p<0.001$ , 95% CI); (b) amyloid severity and beta cell volume/islet volume ( $R^2$  0.7679,  $p<0.001$ , 95% CI); (c) amyloid severity and alpha cell volume/islet volume ( $R^2$  0.1416,  $p<0.05$ , 95% CI); and (d) amyloid severity and delta cell volume/islet volume ( $R^2$  0.1493,  $p<0.05$ , 95% CI) in baboons

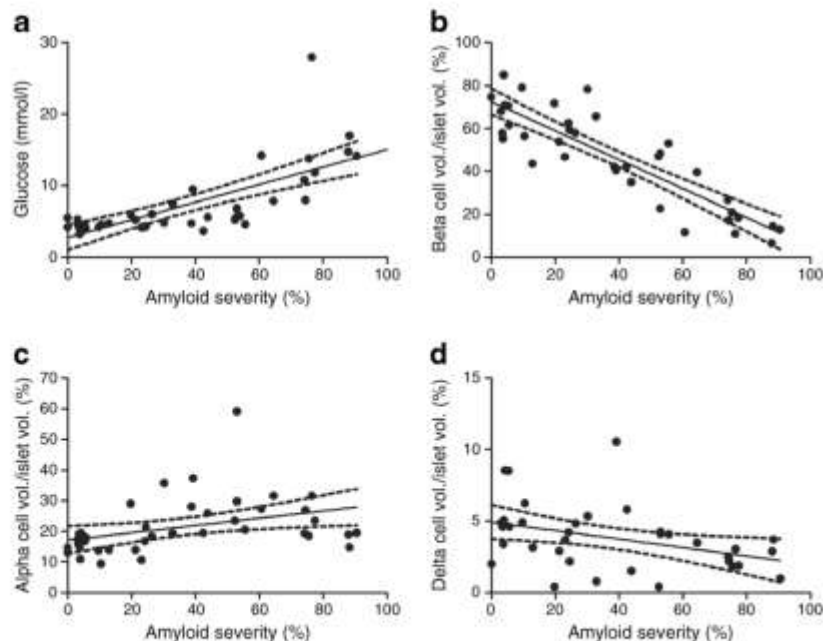
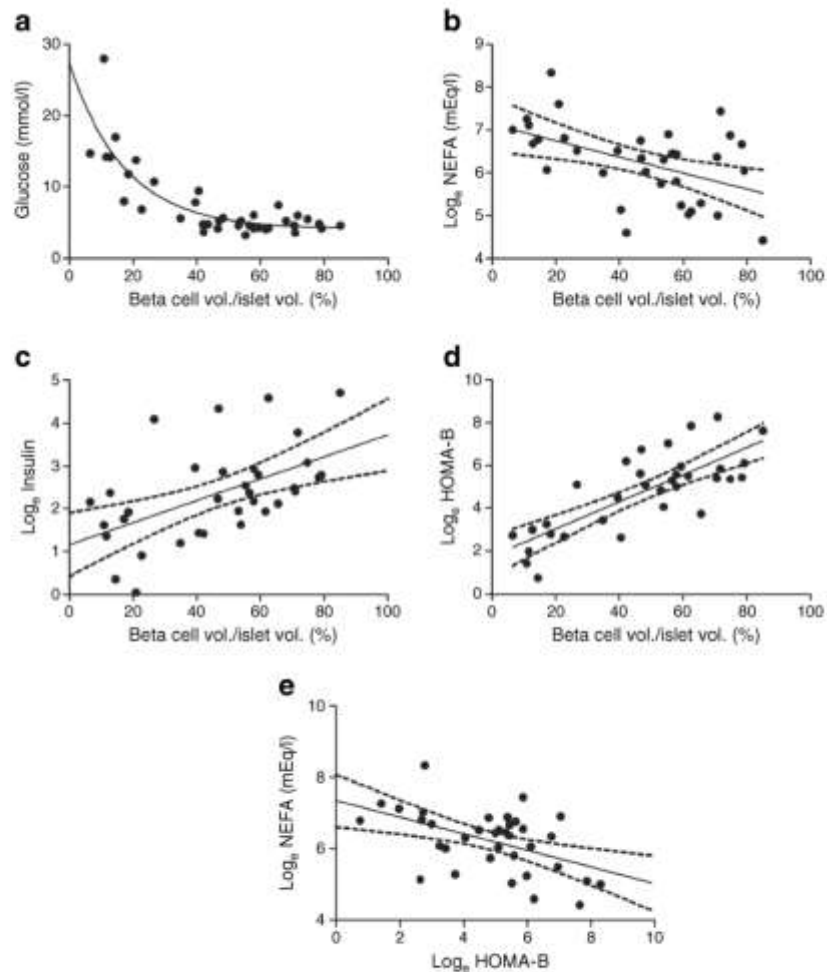


**Fig. 3** Correlation between (a) beta cell volume/islet volume and plasma glucose level ( $R^2$  0.5428,  $p < 0.001$ ); (b) beta cell volume/islet volume and plasma NEFA level ( $\log_e$ ) ( $R^2$  0.2351,  $p < 0.001$ , 95% CI); (c) beta cell volume/islet volume and plasma insulin level ( $\log_e$ ) ( $R^2$  0.2946,  $p < 0.001$ , 95% CI); (d) beta cell volume/islet volume and  $\log_e$  HOMA-B ( $R^2$  0.6092,  $p < 0.001$ , 95% CI); and (e)  $\log_e$  HOMA-B and plasma  $\log_e$  NEFA ( $R^2$  0.2451,  $p < 0.01$ , 95% CI) in baboons



with HOMA-B (Fig. 3c,  $R^2$  0.2946,  $p < 0.001$ ; Fig. 3d,  $R^2$  0.6092,  $p < 0.001$ ). HOMA-B was inversely correlated with NEFA levels (Fig. 3e,  $R^2$  0.2451,  $p < 0.01$ ).

**Correlation between FPG and NEFA levels and volumes of alpha and delta cells** The correlations between FPG and alpha and delta cell volumes were not significant (Fig. 4a, b). Conversely, delta cell volume was inversely correlated with  $\log_e$  NEFA, suggesting a potential toxic effect of increased levels of NEFA, which are observed in G3 and G4 animals in delta cells (Fig. 4c,  $R^2$  0.1926,  $p < 0.05$ ). Delta cell volume positively correlated with beta cell volume (Fig. 4d,  $R^2$  0.2110,  $p < 0.01$ ).

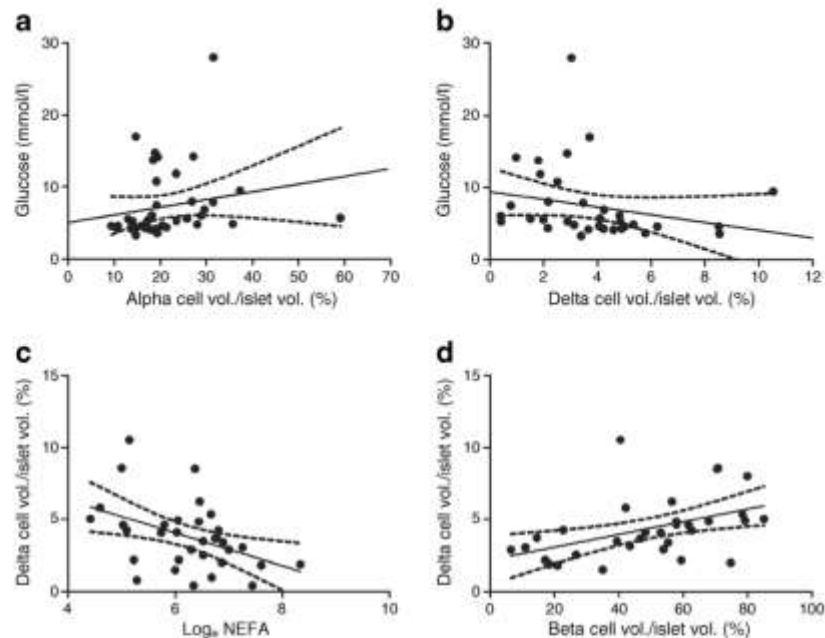
**Correlation of plasma glucagon levels and beta, alpha and delta cell volumes** Plasma glucagon levels did not correlate significantly with either beta or alpha cell volume (ESM Fig. 1a, b), while glucagon levels showed a significant inverse correlation with delta cell volume (ESM Fig. 1c,  $R^2$  0.2696,  $p < 0.01$ ).

**Pancreatic delta and beta cell apoptosis** To explore the mechanisms involved in the reduction of both delta and beta cell volume we performed a TUNEL assay on pancreatic sections obtained from G1 and G4 baboons. In triple immunofluorescence experiments with antibodies against hormones, ~5% of delta and ~3.5% of beta cells were TUNEL positive (apoptotic) in G4 diabetic pancreases (Fig. 5e, f, h, i, k, l), compared with control non-diabetic pancreases (G1 group) where no apoptotic delta cells ( $p < 0.05$ ) and beta cells ( $p < 0.005$ ) were observed (Fig. 5d, g, j, m).

To confirm the presence of apoptotic delta cells in diabetic pancreases, in both G1 and G4 pancreases we also performed double label immunohistochemical and triple immunofluorescence staining with antibodies directed against two additional apoptotic cell markers: M30 and CC-3 antibodies.

In G3 and G4 diabetic pancreases, the volume and the number of somatostatin-producing delta cells was greatly reduced compared with G1 control pancreases (Fig. 1k, l and ESM Fig. 2a, b).

**Fig. 4** Correlation between (a) alpha cell volume/islet volume and plasma glucose ( $R^2$  0.04,  $p=0.22$ , 95% CI); (b) delta cell volume/islet volume and plasma glucose ( $R^2$  0.058,  $p=0.16$ , 95% CI); (c)  $\log_e$  NEFA and delta cell volume/islet volume ( $R^2$  0.1926,  $p<0.05$ , 95% CI); and (d) beta cell volume/islet volume and delta cell volume/islet volume ( $R^2$  0.2110,  $p<0.01$ , 95% CI) in baboons



We observed M30-positive islet cells that were somatostatin negative, likely corresponding to insulin-positive beta cells as previously demonstrated [31] (ESM Fig. 2c, d, e). Using double label immunohistochemistry we were able to quantify that in diabetic pancreatic islets ~3% of delta cells (Fig. 5m and ESM Fig. 2f) and ~2% of insulin-producing beta cells were positive for the M30 antibody (i.e. apoptotic cells). Conversely, in non-diabetic pancreases (G1 group) no apoptotic delta cells ( $p<0.001$ ) or beta cells ( $p<0.001$ ) were observed. These findings confirm and reinforce the data obtained by TUNEL (Fig. 5m). Finally, consistent with the data obtained by TUNEL confocal microscopy and M30 immunohistochemistry, we could also detect both insulin/CC-3-positive beta as well as somatostatin/CC-3-positive delta cells in G4 (type 2 diabetes) islets of Langerhans (ESM Fig. 3). The number of delta cells per islet area in a subset of baboon pancreases was decreased by ~30% in baboon pancreases from G3–G4 animals (ESM Fig. 4).

**Immunoelectron microscopy** While delta cells of G1 baboons were well preserved (Fig. 6a, b and ESM Fig. 5c), in G4 animals, delta cells showed the typical large and uniformly electron-dense secretory granules encircled by a tightly fitting membrane and were immunoreactive for somatostatin, but also presented signs of degeneration, such as pycnotic nuclei and cytoplasmic vacuoles, which are typical features of apoptotic cells (Fig. 6c, d and ESM Fig. 5d).

**Electron microscopy** At the ultrastructural level, the presence of increasing amyloid deposits was associated with signs of cellular injury, including intracellular vacuoles and

pycnotic nuclei involving mainly beta cells, but also delta cells in G3 (impaired fasting glucose [IFG]) and G4 (type 2 diabetic) animals, while alpha cell morphology was unaffected by amyloidosis in G4 animals (Figs 7b, c, d and 8b, f). The degenerative/pro-apoptotic ultrastructural characteristics observed in beta and delta cells were also consistent with the decreases in beta and delta cell volume in diabetic animals.

## Discussion

Several studies have shown that the pancreases of subjects with type 2 diabetes display a severe beta cell deficit due to increased beta cell apoptosis [16, 17, 37, 38], and normal or increased alpha cell number [5, 13–15, 19]; interestingly, these alterations are also present in diabetic and insulin resistant/obese baboons [31, 33]. However, little is known regarding islet cell composition in prediabetic conditions such as IFG and impaired glucose tolerance [16]. We believe that another important unresolved question is related to the function and fate of the delta cells in type 2 diabetes. To learn more about these issues, we analysed the islet cell composition in the pancreases of baboons stratified into four quartiles of FPG levels spanning the NGT, IFG and type 2 diabetes ranges (G1–G4; Table 1).

We already reported that FPG levels in baboons are linearly correlated with islet amyloidosis [31]. In the present study, we confirm this finding by showing that as little as 0.83 mmol/l of FPG increase is associated with a significant increase in amyloid deposits that, remarkably, precede the changes in beta cell volumes (Fig. 1p). In fact, beta cell volumes were identical in

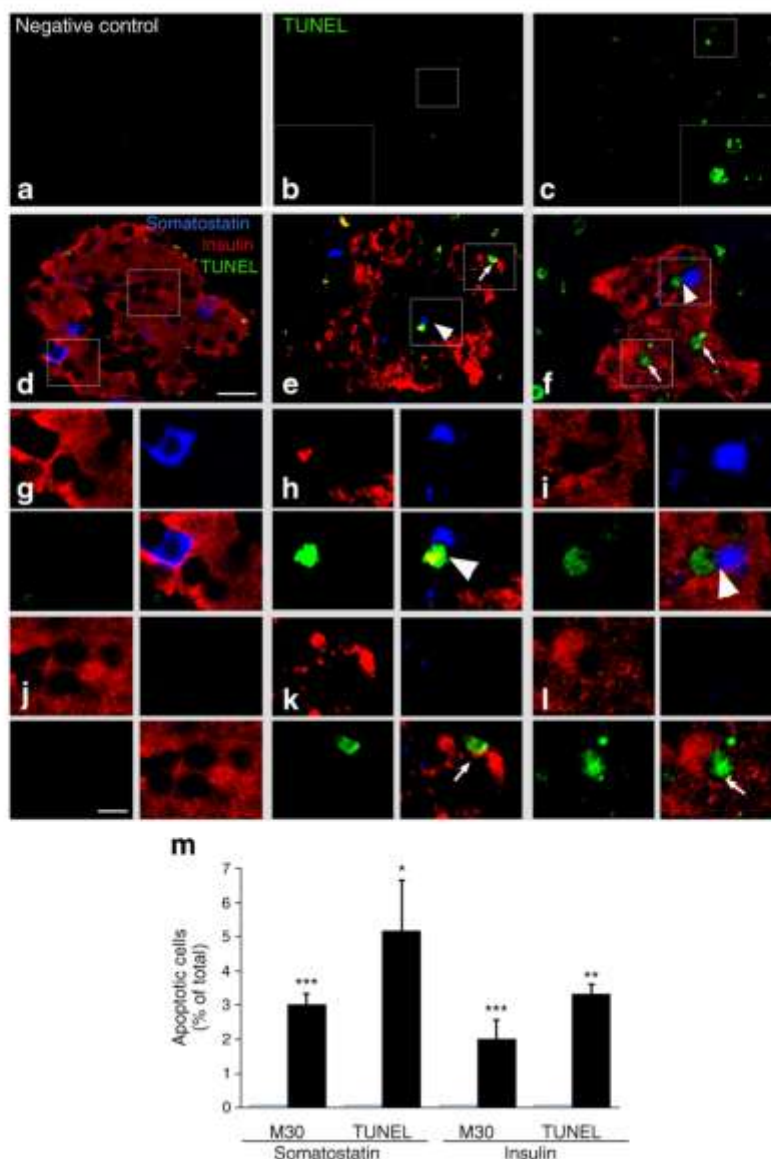


**Fig. 5** Triple immunofluorescence staining showing apoptotic beta and delta cells in baboons with type 2 diabetes. To reveal the presence of apoptotic cells, a TUNEL assay was performed in pancreas sections from controls (**a, b, d, g, j**) and two different G4 baboons with type 2 diabetes (**c, e, f, h, i, k, l**). (**a**) Negative control (secondary antibodies only); (**b, c**) TUNEL assay; (**d–f**) triple immunofluorescence staining with TUNEL (green), insulin (red) and somatostatin (blue). Representative TUNEL-positive somatostatin-labelled cells are shown at high magnification ( $\times 2.5$ ) in (**g–i**). Representative TUNEL-positive insulin-labelled cells are shown at high magnification ( $\times 2.5$ ) in (**j–l**). TUNEL-positive nuclei were detected in a fraction of somatostatin-positive cells (blue,

arrowheads) and in insulin-positive cells (red, arrows), only in the pancreas of baboons with type 2 diabetes (**a–f**; scale bar, 20  $\mu\text{m}$  and **g–l**; scale bar, 10  $\mu\text{m}$ ). Quantification of apoptotic delta and beta cells detected using both TUNEL and M30 assay in normal and diabetic baboons is shown in (**m**). The number of M30-positive and TUNEL-positive delta or beta cells was counted in a total of 100 somatostatin- or insulin-immunoreactive cells in three different baboons for each group. Black bars, type 2 diabetic pancreas (G4); white bars, control pancreas (G1). Data are expressed as means  $\pm$  SD. \* $p < 0.05$ ; \*\* $p < 0.01$ ; \*\*\* $p < 0.001$  type 2 diabetes vs relative control

G1 and G2, decreased in G3 but without reaching statistical significance, and fell dramatically only in G4 (Fig. 1m). These data further strengthen the evidence that amyloid deposition is an early event in islet pathology in baboons and that amyloidosis is an important cause of beta cell death in humans, non-human primates and other species [16, 31, 38, 39].

Similarly to the beta cell, the alpha and delta cell volumes also did not change significantly between G1 and G2. Alpha cell volume increased sharply in G3 (Fig. 1n), while delta cell volume showed a remarkable decrease in this group (Fig. 1o). Thus, alterations in alpha and delta cell composition seemed to occur earlier than changes in beta cell volume. In G4, alpha

**Fig. 6** Immunogold electron microscopy showing a normal delta cell with the classical trumpet-like shape in a control G1 baboon; (a) scale bar 2,000 nm and (b) scale bar 1,000 nm. The nucleus is well preserved and in the cytoplasm there are numerous secretory granules. At higher magnification (b), secretory granules are immunostained with an anti-somatostatin antibody and an anti-somatostatin gold-labelled antibody. In G4 baboons (c, scale bar 1,000 nm), the delta cell shows signs of degeneration including pycnotic nucleus and cytoplasmic vacuoles. At higher magnification (d, scale bar 500 nm), secretory granules are immunostained with an anti-somatostatin antibody and an anti-somatostatin gold-labelled antibody

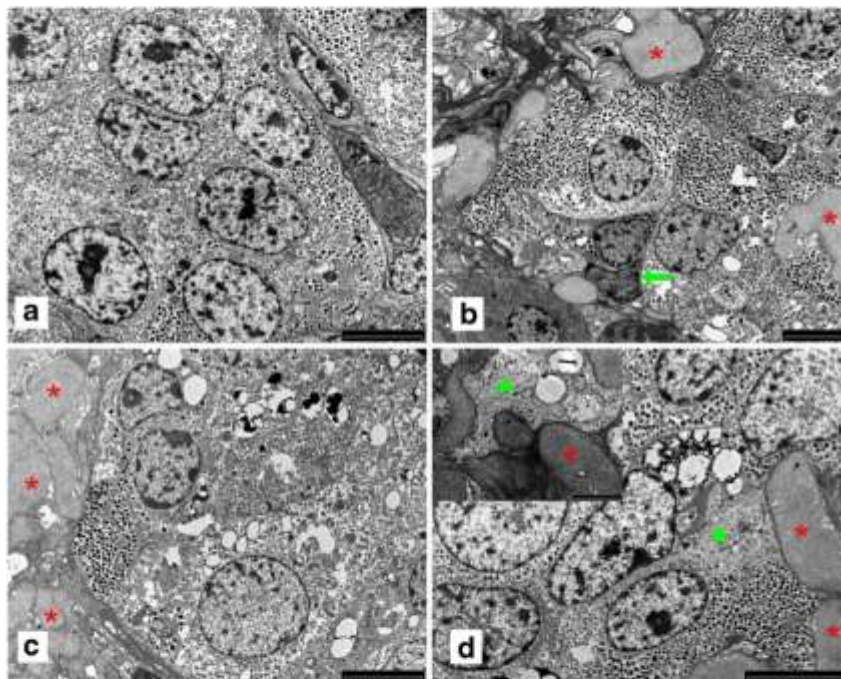
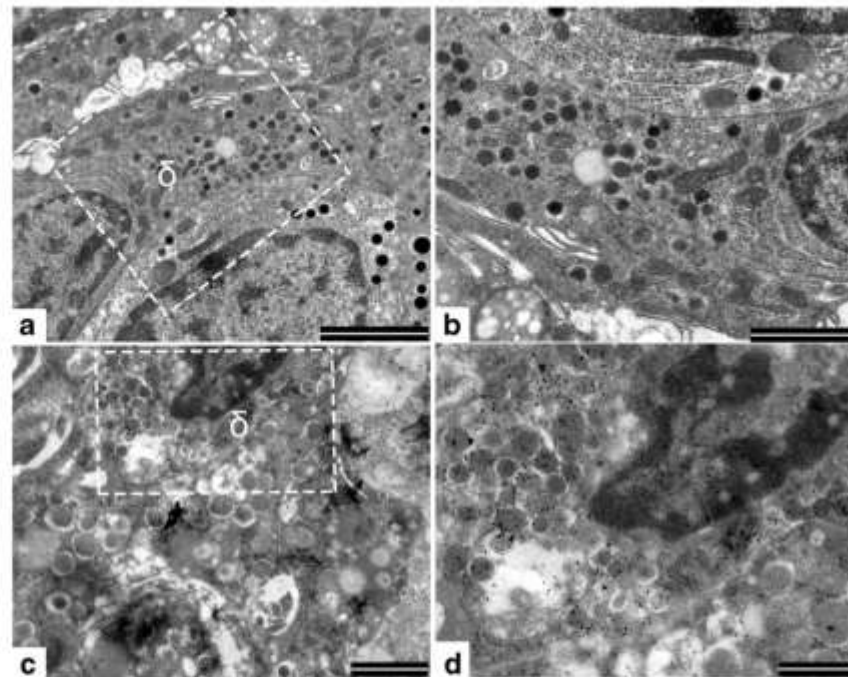
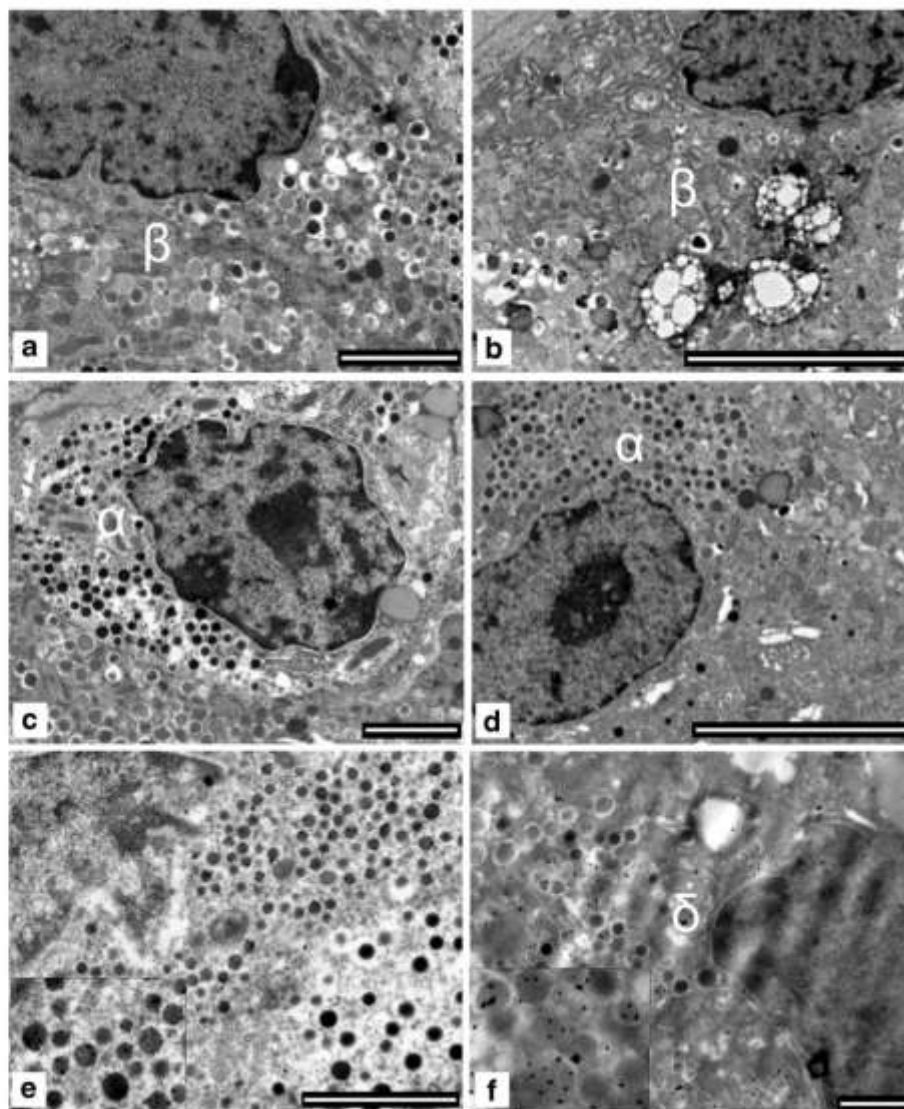


**Fig. 7** Example of a normal islet in control pancreatic tissue (G1 animal); islet cells are all well granulated, do not show any sign of degeneration and amyloid fibrils are absent (a, scale bar 5  $\mu$ m). Example of mild insular amyloidosis (G2 animal): some amyloid fibrils are accumulated in extracellular spaces (asterisks) and some cells show signs of degeneration (pre-pycnotic nuclei [arrow] and faint cytoplasmic vacuolisation) (b, scale bar 5  $\mu$ m). Moderate amyloidosis (G3 animal): numerous amyloid fibrils are

accumulated in extracellular spaces (asterisks) and cells show signs of degeneration, scarce secretory granules and numerous cytoplasmic vacuoles and lysosomes; (c, scale bar 5  $\mu$ m). Severe amyloidosis (G4 animal): amyloid deposits are accumulated in both extracellular spaces (asterisks) and cell cytoplasm (triangle), as better shown in the inset. Some cells show significant degeneration, cytoplasmic condensation and vacuolation; d, scale bar 5  $\mu$ m)

**Fig. 8** In a control baboon, beta (a,  $\beta$ , scale bar 2,000 nm), alpha (c,  $\alpha$ , scale bar 2,000 nm), and delta (e,  $\delta$ , scale bar 2,000 nm) cells are well granulated and show normal nuclei. In a baboon with type 2 diabetes, beta (b, scale bar 5  $\mu$ m) and delta (f, scale bar 1,000 nm) cells show signs of degeneration including pyknotic nuclei and large cytoplasmic vacuoles, while alpha cells (d, scale bar 5  $\mu$ m) show normal features. In the insets of figures (e) and (f), secretory granules are immunostained using anti-somatostatin antibody and an anti-somatostatin gold-labelled antibody



and delta cell volumes did not change further as compared with G3. This and previous studies indicate that in humans and baboons, alpha cells are resistant to various conditions of beta cell stress, and that delta cells are also involved in the islet remodelling that occurs in type 2 diabetes [20, 21, 40–44].

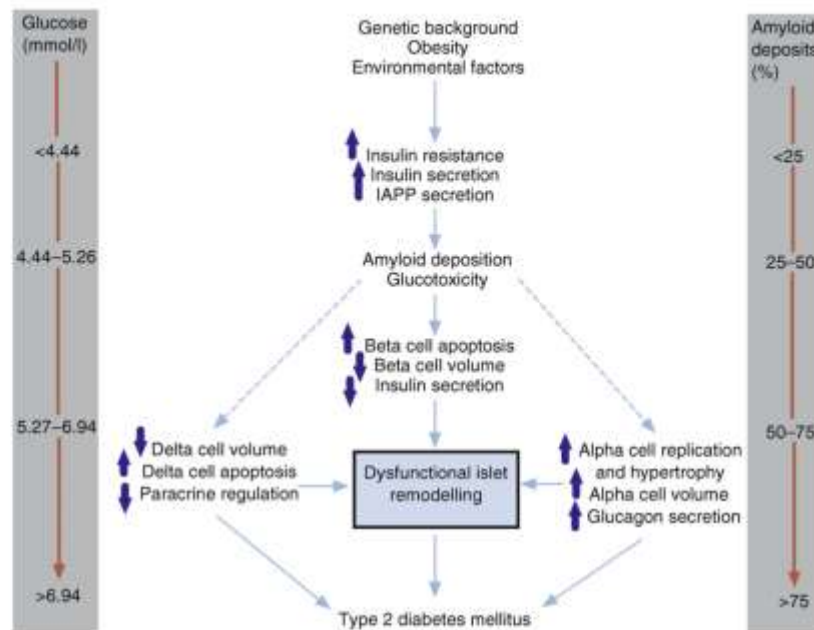
It has been suggested that metabolic stress and type 2 diabetes in mice can result in beta cell dedifferentiation into a progenitor-like stage followed by the conversion of a subpopulation of dedifferentiated beta cells into alpha cells [45]. Similar results have been shown in primary human beta cells that, when incubated *in vitro* under conditions of stress, lose insulin granules and transdifferentiate into alpha cells [46].

There is little information about delta cell fate in diabetes, but previous studies reported increased delta cell volumes in type 1 diabetes [47] as well as in type 2 diabetes [19] and in

diabetes associated with cystic fibrosis [43]. Delta cell expansion has been interpreted as a compensatory adaptation to hyperglucagonaemia. These studies, however, have the limitation of being performed on a small number of subjects and in the presence of severe beta cell depletion, so that apparent delta cell hyperplasia might be relative to beta cell loss rather than absolute.

Furthermore, together with the evidence of reduced delta cell volumes, we here provide for the first time the direct evidence of ongoing delta cell death in type 2 diabetes. Confocal microscopy examination of control (G1) and G4 pancreatic tissues triple-stained for insulin, somatostatin and TUNEL showed that apoptotic delta cells were absent in pancreases from G1 baboons but present in those from G4 baboons (Fig. 5). Electron microscopy and immune-electron

**Fig. 9** Proposed dysfunctional islet remodelling in the natural history of type 2 diabetes. As glucose levels and amyloid deposits progressively increase, different anatomical and physiological changes occur in beta, alpha and delta cells leading to a dysfunctional islet remodelling and progression to type 2 diabetes, IAPP, islet amyloid polypeptide



microscopy analysis of G4 baboon pancreases showed somatostatin-positive delta cells with ultrastructural degenerative features and fragmented pycnotic nuclei (Fig. 6 and ESM Fig. 5). Moreover, double immunohistochemical and triple immunofluorescence studies showed co-localisation of somatostatin and the apoptotic markers M30 and CC-3 in islet delta cells of diabetic baboons (ESM Figs 2, 3). The evidence that amyloid severity is inversely correlated to delta cell volumes (Fig. 2d) may suggest that delta cells, like beta cells, are also sensitive to amyloid toxicity. In contrast to beta cell volume (Fig. 3a), delta cell volume did not show a clear negative correlation with FPG (Fig. 4b). Nevertheless, similarly to beta cell volume, delta cell volume correlated inversely with NEFA levels (Figs 3b and 4c). Thus, delta cells appear resistant to glucose-toxicity but sensitive to lipotoxicity [48]. In spite of a slightly different sensitivity to hyperglycaemia, amyloid and NEFA, beta and delta cells share a common fate as their volumes are positively correlated with each other (Fig. 4d). Owing to the known negative paracrine effect of somatostatin on alpha cell secretion, loss of delta cells (in concert with the relative or absolute increase in alpha cell volume) can also play a role in insulin and glucagon secretory changes associated with type 2 diabetes. This possibility is supported by evidence that fasting glucagon concentrations are inversely correlated to delta cell volume (ESM Fig. 1c). Finally, a decrease in delta cell number (considering the negative paracrine effect of somatostatin on insulin secretion) could be viewed as a compensatory adaptation in a situation of beta cell deficiency.

We would like to propose that as glucose and amyloid increase within the islet, dysfunctional islet remodelling occurs that involves not only beta and alpha cells, but also delta cells (Fig. 9).

In conclusion, additional studies should be carried out to confirm the loss of delta cells in human type 2 diabetes and to explore the molecular mechanisms involved, and to investigate novel therapeutic options directed at preserving not only beta cells, but also delta cells.

**Acknowledgements** We thank M. Silva for pathology support and expert assistance in tissue processing (Texas Biomedical Research Institute, San Antonio, Texas, TX, USA). We also thank P. Zuo for performing insulin and glucagon RIA and NEFA determinations. Portions of this work were presented in abstract form at the 2014 Endocrine Society Meeting, Chicago, IL, USA. This work is dedicated to the memory of my beloved nephew Matteo Folli (17 April 1995–2 April 2015), who left us in the prime time of his life.

**Funding** This research was supported in part by NIH-NCRR grant P51 RR013986 to the Southwest National Primate Research Center and conducted in facilities constructed with support from Research Facilities Improvement Program Grant C06 RR014578 and C06 RR015456. FF was partially supported by NIH RO1 DK080148. FF is a visiting professor in the Department of Medicine and the Obesity and Comorbidities Research Center (OCRC), University of Campinas, Campinas, São Paulo State, Brazil, and is supported by FAPESP and CNPq, Brazil. He is on sabbatical leave from the University of Texas Health Science Center at San Antonio, TX, USA. LAV and MJAS are supported by OCRC and FAPESP, Brazil.

**Duality of interest** The authors declare that there is no duality of interest associated with this manuscript.

**Contribution statement** FF is responsible for the integrity of the study and conceived the study. RGM and FF performed experiments and generated, analysed and interpreted the data, wrote the manuscript and reviewed the final version of the manuscript. CP, GF, SL, CC, FS and SM performed experiments, analysed and interpreted the data, wrote the manuscript and contributed to the discussion and the final review of the

manuscript. LMJC performed data quantification, analysed and interpreted the data and critically revised the manuscript for important intellectual content. LAV, MJAS and FB analysed and interpreted the data and critically revised the manuscript for important intellectual content. EJD and AD performed experiments, analysed and interpreted the data, wrote the manuscript, contributed to the discussion and reviewed the final version of the manuscript. All authors gave final approval of the version of the manuscript to be published.

## References

- Gannon M, Ray MK, van Zee K, Rausa F, Costa RH, Wright CV (2000) Persistent expression of HNF6 in islet endocrine cells causes disrupted islet architecture and loss of beta cell function. *Development* 127:2883–2895
- Orci L, Unger RH (1975) Functional subdivision of islets of Langerhans and possible role of D cells. *Lancet* 2:1243–1244
- Samols E, Stagner JJ (1990) Islet somatostatin—microvascular, paracrine, and pulsatile regulation. *Metabolism* 39:55–60
- Unger RH, Orci L (2010) Paracrinology of islets and the paracrinopathy of diabetes. *Proc Natl Acad Sci U S A* 107:16009–16012
- Gromada J, Franklin I, Wollheim CB (2007) Alpha-cells of the endocrine pancreas: 35 years of research but the enigma remains. *Endocr Rev* 28:84–116
- Bonner-Weir S, Orci L (1982) New perspectives on the microvasculature of the islets of Langerhans in the rat. *Diabetes* 31:883–889
- Unger RH, Orci L (1977) Possible roles of the pancreatic D-cell in the normal and diabetic states. *Diabetes* 26:241–244
- Bonner-Weir S, O'Brien TD (2008) Islets in type 2 diabetes: in honor of Dr. Robert C. Turner. *Diabetes* 57:2899–2904
- Bosco D, Armanet M, Morel P et al (2010) Unique arrangement of alpha- and beta-cells in human islets of Langerhans. *Diabetes* 59:1202–1210
- Cabrera O, Berman DM, Kenyon NS, Ricordi C, Berggren PO, Caicedo A (2006) The unique cytoarchitecture of human pancreatic islets has implications for islet cell function. *Proc Natl Acad Sci U S A* 103:2334–2339
- Quinn AR, Blanco CL, Perego C et al (2012) The ontogeny of the endocrine pancreas in the fetal/newborn baboon. *J Endocrinol* 214:289–299
- Orci L (1982) Macro- and micro-domains in the endocrine pancreas. *Diabetes* 31:538–565
- Clark A, Wells CA, Buley ID et al (1988) Islet amyloid, increased A-cells, reduced B cells and exocrine fibrosis: quantitative changes in the pancreas in type 2 diabetes. *Diabetes Res* 9:151–159
- Yoon KH, Ko SH, Cho JH et al (2003) Selective beta-cell loss and alpha-cell expansion in patients with type 2 diabetes mellitus in Korea. *J Clin Endocrinol Metab* 88:2300–2308
- Sakuraba H, Mizukami H, Yagihashi N, Wada R, Hanyu C, Yagihashi S (2002) Reduced beta-cell mass and expression of oxidative stress-related DNA damage in the islet of Japanese type II diabetic patients. *Diabetologia* 45:85–96
- Butler AE, Janson J, Bonner-Weir S, Ritzel R, Rizza RA, Butler PC (2003) Beta-cell deficit and increased beta-cell apoptosis in humans with type 2 diabetes. *Diabetes* 52:102–110
- Folli F, Okada T, Perego C et al (2011) Altered insulin receptor signalling and beta-cell cycle dynamics in type 2 diabetes mellitus. *PLoS One* 6, e28050
- Dunning BE, Gerich JE (2007) The role of alpha-cell dysregulation in fasting and postprandial hyperglycemia in type 2 diabetes and therapeutic implications. *Endocr Rev* 28:253–283
- Iki K, Pour PM (2007) Distribution of pancreatic endocrine cells including IAPP-expressing cells in non-diabetic and type 2 diabetic cases. *J Histochem Cytochem* 55:111–118
- Unger RH, Dobbs RE, Orci L (1978) Insulin, glucagon, and somatostatin secretion in the regulation of metabolism. *Annu Rev Physiol* 40:307–343
- Ludvigsen E, Olsson R, Stridsberg M, Janson ET, Sandler S (2004) Expression and distribution of somatostatin receptor subtypes in the pancreatic islets of mice and rats. *J Histochem Cytochem* 52:391–400
- Hauge-Evans AC, King AJ, Carnignac D et al (2009) Somatostatin secreted by islet delta-cells fulfills multiple roles as a paracrine regulator of islet function. *Diabetes* 58:403–411
- Patel YC, Pierzchala I, Amherdt M, Orci L (1985) Effects of cysteamine and antibody to somatostatin on islet cell function in vitro. Evidence that intracellular somatostatin deficiency augments insulin and glucagon secretion. *J Clin Invest* 75:1249–1255
- D'Alessio DA, Fujimoto WY, Ensink JW (1989) Effects of glucagonlike peptide 1-(7-36) on release of insulin, glucagon, and somatostatin by rat pancreatic islet cell monolayer cultures. *Diabetes* 38:1534–1538
- Guenifi A, Ahren B, Abdel-Halim SM (2001) Differential effects of glucagon-like peptide-1 (7-36)amide versus cholecystokinin on arginine-induced islet hormone release in vivo and in vitro. *Pancreas* 22:58–64
- Heller RS, Aponte GW (1995) Intra-islet regulation of hormone secretion by glucagon-like peptide-1-(7–36) amide. *Am J Physiol* 269:G852–G860
- Silvestre RA, Rodriguez-Gallardo J, Egado EM, Marco J (2003) Interrelationship among insulin, glucagon and somatostatin secretory responses to exendin-4 in the perfused rat pancreas. *Eur J Pharmacol* 469:195–200
- Vieira E, Salehi A, Gylfe E (2007) Glucose inhibits glucagon secretion by a direct effect on mouse pancreatic alpha cells. *Diabetologia* 50:370–379
- Chavez AO, Gastaldelli A, Guardado-Mendoza R et al (2009) Predictive models of insulin resistance derived from simple morphometric and biochemical indices related to obesity and the metabolic syndrome in baboons. *Cardiovasc Diabetol* 8:22
- Chavez AO, Lopez-Alvarenga JC, Tejero ME et al (2008) Physiological and molecular determinants of insulin action in the baboon. *Diabetes* 57:899–908
- Guardado-Mendoza R, Davalli AM, Chavez AO et al (2009) Pancreatic islet amyloidosis, beta-cell apoptosis, and alpha-cell proliferation are determinants of islet remodeling in type-2 diabetic baboons. *Proc Natl Acad Sci U S A* 106:13992–13997
- Kamath S, Chavez AO, Gastaldelli A et al (2011) Coordinated defects in hepatic long chain fatty acid metabolism and triglyceride accumulation contribute to insulin resistance in non-human primates. *PLoS One* 6, e27617
- Guardado-Mendoza R, Jimenez-Ceja L, Majluf-Cruz A et al (2013) Impact of obesity severity and duration on pancreatic beta- and alpha-cell dynamics in normoglycemic non-human primates. *Int J Obes (Lond)* 37:1071–1078
- Freere RH, Weibel ER (1967) Stereologic techniques in microscopy. *J R Microsc Soc* 87:25–34
- Mandarim-de-Lacerda CA (2003) Stereological tools in biomedical research. *An Acad Bras Cienc* 75:469–486
- Matthews DR, Hosker JP, Rudenski AS, Naylor BA, Treacher DF, Turner RC (1985) Homeostasis model assessment: insulin resistance and beta-cell function from fasting plasma glucose and insulin concentrations in man. *Diabetologia* 28:412–419
- Lupi R, del Prato S (2008) Beta-cell apoptosis in type 2 diabetes: quantitative and functional consequences. *Diabetes Metab* 34(Suppl 2):S56–S64

38. Jurgens CA, Toukatly MN, Fligner CL et al (2011) Beta-cell loss and beta-cell apoptosis in human type 2 diabetes are related to islet amyloid deposition. *Am J Pathol* 178:2632–2640
39. Westermark GT, Westermark P (2013) Islet amyloid polypeptide and diabetes. *Curr Protein Pept Sci* 14:330–337
40. Di Cairano ES, Davalli AM, Perego L et al (2011) The glial glutamate transporter 1 (GLT1) is expressed by pancreatic beta-cells and prevents glutamate-induced beta-cell death. *J Biol Chem* 286:14007–14018
41. Federici M, Hribal M, Perego L et al (2001) High glucose causes apoptosis in cultured human pancreatic islets of Langerhans: a potential role for regulation of specific Bcl family genes toward an apoptotic cell death program. *Diabetes* 50:1290–1301
42. Fontes G, Zarrouki B, Hagman DK et al (2010) Glucolipotoxicity age-dependently impairs beta cell function in rats despite a marked increase in beta cell mass. *Diabetologia* 53:2369–2379
43. Soejima K, Landing BH (1986) Pancreatic islets in older patients with cystic fibrosis with and without diabetes mellitus: morphometric and immunocytologic studies. *Pediatr Pathol* 6:25–46
44. Menge BA, Gruber L, Jorgensen SM et al (2011) Loss of inverse relationship between pulsatile insulin and glucagon secretion in patients with type 2 diabetes. *Diabetes* 60:2160–2168
45. Talchai C, Xuan S, Lin HV, Sussel L, Accili D (2012) Pancreatic beta cell dedifferentiation as a mechanism of diabetic beta cell failure. *Cell* 150:1223–1234
46. Spijker HS, Ravelli RB, Mommaas-Kienhuis AM et al (2013) Conversion of mature human beta-cells into glucagon-producing alpha-cells. *Diabetes* 62:2471–2480
47. Orci L, Baetens D, Rufener C et al (1976) Hypertrophy and hyperplasia of somatostatin-containing D-cells in diabetes. *Proc Natl Acad Sci U S A* 73:1338–1342
48. Collins SC, Salehi A, Eliasson L, Olofsson CS, Rorsman P (2008) Long-term exposure of mouse pancreatic islets to oleate or palmitate results in reduced glucose-induced somatostatin and oversecretion of glucagon. *Diabetologia* 51:1689–1693

## 2) TIRFM e GFP-sonde pH-sensative to evaluate Neurotransmitter Vesicle Dynamics in SH-SY5Y Neuroblastoma cells: cell imaging and data analysis

Published on Jove, January 2015

### AIM and INTRODUCTION

This article purpose was to optimize a TIRF microscopy protocol for vesicles dynamic evaluation and analysis. The protocol was initially thought to study the mechanisms of neurotransmitters release from neuroblastoma cells but can be applied to all the membrane trafficking mechanisms that provide the fusion of intracellular vesicles with the cell surface, such as for example the study of constitutive membrane trafficking and release of pancreatic hormones.

Genetic studies have provide many evidences of the proteins involved in vesicle dynamics however their specific contribution to the phenomenon remains to be clarified (Sudhof 2004). Our understanding of synaptic proteins involvement in exocytosis, endocytosis and recycling is limited by the fact that the most extensively used assays for exo/endocytosis are not always the most appropriate. Numerous studies related to vesicle fusion and dynamics rely on electrophysiological techniques. This approach provides an optimal temporal resolution and is excellent for investigating the initial fusion of vesicles to the plasma membrane but is unable to detect many of the underlying molecular events. Electron microscopy, on the other side, provides the optimal morphological description of each singular step, but the dynamic aspect of the event cannot be captured, because samples must be fixed before the analysis. The advent of new optical recording techniques (Denk and Svoboda 1997; Helmchen et al., 1999), in association with advances in fluorescent molecular probes development (Tsien,1998; Matz et al., 1999; Ribchester et al., 1994), enables the visualization of exocytic processes *in live* cells, thus providing new levels of information about the synaptic structure and function.

In this context the optical technique that provides the necessary spatio-temporal resolution to follow vesicle dynamics at the plasma membrane is total internal reflection fluorescence microscopy (TIRFM), an application of fluorescence microscopy.

Total internal reflection occurs at the interface between the glass cover-slip and the sample. When the light path reaches the glass cover-slip with an incident angle larger than the critical angle, the excitation light is not transmitted into the sample but is completely reflected back. Under these conditions, an evanescent light wave forms at the interface and propagates in the medium with less optical density (the sample). As the intensity of the evanescent field decays exponentially with distance from the interface (with a penetration depth of about

100 nm) only the fluorophores in closest proximity to the cover-slip can be excited while those further away from the boundary are not. In cells transfected with GFP-constructs, this depth corresponds to proteins expressed on the plasma membrane or in vesicular structures approaching it. As fluorophores in the cell interior cannot be excited, the background fluorescence is minimized, and an image with a very high signal/background ratio is formed (Sankaranarayanan et al., 2000).

Several characteristics make TIRFM the technique of choice for monitoring vesicles dynamics. The perfect contrast and the high signal-to-noise-ratio allow the detection of very low signals deriving from single vesicles. Chip-based image acquisition in each frame provides the temporal resolution necessary to detect highly dynamic processes. Finally, the minimal exposure of cells to light at any other plane in the sample strongly reduces phototoxicity and enables long lasting time-lapse recording (Mattheyses et al., 2010).

## **METHODS**

The method requires the growth of cell, like SH-SY5Y, as adherent cells; the transfection of them with specific probes, such the synapto-pHluorin, and the TIRFM technique.

*The Cells.* The SH-SY5Y human neuroblastoma cells were proposed as a valuable model for studying neurotransmitter release at the single-vesicle level by TIRFM, because they are sufficiently flat to allow stable visualization of membranes and fusion events in TIRFM mode (particularly in the cell body) and vesicles are relatively dispersed. Additionally this type of cells are easy to handle, to maintain in culture and to transfect with the constructs of interest and are therefore a good starting point for the optimization of this type of analysis. In the protocol we suggest the PEI, which is the basis of most commercially available transfection agents and alone acts as a very low cost effective transfection vector.

*Probes.* In cells transfected with GFP-constructs, the TIRF procedure can reveal the dynamics of proteins expressed at the plasma membrane or in vesicular structures approaching it. The advanced application of this technique is the use of pH-sensitive variants of the Green Fluorescent Protein (GFP) (pHluorin) tethered to luminal vesicles proteins (Miesenböck et al., 1998). These probes are normally switched off when present in the vesicles, because of the low luminal pH. After fusion with the plasma membrane, the vesicle interior is exposed to the neutral extracellular space, the pH abruptly increases, relieves the proton-dependent quenching of pHluorin and the fluorescent signal rapidly appears. As the change in pHluorin is faster than the fusion event, by monitoring fluorescence increases, vesicle fusion with the membrane can be measured and analyzed. Because surface pHluorin-tagged molecules are endocytosed, the fluorescence signal subsequently returns to

basal level, therefore the same construct may be used also to monitor vesicle recycling (Miesenböck et al., 1998).

In this work I have contributed to the samples preparation (cell culture and transfection), in video acquisition by TIRF microscopy, and together with my lab team and my tutor, Carla Perego, in the development of a *macro* for data analysis.

## **CONCLUSION AND DISCUSSION**

This paper presents a protocol to image and analyze vesicles dynamics in secreting cells, using fluorescent cDNA-encoded vectors and TIRFM. Vesicles should ideally be dispersed in the cell so that their trafficking, fusion and endocytosis can be imaged and quantified at single-vesicle level. TIRFM facilitates the collection of information regarding processes that occur at or near the membrane in living cells and enables the analysis of individual molecular events through detection of changes in the fluorescent signal derived from tagged proteins that move in or out the evanescent field.

This technique can be used in different cell types (neurons and endocrine cells) to visualize and dissect the various steps of exo/endocytosis, to reveal the role of proteins and their pathogenic mutants in the regulation of vesicle dynamics and to uncover the mechanisms of action of drugs targeting constitutive and regulated exocytosis.

## Video Article

**TIRFM and pH-Sensitive GFP-Probes to Evaluate Neurotransmitter Vesicle Dynamics in SH-SY5Y Neuroblastoma Cells: Cell Imaging and Data Analysis**Federica Daniele<sup>1</sup>, Eliana S. Di Cairano<sup>1</sup>, Stefania Moretti<sup>1</sup>, Giovanni Piccoli<sup>2</sup>, Carla Perego<sup>1,3</sup><sup>1</sup>Department of Pharmacological and Biomolecular Sciences, Università degli Studi di Milano<sup>2</sup>San Raffaele Scientific Institute and Vita-Salute University<sup>3</sup>CEND Center of Excellence in Neurodegenerative diseases, Università degli Studi di MilanoCorrespondence to: Carla Perego at [carla.perego@unimi.it](mailto:carla.perego@unimi.it)URL: <http://www.jove.com/video/52267>DOI: [doi:10.3791/52267](https://doi.org/10.3791/52267)

Keywords: Synaptic vesicles, neurotransmission, Total Internal Reflection Fluorescence Microscopy, pHluorin, neuroblastoma cells

Date Published: 11/30/2014

Citation: Daniele, F., Di Cairano, E.S., Moretti, S., Piccoli, G., Perego, C. TIRFM and pH-Sensitive GFP-Probes to Evaluate Neurotransmitter Vesicle Dynamics in SH-SY5Y Neuroblastoma Cells: Cell Imaging and Data Analysis. *J. Vis. Exp.* (), e52267, doi:10.3791/52267 (2014).**Abstract**

Synaptic vesicles release neurotransmitters at chemical synapses through a dynamic cycle of fusion and retrieval. Monitoring synaptic activity in *real time* and dissecting the different steps of exo-endocytosis at the single-vesicle level are crucial for understanding synaptic functions in health and disease.

Genetically-encoded pH-sensitive probes directly targeted to synaptic vesicles and Total Internal Reflection Fluorescence Microscopy (TIRFM) provide the spatio-temporal resolution necessary to follow vesicle dynamics. The evanescent field generated by total internal reflection can only excite fluorophores placed in a thin layer (<150 nm) above the glass cover on which cells adhere, exactly where the processes of exo-endocytosis take place. The resulting high-contrast images are ideally suited for vesicle tracking and quantitative analysis of fusion events.

In this protocol, SH-SY5Y human neuroblastoma cells are proposed as a valuable model for studying neurotransmitter release at the single-vesicle level by TIRFM, because of their flat surface and the presence of dispersed vesicles. The methods for growing SH-SY5Y as adherent cells and for transfecting them with synapto-pHluorin are provided, as well as how to perform TIRFM and imaging. Finally, a strategy aiming to select, count, and analyze fusion events at whole-cell and single-vesicle levels is presented.

To validate the imaging procedure and data analysis approach, the dynamics of pHluorin-tagged vesicles have been analyzed under resting and stimulated (depolarizing potassium concentrations) conditions. Membrane depolarization increases the frequency of fusion events and causes a parallel raise of the net fluorescence signal recorded in whole cell. Single-vesicle analysis reveals modifications of fusion-event behavior (increased peak height and width). These data suggest that potassium depolarization not only induces a massive neurotransmitter release but also modifies the mechanism of vesicle fusion and recycling.

With the appropriate fluorescent probe, this technique can be employed in different cellular systems to dissect the mechanisms of constitutive and stimulated secretion.

**Video Link**

The video component of this article can be found at <http://www.jove.com/video/52267/>

**Introduction**

Chemical synaptic transmission between neurons is a major mechanism of communication in the nervous system. It relies on the release of neurotransmitters through a dynamic cycle of vesicle fusion and retrieval at the presynaptic site. Many of the proteins involved in vesicle dynamics have been identified; however, their specific contribution to the phenomenon remains to be clarified<sup>1</sup>.

Our understanding is partly limited by the fact that the most widely used assays for exo/endocytosis are not always the most appropriate. Several studies related to vesicle fusion and dynamics rely on electrophysiological techniques. This technique provides an optimal temporal resolution and is excellent for investigating the initial fusion of vesicles to the plasma membrane but is unable to detect many of the underlying molecular events that support presynaptic function. Electron microscopy, on the other side, provides the finest morphological description of each singular step, but the dynamic aspect of the event cannot be captured, because samples must be fixed in order to be analyzed.

The advent of new optical recording techniques<sup>2,3</sup>, in combination with advances in fluorescent molecular probes development<sup>4-6</sup>, enable the visualization of exocytic processes in *live* cells, thus providing new levels of information about the synaptic structure and function.

Initial studies exploited activity-dependent styryl dyes (FM1-43 and related organic dyes)<sup>7,8</sup>. State-of-the-art imaging techniques employ pH-sensitive variants of the Green Fluorescent Protein (GFP) (pHluorin) tethered to luminal vesicles proteins<sup>9</sup>. These probes are normally switched off when present in the vesicles because of the low luminal pH. After fusion with the plasma membrane, the vesicle interior is exposed to the

neutral extracellular space, the pH abruptly increases, relieves the proton-dependent quenching of pHluorin and the fluorescent signal rapidly appears. As the change in pHluorin is faster than the fusion event, by monitoring fluorescence increases, vesicle fusion with the membrane can be measured and analyzed. Because surface pHluorin-tagged molecules are endocytosed, the fluorescence signal subsequently returns to basal level, therefore the same construct may be used also to monitor vesicle recycling<sup>9</sup>.

While the vesicle-tagged pH-sensor ensures the visualization only of those vesicles that really fuse with the plasma membrane, imaging at high spatial and temporal resolution is required to describe in details the steps involved in the exo/endocytosis processes. The optical technique that provides the necessary spatio-temporal resolution is total internal reflection fluorescence microscopy (TIRFM), an application of fluorescence microscopy.

Total internal reflection occurs at the interface between the glass cover-slip and the sample. When the light path reaches the glass cover-slip with an incident angle larger than the critical angle, the excitation light is not transmitted into the sample but is completely reflected back. Under these conditions, an evanescent light wave forms at the interface and propagates in the medium with less optical density (the sample). As the intensity of the evanescent field decays exponentially with distance from the interface (with a penetration depth of about 100 nm) only the fluorophores in closest proximity to the cover-slip can be excited while those further away from the boundary are not. In cells transfected with GFP-constructs, this depth corresponds to proteins expressed on the plasma membrane or in vesicular structures approaching it. As fluorophores in the cell interior cannot be excited, the background fluorescence is minimized, and an image with a very high signal/background ratio is formed<sup>11</sup>.

Several characteristics make TIRFM the technique of choice for monitoring vesicles dynamics. The perfect contrast and the high signal-to-noise-ratio allow the detection of very low signals deriving from single vesicles. Chip-based image acquisition in each frame provides the temporal resolution necessary to detect highly dynamic processes. Finally, the minimal exposure of cells to light at any other plane in the sample strongly reduces phototoxicity and enables long lasting time-lapse recording<sup>12</sup>.

Data analysis remains the most challenging and crucial aspect of this technique. The simplest way to monitor vesicle fusion is to measure the accumulation of reporter fluorescent proteins at the cell surface, over time<sup>13</sup>. As fusion increases, net fluorescence signal increases as well. However, this method may underestimate the process, particularly in large cells and in resting conditions, because endocytosis and photobleaching processes offset the increase in fluorescence intensity due to vesicle exocytosis. An alternative method is to follow each single fusion event<sup>14</sup>. This latter method is very sensitive and can reveal important details about the fusion mechanisms. However, it requires the manual selection of single events, because completely automated procedures to follow vesicles and to register the fluctuation of their fluorescent signals are not always available. Observation of vesicle dynamics requires sampling cells at high frequency. This generates a large amount of data that can hardly be analyzed manually.

The proposal of this paper is to optimize the TIRFM imaging technique for monitoring the basal and stimulated neurotransmitter release in the SH-SY5Y neuroblastoma cell line, and to describe, step-by-step, a procedure developed in the laboratory to analyze data, both at whole-cell and single-vesicle levels.

## Protocol

### 1. Cell Culture and Transfection

#### 1. SH-SY5Y cell culture

NOTE: The experiments have been performed using the human neuroblastoma SH-SY5Y (ATCC# CRL-2266)<sup>15</sup>. SH-SY5Y cells grow as a mixture of floating clusters and adherent cells. Follow the instructions reported in the protocol (cell density, splitting ratio, etc.) to have cells that grow firmly attached to glass cover, which is crucial for TIRFM.

- Before starting, under the laminar flow biosafety cabinet, make the opportune volume of sterile phosphate buffer saline solution (PBS) and culture medium.
  - Make 50 ml of PBS with concentrations of 150 mM NaCl, 24 mM phosphate buffer, pH 7.4. Filter the solution.
  - Make 50 ml of cell medium from Dulbecco's modified Eagle medium (DMEM) with high glucose, 10% heat-inactivated fetal bovine serum (FBS), penicillin (100 U/ml), streptomycin (100 µg/ml), L-glutamine (2 mM), and sodium pyruvate (1 mM). Filter the solution.
- Remove complete growth medium and wash the cells with 3 ml of PBS.
- Incubate cells with 2 ml of 0.05% trypsin-ethylenediaminetetraacetic acid (EDTA) (for 6 cm Petri dish) for 5 min at 37 °C, 5% CO<sub>2</sub> and detach cells using pipette.
- Inactivate trypsin by adding 2 ml of DMEM, and collect cells by centrifugation at 300 x g for 5 min.
- Remove the supernatant, add 1 ml of DMEM to the pellet and pipette the solution up and down sufficiently to disperse cells into a single cell suspension.
- Split them 1:4 in a new 6 cm diameter Petri dish containing 3 ml of complete medium. Maintain cells in culture in 6 cm diameter Petri dishes, at 37 °C in a 5% CO<sub>2</sub> incubator. Sub-culture once a week or when they have covered 80 - 90% of the surface area.

#### 2. SH-SY5Y cell plating for imaging

- For TIRFM experiments, plate cells onto glass covers. Employ glass covers with 0.17 ± 0.005 mm thickness and a 1.5255 ± 0.00015 refractive index. Before starting, prepare the glass coverslips as follow:
  - Clean glass covers with 90% ethanol, overnight.
  - Rinse them thoroughly in distilled water (three changes of distilled water). Dry glass covers in a drying oven.
  - Place covers in glass Petri dishes and sterilize in a preheated oven at 200 °C for 3 hr.
- The day before transfection, place each coverslip in a 3.5 cm Petri dish, add 1 ml of culture medium and incubate at 37 °C in a 5% CO<sub>2</sub> incubator.

3. Trypsinize cells as described in **steps 1.1.3 - 1.1.5**, suspend the cell pellet in 1 ml of complete medium and count. Calculate the correct volume of cell suspension to add to each Petri dish to yield  $3 \times 10^5$  cells/well. This density is required for optimal cell growth and efficient transfection. Incubate at 37 °C in a 5% CO<sub>2</sub> incubator overnight.
- 3. SH-SY5Ytransfection by polyethylenimine (PEI)**
- NOTE: To visualize synaptic vesicles dynamics, pCB6 vector containing synapto-pHluorin has been used. The synapto-pHluorin has been generated by in frame fusion of a pH-sensitive variant of the green fluorescent protein (GFP)<sup>16</sup> and the vesicular membrane protein synaptobrevin 2. The construct has been extensively employed to investigate synaptic vesicle properties within neurons<sup>9</sup>.
1. Before starting transfection, make 10 ml of the following solutions. Keep the solutions as maximal as 1 month.
    1. Make a 150 mM NaCl solution. Adjust to pH 5.5 with 0.01 N HCl.
    2. Make a PEI solution at 10% polyethylenimine (PEI; 25 kDa linear) in 150 mM NaCl solution. The pH of solution rises to 8.8. Adjust pH to 7.8 with 0.01 N HCl.
  2. 24 hr after plating, remove the medium and refresh with 1.5 ml of complete medium. Keep the cells at 37 °C, in a 5% CO<sub>2</sub> incubator.
  3. Under the laminar flow biosafety cabinet, in a 1.5 ml microfuge tube, add 3 µg of plasmid DNA to 25 µl of 150 mM NaCl solution and 100 µl of PEI solution per 3.5 cm Petri dish.
  4. Vortex for 10 sec, then incubate the DNA/PEI mixture for 30 min at room temperature.
  5. Carefully add the DNA/PEI mixture to the Petri dish containing coverslips with cells and gently shake to equally distribute the reagent in the Petri dish.
  6. After 4 hr change the medium and incubate the cells overnight at 37 °C in a 5% CO<sub>2</sub> incubator. Perform imaging experiments 24 - 48 hr after transfection.

## 2. Cell Imaging by Total Internal Reflection Fluorescence Microscopy (TIRFM)

1. **Imaging set-up**
  1. Perform TIRF imaging with the set-up described in **Figure 1**. It comprises a motorized inverted microscope (**Figure 1, inset A**), the laser source (**Figure 1, inset B**) and the TIRF-slider (**Figure 1, inset C**). Reach TIRFM illumination through a high numerical aperture (NA 1.45 Alpha Plan-Fluar) 100X oil, immersion objective.
  2. For TIRFM illumination, employ a multi-line (458/488/514 nm) 100 mW argon-ion laser. Using a mono mode fiber, introduce the linearly polarized laser light into the beam path, via the TIRF slider. Insert the TIRF slider into the luminous field diaphragm plane of the reflected-light beam path.
    1. For wide field illumination, connect the microscope to a conventional mercury short-arc lamp HBO white light. A polarization-maintaining double prism in the slider ensures the simultaneous combination of TIRF illumination and white light.
  3. Filter the laser light with an excitation filter (band width 488/10 nm) mounted on a filter wheel, introduced into the laser path. Employ a high speed, software-controlled, shutter to allow fast control of laser illumination. For pHluorin analysis, mount a band pass 525/50 nm emission filter. Capture digital images (512 x 512 pixels) on a cooled Fast CCD camera with the Image ProPlus software.
2. **Achieving TIRF illumination (Figure 2)**
  1. Turn on the lasers, the computer, the camera, the filter wheel, and the shutter controllers; then, wait 20 min before starting the experiment as the lasers need to warm up and stabilize.
  2. Before imaging, make the opportune volume of the following solutions.
    1. Make 50 ml of Krebs (KRH) solution at 125 mM NaCl, 5 mM KCl, 1.2 mM MgSO<sub>4</sub>, 1.2 mM KH<sub>2</sub>PO<sub>4</sub>, 25 mM 4-(2-Hydroxyethyl)piperazine-1-ethanesulfonic acid (HEPES) (buffered to pH 7.4), 2 mM CaCl<sub>2</sub>, and 6 mM glucose.
    2. Make 10 ml of KCl-KRH solution (pH 7.4) at 80 mM NaCl, 50 mM KCl, 1.2 mM MgSO<sub>4</sub>, 1.2 mM KH<sub>2</sub>PO<sub>4</sub>, 25 mM HEPES (buffered to pH 7.4), 2 mM CaCl<sub>2</sub>, and 6 mM glucose.
  3. Remove the glass cover with transfected cells and insert it in the appropriate imaging chamber. Assemble the chamber and add 500 µl of KRH solution in the center of the glass.
  4. Add oil over the objective. Place the imaging chamber on the stage of the microscope and position the objective under the glass coverslip. Position the safe cover over the sample.
  5. In epifluorescence mode, focus on the coverslip (upper surface) and choose transfected cells placed in the chamber center. Select cells whose fluorescent signal can be clearly recorded using an exposure time below 80 msec.
  6. Under software control, switch to TIRF illumination *in live* mode.
  7. To set the TIRF configuration, check the position of beam that emerges out of the objective, on the sample cover (**Figure 2B**). When the beam is positioned in the center of the objective lens (**Figure 2A, left**), a spot is visible in the center of the TIRF sample cover (**Figure 2B, left**) and the cell is imaged in epifluorescence mode (several focus planes, high background fluorescence; **Figure 2C, left**).
  8. To reach the critical angle, move the focused spot in the Y direction (forward or backward; **Figure 2B, center**) using the angle adjustment screw on the TIRF slider (**Figure 1, C**). When the beam converges on the sample plane at an angle larger than the critical angle (**Figure 2A, right**), the spot disappears and a straight, thin, focused line is evident in the middle of the sample cover (**Figure 2B, right**).
  9. To fine-tune the TIRF angle use the cell sample (**Figure 2C**). Watch the fluorescence image on the video, at this stage, an epifluorescence-like image is still visible. Gently, move the screw until TIRF condition is achieved: only one optical plane of the cell is in focus (*i.e.*, the plasma membrane in contact with the cover-slip), this results in a flat image with high contrast (**Figure 2C, right**).
3. **Sample imaging**

1. Set the single-channel time-lapse experiment. To minimize photobleaching, capture the image using low exposure time and high gain. Appropriate exposure times are between 40 - 80 msec. Acquire images at 1 - 2 Hz sampling frequency. Vesicle kinetics may be better appreciated sampling at higher frequency (10 Hz). The regular time of observation is usually 2 min.
2. Add 500  $\mu$ l of KRH solution and record cells in TIRFM mode. This is the resting condition. Save the time sequential images.
3. Focus on the same cell and record under the same conditions of resting (laser power, time exposure, frame number). After five frames, add 500  $\mu$ l of KCl-KRH solution and keep KCl in the chamber. This is the stimulated condition; save the time sequential images.

### 3. Image Analysis and Data Processing

NOTE: To analyze images, macros have been developed in the lab, based on existing functions of the image analysis software; similar macros are available online (URL provided in **Table of Materials and Equipment**).

1. **Fluorescence intensity quantification**
  1. Use a "Sequence fluorescence intensity" macro for fluorescence intensity quantification in a region of interest (ROI) of the image, over the course of the movie.
  2. Open the time-sequential images. Go to the macro menu and select 'Sequence fluorescence intensity'. In the 'Analysis' window appears "select the ROI".
  3. Choose one of the selection tools in the menu to create the ROI. Place 3 ROIs in regions of the cell membrane without spots (background ROI). Employ this "background ROI" to evaluate the photobleaching and to set the threshold for fusion event analysis (**Figure 3A**).
2. **Photobleaching correction and threshold determination (Figure 3B)**
  1. To evaluate the photobleaching, open the fluorescence intensity rows "background ROIs", (**Figure 3Ba**). Normalize the fluorescence intensity values in each frame to the initial intensity value ( $F_0$ ) ( $F/F_0$ ) (**Figure 3Bb**). Average the values.
  2. Highlight the average data and create a line plot using the chart menu options.
  3. From the data analysis menu, select "trendline" to open the plot analysis dialog. Select the type of regression. Set "exponential" regression. Then select "display equation on chart". In the graph window, the exponential equation appears and the parameter values are automatically assigned, (**Figure 3Bc**).
  4. Apply the exponential correction to the intensity values in each frame as follow:  

$$F_n (\text{corrected}) = F_n / \exp(-n * a)$$

$$F_n = \text{experimental fluorescence intensity measured at frame}; n = \text{number of frames}; a = \text{bleaching factor (constant that expresses the rate of intensity loss due to photobleaching; Figure 3Bd)}$$
  5. To set the threshold, open a normalized and corrected "background ROI", calculate the average fluorescence signal and its standard deviation (SD). The average value plus 3 SD represents the threshold (**Figure 3Be**). Use this threshold for data analysis.
3. **Selection of fusion events using a semiautomatic procedure**
  1. Open the time-sequential images with image analysis software. Apply a Gaussian filter to the active image sequence.
  2. Analyze images using the tool "count objects" or a macro which allows the selection of an object whose pixels have average fluorescence intensity within a defined range. Set the intensity range manually, using the threshold function (go to the bar menu, set measure  $\rightarrow$  threshold to highlight the area of interest). An adequate threshold is 30% over the local fluorescent background signal.
  3. Apply a macro "Filters objects" to select only objects meeting the following criteria:
    1. Apply ranges option (min and max inclusive) for aspect. **Aspect** reports the ratio between the major axis and the minor axis of the ellipse equivalent to the object. Aspect is always  $\geq 1$ . Adequate values are min = 1, max = 3.
    2. Apply ranges for diameter. **Diameter** reports the average length of the diameters measured at two degree intervals joining two outline points and passing through the centroid of the object. Set the range in pixels (or in  $\mu$ m, if using a calibrated system).
    3. Define the optimal range in preliminary experiments: select manually the spots of interest and then measure their diameter using the plot profile function.
  4. Select "display objects": selected objects will appear superimposed to the TIRFM image (**Figure 4B**).
  5. Include in the analysis only those spots that show a short (one to three frames) transient increase in fluorescence intensity, immediately followed by a marked loss of signal (transient spots). Employ the circular selection to create a ROI approximately one-spot diameter radially around the selected vesicle/spots (experimental ROIs). Perform this step manually.
  6. With the ROIs selected, calculate the average fluorescence intensity of each ROI over the course of the movie.
4. **Data analysis (Figure 3C-D)**
  1. Export the time-course of the fluorescence changes measured in each "experimental ROI" to a spreadsheet; (**Figure 3Da**). Normalize the intensity value in each frame to the initial fluorescence intensity ( $F/F_0$ ), (**Figure 3Db**).
  2. Apply the exponential correction to the intensity values in each frame as reported in **step 3.2.4 (Figure 3Dc)**.
  3. To calculate the total number of fusion events (peak number), the time each fusion occurs (peak width) and the amplitude of fluorescent peak (peak height and AUC) apply logical functions using spreadsheet or math packages. An example of fusion event analysis using logical formulas is reported in **Figure 3Dd and 3De**.
  4. Assume the increase of fluorescence intensity exceeding the threshold (average background fluorescence intensity  $\pm$  3SD) as vesicle fusion to the plasma membrane and the resulting peak as a fusion event.
  5. Calculate the peak width as difference between the last and the first x value of each peak. Multiply this value for 1 / (sampling frequency). Consider this value as the time of vesicle fusion and adhesion at the plasma membrane before vesicle re-acidification and recycling (**Figure 3De**).
  6. Calculate the whole-cell AUC as a sum of values over threshold. Consider this value as net fluorescent change during the recording time due to the spontaneous (resting) or evoked (stimulated) synaptic activity.

7. Calculate the peak height as the difference between the maximal y value of each peak and the threshold. Consider this value as indicative of the fusion type (single vs. simultaneous/sequential fusion or transient vs. full fusion).

## Representative Results

The TIRF imaging and data analysis procedures described are designed to study vesicles dynamics in cellular systems. This technique can be used to determine the effects of signaling molecules and drugs on fusion events and neurotransmitter vesicle dynamics<sup>17</sup>. Using GFP-tagged plasma membrane proteins, the TIRFM analysis has been employed to characterize the constitutive trafficking of GFP-tagged glutamate transporters in glial and epithelial cells<sup>18,19</sup>.

To validate the imaging procedure and data analysis strategy reported, fusion events have been recorded under basal and stimulated conditions (potassium-induced depolarization), in SH-SY5Y neuroblastoma cells transfected with synapto-pHluorin. (Video 1, 2, respectively). Two different analyses have been performed: whole-cell (Figure 4) and single-vesicle analyses (Figure 5).

Whole cell analysis measures the total number of fusion events in the cell and the resulting net fluorescence changes induced by stimulation. In Figure 4, synapto-pHluorin transfected cells are recorded under resting and stimulated conditions (KCl stimulation), using the same experimental protocol (time exposure, laser power, etc). Figure 4A shows that synapto-pHluorin accumulates in fluorescent puncta scattered on the cell membrane. As described in literature, a faint fluorescent signal is also present at the plasma membrane<sup>2</sup>; this signal is useful to identify cells to be imaged. In Figure 4B, spots selected by the automatic procedure described in the paper (section 3.3) are superimposed to the TIRFM image reported in Figure 4A. Figure 4C shows the normalized fluorescent intensity profiles of selected spots under resting conditions. These profiles reveal the presence of individual peaks of similar fluorescent intensity that come out at various times during the recording and probably correspond to vesicles that occasionally fuse with the membrane. Figure 4D shows the effects of KCl stimulation. As expected, depolarization with 25 mM KCl elicits a prompt response and several very bright fluorescent puncta appear at the cell membrane (Video 2). These puncta correspond to the 'readily releasable' pool of synaptic vesicles present beneath the plasma membrane. The time course analysis of fluorescent changes measured in correspondence of individual spots indicates the presence of peaks, of variable fluorescence intensity, that appear suddenly after application of the secretory stimulus (Figure 4D and 4F). Results of whole cell analysis during the time of recording are reported in Figure 4E-H. KCl stimulation causes a rapid marked increase in the number of fusion events (2.5 fold increase over resting conditions) (Figure 4E-F) and in the resulting fluorescence intensity changes (9.3 fold increase over resting conditions) (Figure 4G-H), thus indicating massive neurotransmitter release.

Single-peak analysis allows the characterization of single-fusion events (Figure 5). Figure 5A shows the sequential images of a representative "experimental ROI" recorded under resting conditions. The particular highlights a synapto-pHluorin labeled vesicle which fuses with the membrane under the TIRF zone. After two frames, the fluorescent signal disappears, indicating probable vesicle retrieval and re-acidification. The normalized fluorescence profile of the region of interest (Figure 5B) measures an increase in the fluorescent signal in correspondence of the spot appearance in the TIRF zone. Conversely, the fluorescence returns to basal level after spot disappearance (single peak average width  $1.91 \pm 0.32$  sec; average peak height  $0.042 \pm 0.005$  normalized fluorescence intensity). Figure 5C and 5D show the sequential images of an "experimental ROI" recorded under KCl stimulation and the corresponding normalized fluorescence intensity profiles. Note the increase in the movement of vesicles in and out the TIRF zone after KCl depolarization.

40 fusion events have been selected and analyzed in resting and stimulated conditions. The following parameters have been measured: average peak AUC, peak width and height. Peak width specifies the time of vesicle fusion, attachment and endocytosis before re-acidification and recycling, Figure 5G. Peak height measures the fluorescence intensity changes induced by vesicle fusion, Figure 5F. Changes in these parameters are indicative of different exocytosis mechanisms. Single-peak analysis reveals that KCl depolarization modifies the mode of vesicle fusion to the plasma membrane. Indeed, increase in the average peak area ( $3.8 \pm 0.2$  fold increase over resting conditions,  $P < 0.01$  by paired t-test, Figure 5E), peak height ( $2.75 \pm 0.03$  fold increase,  $P < 0.01$  by paired t-test, Figure 5F) and width ( $2.6 \pm 0.5$  fold increase,  $P < 0.05$  by paired t-test, Figure 5G) are detected under stimulated conditions. Several explanations can be envisaged for these results. A possibility is that KCl depolarization causes the simultaneous and/or sequential fusion of vesicles in a constrained region of the cells. An alternative explanation is that strong depolarization favors full fusion versus transient fusion. Under basal conditions, the prevailing mechanism is a transient fusion: a fusion pore forms, the pH in the vesicle increases and the fluorescent signal appears, but the pore immediately closes, thus allowing rapid re-acidification and recycling. Under stimulated conditions, the vesicle completely fuses with the plasma membrane, the peak height and width increase as recapture of membrane vesicle components, re-acidification and recycling may require a longer period. A similar result has been recently obtained analyzing synaptic-like microvesicle exocytosis in endocrine  $\beta$ -cells<sup>20</sup>.

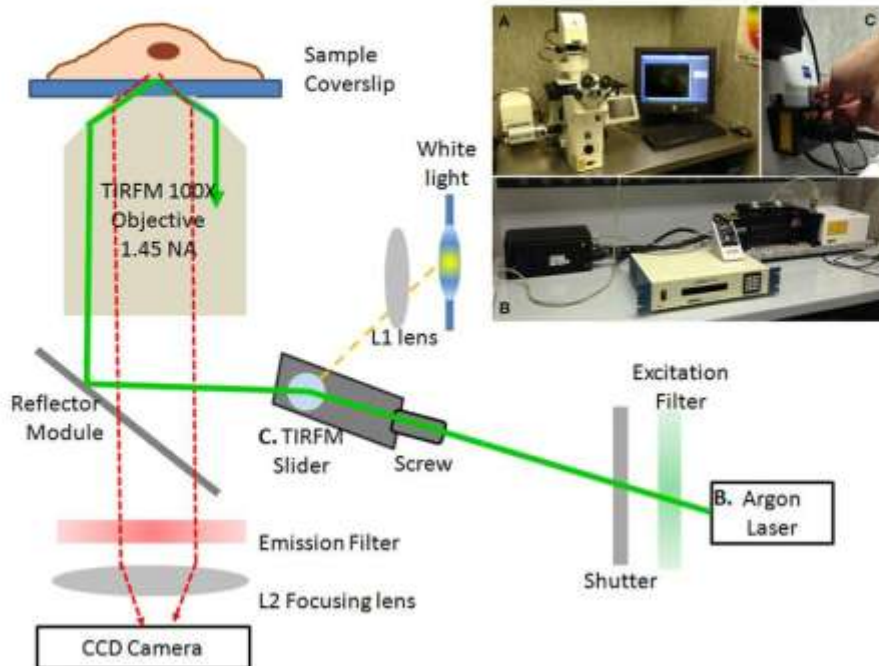


**Figure 1. TIRF microscope set up.** Schematic view and image (inset) of the TIRF microscope system. The set up comprises the Axio Observer Z1 motorized inverted microscope (A), a multi-line 100 mW Argon-ion laser (B) and a TIRF-slider (C). The laser light (green line) and white light (yellow line) are shown. Cells are imaged using a 100 × oil immersion objective. Digital images are captured on a cooled RetigaSRV Fast CCD camera. The reflector module, the emission (488/10 nm) and the excitation (band pass 525/50 nm) filters, the collimator (L1) and focusing (L2) lens are indicated. [Please click here to view a larger version of this figure.](#)

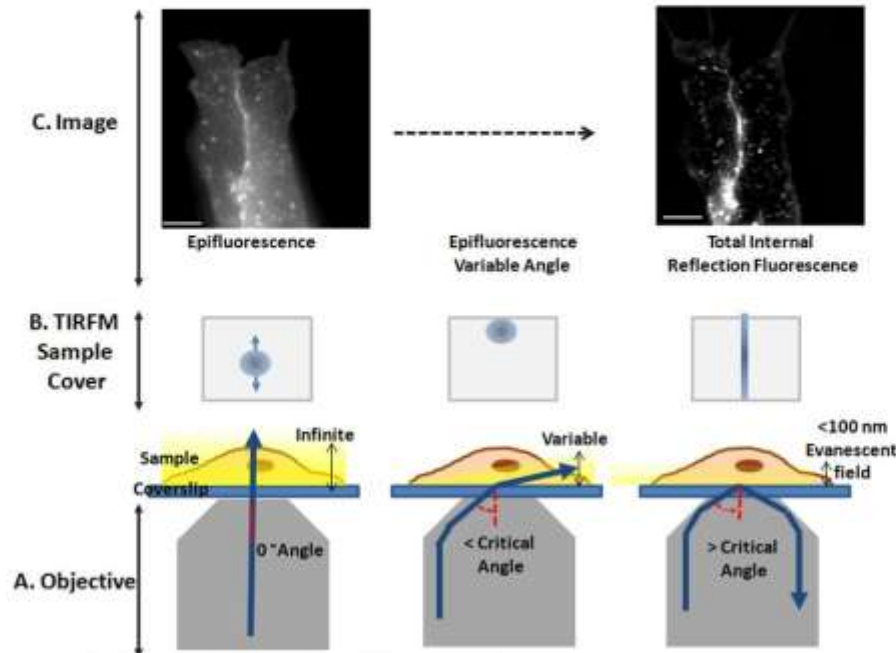


**Figure 2. Getting TIRFM configuration.** (A) Schematic cartoon illustrating the objective, the cover-slip, the sample and the position of the laser beam (blue line). *Left*, the excitation beam travels directly through the cover-slip-sample interface. The sample is excited as in epifluorescence mode. *Center*, the excitation beam forms with the sample an incident angle lower than the critical angle, the light illuminates the sample at a variable angle. *Right*, the excitation beam forms an incident angle greater than the critical angle, the light is completely reflected back into the objective lens, and an evanescent field propagates in the sample. (B) Cartoon showing the sample cover and the position of the excitation beam (blue circle), that emerges out of the objective, during the transition from epifluorescence (*left*) toward TIRF illumination (*right*). (C) epifluorescence (*left*) and TIRFM (*right*) images of synapto-pHluorin fluorescence in a live SH-SY5Y cell. Scale bar: 10  $\mu\text{m}$ . [Please click here to view a larger version of this figure.](#)

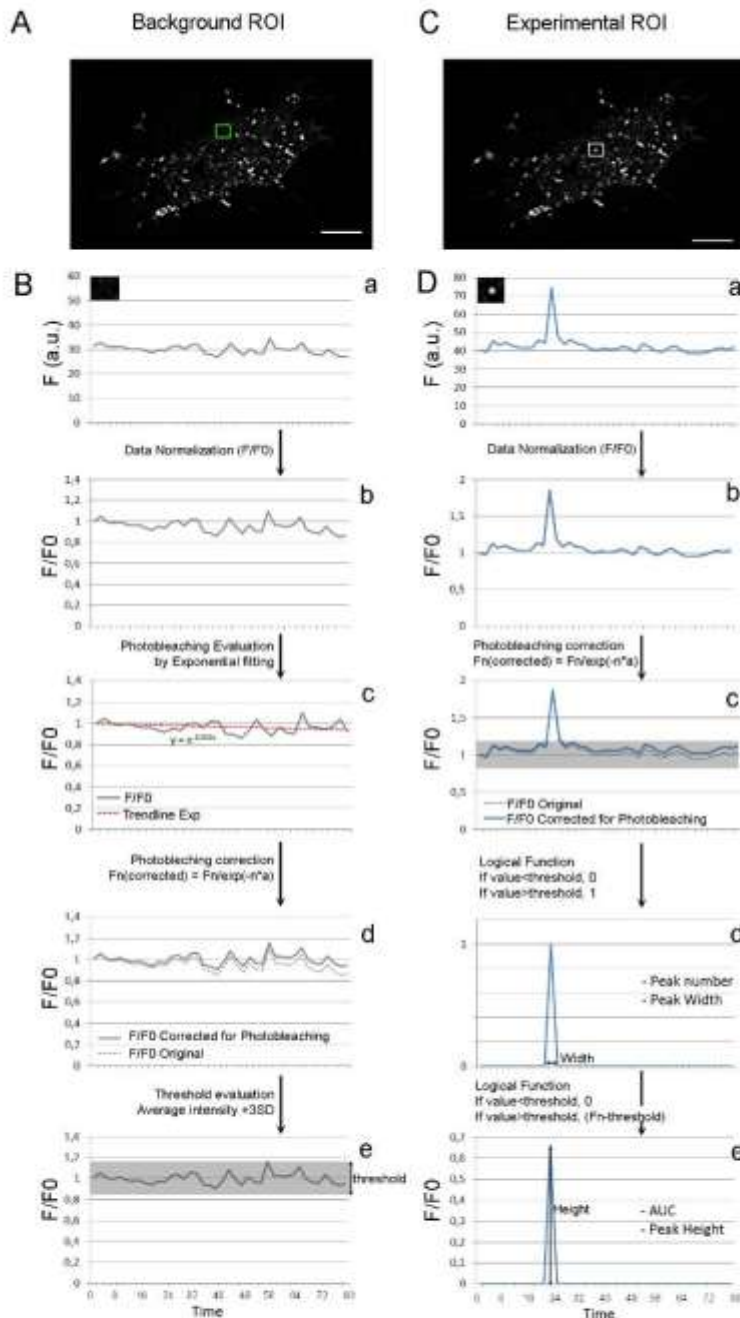


**Figure 3. Data processing and analysis.** (A) TIRFM image of synapto-pHluorin fluorescence in a live SH-SY5Y cell. The green square indicates a representative "background ROI". Scale bar 10  $\mu\text{m}$ . (B) Proposed workflow for background ROI. From top to bottom: a. time course of fluorescence intensity changes measured in the background ROI; b. normalization of fluorescence changes to the initial fluorescence value ( $F/F_0$ ); c. application of the exponential regression; d. correction for photobleaching; e. threshold evaluation (transparent gray square). (C) TIRFM image of synapto-pHluorin fluorescence in a live SH-SY5Y cell. The white square indicates a representative "experimental ROI". Scale bar 10  $\mu\text{m}$ . (D) Proposed workflow for experimental ROI. From top to bottom: a. time course of the fluorescence intensity changes; b. data normalization to the initial fluorescence value ( $F/F_0$ ); c. photobleaching correction; d-e. application of logical functions to detect peak number, AUC, width and height. Please click here to view a larger version of this figure.

### Whole cell analysis

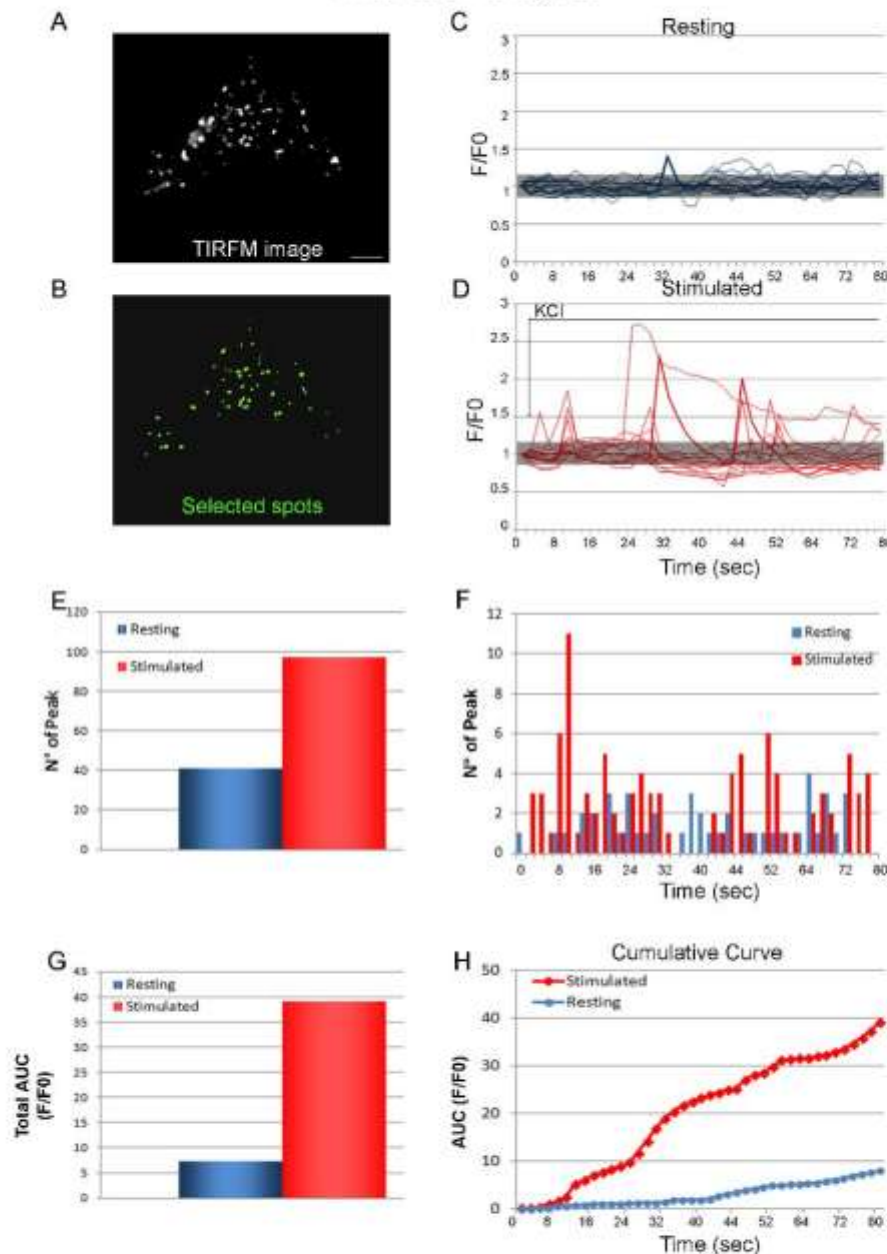


**Figure 4. Whole cell analysis.** (A) TIRFM image of synapto-pHluorin fluorescence in a live SH-SY5Y cell. Cells are recorded under resting and stimulated (25 mM KCl application) conditions (sampled at 1 Hz). Scale bar: 10 µm. (B) spots identified by the automatic procedure are shown superimposed (green color) on the TIRFM image. (C) Normalized fluorescence intensity profiles (F/F0) of spots selected by the automatic procedure in the whole cell under resting conditions. (D) Normalized fluorescence intensity profiles (F/F0) of selected spots under stimulated conditions. The bar over the traces indicates KCl application. (E-H) Number of events and fluorescence intensity changes recorded in the whole cell under resting (blue) and stimulated (red) conditions. (E) Histograms representing changes (Total AUC) in pHluorin fluorescence intensity occurring in the whole-cell. (F) Temporal distribution of fusion events. (G) Histograms representing changes (Total AUC) in pHluorin fluorescence intensity occurring in the whole-cell. (H) Curves showing the cumulative pHluorin fluorescence intensity changes as a function of time. [Please click here to view a larger version of this figure.](#)

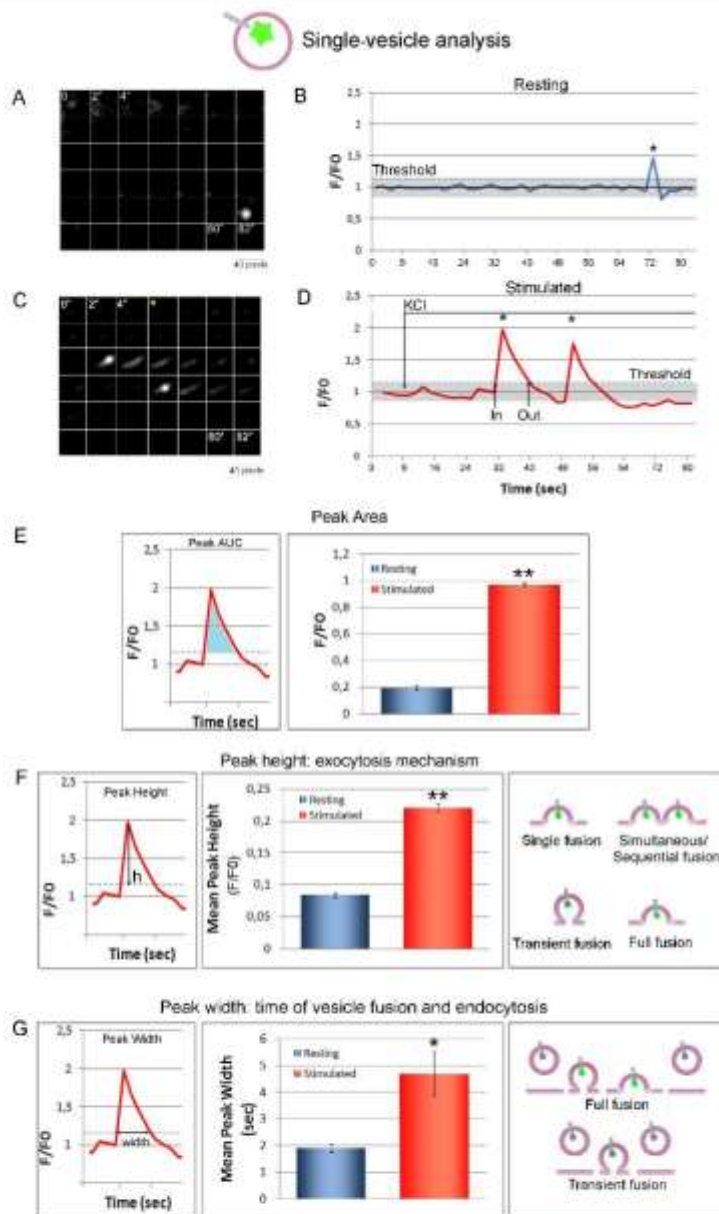


**Figure 5. Single-vesicle analysis.** (A) SH-SY5Y cells expressing synapto-pHluorin are imaged at 1 Hz, under resting conditions. Representative TIRFM sequential images (every 2 sec) of a ROI showing a synapto-pHluorin labeled vesicle. ROI = 40 x 35 pixels. (B) Normalized fluorescence profile (F/F0) of the ROI shown in A. The black asterisk indicates a fusion event, the threshold line is shown. (C) The same cell is recorded under stimulated conditions (25 mM KCl), representative TIRFM sequential images of a ROI are shown. KCl application is indicated by the yellow asterisk. (D) The normalized fluorescence profile of the region shown in C highlights the arrival (in) and disappearance (out) of vesicles. Black asterisks indicate fusion events, the threshold line is shown. (E-G) properties of single-vesicle events recorded under resting (blue bar) and stimulated (red bar) conditions. *n* = 40 fusion events. (E) *Left*, peak area (AUC) is indicated by light blue; *right*, histograms of average peak areas; \*\**p* < 0.01. (F) *Left*, peak height (*h*) is indicated by a double-headed arrow; *center*, histograms of the average peak height; \*\**p* < 0.01; *right*, peak height specifies the fusion mechanism. The star in the cartoon indicates synapto-pHluorin. (G) *Left*, peak width is indicated by a double-headed arrow; *center*, histograms of the average peak width; \**p* < 0.05; *right*, peak width specifies the time of vesicle exocytosis, attachment and endocytosis. The star color is green when synapto-pHluorin fluorescence is visible and gray when it is switched-off. [Please click here to view a larger version of this figure.](#)

**Video 1.** SH-SY5Y cells expressing synapto-pHluorin are recorded under resting conditions (sampled at 1 Hz). [Please click here to view this video.](#)

**Video 2.** SH-SY5Y cells expressing synapto-pHluorin are recorded under stimulated conditions (sampled at 1 Hz). KCl perfusion is indicated. [Please click here to view this video.](#)

## Discussion

This paper presents a protocol to image and analyze vesicles dynamics in secreting cells, using fluorescent cDNA-encoded vectors and TIRFM. Key elements of successful imaging by TIRFM are the selection of the cellular model and cell transfection with genetically-encoded optical indicators of vesicle release and recycling.

TIRFM is ideally suited for cells growing adherent to a glass cover and sufficiently flat to allow stable visualization of membranes and fusion events. Vesicles should ideally be dispersed in the cell so that their trafficking, fusion and endocytosis can be imaged and quantified at single-vesicle level. Unfortunately, neurons do not meet these criteria: they have irregular shapes, neurites which frequently cross over each other, and vesicles fusion is prevalently concentrated in small regions (active zones). For these regions is very difficult to study vesicle dynamics by TIRFM in primary cultures of neurons.

We demonstrate for the first time that the SH-SY5Y human neuroblastoma cell line can be a valuable alternative model to investigate neurotransmitter release under resting and stimulated conditions, by TIRFM. This cell line has a neuronal phenotype with a cellular body and thin processes, possesses enzymes for neurotransmitter synthesis, proteins of the synaptic machinery, and a regulated secretion. Furthermore, it can be differentiated into a functionally mature neuronal phenotype in the presence of various agents, including retinoic acid, phorbol esters, and dibutyryl cyclic AMP<sup>21,22</sup>. Cells are sufficiently flat to allow stable visualization of membranes and fusion events in TIRFM mode (particularly in the cell body) and vesicles are relatively dispersed. Finally, cells can be easily transfected with plasmid encoding GFP-labeled proteins or pH-sensitive protein tags using different transfection reagents. In this protocol, PEI has been used to transfect the cells. This reagent constitutes the basis of most commercially available transfection agents and alone acts as a very cost-effective transfection vector. A 20% efficiency of transfection is expected using the above reported protocol which is adequate for single cell imaging.

While the availability of different transfection reagents and procedures makes transfection almost a standard procedure in SH-SY5Y and even in primary neuronal cultures, care must be taken when recording, analyzing and interpreting TIRFM data. TIRFM facilitates the collection of information regarding processes that occur at or near the membrane in living cells, and enables the analysis of individual molecular events through detection of changes in the fluorescent signal derived from tagged proteins that move in or out the evanescent field. However, several factors can modify the fluorescent signals in this zone, without necessarily implying exo/endocytic events, and this must be taken into consideration when recording and analyzing data. Among these are morphological changes in the cell, particularly those concerning the plane in focus under the evanescent field and fluorophore modifications during recording.

### Morphological Changes

The high resolution of the TIRF technique relies on the excitation of fluorophores within the evanescent field, with the depth of 100 nm from the glass interface<sup>11</sup>. This is a very thin zone and imperceptible morphological modifications are expected to change the cell plane in focus. This particularly applies to neurons and cells that present several processes and exhibit pronounced ruffling. In these cells, the membrane area in contact with the cover-slip during recording is irregular and can rapidly change, thus causing inaccurate evaluation of exocytosis. For this reason, whenever possible, it is important to select the cellular model of investigation. To limit cell movements can be helpful to coat glass-covers with extracellular matrix proteins or poly-L-lysine. However, one must keep in mind that these substrates may modify cell behavior and vesicle dynamics.

Other possible sources of morphological modifications during recording are cell stimulation, addition of solutions, and temperature changes. Stimuli able to induce massive vesicles release (*i.e.*, KCl depolarization) often cause cell shrinkage which obviously modifies the cell surface under the TIRF zone. It is therefore important to select accurately the type, concentration, and application time of the stimulus in preliminary experiments.

The simple introduction of solutions into the bath with a pipette, independently of the composition, may cause modification of cell morphology by shear stress. To solve this artifact, add medium preferably using a perfusion system, possibly connected with a vacuum pump to reduce noise.

Cell morphology and function are extremely sensitive to temperature variations due to experimental environment, medium addition and intense laser illumination. The temperature control in live-cell imaging is normally achieved using incubators; small (stage-top) and large (chamber) incubators are available. The former are particularly handy and well suited for the observation of cell cultures, the latter guarantee a constant temperature of all devices inside the incubator, including a large part of the microscope, thus minimizing the focus drift resulting from temperature gradient. In the absence of a temperature regulatory system, it is critical to equilibrate cells, live-cell imaging chamber, and solutions to room temperature and to avoid long-term imaging experiments.

### Fluorophore

Alteration of fluorescent signals may also be due to modification of the fluorophore during recording. The most important is photobleaching<sup>23</sup>. Photobleaching is the photon-induced decomposition of a fluorophore. It generally causes a permanent loss of fluorescence and dimming of the observed sample over time. In TIRFM, only fluorophores closed to the origin of the evanescent field can be photobleached and GFP-tagged membrane proteins are photobleached because they reside in this field. The prevention of the fading of fluorescence emission intensity is very important to obtain high-quality images, and obligatory for quantitative fluorescence microscopy. With a reasonable approximation, for a given molecule in a constant environment, photobleaching depends on the time and the cycle of exposure to the excitation source. In many instances, photobleaching follows a simple exponential decay function, which makes its assessment and its correction easier by performing

control recordings<sup>23</sup>. Different correction formulas/macros are available online (see Table of materials and equipments); in the protocol a simple exponential function has been used.

There are several strategies to overcome photobleaching. A good strategy is to prevent photobleaching at the source, for example, using fluorophores with high photostability. Unfortunately, right now, the choice of DNA-encoded probes is still limited. In this case, loss of activity caused by photobleaching can be minimized during imaging acquisition, optimizing time-span of light exposure, the photon energy of the input light and the frequency of sampling.

When using pH-sensitive probes, a further source of fluorophore modification during recording is the pH shift in the medium. The liquid volume of the recording chamber is usually very low and drug application, cell activity and metabolism may modify the pH of the medium, particularly in the tiny volume between the cell and the surface of the coverslip. This in turn, changes the pHluorin fluorescent signal, thus causing over/under-estimate vesicle release. For example, strong stimulations may lead to a calcium-dependent acidification of the cytosol and mirrored alkalization in the extracellular space, thus resulting in an exaggerated increase in the fluorescent signal<sup>24</sup>.

To avoid this problem, always use buffered solutions and monitor possible pH modifications introduced by the established protocol, in preliminary experiments. For a more accurate estimate of evoked vesicle release, when analyzing data, monitor the fluorescence signal in a region of the cell surface without fusion events, and use modifications of the fluorescent signal within this region as adjustment factor.

In conclusion, a method for monitoring and analyzing vesicle fusion and dynamics has been described. This technique can be used in different cell types (neurons and endocrine cells) to visualize and dissect the various steps of exo/endocytosis, to reveal the role of proteins and their pathogenic mutants in the regulation of vesicle dynamics and to uncover the mechanisms of action of drugs targeting constitutive and regulated exocytosis.

## Disclosures

The authors declare that they have no competing financial interests.

## Acknowledgements

The authors would like to acknowledge the Università degli Studi di Milano for support to Eliana Di Cairano (Post-doctoral fellowship) and Stefania Moretti (Ph.D. fellowship). This work was supported by the University Research Program PUR to C.P.

We would like to thank Prof. Jeremy M. Henley, School of Biochemistry, University of Bristol, United Kingdom, for the pHluorin construct and Dr. Doti Francesco for assistance in data analysis, and Silvia Marsicano for technical assistance.

## References

1. Sudhof, T. C., The synaptic vesicle cycle. *Annu. Rev. Neurosci.* **27**, 509–547, DOI: 10.1146/annurev.neuro.26.041002.131412 (2004).
2. Denk, W., Svoboda, K. Photon upmanship: why multiphoton imaging is more than a gimmick. *Neuron*. **18** (3), 351–7, DOI: 10.1016/S0896-6273(00)81237-4 (1997).
3. Helmchen, F., Svoboda, K., Denk, W., Tank, D.W. In vivo dendritic calcium dynamics in deep-layer cortical pyramidal neurons. *Nat Neurosci.* **2** (11), 989–96, DOI: 10.1038/14788 (1999).
4. Tsien, R.Y. The green fluorescent protein. *Annu Rev Biochem.* **67**, 509–44, DOI: 10.1146/annurev.biochem.67.1.509 (1998).
5. Matz, M.V., et al. Fluorescent proteins from non bioluminescent Anthozoa species. *Nat Biotechnol.* **17** (10), 969–73, DOI: 10.1038/13657 (1999).
6. Ribchester R.R., Mao, F., Betz, W.J. Optical measurements of activity-dependent membrane recycling in motor nerve terminals of mammalian skeletal muscle. *Proc Biol Sci.* **255** (1342), 61–6, DOI: 10.1098/rspb.1994.0009 (1994).
7. Polo-Parada, A.L., Bose, C.M., Landmesser, L.T. Alterations in transmission, vesicle dynamics, and transmitter release machinery at NCAM-deficient neuromuscular junctions. *Neuron*. **32** (5), 815–28, DOI: 10.1016/S0896-6273(01)00521-9 (2001).
8. Gaffield, M.A., Betz, W.J. Imaging synaptic vesicle exocytosis and endocytosis with FM dyes. *Nat Protoc.* **1** (6), 2916–21, DOI: 10.1038/nprot.2006.476 (2006).
9. Miesenböck, G., De Angelis, D.A., Rothman, J.E. Visualizing secretion and synaptic transmission with pH-sensitive green fluorescent proteins. *Nature*. **394** (6689), 192–5, DOI: 10.1038/28190 (1998).
10. Axelrod, D. Total internal reflection fluorescence microscopy. *Methods Cell Biol.* **89**, 169–221, DOI: 10.1016/S0091-679X(08)00607-9 (2008).
11. Sankaranarayanan, S., De Angelis, D., Rothman, J.E., Ryan, T. A. The Use of pHluorins for Optical Measurements of Presynaptic Activity. *Biophys. J.* **79**, 2199–2208, DOI: 0006-3495/00/10/2199/10 (2000).
12. Mattheyses, A.L., Simon, S.M., Rappoport, J.Z. Imaging with total internal reflection fluorescence microscopy for the cell biologist. *J. Cell Sci.* **123**, 3621–28, DOI: 10.1242/jcs.056218 (2010).
13. Wyatt, R.M., Balice-Gordon R.J. Heterogeneity in Synaptic Vesicle Release at Neuromuscular Synapses of Mice Expressing SynaptopHluorin. *J. Neurosci.* **28**(1), 325–335, DOI: 10.1523/JNEUROSCI.3544-07.2008 (2008).
14. Tsuboi, T., Rutter, G.A. Multiple forms of "kiss-and-run" exocytosis revealed by evanescent wave microscopy. *Curr Biol.* **13**, 563–567, DOI: 10.1016/S0960-9822(03)00176-3 (2003).
15. Miloso, M., et al. Retinoic Acid-Induced Neurogenesis of Human Neuroblastoma SH-SY5Y Cells Is ERK Independent and PKC Dependent. *J. Neurosci. Res.* **75**, 241–252, DOI: 10.1002/jnr.10848 (2004).
16. Jaskolski, F., Mayo-Martin, B., Jane, D., Henley, J.M. Dynamin-dependent Membrane Drift Recruits AMPA Receptors to Dendritic Spines. *J Biol Chem.* **284** (18), 12491–503, DOI: 10.1074/jbc.M808401200 (2009).
17. Treccani, G., et al. Stress and corticosterone rapidly increase the readily releasable pool of glutamate vesicles in synaptic terminals of prefrontal and frontal cortex. *Mol Psychiatry.* **19** (4), 433–43, DOI: 10.1038/mp.2014.5 (2014).

18. D'Amico, A., *et al.* The surface density of the glutamate transporter EAAC1 is controlled by interactions with PDZK1 and AP2 adaptor complexes. *Traffic*. **11** (11), 1455-70, doi: 10.1111/j.1600-0854.2010.01110.x (2010).
19. Perego, C., Di Cairano, E.S., Ballabio, M., Magnaghi, V. Neurosteroid allopregnanolone regulates EAAC1-mediated glutamate uptake and triggers actin changes in Schwann cells. *J Cell Physiol*. **227** (4), 1740-51, DOI: 10.1002/jcp.22898 (2012).
20. Bergeron, A., Pucci, L., Bezzi, P., Regazzi, R. Analysis of synaptic-like microvesicles exocytosis of B-cells using a live imaging technique. *PlosOne*. **9**, e87758, DOI: 10.1371/Journal.pone.0087758 (2014).
21. Encinas, M., *et al.* Sequential treatment of SH-Sy5Y cells with retinoic acid and brain-derived neurotrophic factor gives rise to fully differentiated, neurotrophic factor-dependent, human neuron-like cells. *J. Neurochem*. **75** (3), 991-1003, DOI: 10.1046/j.1471-4159.2000.0750991.x (2000).
22. Kume, T., *et al.* Dibutyl cAMP Induces differentiation of human neuroblastoma SH-SY5Y cells into a noradrenergic phenotype. *Neurosci Lett*. **443** (3), 199-203, DOI: 10.1016/j.neulet.2008.07.079 (2008).
23. Diaspro, A., Chirico, G., Usai, C., Ramoino, P., Dobrucki, J. Photobleaching. In *Handbook of Biological Confocal Microscopy*. J.B. Pawley, editor. Springer-Verlag New York, Inc., New York. 690-699. DOI: 10.1007/978-0-387-45524-2\_39 (2006).
24. Rossano, A.J., Chouhan A. K., Macleod G.M. Genetically encoded pH-indicators reveal activity-dependent cytosolic acidification of *Drosophila* motor nerve termini in vivo. *J Physiol*. **591.7**, 1691-1706, DOI: 10.1113/jphysiol.2012.248377 (2013).

## Bibliography Chapter IV

1. Bonner-Weir S and Orci L (1982). New perspectives on the microvasculature of the islets of Langerhans in the rat. *Diabetes* 31:883–889.
2. Butler AE, Janson J, Bonner-Weir S, Ritzel R, Rizza RA, Butler PC (2003). Beta-cell deficit and increased beta-cell apoptosis in humans with type 2 diabetes. *Diabetes* 52:102–110.
3. Chavez A, Gastaldelli A, Guardado-Mendoza R, Lopez-Alvarenga JC, Leland MM, Tejero ME, Sorice G, Casiraghi F, Davalli A, Bastarrachea RA, Comuzzie AG, DeFronzo RA, Folli F. (2009). Predictive models of insulin resistance derived from simple morphometric and biochemical indices related to obesity and the metabolic syndrome in baboons. *Cardiovasc Diabetol* 8:22.
4. Chavez A, Lopez-Alvarenga JC, Tejero ME, Triplitt C, Bastarrachea RA, Sriwijitkamol A, Tantiwong P, Voruganti VS, Musi N, Comuzzie AG, DeFronzo RA, Folli F (2008). Physiological and molecular determinants of insulin action in the baboon. *Diabetes* 57:899–908.
5. Denk W. and Svoboda K. (1997). Photon upmanship: why multiphoton imaging is more than a gimmick. *Neuron*. 18 (3), 351-7, DOI: 10.1016/S0896-6273(00)81237-4.
6. Di Cairano ES, Davalli AM, Perego L, Sala S, Sacchi VF, La Rosa S, Finzi G, Placidi C, Capella C, Conti P, Centonze VE, Casiraghi F, Bertuzzi F, Folli F, Perego C. (2011). The glial glutamate transporter 1 (GLT1) is expressed by pancreatic beta-cells and prevents glutamate-induced beta-cell death. *J Biol Chem* 286:14007–14018.
7. Federici M, Hribal M, Perego L, Ranalli M, Caradonna Z, Perego C, Usellini L, Nano R, Bonini P, Bertuzzi F, Marlier LN, Davalli AM, Carandente O, Pontiroli AE, Melino G, Marchetti P, Lauro R, Sesti G, Folli F. (2001) High glucose causes apoptosis in cultured human pancreatic islets of Langerhans: a potential role for regulation of specific Bcl family genes toward an apoptotic cell death program. *Diabetes* 50:1290–1301.
8. Fontés G, Zarrouki B, Hagman DK, Latour MG, Semache M, Roskens V, Moore PC, Prentki M, Rhodes CJ, Jetton TL, Poitout V. (2010). Glucolipotoxicity age-dependently impairs beta cell function in rats despite a marked increase in beta cell mass. *Diabetologia* 53:2369–2379.
9. Gannon M, Ray MK, van Zee K, Rausa F, Costa RH, Wright CV (2000). Persistent expression of HNF6 in islet endocrine cells causes disrupted islet architecture and loss of beta cell function. *Development* 127:2883–2895.
10. Gromada J, Franklin I, Wollheim CB (2007). Alpha-cells of the endocrine pancreas: 35 years of research but the enigma remains. *Endocr Rev* 28:84–116.
11. Guardado-Mendoza R, Davalli AM, Chavez AO, Hubbard GB, Dick EJ, Majluf-Cruz A, Tene-Perez CE, Goldschmidt L, Hart J, Perego C, Comuzzie AG, Tejero ME, Finzi G, Placidi C, La Rosa S, Capella C, Halff G, Gastaldelli A, DeFronzo RA, Folli F. (2009). Pancreatic islet amyloidosis, beta-cell apoptosis, and alpha-cell proliferation are determinants of islet remodeling in type-2 diabetic baboons. *Proc Natl Acad Sci U S A* 106:13992–13997.
12. Guardado-Mendoza R, Jimenez-Ceja L, Majluf-Cruz A, Kamath S, Fiorentino TV, Casiraghi F, Velazquez AO, DeFronzo RA, Dick E, Davalli A, Folli F. (2013). Impact of obesity severity and duration on pancreatic beta- and alpha-cell dynamics in normoglycemic non-human primates. *Int J Obes (Lond)* 37:1071–1078.
13. Hauge-Evans AC, King AJ, Carmignac D, Richardson CC, Robinson IC, Low MJ, Christie MR, Persaud SJ, Jones PM. (2009). Somatostatin secreted by islet delta-cells fulfills multiple roles as a paracrine regulator of islet function. *Diabetes* 58:403–411.
14. Helmchen F, Svoboda K., Denk W., Tank D.W. (1999). In vivo dendritic calcium dynamics in deep-layer cortical pyramidal neurons. *Nat Neurosci*. 2 (11), 989-96, DOI: 10.1038/14788.
15. Jurgens CA, Toukatly MN, Fligner CL, Udayasankar J, Subramanian SL, Zraika S, Aston-Mourney K, Carr DB, Westermark P, Westermark GT, Kahn SE, Hull RL. (2011). Beta-cell loss and beta-cell apoptosis in human type 2 diabetes are related to islet amyloid deposition. *Am J Pathol* 178:2632–2640.
16. Kamath S, Chavez AO, Gastaldelli A, Casiraghi F, Halff GA, Abrahamian GA, Davalli AM, Bastarrachea RA, Comuzzie AG, Guardado-Mendoza R, Jimenez-Ceja LM, Mattern V, Paez AM, Ricotti A, Tejero ME, Higgins PB, Rodriguez-Sanchez IP, Tripathy D, DeFronzo RA, Dick EJ Jr, Cline GW, Folli F. (2011). Coordinated defects in hepatic long chain fatty acid metabolism and triglyceride accumulation contribute to insulin resistance in non-human primates. *PLoS One* 6, e27617.
17. Ludvigsen E, Olsson R, Stridsberg M, Janson ET, Sandler S (2004). Expression and distribution of somatostatin receptor subtypes in the pancreatic islets of mice and rats. *J Histochem Cytochem* 52:391–400.
18. Mattheyses A. L., Simon S. M., Rappoport J. Z. (2010). Imaging with total internal reflection fluorescence microscopy for the cell biologist. *J. Cell Sci.* 123, 3621-3628.

19. Matz MV, Fradkov AF, Labas YA, Savitsky AP, Zaraisky AG, Markelov ML, Lukyanov SA. (1999). Fluorescent proteins from non bioluminescent Anthozoa species. *Nat Biotechnol.* 17, (10), 969-9673.
20. Menge BA, Grüber L, Jørgensen SM, Deacon CF, Schmidt WE, Veldhuis JD, Holst JJ, Meier JJ. (2011). Loss of inverse relationship between pulsatile insulin and glucagon secretion in patients with type 2 diabetes. *Diabetes* 60:2160–2168.
21. Miesenböck G., De Angelis D. A., Rothman J. E. (1998). Visualizing secretion and synaptic transmission with pH-sensitive green fluorescent proteins. *Nature.* 394, (6689), 192-195.
22. Orci L and Unger RH (1975). Functional subdivision of islets of Langerhans and possible role of D cells. *Lancet* 2:1243–1244.
23. Patel YC, Pierzchala I, Amherdt M, Orci L (1985). Effects of cysteamine and antibody to somatostatin on islet cell function in vitro. Evidence that intracellular somatostatin deficiency augments insulin and glucagon secretion. *J Clin Invest* 75:1249–1255.
24. Ribchester R. R., Mao F., Betz W. J. (1994). Optical measurements of activity-dependent membrane recycling in motor nerve terminals of mammalian skeletal muscle. *Proc Biol Sci.* 255, (1342), 61-66.
25. Samols E and Stagner JI (1990). Islet somatostatin—microvascular, paracrine, and pulsatile regulation. *Metabolism* 39:55–60.
26. Sankaranarayanan S., De Angelis D., Rothman J. E., Ryan T. A. (2000). The Use of pHluorins for Optical Measurements of Presynaptic Activity. *Biophys. J.* 79, 2199-2208.
27. Soejima K and Landing BH (1986). Pancreatic islets in older patients with cystic fibrosis with and without diabetes mellitus: morphometric and immunocytologic studies. *Pediatr Pathol* 6:25–46.
28. Sudhof T. C. (2004). The synaptic vesicle cycle. *Annu. Rev. Neurosci.* 27, 509–547, DOI:10.1146/annurev.neuro.26.041002.131412
29. Tsien R. Y. (1998). The green fluorescent protein. *Annu Rev Biochem.* 67, 509-544.
30. Unger RH and Orci L (1977). Possible roles of the pancreatic D-cell in the normal and diabetic states. *Diabetes* 26:241–244.
31. Unger RH and Orci L (2010). Paracrinology of islets and the paracrinopathy of diabetes. *Proc Natl Acad Sci U S A* 107:16009–16012.
32. Vieira E, Salehi A, Gylfe E (2007). Glucose inhibits glucagon secretion by a direct effect on mouse pancreatic alpha cells. *Diabetologia* 50:370–379.
33. Westermark GT and Westermark P (2013). Islet amyloid polypeptide and diabetes. *Curr Protein Pept Sci* 14:330–337.

# Chapter V

**Stefania Moretti**

## Original research papers on peer reviewed international journals

1. Di Cairano ES, **Moretti S**, Daniele F, Sacchi VF, Perego C. (2015) Total internal reflection fluorescence microscopy as a powerful tool to follow dynamic events at the cell membrane. *J Biol. Research.* 88:5161, 57-58. (IF:0.834)
2. Daniele F, Di Cairano E, **Moretti S**, Piccoli G, Perego C. (2015) Total internal reflection fluorescence microscopy and pH-sensitive GFP-based sensors to evaluate neurotransmitter vesicle dynamics. *J. Vis. Exp. (JoVE).* 95: e52267, doi:10.3791/52267. (IF:1.325).
3. Guardado-Mendoza R, Perego C, **Moretti S**, Jimenez-Ceja L. M., Abrahamian G, Dick Jr E J., Chavez A V, Kamath S, Davalli A, Half G, De Fronzo R, Gastaldelli A, Folli F. (2015) Delta-cell death in the islet of Langerhans and the progression from normal glucose tolerance to type 2 diabetes mellitus in non-human primates (Baboon, *Papio hamadryas*). *Diabetologia.* 58(8):1814-26. doi: 10.1007/s00125-015-3625-5. (IF: 6.88)
4. Di Cairano ES, **Moretti S**, Marciani P, Sacchi VF, Castagna M, Davalli A, Folli F, Perego C. (2015) Neurotransmitters and Neuropeptides: New Players in the Control of Islet of Langerhans' Cell Mass and Function. *Journal of Cellular Physiology. Epub 2015 Sep.* (IF: 3.88)

## In preparation

1. Di Cairano E.S.\*, **Moretti S.\***, Fino E., Bazzicaluppi E, Amalia G., Froelich F., Piccoli G, Bertuzzi F., Davalli AM and F. Folli, Perego C., Identification of a novel autoantibody in type 1 Diabetes Mellitus.\*Co-first author
2. Moretti S, Di Cairano ES, Bertuzzi F, La Rosa S, Davalli A, Folli F, Perego C. Modulation of glutamate signalling in human islets of Langerhans under hyperglycaemia.
3. Di Cairano ES\*, **Moretti S\***, Castagna P, D'Amico A, Soragna A, and Perego C. Glutamate transporter dynamics and protein interactions: roles in the control of glutamate clearance and in the maintenance of oxidative defense.\*Co-first author

## Proceedings published on international journals

1. Perego C, **Moretti S**, Di Cairano ES, Santi C, La Rosa S, Bertuzzi F, Folli F. Plasticity in islets of Langerhans in type 2 diabetes. *Diabetologia* 2015; Vol 58 (Suppl 1), Pag S116-117 #232. DOI 10.1007/s00125-015-3687-4

(Oral communication, 51th EASD Annual Meeting. Section OP40: The perfect cellular environment for beta cell differentiation. Stockholm. 14-18 September 2015). (IF: 6.88)

2. Cosentino C, Di Cairano ES, **Moretti** S, Perego C, MC. Proverbio, E. Mangano, C. Perego, C. Battaglia. 5S561F-CDKAL1 variant, identified by whole exome sequencing of Congenital Hyperinsulinism patients, affects protein localization and insulin content in INS1-E cells. *Diabetologia* 2015; Volume 58 (Suppl 1), Pag S216 #435. DOI 10.1007/s00125-015-3687-4 (Poster, 51th EASD Annual Meeting. Section PS23: Mechanisms of Insulin secretion. Stockholm. 14-18 September 2015). (IF: 6.88).
3. Di Cairano ES, Meraviglia V, Ulivi A, Rosa P, **Moretti** S, Daniele F., Bertuzzi F, La Rosa S, Sacchi VF, Perego C. Expression and function of the atypical purinergic receptor GPR17 in the endocrine pancreas. *Diabetologia* - ISSN: 1432-0428 – Volume 57, Issue 1 Supplement. 2014 (Poster n°612. 50th EASD Annual Meeting. Section PS039: Glucagon, somatostatin secretion. 15-19 September 2014, Vienna).
4. Perego C, **Moretti** S, Di Cairano ES, Daniele F, La Rosa S, Bertuzzi F, Davalli A, Folli F. Modulation of glutamate signalling in human islets of Langerhans under hyperglycaemia. *Diabetologia* - ISSN: 1432-0428 - Volume 57, Issue 1 Supplement. 2014. (Poster, 50th EASD Annual Meeting. Section PS022: Beta cell ER stress and apoptosis. Poster N°462. 2014. 15-19 September 2014, Vienna).
5. Perego C, **Moretti** S, Fino E, Iaquinto M, Di Cairano E, Bertuzzi F, Davalli A, Folli F (2012). The glutamate transporter GLT1/EAAT2 in islet of Langerhans: a key player in the control of  $\beta$ -cell function and integrity in health and disease. *Acta Physiologica* 2012; Volume 206, Supplement 692. (Poster, 63rd National Congress of the Italian Physiological Society. 21/09/2012-23/09/2012. Verona, Italy).
6. Davalli AM, Di Cairano ES, Iaquinto M, **Moretti** S, Bazzini C, La Rosa S, Bertuzzi F, Folli F (2012). The Glutamate transporter GLT1/EAAT2: a promising target to arrest beta cell dysfunction and death in diabetes mellitus. 48th EASD Annual Meeting of the European Association for the Study of Diabetes. *Diabetologia*. October 2012, Volume 55, Issue 1, pp 1-538. DOI: 10.1007/s00125-012-2688-9.
7. Perego C, Iaquinto M, **Moretti** S, Di Cairano ES, Bazzini C, La Rosa S, Bertuzzi F, Davalli AM, Folli F. The Glutamate transporter GLT1/EAAT2: a promising target to arrest  $\beta$ -cell dysfunction and death in diabetes mellitus. . *Diabetologia* - ISSN: 1432-0428 - Volume 55, Issue 1, P495, 2015 (poster, 48th EASD Annual Meeting. 1-5 October 2012, Berlin)

#### **Proceedings published in conference proceedings and oral communication**

1. Perego C, Daniele F, Marsicano S, Di Cairano ES, **Moretti** S, Cirnaru M.D., Perez Carrion M., Piccoli G. (2015). Expression of G2385R LRRK2/PARK8 mutant in human SH-SY5Y neuroblastoma cells alters

neurotransmitter vesicle dynamics. Molecular Mechanisms of Neurodegeneration Milan, Italy. May 24-27 2015.

2. **Moretti S**, Di Cairano ES, Daniele F, La Rosa S, Bertuzzi F, Folli F, Perego C.(2015) The glutamate signalling in islets of Langerhans: molecular mechanisms of modulation. Italian Physiological Society (SIF). Annual Meeting of Young Researchers. Fiesole, 28-may-2015. (Oral communication).
3. Di Cairano ES, Meraviglia V, Ulivi A, Rosa P, **Moretti S**, Daniele F., Bertuzzi F, La Rosa S, Sacchi VF, Perego C. Expression and function of the atypical purinergic receptor GPR17 in the endocrine pancreas. Physiological Society. London, 2014.
4. C. Perego, F. Daniele, S. Marsicano, **Moretti S**, Di Cairano ES, MD. Cinaru, M. Perez Carrion, G. Piccoli. Total Internal Reflection Fluorescence Microscopy to unravel the impact of LRRK2/Park8 and its pathogenic mutants on neurotransmitter vesicle trafficking. Section: Neurobiology and Neurophysiology. 65th Congress of the Italian Physiological Society (SIF). Anacapri 30 September -2 October, 2014.
5. Perego C, **Moretti S**, Di Cairano ES, Mengacci D, Daniele F, Larosa S, Bertuzzi F, Folli F (2014). The glutamate signalling in islet of Langerhans: molecular mechanisms of modulation. 64. Congress of the Italian Physiological Society held in Portonovo in 2013 (21-sept-2014).(oral communication)
6. F. Folli, C. Perego, R. Guardado-Mendoza, S. **Moretti**, S. Larosa, G. Finzi, A. Davalli (2014). Remodeling pancreatic island in type 2 diabetes: study in non-human primates. 25th Conference National Congress Italian Society of Diabetes. SID held in Bologna in 2013 (28-may-2014). URL: <http://www.siditalia.it/congressi/25-congresso-nazionale-2014.html>. (oral communication)
7. Perego C, **Moretti S**, Di Cairano ES, La Rosa S, Bertuzzi F, Davalli AM (2014). Modulation of glutamate signalling in human islets of Langerhans under hyperglycaemia. 25th Conference National Congress Italian Society of Diabetes. SID "Symposium: molecular mechanisms of disease" held in Bologna in 2014 (28-june-2014) (oral communication)
8. Di Cairano ES, V. Meraviglia, A. Ulivi, P. Rosa, S. Moretti, F. Daniele, F. Bertuzzi, S. La Rosa, V. Sacchi, C. Perego (2014). Expression and function of the atypical purinergic receptor GPR17 in the endocrine pancreas. Physiology Congress in London in 2014 (31-mar-2014) (oral communication)
9. **Moretti S** , Di Cairano E., Bertuzzi F , F. Folli , C. Perego . Signalling pathways responsible for the regulation of the Glutamate Transporter 1 (GLT1/EAAT2) in pancreatic beta cells". Iniziativa NEXT STEP5 - La giovane ricerca avanza". Università degli Studi di Milano. Mercoledì 4 luglio 2014 ,Aula Magna, via Balzaretti, 9, Milano. (Oral communication).
10. **Moretti S**, Di Cairano ES, F. Bertuzzi F , F. Folli , C. Perego. (2014) Signalling pathways responsible for the regulation of the glutamate transporter 1 (GLT1/EAAT2) in pancreatic beta cells. Italian Physiological Society (SIF). Annual Meeting of Young Researchers. Firenze, 01-may-2014. (Oral communication).

11. **Moretti S**, E. Di Cairano , D. Mengacci , A. Davalli , F. Bertuzzi , F. Folli , C. Perego. (2013) "The glutamate transporter GLT1 in islet of langerhans: molecular mechanisms", NEXT STEP4 - La giovane ricerca avanza". Università degli Studi di Milano. Mercoledì 17 luglio 2013 , Aula Magna, via Balzaretti, 9, Milano. (Oral communication).
12. **Moretti S**, Di Cairano E, Mengacci D, Davalli A, Bertuzzi F, Folli F and Perego C. (2013)The glutamate transporter GLT1 in Islets of Langerhans: localization and function. Italian Physiological Society (SIF). Annual Meeting of Young Researchers. Maggio 2013, Anacapri (oral communication).
13. **Moretti S**, Fino E, Iaquinto M, Di Cairano ES, Davalli A, Sacchi VS, La Rosa S, Bertuzzi F, Folli F and Perego C. (2012) The Glial Glutamate transporter 1 is expressed by pancreatic  $\beta$  -cells and preserves their integrity by controlling glutamate homeostasis in islet of Langerhans. Iniziativa "NEXT STEP3 - La giovane ricerca avanza". Università degli Studi di Milano. 26 giugno 2012. Milano. (oral communication).
14. Perego C, Iaquinto, **Moretti S**, Di Cairano ES, S. La Rosa, F. Bertuzzi, A. Davalli, F. Folli.(2012) Expression and activity of the glutamate transporter GLT1 / EAAT2 in Type 2 Diabetes. 24th National Congress of the Italian Society Diabetes. Section CO81 Molecular mechanism of pathology. conference held in Turin in 2012 (21-may-2012). (Oral communication)

### Professional Courses

- Selected for the Advanced Imaging and Fluorescence Techniques, advance course of EMBL (European Molecular Biology Laboratory) 28 Jun - 5 Jul 2014, Heidelberg (Germany) for researchers selected across the Europe (one representative researcher from each European state).
- Course of EXCEL of Informatics and Advanced Statistics. Università degli Studi di Milano, Department of Pharmacological and Biomolecular sciences, February 2013 and May 2014 (DiSfeb Department), Milano
- Practical Course of Muse<sup>®</sup> Cell, Mini Flow Cytometry, which uses miniaturized fluorescence detection and microcapillary cytometry to deliver single-cell analysis, which is highly quantitative. Università degli Studi di Milano, Department of Pharmacological and Biomolecular sciences, October 2013 (DiSfeb Department), Milano
- Practical Course of flow cytometers and FACS Aria, Università degli Studi di Milano, Department of Biosciences (Dbs) June 2014, Milano
- Workshop on Safety. Università degli Studi di Milano, Department of Pharmacological and Biomolecular sciences (DiSfeb Department) January 2012, Milano
- Course on the Management and Disposal of Toxic and Hazardous Waste. Università degli Studi di Milano,

**Teaching and tutoring**

2014-2015. Physiology of Integrated system. Two sections of Physiology laboratory for Students of Pharmaceutical Biotechnology at the Department of Pharmacological and Biomolecular sciences (DiSfeb Department), Università degli Studi di Milano.

Provided scientific tutoring for graduating students in Pharmaceutical Biotechnology (I Level) and Drug Biotechnology (II Level) at DISMAB, Dept. of Molecular Sciences Applied to Biosystems, Università degli Studi di Milano.